

**ISOLATION, CHARACTERIZATION, AND SYNTHESIS
OF BIOACTIVE NATURAL PRODUCTS FROM RAINFOREST FLORA**

John Michael Berger

Dissertation submitted to the Faculty of the
Virginia Polytechnic Institute and State University
in partial fulfillment of the requirement for the degree of

DOCTOR OF PHILOSOPHY

in

Chemistry

David G. I. Kingston, Chair

Neal Castagnoli, jr.

James Tanko

Richard Gandour

Paul Deck

June 4, 2001

Blacksburg, Virginia

Keywords: Saponins, Benzoquinones, Diterpenes, Antineoplastics, Anticancer

Copyright 2001, John M. Berger

ABSTRACT

ISOLATION, CHARACTERIZATION, AND SYNTHESIS OF BIOACTIVE NATURAL PRODUCTS FROM SURINAMESE FLORA

John Michael Berger

As part of our ongoing investigations for anticancer drugs from rainforest flora, five plant extracts were determined to contain interesting bioactivity. These extracts were subjected to various separation techniques, affording a number of bioactive compounds that were then characterized by spectral and degradative methods.

A methanol extract of *Cestrum latifolium* Lam. yielded the known compound parissaponin Pb. Hydrolysis afforded its aglycone, the known spirostanol diosgenin. GCMS analysis characterized the derivatized, hydrolyzed sugars.

Previous investigations of *Albizia subdimidiata* provided two saponins including the new compound albiziatrioside A. The sugar moieties of these two compounds required further characterization. They were characterized by spectral analysis of the partially hydrolyzed products and by GCMS analysis of the hydrolyzed sugars.

Pittoviridoside, a saponin from *Pittosporum viridiflorum*, was isolated in a previous investigation. Further investigation was required to characterize the stereochemical environment of the sugar moiety. The stereochemistries of the pentose sugars were determined by conversion into thiazolidine acetates of known stereochemistries and analysis with standards by GCMS.

Two new diterpenes were isolated from *Hymenaea courbaril*, which in an earlier investigation provided a new diterpene. The absolute configurations of these diterpenes were assigned on the basis of anisotropic NMR studies, X-ray crystallography, circular dichroism analysis and previously reported literature.

A previous investigation of *Miconia lepidota* isolated two benzoquinones, primin and its *n*-heptyl analog. Fifteen analogs were synthesized for structure-activity relationship determination. It was found that benzoquinones with moderate-length alkyl side chains displayed the strongest activity in our yeast and cancer cell lines.

ACKNOWLEDGEMENTS

This work is the result of many years and the contributions of many people. I could not have done it without them.

I dedicate this work to my parents, Richard and Noele, and the rest of my family. They provided me with every opportunity to succeed in life and the encouragement I needed to succeed.

I would also like to thank Dr. David G. I. Kingston for the patience and support he has shown me over the years. I am also indebted to others who have served on my committee: Dr. James Tanko, Dr. Neal Castagnoli jr., Dr. Paul Deck, Dr. Richard Gandour and Dr. Michael Calter.

The faculty and staff of Virginia Polytechnic Institute and State University never failed to support me in my endeavors. Four in particular deserve my thanks: Dr. Bingnan Zhou, Dr. Youngwan Seo, Dr. Maged Abdel-Kader and Tom Glass. Without these four, I would still be struggling with my work.

Additional thanks to Jeannine Hoch, Jessica Sharp, and Brian Bahler. A medicinal chemist is only as good as those who support him with biological data. These three are the best.

TABLE OF CONTENTS

	Page
LIST OF FIGURES	viii
LIST OF SCHEMES	xi
LIST OF TABLES	xii
I GENERAL INTRODUCTION.	
1.1 Natural Products in Drug Discovery.	13
1.1.1 Natural Products as Antineoplastics.	15
1.2 The ICBG Program.	19
1.3 Bioassay-Guided Fractionation.	21
1.3.1 General Considerations.	21
1.3.2 Bioassays Employed by the ICBG Group.	24
II ISOLATION AND CHARACTERIZATION OF 13-HYDROXY-1(10),14- <i>ENT</i> - HALIMADIEN-18-OIC ACIDS FROM <i>HYMENAEA COURBARIL</i> .	
2.1 Introduction.	28
2.1.1 Previous Investigations of <i>Hymenaea</i> Species.	28
2.1.2 Chemical Investigations of <i>Hymenaea courbaril</i> .	29
Previous Investigations of 13-Hydroxy-1(10),14- <i>ent</i> - halimadien-18-oic Acids	31
2.2 Results and Discussion.	32
2.2.1 Isolation of <i>Ent</i> -Halimadien-18-oic Acids from <i>H. courbaril</i> (Caesalpinaceae).	32
2.2.2 Characterization of Diterpenes from <i>Hymenaea courbaril</i> (Caesalpinaceae).	34

2.2.2.1	Structure of (13 <i>R</i>)-13-Hydroxy-1(10),14- <i>ent</i> -halimadien-18-oic acid (2.10).	34
2.2.2.2	The Structure of (2 <i>S</i> ,13 <i>R</i>)-2,13-Dihydroxy-1(10),14- <i>ent</i> -halimadien-18-oic acid (2.11).	36
2.2.2.3	The Structure of (13 <i>R</i>)-13-Hydroxy-1(10),14- <i>ent</i> -halimadien-18-oic acid (2.12)..	38
2.2.3	Determination of the Absolute Configurations of the (13 <i>R</i>)-13-Hydroxy-1(10),14- <i>ent</i> -halimadien-18-oic acids.	38
2.2.3.1	Circular Dichroism of the (13 <i>R</i>)-13-Hydroxy-1(10),14- <i>ent</i> -halimadien-18-oic acids.	38
2.2.3.2	Subsequent Literature.	46
2.2.3.3	Validation of a New NMR Method for Stereochemical Determination of Carboxylic Acids.	47
2.2.4	Biological Evaluation of Compounds.	54
2.3	Experimental.	54
III	PARISSAPONIN Pb FROM <i>CESTRUM LATIFOLIUM</i> LAM.	
3.1	Introduction.	64
3.1.1	Structure and Basic Properties of Saponins.	64
3.1.2	Saponins: Medicinal Applications and Other Uses.	67
3.1.3	Chemical Investigation of <i>Cestrum latifolium</i> Lam. and <i>Cestrum</i> Saponins.	70
3.2	Results and Discussion.	71
3.2.1	Isolation of Parissaponin Pb from <i>Cestrum latifolium</i> Lam.	71

3.2.2	Structural Elucidation of Parissaponin Pb.	74
3.2.3	Biological Evaluation of Parissaponin Pb.	80
3.3	Experimental.	81
IV	HYDROLYSIS AND CONFIGURATION ANALYSIS OF SAPONINS (ALBIZIATRIOSIDE A) FROM <i>ALBIZIA SUBDIMIDIATA</i>	
4.1	Introduction.	87
4.1.1	Previous Investigations of <i>Albizia</i> Species.	87
4.1.2	Chemical Investigations of <i>Albizia subdimidiata</i> .	90
4.2	Results and Discussion.	94
4.2.1	Isolation of Saponins from <i>Albizia subdimidiata</i> .	94
4.2.2	Characterization of Saponins from <i>Albizia subdimidiata</i> .	97
4.2.3	Characterization of Peracetylated Saponins.	98
4.2.4	Partial Hydrolysis of <i>Albizia</i> Saponins.	98
4.2.5	Determination of the Stereochemistries of the Pentose Sugars.	99
4.2.6	Biological Evaluation of Saponins.	102
4.3	Experimental.	103
V	PITTOVIRIDOSIDE, A NOVEL TRITERPENOID SAPONIN FROM <i>PITTOSPORUM VIRIDIFLORUM</i>	
5.1	Introduction.	113
5.1.1	Previous Investigations of <i>Pittosporum</i> Species.	113
5.1.2	Chemical Investigations of <i>Pittosporum viridiflorum</i> .	115
5.2	Results and Discussion.	118

5.2.1	Isolation of Crude Pittoviridoside from <i>Pittosporum viridiflorum</i> .	118
5.2.2	Determination of Stereochemistries of the Pentose Sugars.	120
5.2.3	NMR Confirmation of Structure.	122
5.2.4	Biological Evaluation of Compounds.	124
5.3	Experimental.	124
VI.	SYNTHESIS OF 2-METHOXY-6- <i>N</i> -ALKYL BENZOQUINONES AND BIS- BENZOQUINONES: POTENTIAL DNA INTERCALATORS AND TOPOISOMERASE INHIBITORS	
6.1	Introduction.	138
6.1.1	Benzoquinones as Potential DNA Intercalators and Topoisomerase Inhibitors.	132
6.1.2	Previous Investigations of Primin and Primin Derivatives.	137
6.2	Results and Discussion.	138
6.2.1	Synthesis of Benzoquinones.	138
6.2.2	Synthesis of Bis-Benzoquinones.	140
6.2.3	Synthesis of Bis-Schiff Bases	142
6.2.4	Biological Evaluation of the Benzoquinones, Bis-Benzoquinones, and Bis-Schiff Bases.	144
6.3	Experimental	150
VII.	CONCLUSIONS	164
	APPENDIX	165
	<i>VITA</i>	210

LIST OF FIGURES

	page
Figure 1-1. Natural Products.	15
Figure 1-2. Antineoplastics.	16
Figure 1-3. Previously Isolated Natural Products.	21
Figure 2-1. Diterpenes from Hymenaeae Species.	29
Figure 2-2. Diterpenes from <i>Hymenaea courbaril</i> (Caesalpinaceae).	30
Figure 2-3. Diterpenes 2.10-12 from <i>Hymenaea courbaril</i> .	30
Figure 2-4. Isolated and Semisynthetic Diterpenes <i>Halimium viscosum</i> .	31
Figure 2-5. Previously Reported Methyl Esters.	34
Figure 2-6. ORTEP Diagrams of 2.10 .	35
Figure 2-7. The Exciton Chirality Method.	39
Figure 2-8. Circular Dichroism Spectrum of 2.10 .	40
Figure 2-9. Circular Dichroism Spectrum of 2.11 .	41
Figure 2-10. Circular Dichroism Spectrum of 2.12 .	42
Figure 2-11. Empirical Model for Predicting Absolute Configuration of Allylic Alcohols.	43
Figure 2-12. Circular Dichroism of the Benzoyl Derivative of 2.11	44
Figure 2-13. Negative Cotton Effect for the Prepared Benzoate Ester	44
Figure 2-14. Projection of 2.12 into Positive and Negative Contributing Quadrants.	45
Figure 2-15. Previously Reported Semisynthesis for Determination of	46

Stereochemistries of *Ent*-Halimediol-18-oic Acids and Esters.

Figure 2-16. Potential Conformations of (<i>R</i>)-PGME Amides.	48
Figure 2-17. NOE Evidence for the Presence of a <i>Gauche</i> + Conformation.	49
Figure 2-18. NOE Evidence for the Existence of a <i>Gauche</i> + Conformation.	50
Figure 2-19. Anisotropic Effects and Predictive Model.	52
Figure 2-20. ¹ H NMR Differences of (<i>R</i>) and (<i>S</i>)-PGME Derivatives of 2.10 .	53
Figure 3-1. Saponins.	65
Figure 3-2. Four Common Triterpene Aglycone Skeletons.	66
Figure 3-3. Basic Steroidal Saponin Skeletons.	67
Figure 3-4. <i>Cestrum</i> Saponins.	72
Figure 3-5. Diosgenin and Related Saponins.	77
Figure 3-6. Predicted and Observed HMBC Correlations.	78
Figure 4-1. Natural Products from <i>Albizia</i> species.	88
Figure 4-2. Previously Isolated and Prepared Samples from <i>Albizia subdimidiata</i> .	90
Figure 4-3. Hydrolysis Products of 4.6 and 4.7 .	91
Figure 4-4. Linkage Analysis via Derivatization and GCMS.	92
Figure 4-5. COSY Correlations Important for Linkages.	93
Figure 4-6. Prosapogenin 10 from <i>Acaia concinna</i> .	99
Figure 4-7. Preparation of Standards for GCMS Analysis of Sugars.	101
Figure 5-1. <i>Pittosporum</i> Terpenes.	114
Figure 5-2. Previously isolated <i>Pittosporum viridiflorum</i> Sapogenins.	116
Figure 5-3. Pittoviridoside from <i>Pittosporum viridiflorum</i> .	116

Figure 5-4. Mass Spectroscopic Fragmentations of Reduced Alditol Acetates from 5.7 .	118
Figure 5-5. Predicted and Observed NOE Correlations.	123
Figure 6-1. Benzoquinones from <i>Miconia Lepidota</i> .	131
Figure 6-2. Biochemically Important Benzoquinones and Hydroquinones.	132
Figure 6-3. Intercalating Drugs.	133
Figure 6-4. Representation of the Intercalation of Anthracycline Antibiotics.	134
Figure 6-5. Bis-Intercalators.	135
Figure 6-6. Intercalation of WP 631 into DNA.	136
Figure 6-7. Synthesis of Benzylic Alcohols.	137
Figure 6-8. Hydrogenolysis and Oxidation of Phenolic Alcohols to Benzoquinones	137
Figure 6-9. Preparation of Bis-Benzoquinones (6.42-6.44).	141
Figure 6-10. Nitrogen Containing Bis-Benzoquinone Target.	142
Figure 6-11. Attempted Preparation of 6.45 .	143
Figure 6-12. Preparation of a Bis-Schiff Base.	144
Figure 6-13. Relationship Between Lipophilicity and Activity in the Sc-7 Cell Line.	147
Figure 6-14. Relationship Between Lipophilicity and Activity in the Sc-7 Cell Line.	147
Figure 6-15. Tautomerism of Hydroxy Primin.	148

LIST OF SCHEMES

	page
Scheme 1. Isolation of Diterpenoids from <i>Hymenaea courbaril</i> (Caesalpinaceae).	33
Scheme 2. Isolation Tree for M980218 (<i>Cestrum Latifolium</i> Lam.)	72
Scheme 3. Isolation Tree for <i>Albizia</i> Saponins.	96
Scheme 4. Isolation of Crude Pittoviridoside.	120

<u>LIST OF TABLES</u>	page
Table 1. Effect of Known Therapeutics on Mutant Yeast Strains.	26
Table 2. Effect of Known Therapeutics on the Sc-7 Mutant Yeast Strain.	27
Table 3. ¹ H NMR Spectral Data for Compounds 2.10-13 .	62
Table 4. ¹³ C NMR Spectral Data for Compounds 2.8-13 .	63
Table 5. ¹ HNMR (Selected Peaks) of A, B, 3.10, 3.13, and 3.14 .	84
Table 6. ¹³ CNMR (Steriodal Structure) of A, B, 3.10, 3.13, and 3.14 .	85
Table 7. ¹³ CNMR (Glycoside Moiety) of A, 3.10, and 3.14 .	86
Table 8. Selected ¹ H NMR Data for Compounds 4.6-4.11 .	111
Table 9. ¹³ C NMR Data for Compounds 4.6 and 4.7 in CD ₃ OD.	112
Table 10. ¹ H and ¹³ C NMR Spectral Data for Pittoviridagenin (5.5).	128
Table 11. ¹ H and ¹³ C NMR Spectral Data for Pittoviridoside (5.7).	129
Table 12. ¹ H and ¹³ C NMR Spectral Data of the Sugar Moiety for Pittoviridoside.	130
Table 13. Biological Activity of the Isolated Benzoquinones.	
138	
Table 14. Bioactivity Data for Compounds 6.1-2, 6.28-6.34 .	140
Table 15. Bioactivity Data for Compounds 6.42-6.44 .	142
Table 16. Bioactivity Data for Compounds 6.1-2, 6.28-34, 6.42-44, and 6.46-48 .	145
Table 17. Physical Properties of 6.1-2, 6.28-34, 6.42-44, and 6.46-48 .	146
Table 18. ¹ H NMR Spectral Data for Compounds 6.1-2, 6.28-34, and 6.42-44 .	160
Table 19. ¹³ C NMR Spectral Data for Compounds 6.1-2, 6.28-34, and 6.42-44 .	161
Table 20. ¹ H NMR Spectral Data for Bis-Benzoquinone Intermediates.	162
Table 21. ¹³ C NMR Spectral Data for Bis-Benzoquinone Intermediates.	163

I. GENERAL INTRODUCTION

1.1 Natural Products in Drug Discovery¹

For at least five thousand years humankind has relied on natural products as the primary source for medicines.² Herbs, bread mold, even leeches were employed to bring relief to the sick and infirm. There was little significant change over much of this time period; however, the last two centuries have brought an explosion of understanding how these natural products are produced and how they interact with other organisms. The last two centuries have seen the isolation of the first commercial drug (morphine),³ the use of microbial products as medicines (penicillin),⁴ and even a use for the lowly leech (the anticoagulant, hirudin).⁵ Who knows what the next two centuries will bring us?

Now, at the start of a new millennium, it is estimated by the World Health Organization that 80% of the world's inhabitants must rely on traditional medicines for health care;⁶ these traditional medicines are primarily plant-based. Even in the remaining population, natural products are important in health care. It is estimated that 25% of all prescriptions dispensed in the USA contained a plant extract or active ingredients derived from plants. It is also estimated that 74% of the 119 currently most important drugs contain active ingredients from plants used in traditional medicine.⁷ Another study of the most prescribed drugs in the USA indicated that a majority contained either a natural

¹ Newman, D.J.; Cragg, G.M.; Snader, K.M. *Nat. Prod. Rep.* **2000**, *17*, 215.

² Mann, J. *Murder, Magic, and Medicine*, Oxford University Press, Oxford, U.K., **1992**, 111.

³ Grabley, S.; Thiericke, R. *Adv. Biochem. Eng./Biotech.* **1999**, *64*, 104.

⁴ Miller, J.B., *the Pharma Century: Ten Decades of Drug Discovery*, Supplement to ACS Publications, **2000**, 52.

⁵ Budavari, S. (editor) *The Merck Index*, twelfth edition, Merck & Co., Whitehouse, NJ, **1996**, 806.

⁶ Farnsworth, N.R.; Akerele, O.; Bingel, A.S.; Soejarto, D.D.; Guo, Z. *Bull. WHO*, **1985**, *63*, 965.

⁷ Arvigo, R.; Balick, M. *Rainforest Remedies*, Lotus Press, Twin Lakes, **1993**.

product or a natural product was used in the synthesis or design of the drug.⁸ All of these investigations demonstrate the importance of natural products in drug discovery.

Until the 1970's, drug discovery was essentially based on serendipity.⁹ Rational drug discovery only began with the advent of molecular biology and computers. With the cost of drug development approaching \$350 million (USA) per drug,¹⁰ many discovery groups are debating "quantity" vs. "quality" strategies in an effort to reduce costs. The "quantity" approach is that of combinatorial chemistry, which can provide libraries of thousands of compounds in a short period of time. For example, this approach can provide thousands of analogs of the decapeptide gramicidin S₁ (**1.1**) for testing, a task impossible for natural product isolation. However, these libraries tend to lack novelty and are usually based on natural product targets anyway. One "quality" approach is natural product screening and isolation, which provides fewer compounds over a longer period of time. However, this strategy can lead to novel molecular structures not foreseen through combinatorial chemistry. The unique peroxy-bond of artemisinin (**1.2**), the ring system of paclitaxel (Taxol[®]) (**1.3**), and the stereochemistry of erythromycin A (**1.4**) are synthetically challenging and are unlikely to have been discovered through a combinatorial approach. Many pharmaceutical companies are now pursuing both combinatorial and isolation strategies. Only time will tell which strategy will predominate, but to paraphrase a respected natural product chemist,¹¹ perhaps Nature is the world's best combinatorial chemist.

⁸ Grifo, F.; Newman, D.; Fairfield, A.S.; Bhattacharya, B.; Grupenhoff, J.T. *The Origins of Prescription Drugs* (F. Grifo and J. Rosenthal, ed.) Island Press, Washington, D.C., **1997**, 131.

⁹ Pushkar, P. *Prog. Drug. Res.*, **1998**, *50*, 9.

¹⁰ Grabley, S.; Thiericke, R. *Adv. Biochem. Eng./Biotech.* **1999**, 64101.

¹¹ Potier, P. *Actual. Chim.* **1999**, *11*, 9.

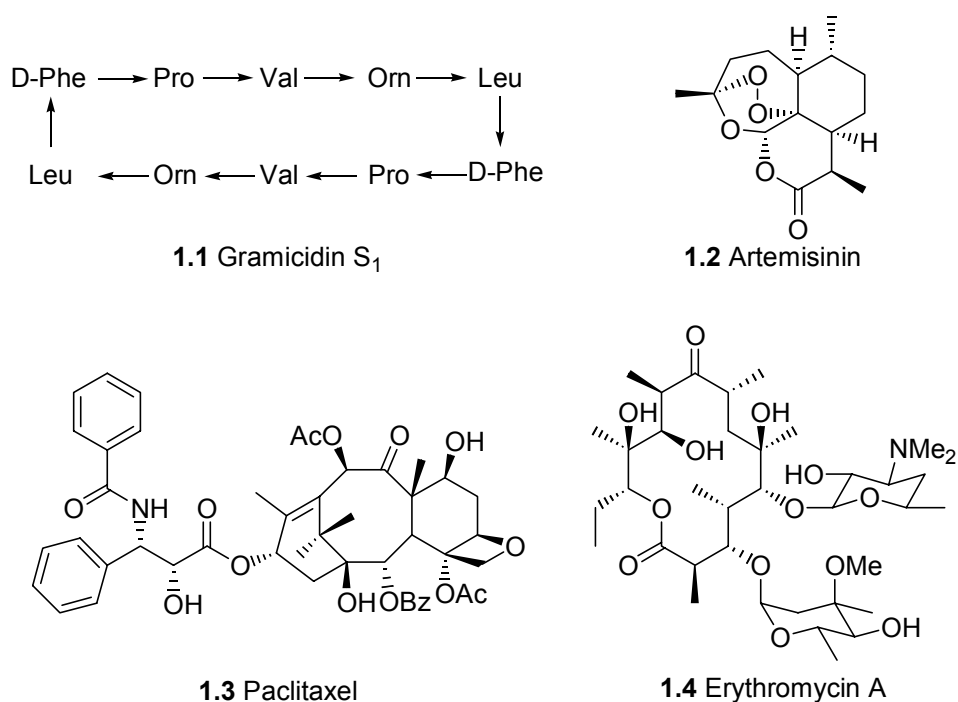


Figure 1-1. Natural Products

1.1.1 *Natural Products as Antineoplastics*

According to the American Cancer Society,¹² cancer is the second leading cause of death in the United States, second only to heart disease. One in four deaths in the USA were reportedly due to cancer. Five million lives have been lost to cancer since 1990 and more than a million cancer cases were expected to be diagnosed in 2000. Thirteen million cases of cancer were diagnosed since 1990. While the death rates for the sufferers of most cancers have stayed essentially the same since 1940, there was a dramatic increase in death rate due to smoking that has only recently started to taper off.

Initially, surgery was the treatment of choice for many cancers; however surgery is only applicable to those patients whose cancer is localized (non-metastasized). Those

patients whose cancer is in metastasis (spreadable) must rely on chemotherapy. Very few clinically useful anticancer drugs (antineoplastics) have been developed by rational design (5-fluorouracil is one of the exceptions). Many of the anticancer drugs in current use are natural products or are derived from natural products. The introduction of anticancer drugs such as the *Vinca* alkaloids vinblastine (**1.5**) and vincristine (Oncovin[®]) (**1.6**) has wrought modern day miracles. The five-year survival rate of Hodgkin's disease sufferers in 1970 was a tragic 5%; yet by 1982 it had increased to 98%.²

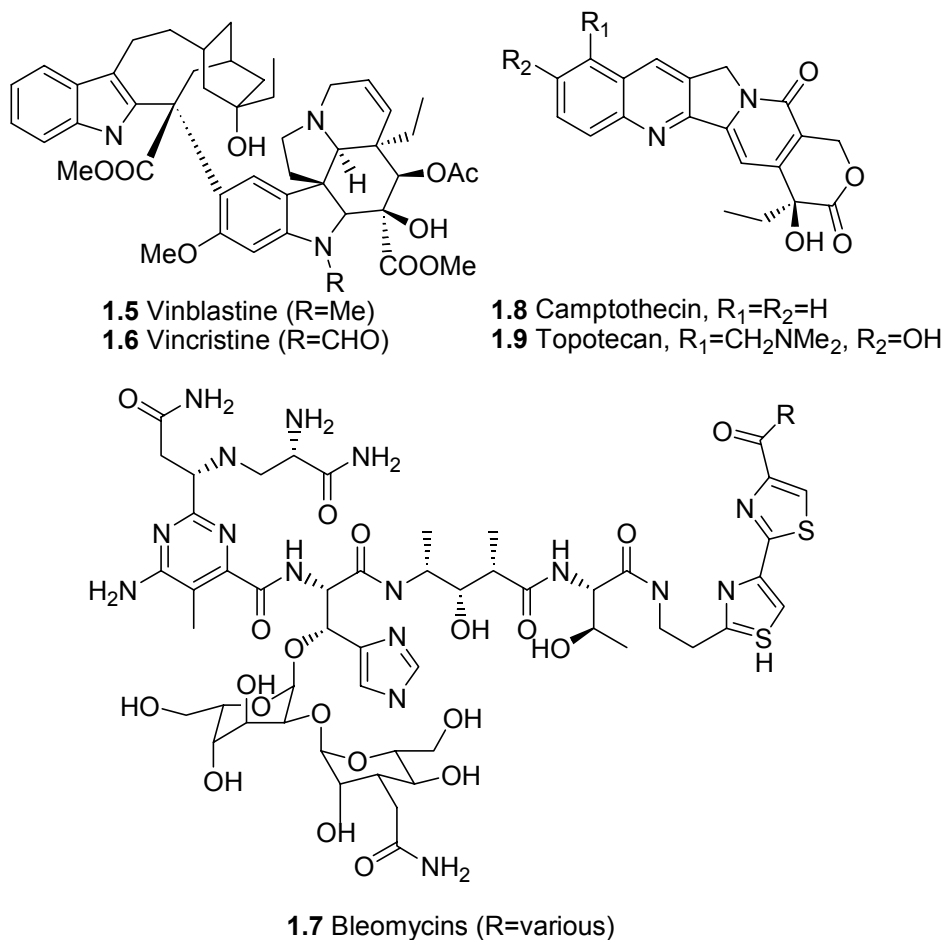


Figure 1-2. Antineoplastics

¹² The American Cancer Society has a very informative website at www.cancer.org.

Acute lymphoblastic leukemia patients also had the same depressing survival rate in 1970; but by 1982 it had risen to 60%. Testicular cancer sufferers now have over a 90% survival rate, thanks to a mold product, bleomycin (**1.7**).

In 1957, the United States National Cancer Institute (NCI) embarked on an ambitious search for anticancer compounds from higher plants;¹³ since then (circa 1991) more than 120,000 plant extracts from 35,000 species have been investigated. Compounds such as paclitaxel (**1.3**) and camptothecin (**1.8**) were developed through this undertaking. Three cytotoxic test methods were developed and employed as bioassays: the 3PS(P388) *in-vivo* (methylchloanthrene-induced) mouse leukemia, the *in-vitro* 9KB human nasopharyngeal carcinoma, and the 9PS *in-vitro* murine leukemia. Eventually (1986) these cell lines were shut down and a panel of 60 human cancer cells was employed for testing purposes.

Since the 1970s, significant progress in the understanding of cell division and replication has led to a number of strategies to inhibit cell reproduction. A number of anticancer drugs either directly damage DNA (bleomycins **1.7**) or inhibit enzymes that are responsible for the uncoiling of DNA (the topoisomerase I inhibitor camptothecin, **1.8**). Another approach is to interfere with the assembly or disassembly of the mitotic spindles that form during cell reproduction. Paclitaxel (Taxol[®]) (**1.3**) promotes tubulin polymerization, preventing cell reproduction. The *Vinca* alkaloids vinblastine (**1.5**) and vincristine (Oncovin[®]) (**1.6**), on the other hand, inhibit tubulin polymerization by binding to tubulin; the result is still the same: cell reproduction is stopped.¹⁴

¹³ McLaughlin, J.L. in *Methods in Plant Biochemistry* (K. Hostettmann, ed.) Academic Press Inc. San Diego, **1991**.

¹⁴ Dewick, P.M. *Medicinal Natural Products: A Biosynthetic Approach*, John Wiley and Sons, New York, **1999**.

The most significant problems facing the use of natural products as antineoplastics are their solubilities, toxicities, and supply problems. Camptothecin (**1.8**) was too insoluble for clinical use and was originally administered as the sodium salt of the ring-opened lactone; this proved to be inactive. It was revived for drug use by the synthesis of water soluble derivatives such as topotecan (**1.9**). Paclitaxel (**1.3**) suffered from solubility and supply problems. It was isolated from the bark of the slow growing *Taxus brevifolia* (Pacific Yew); bark removal results in the death of the tree. This supply issue was addressed by semisynthetic production from the renewable needles of a similar tree, *Taxus baccata* (English Yew). The solubility issue was addressed (barely adequately) by formulation.

Current research in natural products indicates that the future holds great rewards through the use of recently developed technology. Synthesis of novel compounds may be achievable not through synthetic organic chemistry but through genetics; recombinant DNA techniques have been used to create hybrid strains of *Streptomyces* resulting in isolation of over 50 new erythromycins (**1.4**) by manipulating the polyketide synthases.¹⁵ Combinatorial chemistry can possibly perform lead-structure optimization faster than classical synthesis. Newer, more focused drug delivery systems may permit the use of toxic drugs at safe dosages. These and many other advances can give hope to those who suffer from cancer.

¹⁵ McDaniel, R.M.; Thamchaipenet, A.; Gustafsson, C.; Fu, H.; Betlach, M.; Betlach, M.; Ashley, G. *Proc. Natl. Acad. Sci. USA*, **1999**, *96*, 1846.

1.2 The ICBG Program

As our understanding of natural products has increased, the biodiversity of our planet has decreased predominately due to development by man. In this day of biotechnology, genetic material is becoming a valuable resource; it is ironic that while we value genetic material more every day, genetic material is becoming less available.

The International Cooperative Biodiversity Group (ICBG) program was initiated by a consortium of three U.S. government agencies in 1992 as a response to the ongoing loss of biodiversity. Virginia Polytechnic Institute and State University (under the direction of Dr. David G.I. Kingston) (VPI&SU) is the lead organization of an ICBG program initially funded in 1993. Other participants are the Missouri Botanical Gardens (Dr. James S. Miller), Conservation International (Dr. Russell Mittermeier), Centre National d'Application et des Recherches Pharmaceutiques (Madagascar, Dr. Rabodo Andriantsiferana), Bedrijf Geneesmiddelen Voorziening Suriname (Dr. Jan H. Wisse), Bristol-Myers Squibb Pharmaceutical Research Institute (Dr. J.J. Kim Wright), and Dow Agrosciences (Dr. Cliff Gerwick). The program focuses on two regions: the South American country Suriname (formerly Dutch Guiana) and the African country Madagascar. They have been previously determined to be strategically important for biodiversity. The program has many diverse goals besides natural product isolation or drug discovery; the program seeks to promote conservation, the development of alternative uses for natural resources, education, and economic benefits for the people of these countries. The research program at VPI&SU focuses on the isolation and characterization of anticancer compounds.

The process of isolation of compounds occurs as follows: plants are identified and collected (under the supervision of the Missouri Botanical Gardens or Conservation International) in Suriname and in Madagascar. Voucher samples are stored at local herbaria. The plants are then extracted individually with ethyl acetate and methanol by local support (Bedrijf Geneesmiddelen Voorziening Suriname or Centre National d'Application et des Recherches Pharmaceutiques). The extracts are shipped in triplicate to VPI&SU, which then sends one set of extracts to Bristol Myers Squibb. They are then prescreened (to determine if they are active), screened (to determine their level of activity), and then submitted for isolation (prioritized based on bioactivity).

Under the ICBG program a number of new and previously known structures have been published (some are shown below).¹⁶

¹⁶ (a) Yang, S.-W.; Zhou, B.-N.; Wisse, J.; Evans, R.; van der Werff, H.; Miller, J.S.; Kingston, D.G.I. *J. Nat. Prod.* **1998**, *61*, 901. (b) Yang, S.-W.; Abdel-Kader, M.; Malone, S.; Werkhoven, M.C.M.; Wisse, J.H.; Bursuker, I.; Neddermann, K.; Fairchild, C.; Raventos-Suarez, C.; Menendez, A.T.; Lane, K.; Kingston, D.G.I. *J. Nat. Prod.* **1999**, *62*, 976. (c) Abdel-Kader, M.; Bahler, B.; Malone, S.; Werkhoven, M.C.M.; van Troon, F.; David; Wisse, J.H.; Bursuker, I.; Neddermann, K.M.; Mamber, S.W.; Kingston, D.G.I. *J. Nat. Prod.* **1998**, *61*, 1202.

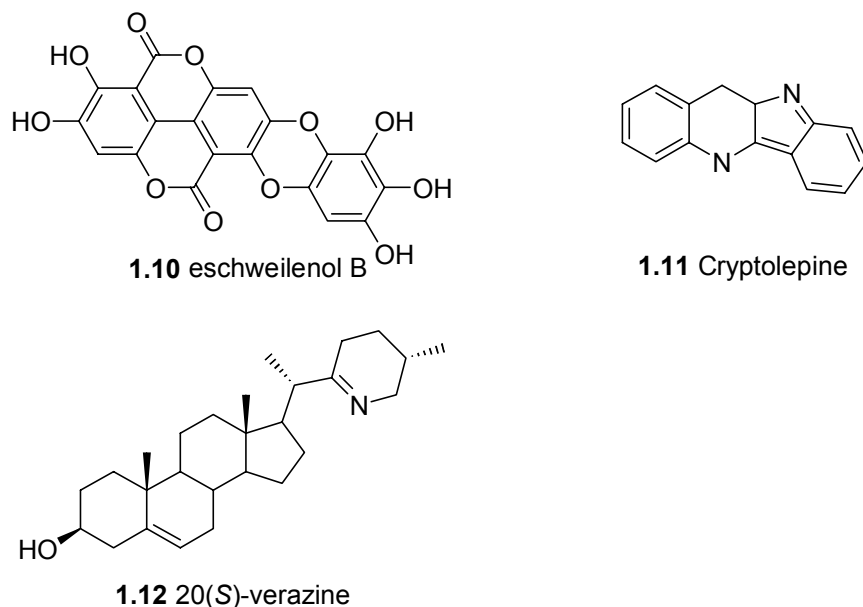


Figure 1-3. Previously Isolated Natural Products

1.3 Bioassay-Guided Fractionation

1.3.1 *General Considerations*

Bioassays are the foundation of a natural products discovery group. No discovery group has the manpower, financial resources, or time to extract every compound from an extract. Bioassays permit the researcher to prioritize their investigations.

Bioassays can be used in three ways. The first way is used to determine if extracts are active (prescreening). As the chance that an extract is active is quite low, large numbers of extracts should be tested. This is usually performed at a specific concentration (dose) previously determined to be “interesting”. If the extract responds positively, it will be subjected to further testing.

The second manner (screening) permits the prioritizing of the active extracts. The extracts are tested over a range of concentrations and their responses quantified (i.e. an

IC₅₀ is assigned which is the concentration required to inhibit the growth of a microorganism by 50%). More active fractions should be investigated first with greater resources than a less active extract.

The third use of bioassays is as a monitoring tool. Once an extract is subjected to a given separation technique, a number of fractions are collected. These fractions can then be tested (monitored); the more active fractions are submitted for further separation and monitoring whereas less active fractions are set aside. Eventually the most active component of an extract will be isolated.

Bioassays should be simple, fast, reliable, inexpensive, and reproducible. The assay should also correlate to the problem. They should model a living organism well. Unfortunately, no bioassay can meet all of the above criteria. *In-vivo* testing (such as on animals) can provide more valid data than *in-vitro* cellular testing; however, animal testing is complicated, slow, and expensive. Cellular assays can be fast, simple, and inexpensive but do not model higher organisms well. Due to costs and time, *in-vitro* assays are usually employed initially and *in-vivo* testing is reserved only for those pure compounds with potential clinical use.

Bioassays for potential anticancer agents can be grouped into two types: cytotoxicity assays and mechanism-based assays.¹⁷ Cytotoxicity tests usually determine the concentration of sample required to inhibit cell growth of a single cell line by 50%. An example of a cell line employed in a cytotoxicity assay is the A2780 human ovarian cancer cell line, originally developed at NCI¹⁸ and in use at Bristol Myers-Squibb and the

¹⁷ Suffness, M. in *Biologically Active Natural Products* (Hostettmann, K. and Lea, P.J. editors), Oxford University Press, Oxford, UK, **1987**, 85.

¹⁸ Skehan, P.; Storeng, R.; Scudiero, D.; Monks, A.; McMahon, J.; Vistica, D.; Warren, J.T.; Bokesch, H.; Kenney, S.; Boyd, M.R. *J. Nat. Can. Inst.* **1990**, *82*, 1107.

ICBG program at VPI&SU. The A2780 method is a general assay, not limited to any specific mechanism of action. However, there are many cytotoxic compounds that are not viable drug candidates, since many cytotoxic compounds are just too toxic for clinical use.

Mechanism-based assays are based on a known strategy to defeat a specific problem. They are usually non-cellular tests that measure the concentration required to inhibit the rate of a given reaction by 50%. An example of a mechanism based assay is the tubulin-polymerization reaction first employed by Susan Horwitz to discover the mechanism of action of paclitaxel (**1.3**).¹⁹

There are also bioassays that are a mixture of these two types: the mechanism-based cellular bioassay. Cell lines have been developed that are selectively susceptible to inhibitors that operate by specific mechanisms of action. A number of *Saccharomyces cerevisiae*²⁰ strains have been developed that are more sensitive to topoisomerase inhibitors than the original strain. Another example is that of drug-resistant microorganisms (such as penicillin-resistant bacteria), which have developed over time; these microorganisms have developed defense mechanisms (such as the β -lactamases). These cell lines are useful for development of inhibitors of the defense mechanism.

Bioassays suffer from one or more limitations. Cytotoxicity tests are unspecific, can result in false positives, and can lead to highly toxic compounds. The more active compounds can overshadow less cytotoxic compounds of interest. Mechanism-based assays suffer from high specificity; useful compounds that interact via different

¹⁹ Horwitz, S.B. *Trends Pharmacol. Sci.* **1992**, *13*, 134.

²⁰ a. Nitiss, J.; Wang, J.C. *Proc. Natl. Acad. Sci. USA*, **1988**, *85*, 7501. b. Abdel-Kader, M.S.; Bahler, B.D.; Malone, S.; Werkhoven, M.C.M.; van Troon, F.; David, Wisse, J.H.; Bursuker, I.; Neddermann, K.M.; Mamber, S.W.; Kingston, D.G.I. *J. Nat. Prod.* **1998**, *61*, 1202.

mechanisms will not be isolated. Only through testing with multiple assays and eventual clinical studies can a drug candidate finally enter the marketplace.

1.3.2 *Bioassays Employed by the ICBG Group.*

The main characteristic of cancer cells as opposed to normal cells is unregulated growth. A common misconception is that cancer cells grow faster than normal cells; this is not necessarily true.² Rather the lack of regulation leads to the growth of cancer cells. Cancer cells also possess two more characteristics: the ability not to be recognized by the immune system as an aberration and the ability to metastasize (to break off from the primary tumor and move to other sites where they can produce secondary tumors).

One method for treatment is to prevent reproduction of cancer cells. Reproduction can be prevented either through disrupting mitosis (paclitaxel or *Vinca* alkaloids, **1.3**, **1.5-1.6**), direct DNA damage (bleomycin, **1.7**), or by interfering with DNA repair pathways.

The ICBG group has employed the last method as a mechanism-based cellular assay. Mutant yeast strains (*Saccharomyces cerevisiae*, baker's yeast) have been developed whose DNA repair mechanisms have been compromised. The RAD52 gene is responsible for the repair of double-strand breaks and meiotic recombination.^{21,22} Yeast strains without this gene are more sensitive to agents that damage DNA due to the lack of a repair mechanism. However, yeast cell walls are not very permeable to foreign compounds; to overcome this resistance *ise1* or *ISE2* permeability mutations were

²¹ Game, J.C. *Yeast Genetics: Fundamental and Applied Aspects*. (J.F.T. Spencer, D.M. Spencer, and A.R.W. Smith, Eds.) Springer Verlag, New York. **1983**. 109.

²² Wu, C. *Structural and Synthetic Studies of Potential Antitumor Natural Products*. Thesis, Virginia Polytechnic Institute and State University, **1998**.

introduced. These vulnerable strains have been developed in which the topoisomerase genes have been selectively removed. Three strains have been developed: the 1138 strain (which possesses the ISE2 mutation and a deficient RAD52 repair pathway), the 1140 strain (which possesses the *ise1* mutation and a deficient RAD52 repair pathway), and the 1353 strain (which lacks the topoisomerase I gene, possesses a deficient RAD52 repair pathway but does not possess a permeability mutation).

These strains are deployed on an agar gel medium in a standard 10 cm x 10 cm plates. Wells are cut into the agar and 100 μ L of diluted extract (or compound) is placed in each of the wells. The cells are allowed to incubate for approximately two days. Zones of cell growth inhibition are measured and quantified as IC_{12} 's. An IC_{12} is a measure of the concentration required to inhibit the cell growth in a 12 mm diameter about the well.

The effects of several known anticancer and antifungal agents in these yeast strains are shown in Table 1 below.

Table 1. Effect of Known Therapeutics on Mutant Yeast Strains.

Test Sample	Type	Dose ($\mu\text{g}/\text{mL}$)	Zone of Inhibition (mm)		
			<i>ISE2</i> 1138	<i>Ise1</i> 1140	<i>ISE</i> ⁺ 1353
Camptothecin	Topo I inhibitor	200	26	25	7
Etoposide	Topo II inhibitor	1000	18	7	7
Teniposide	Topo II inhibitor	1000	20	7	7
Streptonigrin	DNA cleavage, Topo II inhibitor	100	13	10	15
Doxorubicin	DNA intercalator Topo II inhibitor	1000	16	16	19
Mitomycin C	DNA damage	500	15	7	7
Mystatin	Antifungal	40	12	12	12
Amphotericin B	Antifungal	250	20	17	19

When the results of these three strains are compared certain trends can be deduced. The 1138 and 1140 strains are selectively sensitive to topoisomerase I inhibitors, whereas 1353 is insensitive (since there is no topoisomerase I pathway to interfere with). Strain 1353 has shown hypersensitivity towards certain topoisomerase II inhibitors. Strains 1138 and 1140 differ only in permeability. General DNA damaging agents and antifungal agents show unselective activity on all three strains. Selective activity is defined as a three-fold greater response to one strain versus another (as IC_{12} 's).

Another yeast strain available is the Sc-7 (*Saccharomyces cerevisiae*) mutant yeast strain. This strain has been employed in a similar manner as a general (i.e. not mechanism based) cytotoxicity assay. This assay has shown hypersensitivity to a number of anticancer and antifungal compounds; it was essentially used as a secondary screen since it does not provide interesting mechanistic information.

Table 2. Effect of Known Therapeutics on the Sc-7 Mutant Yeast Strain.

Compound	Concentration $\mu\text{g/mL}$	<i>S. Cerevisiae</i> 1600 Normal Yeast Inhibition Zone mm	<i>S Cerevisiae</i> Sc-7 Mutant Yeast Inhibition Zone Mm
Chloramphenicol	2000	7	14
Tunicamycin	1000	14	29
Esperamicin A1	20	14	29
Streptonigrin	100	7	26
5-Flurouracil	100	26	34
Amphotericin B	250	14	17
Nystatin	40	17	28

These strains and, in recent years, the A2780 mammalian cytotoxicity assay¹⁸ have been employed by VPI&SU and its collaborators to investigate over 16,000 plant extracts since 1995. They have been used in bioactivity-guided fractionations in the discussions that follow.

II. ISOLATION AND CHARACTERIZATION OF 13-HYDROXY-1(10),14-ENT-HALIMADIEN-18-OIC ACIDS FROM *HYMENAEA COURBARIL* (CAESALPINACEAE)

2.1 Introduction

Extracts from *Hymenaea courbaril* were weakly active in the mutant yeast assays indicative of possible anticancer activity. Initial work on this extract was carried out by Dr. Maged Abdel-Kader, who succeeded in isolating and partially characterizing (13*R*)-13-hydroxy-1(10),14-*ent*-halimadien-18-oic acid as the major active constituent. On Dr. Abdel-Kader's departure investigation of this extract was continued by the present author. Two additional diterpenes, (2*S*,13*R*)-2,13-dihydroxy-1(10),14-*ent*-halimadien-18-oic acid and 2-oxo-(13*R*)-13-hydroxy-1(10),14-*ent*-halimadien-18-oic acid, were isolated and characterized. The configurations of these compounds were determined by X-ray crystallography, circular dichroism, and NMR of anisotropic derivatives.

2.1.1 Previous Investigations of *Hymenaea* Species.

The *Hymenaea* genus is a member of the *Leguminosae* (bean) family; these plants are typically found in tropical South America and Africa. They have been investigated primarily for the oligo- and polysaccharides that can be isolated from the seeds.¹ A number of investigations have also focused on amber and other resins that originate from them.² Some medicinally oriented groups report investigating *Hymenaea* species for various activities such as inhibition of tyrosinase,³ 5-lipoxygenase,⁴ and testosterone-5- α -reductase⁵ enzymes.

¹ a. Tine, M.A.S.; Cortelazzo, A.; Buckeridge, M.S. *Rev. Bras. Bot.* **2000**, *23*, 413. b. Lima-Nishimura, N.; Quoirin, M.; Wollinger, W.; Kruger, O.; Sierakowaski, M.-R. *Nat. Polym. Compo. [Proc. Third Int. Symp. Workshop Prog. Prod. Process. Cellul Fibres Nat. Polym.]*, **2000**, 114. c. Chang, Y.K.; Silva, M.R.; Gutkoski, L.C.; Sebio, L.; Da Silva, M.A. *J. Sci. Food. Agric.* **1998**, *78*, 59.

² a. Martinez-Richa, A.; Vera-Graziano, R.; Rivera, A.; Joseph-Nathan, P. *Polymer*, **1999**, *41*, 743. b. Stankiewicz, B.A.; Poinar, H.N.; Briggs, D.E.G.; Evershed, R.P.; Poinar, G.O. jr. *Proc. R. Soc. Lond. Ser. B*, **1998**, *265*, 641.

³ a. Takagi, K.; Shimomura, K. *Fragrance J.* **2000**, *28*, 72. b. Takagi, K.; Shimomura, K.; Koizumi, Y.; Mitsunaga, T.; Abe, I. *Nat. Med. (Tokyo)*, **1999**, *53*, 15.

⁴ Braga, F.C.; Wagner, H.; Lombardi, J.A.; De Oliveira, A. *Phytomedicine*, **2000**, *6*, 447.

⁵ Sato, Y.; Kida, H.; Nakahayashi, Y.; Murasugi, S. *Jpn. Kokai Tokkyo Koho*, **2000** (patent application: JP 98-309395 19980925).

Various diterpenes have been isolated from a number of *Hymenaea* species such as *H. verrucosa*, *H. oblongifolia* and *H. parvifolia*;⁶ compounds **2.1-5** are representative examples of these diterpenes.

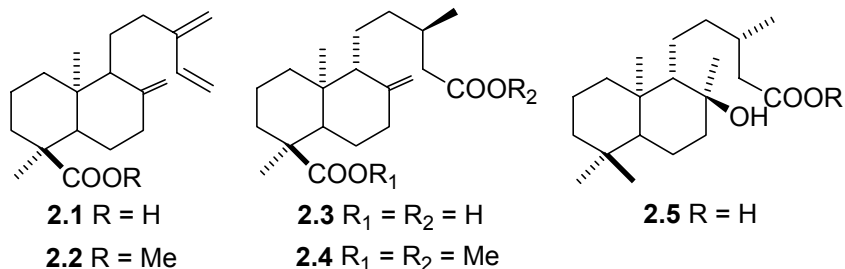


Figure 2-1. Diterpenes from *Hymenaea* species

2.1.2 Chemical Investigations of *Hymenaea courbaril*.

*H. courbaril*⁷ (also known as courbaril, jatoba, the kerosene tree, and the West Indian locust) is useful for its timber; it has been reportedly employed as an anodyne, antiseptic, astringent, expectorant, laxative, purgative, sedative, stimulant, and tonic in folk medicine.⁸ It is a widely distributed large tropical tree commonly found in South America. A selection of diterpenes (**2.6-9**) that have been isolated from the seedpods of this tree are shown below.⁹

⁶ a. Cunningham, A.; Martin, S.S.; Langenheim, J.H. *Phytochemistry*, **1973**, *12*, 633. b. Martin, S.S.; Langenheim, J.H. *Phytochemistry*, **1974**, *13*, 294.

⁷ Duke, J.A. *Handbook of Energy Crops* 1983 (unpublished). http://www.hort.purdue.edu/newcrop/duke_energy/Hymenaea_courbaril.html

⁸ Duke, J.A.; Wain, K.K; *Medicinal Plants of the World*; http://www.hort.purdue.edu/newcrop/duke_energy/Hymenaea_courbaril.html

⁹ a. Khoo, S.F.; Oehlschlager, A.C.; Ourisson, G. *Tetrahedron*, **1973**, *29*, 3379. b. Marsaioli, A.J.; Filho, H. de F. L.; Campello, J. de P. *Phytochemistry*, **1975**, *14*, 1882.

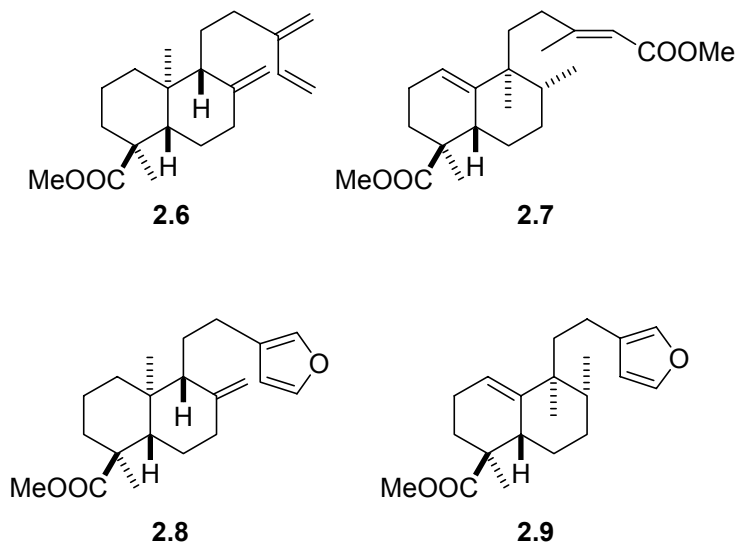


Figure 2-2. Diterpenes from *Hymenaea courbaril* (Caesalpinaceae).

Under an ICBG grant, Dr. Maged Abdel-Kader investigated *H. courbaril* (Caesalpinaceae) (extract M970379 and M980037). A dried methanol extract of this plant exhibited a positive response to the 1138 mutant yeast strain. Bioactivity-guided fractionation afforded a new diterpene identified as 13-hydroxy-1(10),14-*ent*-halimadien-18-oic acid (**2.10**) (Figure 2-3). The structure **2.10** was deduced from ^1H NMR, ^{13}C NMR, and MS data. The methyl ester **2.13** was also prepared; its spectral data were compared to those of the corresponding compound previously reported in the literature.

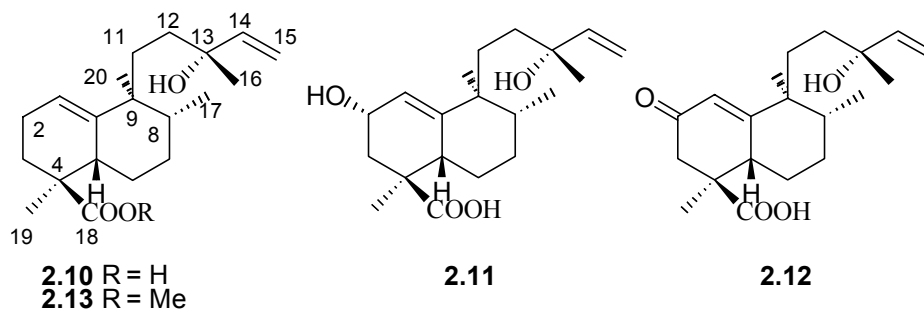


Figure 2-3. Diterpenes **2.10-12** from *Hymenaea courbaril*.

2.1.3 Previous Investigations of 13-Hydroxy-1(10),14-*ent*-halimadien-18-oic Acids.

13-Hydroxy-1(10),14-*ent*-halimadien-18-oic acid has not been previously isolated. Previous phytochemical studies have resulted in the isolation of the methyl esters of diterpenoid acids (**2.14-2.15**) from *Eupatorium turbinatum* and *Halimium viscosum*^{10,11} and a number of similar compounds from *H. courbaril*, **2.6-9**.⁹ The relative configuration of the ring system of **2.14** and **2.15** was determined by NMR. Semisynthesis and NMR studies were used to confirm the absolute stereochemistry at the C-13 position in compounds **2.14-15**, but this work did not permit the direct determination of the absolute stereochemistry of the ring system.

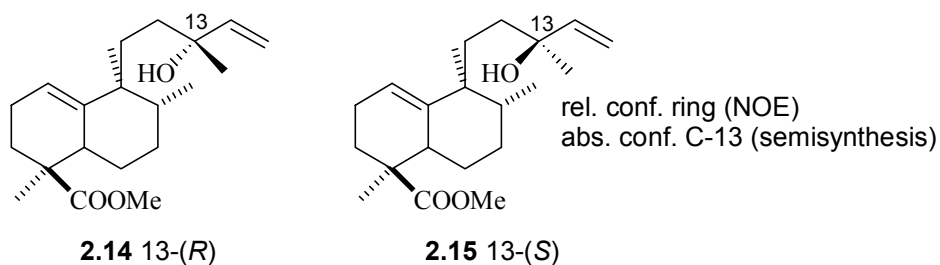


Figure 2-4. Isolated and Semisynthetic Diterpenes *Halimium viscosum*

Further stereochemical investigations were required to complete the unambiguous structural assignment of compound **2.10**, and additional quantities of the compound were required for these investigations. This chapter reports the re-isolation of (13*R*)-13-hydroxy-1(10),14-*ent*-halimadien-18-oic acid, the complete stereochemical characterization of this compound, and the isolation and characterization of two new diterpenes, (2*S*,13*R*)-2,13-dihydroxy-1(10),14-*ent*-halimadien-18-oic acid (**2.11**), and 2-oxo-(13*R*)-13-hydroxy-1(10),14-*ent*-halimadien-18-oic acid (**2.12**).

¹⁰ Jakupovic, J.; Ellmauerer, E.; Bohlmann, F.; Whittetori, A.; Gage, D. *Phytochemistry* **1986**, *25*, 2677.

¹¹ Urones, J.G.; Marcos, I.S.; Basabe, P.; Sexmero, M.J.; Carrillo, H.; Melchor, M.J. *Phytochemistry* **1994**, *37*, 1359.

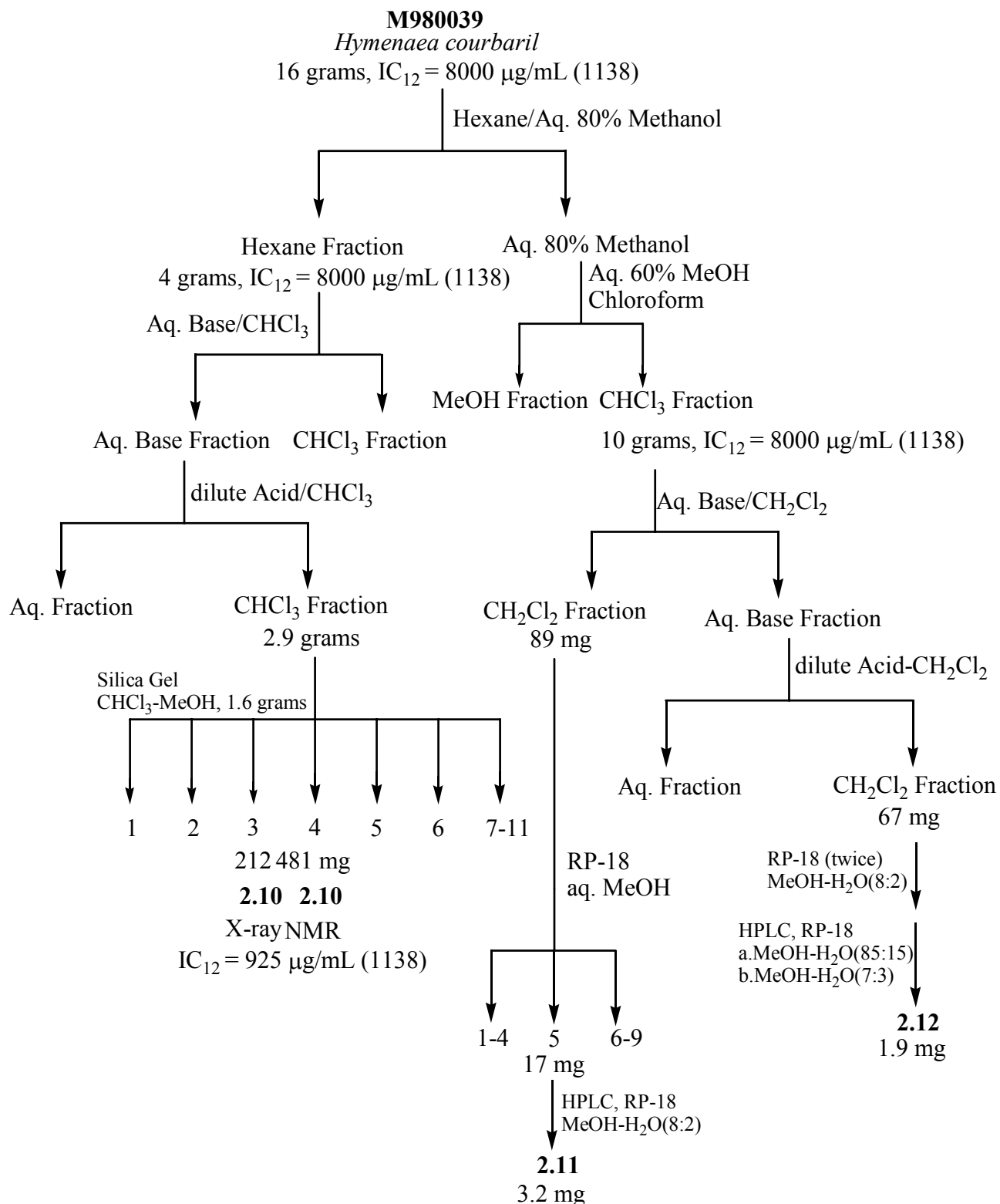
2.2 Results and Discussion.

2.2.1 Isolation of Ent-Halimadien-18-oic Acids from *H. courbaril* (Caesalpinaceae).

(13*R*)-13-Hydroxy-1(10),14-*ent*-halimadien-18-oic acid (**2.10**) (C₂₀H₃₂O₃) was isolated as indicated in Scheme 1. The methanol extract of *H. courbaril* was partitioned between hexane and MeOH-H₂O (8:2), and the aqueous layer was diluted with H₂O to MeOH-H₂O (6:4) and extracted with CHCl₃. Bioactivity testing with the 1138 yeast strain indicated that both the hexane and CHCl₃ fractions were active. Extraction of the hexane fraction with aqueous sodium bicarbonate followed by acidification and re-extraction with CH₂Cl₂ resulted in a diterpene-enriched extract. This extract was subjected to Si gel column chromatography with EtOAc-hexane as eluent to give eleven fractions. Removal of solvent from the third fraction gave a syrupy residue that slowly crystallized to yield good quality crystals of **2.10**. The re-isolated material was subjected to spectral analysis, to confirm it was the same as that isolated by Dr. Abdel-Kader. The negative ion FABMS of **2.10** (C₂₀H₃₂O₃) showed a major signal at *m/z* 319 (M-H)⁻. ¹H and ¹³C NMR data are shown in Table 3 and 4. APT, HMQC, and COSY experiments were in agreement with those reported by Dr. Abdel-Kader.

(2*S*,13*R*)-2,13-Dihydroxy-1(10),14-*ent*-halimadien-18-oic acid (**2.11**) (C₂₀H₃₂O₄) was isolated from the initial chloroform extract described above. This was redissolved in CH₂Cl₂ and extracted with aqueous sodium bicarbonate; the resulting chloroform-soluble fraction was purified by reverse phase column chromatography and reverse phase HPLC to yield 3.2 mg of **2.11**. Since compound **2.11** is acidic, it is presumed that extraction with bicarbonate was incomplete, allowing some of the compound to remain in the chloroform fraction.

The aqueous sodium bicarbonate extract described above was neutralized with dilute acid, the resulting aqueous solution extracted with dichloromethane, and the organic solvent evaporated. The resulting mixture of organic acids was subjected to reverse phase column chromatography and reverse phase HPLC to yield 1.9 mg of compound **2.12**.



Scheme 1. Isolation of Diterpenes from *Hymenaea courbaril* (Caesalpinaceae).

2.2.2 Characterization of Diterpenes from *Hymenaea courbaril* (Caesalpinaceae).

2.2.2.1 Structure of (13*R*)-13-Hydroxy-1(10),14-*ent*-halimadien-18-oic Acid (**2.10**).

(13*R*)-13-Hydroxy-1(10),14-*ent*-halimadien-18-oic acid was previously characterized by Dr. Maged Abdel-Kader by NMR and conversion to the methyl ester. This compound has not been previously reported, but three different methyl esters (**2.14**, **2.15** and **2.16**) were reported.^{10,11} Compounds **2.14** and **2.16** possessed identical ¹³C NMR data, although their optical rotations differed. Dr. Abdel-Kader characterized compound **2.10** by preparing the methyl ester and comparing its spectral data to those of the previously published esters. He prepared the methyl ester **2.13** from **2.10**; its ¹³C NMR data were in agreement with those of compounds **2.14** and **2.16** but not with the data for **2.15**.

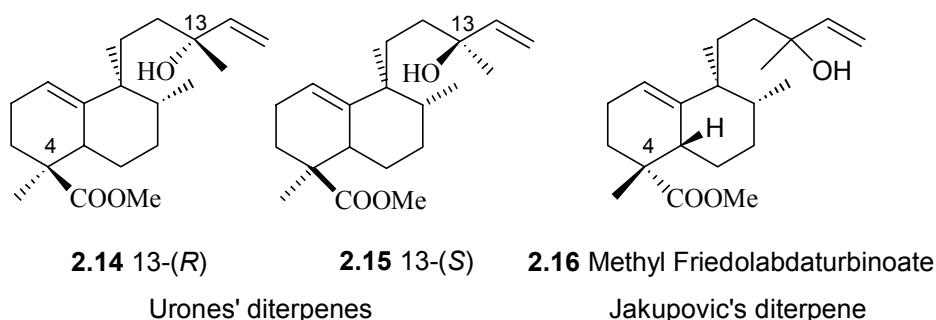


Figure 2-5. Previously Reported Methyl Esters

At this point Dr. Abdel-Kader returned to Egypt and the author assumed control of the project.

Further information was required to fully characterize compound **2.10** and **2.13**. The structures **2.14** and **2.16** were incomplete, in that they lacked full assignment of absolute and relative configurations. In addition, the optical rotation of **2.13** ($[\alpha]_D = +90.3^\circ$ in CHCl_3) did not agree with that of **2.14** ($[\alpha]_D = +26.7^\circ$ in CHCl_3) or **2.16** ($[\alpha]_D = -47^\circ$ in CHCl_3). For these reasons, additional investigations into the relative and absolute configurations of 13-hydroxy-1(10),14-*ent*-halimadien-18-oic acids were initiated.

NOE and GOESY spectra showed interactions between H-1 and H-2, H-1 and H-20, H-18 with H-3 α and H-5; additional experiments were run but other correlations were not seen. These results were not conclusive enough to determine relative stereochemistry. In particular, modeling experiments indicated that the distance between H-18 and H-5 was short enough to permit an NOE interaction with any configuration. Additionally, the absence of a correlation between H-5 and H-20 or H-17 did not adequately indicate the stereochemistry at the C-5 position.

The structure of **2.10** was confirmed and its relative stereochemistry established unambiguously by an X-ray crystallographic structure determination (Figure 2-6, acquired by Dr. Carla Slebodnick). On this basis we have assigned the stereochemistry as that in Figure 2-3.

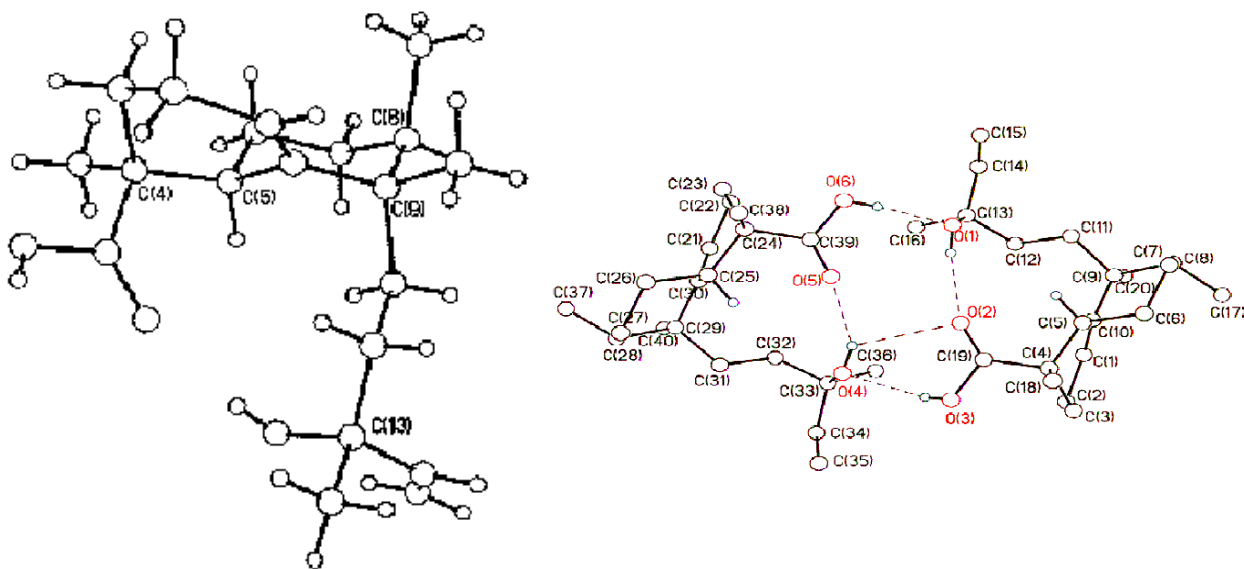


Figure 2-6. ORTEP Diagrams of **2.10**.

2.2.2.2 The Structure of (2*S*,13*R*)-2,13-Dihydroxy-1(10),14-*ent*-halimadien-18-oic Acid (**2.11**).

The negative ion FABMS of **2.11** showed major fragment ions of m/z 335 (M-H)⁻, 318 (M-H₂O)⁻ and 290 (M-HCO₂H)⁻. The positive FABMS did not show a molecular ion, but a sodiated ion at m/z 341 (M-H₂O+Na)⁺ and major fragment ions at 318 (M-H₂O)⁺ and 301 (M-H₂O-OH)⁺ were observed. These data, together with the ¹³C NMR/APT data were consistent with the composition C₂₀H₃₁O₄.

Its ¹H NMR spectrum clearly showed four olefinic proton signals (δ 5.94, 5.82, 5.14 and 4.99), an allylic proton signal (δ 2.22) and four methyl peaks (δ 1.20, 1.18, 0.92 and 0.83). The spectrum was quite similar to that of **2.10**; however H-2 was shifted downfield to δ_{H} 4.76 compared with δ_{H} 2.05 in **2.10**. COSY and DQF-COSY spectra confirmed the assignments of H-2 (correlated with H-1), H-3 (correlated with H-2), H-6 α and β (correlated with H-5), H-8 (correlated with H-17), H-11b (correlated with H-11), H-12a and H-12b (correlated with H-11a and H-11b). The assignments of H-11 were determined from comparison to those of **2.10**. The ¹³C NMR spectrum of **2.11** was very similar to that of **2.10**, with the exception of the C-1, C-2, C-3 and C-10 positions whose shifts were those expected for an allylic alcohol. HMQC was useful for assigning H-7 α and H-7 β (C-7, δ 29.1), H-11a and H-11b (C-11, δ 32.0) along with the remaining carbons.

1D NOE and GOESY spectra showed interactions between H-1 and H-2, H-1 and H-20, and H-18 with H-3 α and H-5. The stereochemistry of the C-2 position was determined by homonuclear decoupling of the C-1 proton; the J values of the C-2 proton were determined to be 4.5 and <1.0 Hz. These results were indicative of equatorial-axial and equatorial-equatorial interactions with the C-3 protons; taking into account the X-ray structure of **2.10** and the use of a model kit, these data assigned the configuration at C-2 as α -OH. On the basis of this information, the similarity to **2.10**, literature and biosynthetic considerations we have assigned the structure and relative configuration as that in Figure 2-3.

2.2.2.3 The Structure of (13*R*)-13-Hydroxy-1(10),14-*ent*-halimadien-18-oic Acid (**2.12**).

The negative ion FABMS of **2.12** showed major fragment ions of m/z 333 ($(M-H)^+$)⁻ and 290 ($(M-CO_2H)^+$)⁻. The positive ion FABMS did not show a molecular ion; instead a sodiated ion (m/z 357) was observed, along with a major fragment of m/z 317 ($(M-OH)^+$)⁺. The high resolution mass spectra revealed a signal corresponding to m/z 333.2042 (Cal. For C₂₀H₂₉O₄: 333.2066). These results and the ¹³C NMR/APT spectra indicate that compound **2.12** had a composition of C₂₀H₂₉O₄. The IR spectrum confirms the presence of an α,β -unsaturated ketone (1658 cm⁻¹). Its ¹H NMR spectrum clearly showed signals for four olefinic protons (δ 5.83, 5.71, 5.16, and 4.99), an allylic proton (δ 3.17), and four methyl peaks (δ 1.25, 1.18, 0.98, and 0.81); the spectrum was quite similar to that of **2.10** and **2.11** indicative of only a minor structural difference. The H-1 olefinic proton in **2.12** was a sharp singlet compared to a broad singlet in **2.10** or a doublet in **2.11**; the H-5 proton was also shifted downfield (δ_H 3.18) compared to that of **2.10** (δ_H 2.64). ¹H COSY, DQF COSY and *J*-coupling measurements along with comparison to **2.10** were used to assign H-3 α and β (¹H-¹H COSY, *J*=15.8 Hz), H-6 (¹H-¹H COSY with H-5), H-7 (¹H-¹H COSY with H-6), H-8 (¹H-¹H COSY with H-17), H-11 α and 11 β (¹H-¹H COSY with COSY, *J*=12.6 Hz), and H-12 α and β (¹H-¹H COSY with H-11). The ¹³C NMR spectrum of **2.12** (see Table 4) was very similar to that of **2.10** with the exception of the C-1, C-2, and C-10 positions, whose shifts (δ 124.3, 201.5, 172.7) were those expected for an α,β -unsaturated ketone. HMQC also helped to identify H-3 α and H-3 β (C-3, δ 41.9), H-11 and H-11' (C-11, δ 33.0) and C-5 (δ 44.1).

NOESY and 1D NOE experiments indicate interactions of H-1 with H-20, H-8 with H-20, H-7 β with H-17, H-15b with H-17, and H-5 with H-7 α ; these interactions, the absence of other significant interactions, literature, biosynthetic considerations and the agreement of the NOE information with the crystal structure of **2.10** leads us to assign the structure and relative configuration of **2.12** as that in Figure 2-3.

2.2.3 Determination of the Absolute Configurations of the (13*R*)-13-Hydroxy-1(10),14-*ent*-halimadien-18-oic Acids.

2.2.3.1 Circular Dichroism of the (13*R*)-13-Hydroxy-1(10),14-*ent*-halimadien-18-oic Acids.

Left and right hand circularly polarized light pass through a chiral medium at different speeds and with different absorbances; thus circular dichroism can provide additional confirmation of the absolute configurations of chiral molecules.¹² These absorbance changes are called Cotton effects.

CD spectra can be explained through two theories: the octant rule and the exciton chirality method. The exciton chirality method (originally the “dibenzoate chirality method”) was first employed by Mason¹³ to determine the absolute configuration of organic compounds; it has been promoted primarily through the work of Nakanishi and coworkers.¹⁴ When two chromophores are close enough to each other, their electronic moments interact with each other. These interactions result in a splitting of the observed excited states (into more stable and less stable states) (Figure 2-7). These interactions are dependent on distance ($1/R^2$), chromophore (λ , ϵ , and μ) projected angle (maximum around 70°), and chirality. Circular dichroism can detect the splitting of states that are typically observed in the ultraviolet range (π to π^* transitions). Chromophores need not be identical. This method is typically used to determine the absolute configuration of 1,2 diols; the diols are converted into benzoate chromophores followed by CD measurement.

Empirical models have been developed to predict absolute configurations (Figure 2-7) based on Newman projections. Those projections that possess a clockwise relationship between the nearer chromophore and the further chromophores (no matter which way they are visualized)

¹² For a good review see: *Circular Dichroism Principles and Applications* (K.Nakanishi, N.Berova, R.W.Woody eds.), **1994**, VCH Publishers, New York, New York, USA.

¹³ Mason, S.F. *J. Chem. Soc. Chem. Comm.* **1963**, 239.

¹⁴ Harada, N.; Nakanishi, K. *J. Am. Chem. Soc.* **1969**, *91*, 3989.

will display “positive chirality”. Similarly, those projections that possess a counterclockwise relationship between the two chromophores will display “negative chirality”.

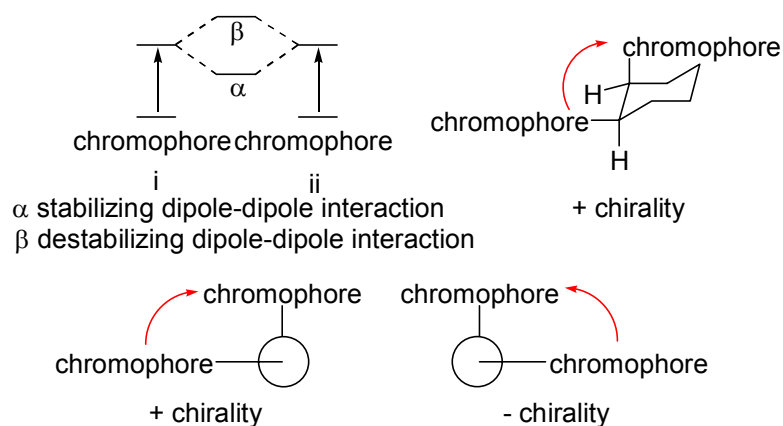


Figure 2-7. The Exciton Chirality Method

CD spectra were acquired for compounds **2.10**, **2.11** and **2.12**. The CD spectrum of **2.10** showed “positive chirality”; this occurs when a single positive Cotton effect exists at a higher wavelength along with the presence of a single negative Cotton effect at a lower wavelength. The reverse of this is “negative chirality”.

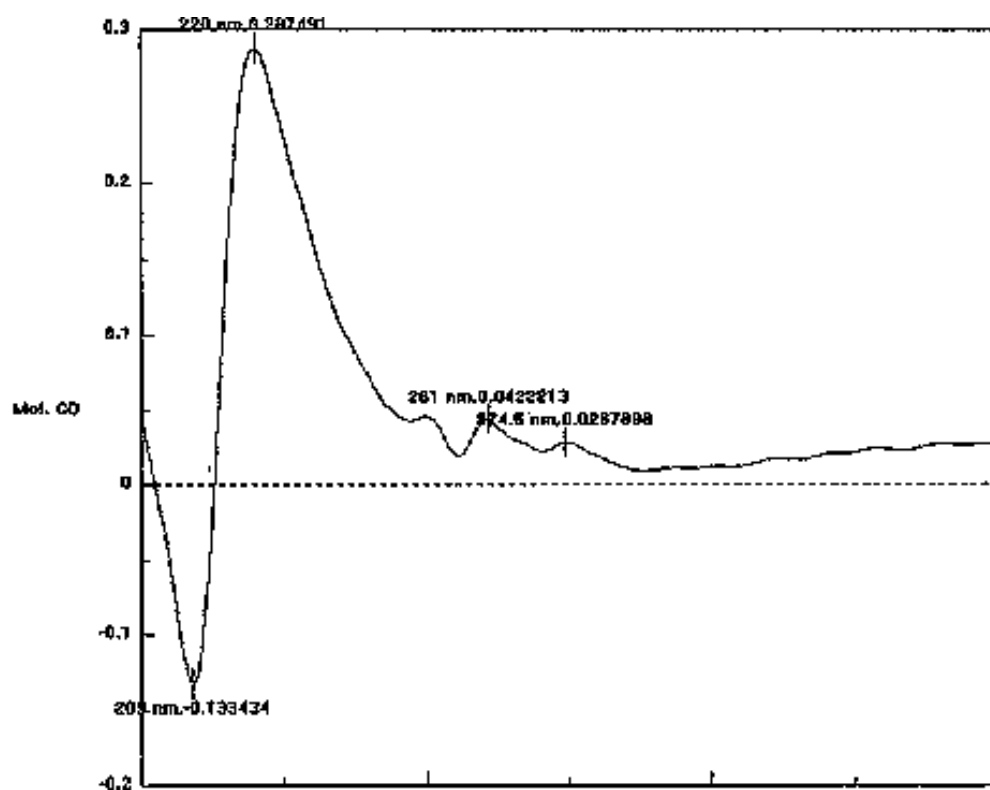


Figure 2-8. Circular Dichroism Spectrum of 2.10.

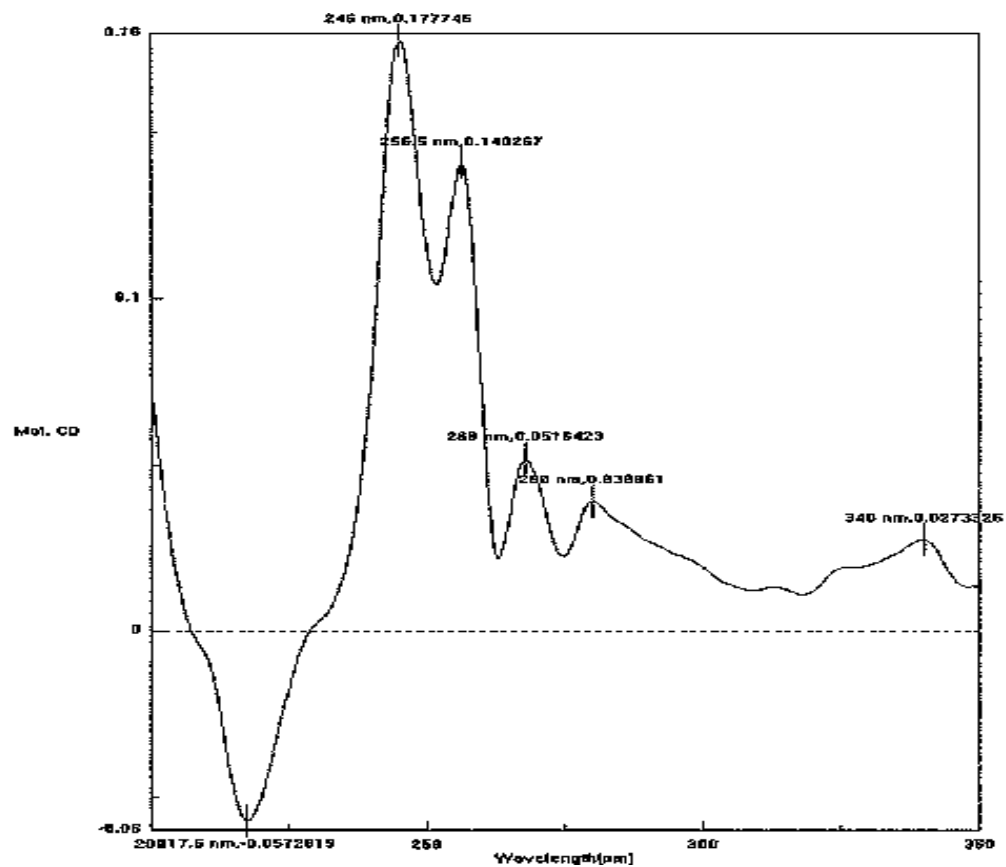


Figure 2-9. Circular Dichroism Spectrum of 2.11.

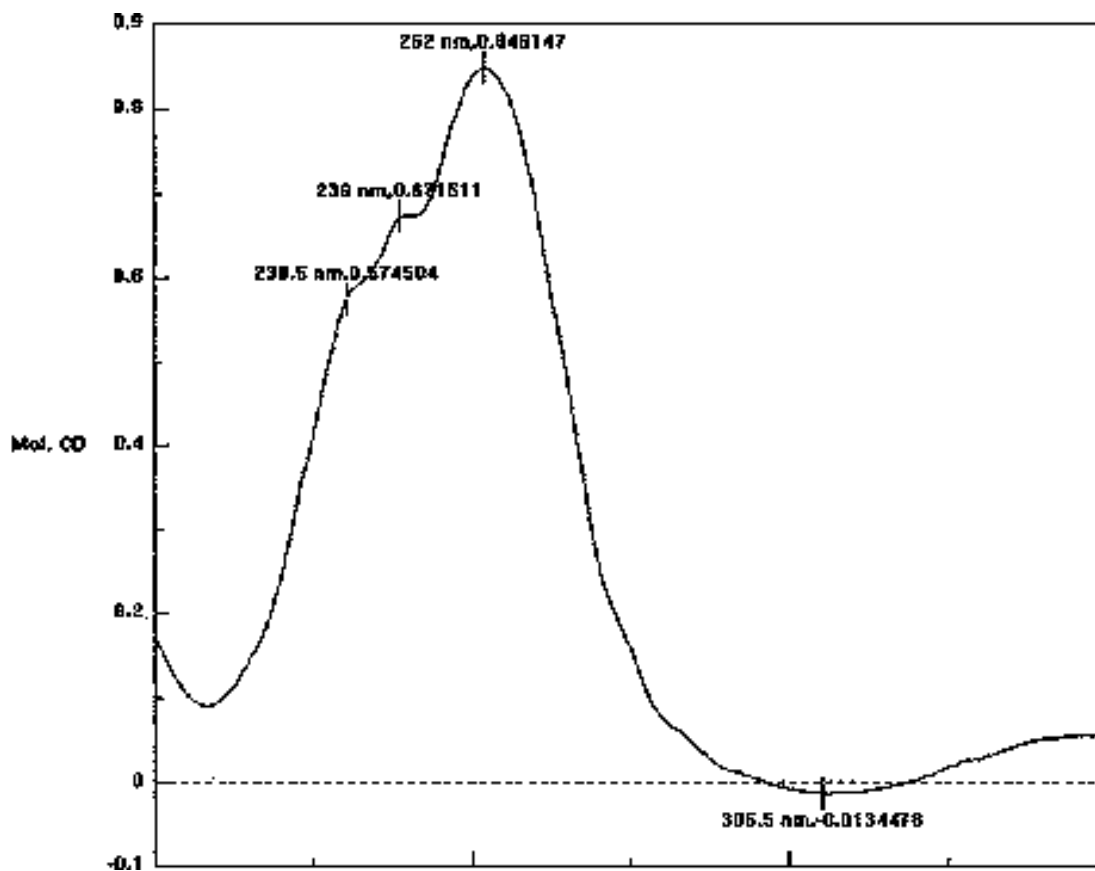


Figure 2-10. Circular Dichroism Spectrum of **2.12**.

CD can determine the absolute configuration of allylic alcohols such as **2.11**; the method is essentially a modification of the commonly employed exciton theory. Both cyclic and acyclic allylic alcohols can be determined by this method. The exciton method requires that a molecule contain two strong chromophores; the stereochemical relationship of the two chromophores will determine the sign of the Cotton shift. For allylic alcohols, the method requires the addition of a second chromophore: a benzoate (chromophore) derivative was synthesized which then had an exciton interaction with the allylic double bond (the nearest chromophore).¹⁵ The use of the benzoate derivative was advantageous for two reasons: it has a large ϵ (which should lead to

¹⁵ a. Harada, N.; Iwabuchi, I.; Yokota, Y.; Hisashi, U.; Nakanishi, K. *J. Am. Chem. Soc.* **1981**, *103*, 5590. b. Gonnella, N.C.; Nakanishi, K.; Martin, V.S.; Sharpless, K.B. *J. Am. Chem. Soc.* **1982**, *104*, 3775.

better amplitudes) and known electronic transitions (230 nm). Other Cotton effects should then be minimized (although these CD's still tend to be complicated). It is unlikely that the C-13 alcohol would undergo esterification; previous esterifications resulted in either no reaction or elimination and neither result would interfere with the results.

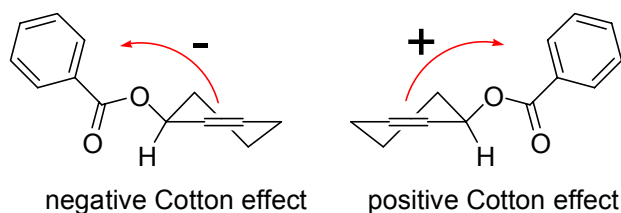


Figure 2-11. Empirical Model for Predicting Absolute Configuration of Allylic Alcohols

Although only a small quantity of **2.11** was available, the strong chromophoric ability of the benzoate made this method practical at the sub-microscale level. The benzoate ester was prepared from the reaction of 140 μg of **2.11** with benzoyl chloride in pyridine. The products were not purified after workup, since neither the achiral side products nor unreacted starting materials would significantly interfere with the results. The products were dissolved in methanol, filtered, and the CD spectrum of the resulting mixture measured. The mixture gave a complicated CD with many negative Cotton effects. The negative Cotton effect at 238 nm, when compared to the reported empirical model, clearly indicated that the absolute configuration about C-2 is *S*.

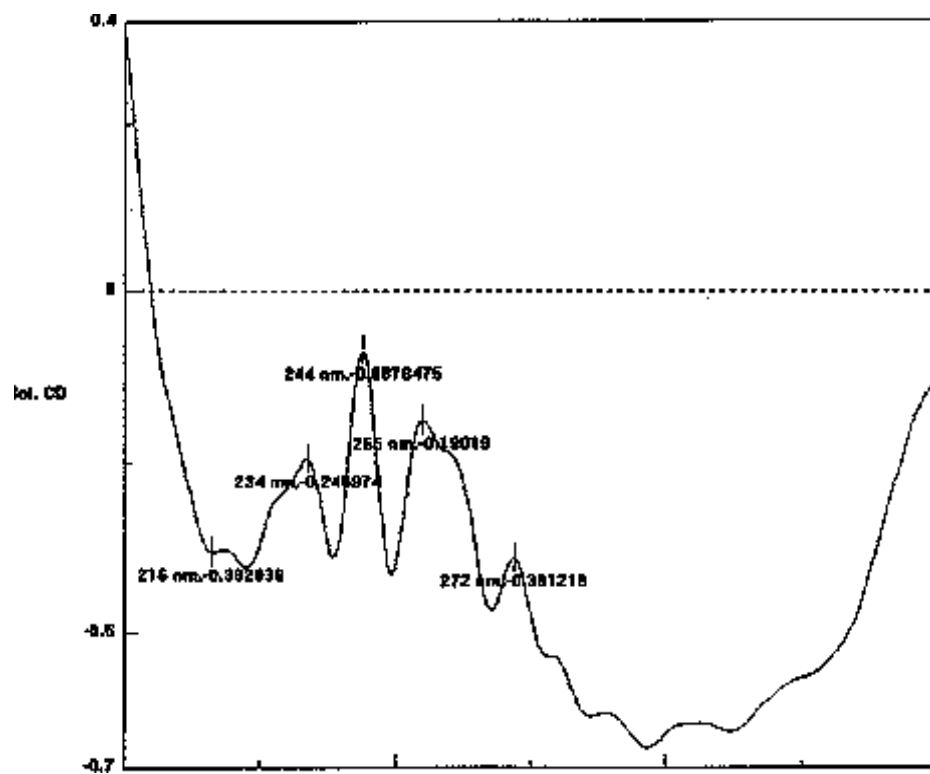


Figure 2-12. Circular Dichroism Spectrum of the Benzoyl Derivative of 2.11.

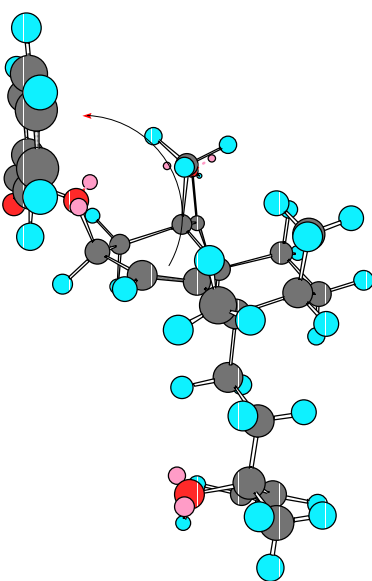


Figure 2-13. Negative Cotton Effect for the Prepared Benzoate Ester

This result permitted us to assign the absolute configuration of **2.11** (*2S,13R*)-2,13-dihydroxy-1(10),14-*ent*-halimadien-18-oic acid.

The CD of **2.12** showed a positive Cotton effect. The absolute configuration of cyclic ketones can be determined by an empirical method called the octant rule; the octant rule is an outgrowth of the old α -haloketone rule of circular dichroism.¹⁶ The geometry of a molecule contributes positively or negatively to the Cotton effect. The expected sign of the Cotton effect can be determined by projecting the molecule (in the desired stereochemistry and conformation) into a three dimensional box of eight octants; more typically, the molecule is instead projected on an xy plane of quadrants, with the carbonyl bond centered on the origin. Any atom in a quadrant (octant) contributes either positively or negatively depending on the sign of the quadrant (octant). Either of these models can then be used to determine the expected sign of the Cotton effect.

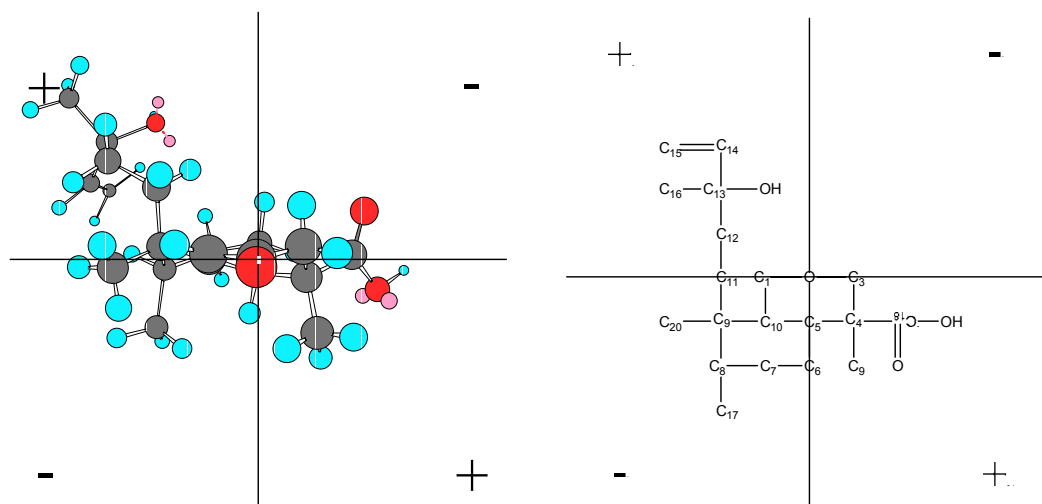


Figure 2-14. Projection of **2.12** into Positive and Negative Contributing Quadrants.

Figure 2-14 shows a single example of **2.12** projected onto the xy plane. The negative contributions cancel out much of the positive contributions (those atoms along an axis do not

¹⁶ Moffitt, W.; Woodward, W.B.; Moscovitz, A.; Klyne, W.; Djerassi, C. *J. Am. Chem. Soc.* **1961**, *83*, 4013.

contribute) except for the side chain. Figure 2-14 shows that the side chain contributes positively; this expectation matches that of the measured CD. All possible stereochemical configurations of **2.12** were drawn in the molecular modeling software Chem-3D. Basic MM2 minimizations were performed and the signs of the expected CD's determined. From these results, it was apparent that the greatest contribution of the sign of the Cotton effect was dependent solely on the configuration at C-9 (the orientation of the side chain). These results indicate the configuration of C-9 is *R*; thus the absolute configuration of **2.12** is 2-oxo-(13*R*)-13-hydroxy-1(10),14-*ent*-halimadien-18-oic acid.

2.2.3.2 Additional Literature Confirmation of the Absolute Configurations of (13*R*)-13-Hydroxy-1(10),14-*ent*-halimadien-18-oic Acids.

Subsequent to the completion of the major portion of this work, a paper was published by Marcos et al.¹⁷ This paper reported an independent investigation into the stereochemistries 13-hydroxy-1(10),14-*ent*-halimadien-18-oic acid methyl esters. *Ent*-halimic acid (**2.17**), which can be prepared from **2.14** or **2.15**,¹⁸ was converted into the chiral lactone **2.18**. The relative configuration of **2.18** was determined by X-ray crystallography. The absolute configuration of the chiral lactone was determined by circular dichroism.

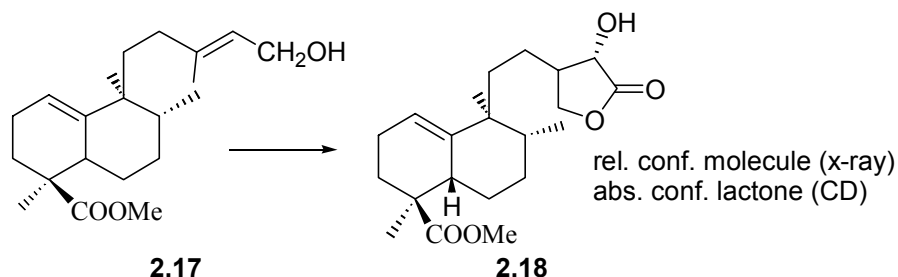


Figure 2-15. Previously Reported Semisynthesis for Determination of Stereochemistries of *Ent*-Halimadien-18-oic Acids and Esters.

¹⁷ Marcos, I.S.; Gonzalez, J.L.; Sexmero, M.J.; Diez, D.; Basabe, P.; Williams, D.J.; Simmonds, M.S.J.; Urones, J.G. *Tetrahedron Letters*, **2000**, *41*, 2553.

¹⁸ Urones, J.G.; Pascual Teresa, J. de; Marcos, I.S.; Diez, D.; Garrido, N.M.; Guerra, R.A. *Phytochemistry*, **1987**, *26*, 1077.

This paper established the stereochemistries of the 13-hydroxy-1(10),14-*ent*-halimadien-18-oic acid methyl esters. The reported results are in agreement with the circular dichroism results reported earlier.

2.2.3.3 Validation of a New NMR Method for Stereochemical Determination of Carboxylic Acids.

The X-ray structure (Figure 2-6) unambiguously assigned the relative stereochemistry of compound **2.10**. Biosynthetic considerations and the spectral agreement of compounds **2.11** and **2.12** to **2.10** permit us to assign the relative stereochemistries of **2.11** and **2.12**. The absolute configuration of 13-hydroxy-1(10),14-halimadien-18-oic acids was determined by circular dichroism spectra of **2.11** and **2.12**, and recent literature has confirmed this absolute configuration.

The availability of compound **2.10** with a known absolute stereochemistry and an α,α,α -trisubstituted acetic acid functionality provided an opportunity to determine whether or not Kusumi's method for determining the absolute stereochemistry of carboxylic acids can be applied to this type of functionality.

The use of chiral derivatizing agents for the determination of absolute chemistry is a well-established structural tool, and the Mosher's ester reagents for secondary alcohols are perhaps the more widely used reagents of this type.¹⁹ Recently similar reagents were developed by Kusumi and his co-workers for the stereochemical analysis of chiral carboxylic acids; the reagents are (*R*) and (*S*)-phenyl glycine methyl esters which can form amides with chiral carboxylic acids.²⁰ These amides act in a similar fashion to Mosher's esters in ¹H NMR, since the phenyl ring can induce the shifting of proton resonances by an anisotropic effect; these effects are geometrically dependent. NMR analysis of the diastereomeric amides can then be

¹⁹ a. Dale, J.; Mosher, H. *J. Am. Chem. Soc.* **1973**, *95*, 512. b. Trost, B.M.; Belletire, J.L.; Godleski, S.; McDougal, P. G.; Balkovec, J.M.; Baldwin, J.J.; Christy, M.E.; Ponticello, G.S.; Varga, S.L.; Springer, J.P. *J. Org. Chem.* **1986**, *51*, 2370.

²⁰ a. Nagai, Y.; Kusumi, T. *Tetrahedron Lett.* **1995**, *36*, 1853. a. Yabuuchi, T.; Kusumi, T. *J. Org. Chem.* **2000**, *65*, 397.

used to determine the absolute configuration of the acid. Determination of absolute confirmation is performed by calculating the ^1H NMR shift differences between those of the (*R*)-PGME isomer and those of the (*S*)-PGME isomer; these results can then be compared to an established empirical model.

While Kusumi's method has been validated for α,α -disubstituted acetic acids, α,α -disubstituted, α -hydroxy acetic acids, and β,β -disubstituted propionic acids, this method in principal can be applied to any carboxylic acid as long as the investigator is fully aware of the conformation of the PGME amides under NMR conditions. These conformations must be determined before absolute configuration determination by NOE and other experiments. Since **2.10** was a carboxylic acid it provided a test of the applicability of this method to α,α,α -trisubstituted acetic acids. Kusumi's PGME analysis assumes that the amide is in a *syn* coplanar conformation (**2.19**); however there are potentially four basic conformations the PGME amide functionality could possess: the *syn*, the *anti*, and two *gauche* (+ and -) forms (**2.19-2.22**). For the purpose of distinguishing between the forms, the dihedral angle was defined as $\text{C}^{18}\text{-C}^4\text{-C}^{19}\text{-N}$.

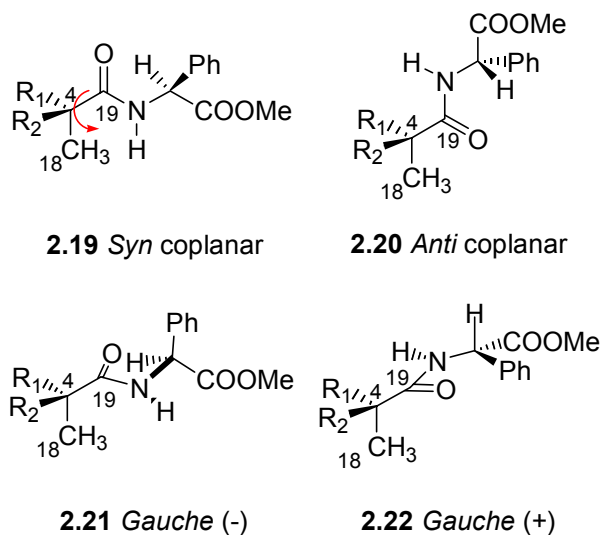


Figure 2-16. Potential Conformations of the (*R*)-PGME Amide of **2.10**.

The amide bond itself (O-C¹⁹-N-H) has been established to be a planar 180° dihedral angle.

Molecular modeling was used to determine the possible conformations of the (*R*) and (*S*) PGME amides of **2.10**. (*R*) and (*S*)-PGME amides were prepared by coupling (*R*) and (*S*) PGME with **2.10** using PyBOP/1-HOBT. NOESY, NOE, and GOESY experiments were used to confirm the conformations. The confirmed conformations were then used to construct a model which was used to interpret the shift data of the (*R*) and (*S*) PGME amides and determine the absolute configuration of **2.10**.

(*R*) and (*S*) PGME structures were modeled on Cambridge Soft Chem3D[®] software.²¹ and minimized with an MM2 force field under gas phase conditions. Numerous modeling experiments indicated that the *syn* conformation was disfavored, but that two *gauche* and the *anti* form were present.

NOE, NOESY, and GOESY experiments were performed to determine the conformations of the PGME amides of **2.10**. These experiments confirmed that the *syn* conformation was not present. This was seen by the fact that the N-H proton has a strong NOE correlation with the H-11A proton, which would be impossible if the compound was in the *syn* conformation. This result indicated that the amide was either not in the *syn* conformation or that this conformation is present only as a minor conformer.

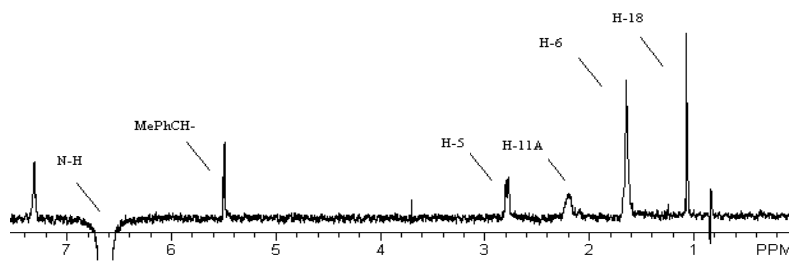


Figure 2-17. NOE Evidence for the Presence of a *Gauche* (+) Conformation.

²¹ Cambridgesoft Corporation, 875 Massachusetts Ave., Cambridge, MA 02139

The experiments indicated that the conformations in solution resemble that of the *gauche* (+) conformer (**2.22**). All three conformers would observe an NOE correlation to H-5 (correlation not shown for better visibility). The *anti* conformer (**2.20**) would not have a correlation with a H-18 proton nor a correlation with the H-6 proton; those protons have been calculated to be too far away by molecular modeling. Similarly the *gauche* (-) conformer would not have a correlation with a H-6 proton nor a correlation with the H-11 proton. The *gauche* (+) structure (**2.22**) did fit the NOE data.

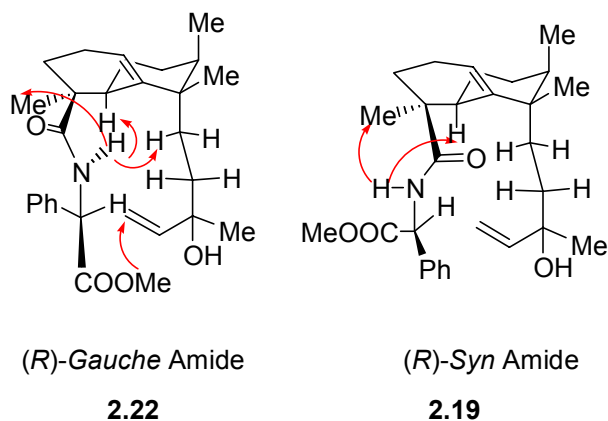


Figure 2-18. NOE Evidence of a *Gauche* (+) Conformation
(*R*)-PGME Amide of **5.10** Shown.

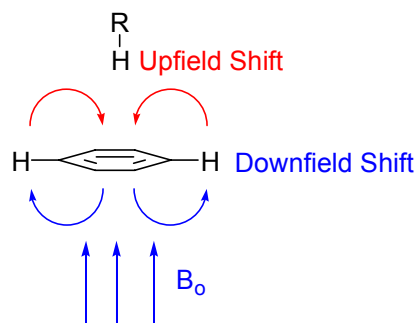
The NOE data for the (*S*)-PGME amide of **2.10** also indicated a *gauche* (+) conformation defining the amide dihedral angle ($C^{18}-C^4-C^{19}-N$).

It was apparent that the energies determined by the modeling program were not in agreement with the data provided by the NOE experiments; in particular, the software predicted the *anti* conformer for the (*R*)-PGME amide (**2.20**) to be the predominant conformer whereas NOE data indicates that a *gauche* conformer is present in solution. Therefore, the conformations determined by the molecular modeling were only used to elucidate NOE data, not to establish the conformations by themselves.

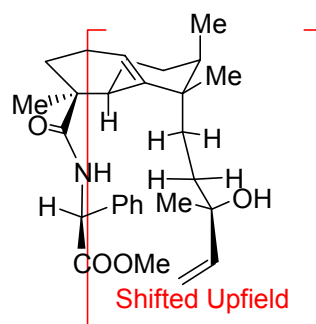
The dihedral angle ($C^{18}-C^4-C^{19}-N$) is not the only dihedral angle significant for anisotropic effects. The orientation of the phenyl ring (defined as dihedral angle $C^{19}-N-C-Ph$) was also investigated. This orientation was determined by NOESY on the (*R*)-PGME amide of **2.10**. A weak NOE interactions by the methoxy group and the absence of expected interactions by the phenyl ring with the olefin side chain indicated that structure **2.22** best represents the conformation of the (*R*)-PGME amide. This conformation was in agreement with the conformation reported by Kusumi. The same evidence for the conformation for the (*S*)-PGME amide of **2.10** was also observed by NOE.

Molecular modeling and NOE results indicate that the phenyl ring prefers to be oriented such that the “face” is orientated towards the molecule as opposed to an “edge” oriented towards the molecule. This is probably due to the local minimization requirements of the $NH-C-Ar-Ar$ dihedral angle, the steric crowding in the “center” of the molecule and in some conformations pi-pi interactions between the phenyl ring and the side chain double bond. This orientation is important because it determines the type of anisotropic contributions of the phenyl ring to 1H NMR shifts (**5.36**).

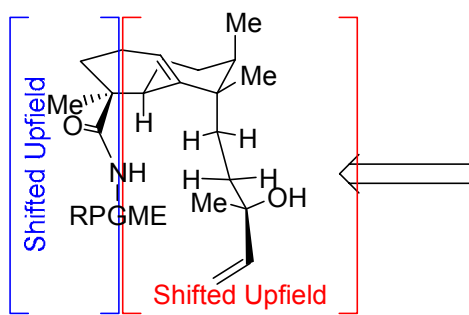
Once the conformations of the (*R*) and (*S*) PGME amides have been determined a model can be constructed to determine the absolute configuration of the molecule. It is the phenyl ring in the PGME amides that is responsible for inducing anisotropic shifts on the rest of the molecule (**5.34**). This is due to the magnetic field induced by aromatic systems which typically results in the downfield shifts of aromatic protons; for those protons oriented towards the ‘face’ of a phenyl ring, however, an upfield shift will occur. Structures **2.24** and **2.25** predict the shift differences due to the anisotropic of the phenyl ring in the (*R*) and (*S*) amides. The easiest way to quantify this data is to represent as a shift difference: $\delta_H (S) - (R)$.



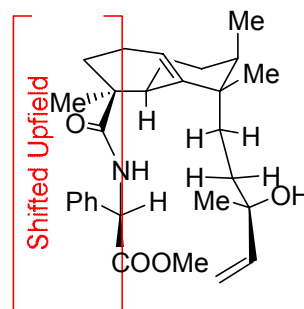
2.23 Anisotropic Shifts



2.24 (*S*)-Gauche Amide
(Subtract)



2.26 Predicted shifts for $\delta(S)-(R)$.



2.25 (*R*)-Gauche Amide

Figure 2-19. Anisotropic Effects and Predictive Model.

The model (2.26) predicts protons on the “right” side of the structure would possess negative shift differences whereas those protons on the “left” would possess positive shift differences. The ^1H NMR shift differences from the PGME amides for **5.10** are shown in Figure 2-20.

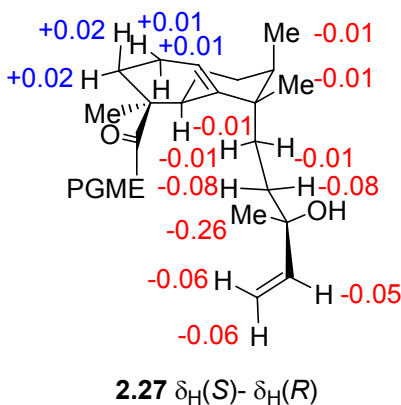


Figure 2-20. ^1H NMR Differences of (*R*) and (*S*)-PGME Derivatives of **2.10**.

The larger shifts of the side chain protons compared to the ring protons merely indicates that those protons are closer to the face of the anisotropic phenyl group than the ring protons; this was further evidence of the *gauche* conformation. Since anisotropic effects are distance dependent, if the PGME side chain was in a *syn* coplanar arrangement we would have expected the H-3, H-5, and H-6 protons to have the largest shift magnitudes and the side chain to have the smallest shift magnitudes.

These results using PGME as a chiral derivatizing agent are in agreement with other results. These results and the agreement of the spectral data with those of the reported methyl ester **2.13**, published literature, and circular dichroism spectra for **2.11** and **2.12** are sufficient to establish the absolute configuration of **2.10** as 13(*R*)-13-hydroxy-1(10),14-*ent*-halimadien-18-oic acid.

These NMR results are not completely conclusive in and of themselves. Since the energies from the modeling results were not in agreement with the NOE results, we could not use the structures for predictions when NOE confirmation was lacking, such as the orientation of the phenyl ring. Slight changes in the orientation of the phenyl ring could have drastic changes to

the anisotropic shifts, leading to a completely different predictive model. Kusumi's method was never validated for α,α,α -trisubstituted acetic acids or for compounds with such complex and flexible conformations but investigations such as these are important for determining future applications for such analytical tools.

2.2.4 *Biological Evaluation of the 13-Hydroxy-1(10),14-Ent-Halimadien-18-oic Acids.*

Compound **2.10** was found to be weakly active in the 1138 mutant yeast strain ($IC_{12}=925$ $\mu\text{g/mL}$) and the A2780 human ovarian cell line ($IC_{50}>40$ $\mu\text{g/mL}$); however the activities are far from sufficient to warrant further investigation. PGME amides of **2.10** showed no activity in the mutant yeast strains. Compound **2.11** displayed no activity in the A2780 assay.

2.3 **Experimental Section.**

General Experimental Procedures. Melting points were determined on a Thermolyne apparatus equipped with microscope. IR spectra were taken on a Midac M-Series FTIR. FABMS spectra were obtained on a Fisons VG Quattro instrument. NMR spectra were taken on either JEOL Eclipse instrument at 500 MHz for ^1H NMR and 125 MHz for ^{13}C NMR or a Bruker Aspect Instrument at 360 MHz for ^1H NMR and 90 MHz for ^{13}C NMR. All J -coupling values were measured, not calculated. Thin layer chromatography was performed on Whatman MKC₁₈F Reverse Phase and EM Science Silica Gel 60 F₂₅₄ TLC plates; visualization was performed by spraying with a vanillin/sulfuric acid mixture followed by heating. MM2 minimizations were performed on Chem3D from CambridgeSoft Corporation (875 Massachusetts Ave., Cambridge, MA 02139) assuming gas phase conditions.

Plant Material. The leaves, stems, and twigs of *Hymenaea courbaril* (*Caesalpinaceae*) were collected near Asindopo village in central Suriname in July 1997 and January 1998. Voucher specimens are deposited at the National Herbarium of Suriname, Paramaribo, Suriname.

Extract Preparation. The plant samples were dried, ground, and extracted with EtOAc to give extracts E970379 and E980037 and then with MeOH to give extracts M970379 and M980037.

Mutant Yeast Strain Bioassays.²² The mutant yeast strains 1138, 1140, and 1353 were acquired from Bristol-Myers Squibb and cultured (48 h, 30 °C) to stationary phase in YEPD (yeast extract, peptone, dextrose) broth. Media was prepared from 500 mL of deionized water, 5 g of Difco (autolysed cell) yeast extract, 10 g of peptone (Glystate™ pancreatic digest of gelatin), (10 g of graduated agar for plates), and 10 g of dextrose. The solution was heated until clear (almost boiling). The media was then dispensed into Erlenmeyer flasks: 50 mL portions dispensed for liquid (shake) cultures or 46 mL dispensed for plates. The flasks are covered then autoclaved for 20 minutes. After removal from the autoclave and cooling, the flasks are transferred to a sterile hood. One mL of the cell suspension is transferred to the shake flasks or transferred to the plates (100 mm by 100 mm). The media is allowed to solidify on the uncovered plates and the plates are then subjected to 30 seconds of UV radiation followed by covering. Two mL of cell culture are then transferred to each of the plates, followed by removal of excess inoculum; the plates were then allowed to dry. Wells (6-7 mm) are cut into the plates and diluted samples (in 1:1 DMSO:MeOH) were added to the wells in 100- μ L aliquots. The plates were incubated at 30 °C for 36-48 h using Nystatin (20 μ g/mL) as a positive control. The resulting zones of inhibition were measured in millimeters. As necessary, a dose-response was determined (extrapolating two concentrations that bracket a 12 mm response) and reported as an IC₁₂ (the dose required to produce a zone of inhibition 12 mm in diameter). Extract M970379 gave an IC₁₂ value of 2000 μ g/mL against the 1138 strain, and extract M980037 gave IC₁₂ values of 8000 μ g/mL against the 1138 strain.²³

Sc-7 Yeast Bioassay. The Sc-7 mutant yeast assay was performed as follows.²³ The *Saccharomyces cerevisiae* mutant yeast strain was acquired from Bristol-Myers Squibb Pharmaceutical Research Institute (Wallingford, Ct.). It was maintained on YEPD broth (yeast extract, peptone, and dextrose) at 4 °C. The culture was maintained with weekly aseptic transfer to fresh broth, which was incubated for 2 days in shaker flasks followed by incubation. Plate inoculum was prepared by transferring the culture into enough distilled water to provide an optical density of 0.12 (25% transmittance) at 600 nm. Yeast morphology agar plates (YMA) were prepared from 500 mL of distilled water, 1 g of yeast nitrogen base (without amino acids or ammonium sulfate), 10 g of dextrose, 10 g of agar, 1.75 g ammonium sulfate, 0.75 g of L-asparagine, 10 mg of D/L tryptophan, 10 mg of D/L methionine, and 5 mg of histidine. The media was heated till clear. Portions (46 mL) of media were distributed to Erlenmeyer flasks, which were then covered and autoclaved for 20 minutes. The flasks were allowed to cool followed by placing in laminar flow biohood. The media was then transferred from the flasks to 100 by 100 mm sterile plates and allowed to solidify. After solidification, 2.5 mL of innoculum was added. After a short period, excess innoculum was removed and the plates were allowed to dry. Wells were then cut into the plates (6-7 mm) and the plates were subjected to 5 minutes of UV light. Samples were prepared in DMSO-Water (1:1) and 100 µL aliquots were added to the wells. The plates were covered and incubated at 30 °C for 2-3 days. Activity was measured with a ruler (in millimeters). IC₁₂ were calculated by extrapolating the concentration required to prevent cell growth in a 12-mm zone. Extract M980037 gave an IC₁₂ value of 3050 µg/mL against the Sc-7 strain

²² a. Nitiss, J.; Wang, J.C. *Proc. Natl. Acad. Sci. USA* **1988**, *85*, 7501. b. Abdel-Kader, M.S.; Bahler, B.D.; Malone, S.; Werkhoven, M.C.M.; van Troon, F.; David; Mamber, S.W.; Kingston, D.G.I. *J. Nat. Prod.* **1998**, *61*, 1202.

²³ Zhou, B.-N.; Baj, N.J.; Glass, T.E.; Malone, S.; Werkhoven, M.C.M.; van Troon, F.; David; Wisse, J.H.; Kingston, D.G.I. *J. Nat. Prod.* **1997**, *60*, 1287.

Cytotoxicity Bioassays.²⁴ *In-vitro* antitumor cytotoxicity assays were performed using the A2780 human ovarian cell line as follows: 200 μ L of RPMI was dispensed to the column 12 well in a 96 well tissue culture plate. RPMI media (20 μ L) was added to column 11. All wells in columns 1 to 11 were seeded with 180 μ L of 2.7×10^{-5} c/mL A2780 DDP-S (Platinol-Sensitive) cells (5×10^{-4} cells/well). Plates were incubated for 3 hours in 5% CO₂ at 37 °C to allow cells to adhere. 20 μ L of the diluted compound (in up to 50% aqueous DMSO) was added to the wells. Column 12 was used for media control. Actinomycin D was the positive control and was run at 4 dilutions with an IC₅₀ ~1-3 ng/mL in Column 11. RPMI (20 μ L) was added to the last 4 rows of Column 11 as a negative control. The plate was incubated for 48 h at 37 °C in a 5% CO₂ incubator. The media was removed from the plates. Fresh RPMI (200 μ L/well) was added plus 10% FCS containing 1% Alamar Blue solution. The plate was incubated for 4 h at 37 °C and at 5% CO₂. The plates were read on a cytofluor at an emission of 530 nm and an excitation of 590 nm with a gain of 40 and IC₅₀ calculated.

Bioactivity-guided Fractionation and Isolation of 13-Hydroxy-1(10),14-*ent*-halimadien-18-oic Acids 2.10-12. The dried bioactive methanol extract M980037 (16 g) was partitioned between hexane and MeOH-H₂O (8:2). Water was added to the MeOH-H₂O fraction to provide a MeOH-H₂O (6:4) solution that was thoroughly extracted with CHCl₃. Evaporation of the solvents gave bioactive hexane and CHCl₃ fractions (4.1 and 10.0 g respectively). The hexane fraction was diluted in 100 mL of CHCl₃ and extracted with 50 mL of aqueous 5% Na₂CO₃ (three times); the aqueous fractions were combined, neutralized with aqueous 1% HCl and re-extracted with CHCl₃. Solvent removal provided 1.6 g of acidic substances. This acidic fraction was chromatographed over silica gel with elution by EtOAc-C₆H₁₂ (2:8). 11 fractions were

²⁴ Skehan, P.; Storeng, R.; Scudiero, D.; Monks, A.; McMahon, J.; Vistica, D.; Warren, J.T.; Bokesch, H.; Kenney, S.; Boyd, M.R. *J. Nat. Can. Inst.*, **1990**, *82*, 1107-1102.

collected of which fractions 3-5 yielded **2.10** (719 mg total) after rotary evaporation; fraction 3 (212 mg) was a syrupy material which slowly crystallized over a one-week period to give crystals of **2.10**; one large crystal was removed and submitted for x-ray analysis.

A small portion (330 mg) of the initial chloroform partition (10.0 g) was dissolved in CH₂Cl₂ (200 mL) and extracted with 0.1M NaHCO₃ (200 mL). Evaporation of the CH₂Cl₂ fraction gave a mixture of neutral and acidic material (89 mg), which was subjected to reverse phase chromatography on a Varian C-18 SPE column (5 g size) using MeOH-H₂O (8:2) as eluant and evaluation of the fractions by ¹H NMR spectroscopy. Fraction 5 (out of 9 fractions) (17 mg) was subjected to reverse phase HPLC using a C18 column and MeOH-H₂O (85:15) as eluant to give **2.11** (3.2 mg). The aqueous NaHCO₃ fraction was acidified with aqueous 10% HCl and then was extracted with 200 mL of CH₂Cl₂. Solvent was removed from the resulting CH₂Cl₂ extract and the product (67 mg) was subjected to reverse phase HPLC (twice) using a C18 column and MeOH-H₂O (85:15 and 70:30) as eluant to yield **2.12** (1.9 mg).

(13R)-13-Hydroxy-1(10),14-ent-halimadien-18-oic Acid (2.10): colorless crystals, mp 94-96 °C, $[\alpha]_D^{25} +22^\circ$ (*c* 0.6, MeOH); IR(neat film) 3403, 2972, 2936, 2875, 1704, 1693, 1463, 1377, 1284, 1243, 1189 cm⁻¹; ¹H NMR (CDCl₃) see Table 3; ¹³C NMR (CDCl₃) see Table 4; FABMS (negative ion) *m/z* 320 (M⁻, 22), 319 (M-H⁺, 100) FABMS (positive ion) *m/z* 303 (M-OH⁻, 17), 257 (20), and 221 (53); HRFABMS (negative ion) *m/z* 319.2273 (M-H⁺, Cal. For C₂₀H₃₁O₃: 319.2275).

(2S,13R)-2,13-Dihydroxy-1(10),14-ent-halimadien-18-oic Acid (2.11): colorless amorphous matrix, $[\alpha]_D^{25} +45^\circ$ (*c* 0.4, MeOH); IR(neat film) 3465, 2966, 2929, 2869, 1762, 1446, 1379 cm⁻¹; ¹H NMR (CDCl₃) see Table 3; ¹³C NMR (CDCl₃) see Table 4; FABMS (negative ion) *m/z* (rel. int.) 336 (M⁻,5), 335 (M-H⁺, 24), 334 (40) 333 (44), 319 (47), 318 (100), 290 (11), 289 (12), 275 (15), 255 (88); FABMS (positive ion) *m/z* (rel. int.) 318 (M-H₂O, 6), 317 (10), 301 (47), 273 (15), 257 (100), 255 (37).

2-Oxo-(13R)-2,13-hydroxy-1(10),14-ent-halimadien-18-oic Acid (2.12): colorless amorphous matrix, $[\alpha]_D^{+15^\circ}$ (*c* 0.3, MeOH); IR(neat film) 3404, 2953, 2923, 2869, 1730, 1658, 1603, 1463, 1372 cm^{-1} ; ^1H NMR (CDCl_3) see Table 3; ^{13}C NMR (CDCl_3) see Table 4; FABMS (negative ion) *m/z* (rel. int.) 334 (M^- , 100), 333 (M-H^+ , 83), 311 (14) 290 (51), 289 (49), 265 (20), 255 (20); FABMS (positive ion) *m/z* (rel. int.) 357 (M+Na^+ , 7), 318 (6), 317 (8), 277 (6), 242 (11), 223 (20), 207 (21); HRFABMS (negative ion) *m/z* 333.2042 (M-H , Cal. For $\text{C}_{20}\text{H}_{29}\text{O}_4$: 333.2066).

X-ray crystallography of (13R)-13-hydroxy-1(10),14-ent-halimadien-18-oic Acid (2.10).^{25,26}

A clear colorless block was crystallized as described above. The crystal was cut (ca. 0.5 x 0.5 x 0.5 mm^3), mounted on a glass fiber with epoxy, and placed on a Siemens (Bruker) P4 diffractometer. Unit cell parameters were determined by least squares refinement of 39 reflections that have been automatically centered on the diffractometer.²⁷ The Laue symmetry and systematic absences were consistent with the orthorhombic space groups $\text{P2}_1\text{2}_1\text{2}_1$. The structure was solved by direct methods and refined using the SHELXTL-NT v5.10 program package.²⁸ The crystal structure consists of the packing of two crystallographically independent molecules in the unit cell. As there were no heavy atoms, the absolute configuration could not be determined from the Friedel pairs; the Friedel pairs were therefore merged for the final refinement. The absolute configuration was assigned based on previous literature (see above) which confirmed R configuration at the C(13) center. The final refinement involved an anisotropic model for all non-hydrogen atoms and a riding model for all hydrogen atoms. The hydrogen attachments of the carboxylic acid groups were assigned to oxygen with the longest C-O bond length. The XP subroutine of the program package SHELXTL-NT was used for the ensuing molecular graphics generation.

²⁵ Crystallographic data for the structure reported in this paper will be deposited with the Cambridge Crystallographic Data Center. Copies of the data can be obtained, free of charge, on application to the Director, CCDC, 12 Union Road, Cambridge CB2 1EZ, UK (Fax: +44-(0)1223-336033 or email: deposit@ccdc.cam.ac.uk).

²⁶ This work was carried out by Dr. Carla Slebodnick who also provided the experimental description.

²⁷ XSCANS v2.1, Siemens Analytical X-ray Instruments: Madison, WI, 1994.

²⁸ Sheldrick, G.M. SHELXTL NT ver. 5.10; Bruker Analytical X-ray Systems: Madison, WI, 1998.

Crystal Data: C₂₀H₃₂O₃, orthorhombic, space group P2₁2₁2₁, a=11.6830(15) Å (α=90°), b=12.4363(18) Å (β=90°), c=27.115(3) Å (γ=90°), V=3939.7(9) Å³, Z=8, density_{calc.} 1.081 g/cm³, absorption coefficient: 0.071 mm⁻¹, F(000) = 1408, crystal size 0.5x0.5x0.5 mm³, theta range for data collection 1.50 to 20.00 °, index ranges -11 ≤ h ≤ 11, -11 ≤ k ≤ 11, -11 ≤ l ≤ 11, reflections collected 4235, independent reflections 2120 [R(int) = 0.0453], completeness to theta = 20.00° = 100.0%, absorption correction none, refinement method full-matrix least squares on F², data/restraints/parameters 2120/0/428, goodness-of-fit on F² 0.840, final R indices [I > 2σ(I)] R1 = 0.0352, wR2 = 0.0529, R indices (all data) R1 = 0.0746, wR2 = 0.0621, absolute structure parameter 0(2), extinction coefficient 0.0047(2), largest difference between peak and hole 0.110 and -0.104 e•Å⁻³.

Preparation of (13R)-13-Hydroxy-1(10),14-ent-halimadien-18-oic Acid Methyl Ester (2.13).

Compound **2.10** (50 mg) was dissolved in 2 mL of DMF; 200 mg (10 eq) of K₂CO₃ and 100 μL (10 eq) of CH₃I were added. The mixture was allowed to react at room temperature for 16h. 50 mL of H₂O and CHCl₃ was added and well shaken. The organic layer was dried then purified by Si gel PTLC (EtOAc:Hexane) to yield 25.4 mg (49 %) of **2.13**.¹¹

13(R)-Hydroxy-1(10),14-halimadien-18-oic Acid Methyl Ester (2.13): oil, [α]_D²⁵ +90.3° (c 0.214, CHCl₃), +37.3° (c 0.061, MeOH); IR(neat film) 3530, 2951, 2926, 1716, 1456, 1378, 1271, 1242, 1196, 995, 915 cm⁻¹; ¹H NMR (CDCl₃) see Table 3; ¹³C NMR (CDCl₃) see Table 4; FABMS (positive ion) m/z (rel. int.) 357 (M+Na⁺, 100); HRFABMS (positive ion) m/z 357.2409 (M+Na⁺, Cal. For C₂₁H₃₄O₃Na: 357.2406).

Preparation of (R) & (S) Phenylglycine Methyl Esters.¹⁵ 16.8 mL of SOCl₂ was added to 50 mL of MeOH at -10 °C. After 10 minutes, 7.0 g of (R)-phenylglycine was added and allowed to stir overnight at room temperature. The products were subjected to rotary evaporation to afford a residue. The residue were recrystallized in methanol resulting in two pure crops (363 mg, 730

mg) and additional material. The optical rotations of both crops were measured in methanol: $[\alpha]_D = -139.25^\circ$, -132.38° . Lit. value $[\alpha]_D = -139.6^\circ$.²⁹ In a similar manner, (*S*)-phenylglycine methyl ester was prepared, resulting in two crops (2.65 g, 0.9 g). The optical rotations of both crops were measured in methanol: $[\alpha]_D = +135.98^\circ$, $+130.60^\circ$. The purest crops of (*R*) and (*S*) phenylglycine methyl ester were used to prepare the chiral amides (below).

Preparation of (*R*) & (*S*) PGME Amides of **2.10.**¹⁴ 20 mg of **2.10** and 14.6 mg (*S*)-PGME were dissolved in 1 mL DMF and cooled to 0 °C. 37.9 mg of PyBOP[®], 10 mg 1-HOBt and 23 μL of *n*-methyl morpholine were added in order. The mixture was stirred at 0 °C for 1.5 h. 15 mL benzene and 30 mL EtOAc were added and the mixture washed with aqueous 5% HCl, aqueous saturated NaHCO₃ and brine. The organic layer was dried with Na₂SO₄ and solvent removed by rotary evaporation. The residue was chromatographed over Si gel PTLC first with CHCl₃-MeOH(97:3) then with CHCl₃ to yield 12.3 mg (42%) of (*S*)-PGME amide of **2.10**. In a similar fashion (except for a chromatographic eluant of EtOAc:Hexane:1:4) 13.8 mg (47%) of (*R*)-PGME amide of **2.10** was prepared.

Preparation of the (2*S*,13*R*)-2,13-Dihydroxy-1(10),14-*ent*-halimadien-18-oic Acid Benzoate Ester. Approximately 140 μg of **2.11** was placed in 200 μL of pyridine and allowed to stir at room temperature. 20 μL of benzoyl chloride was added along with a small quantity of DMAP. The mixture was allowed to react overnight. Pyridine was removed by blowing with argon. Water (1 mL) and CHCl₃ (1 mL) were added and the mixture shaken. The organic layer was removed by pipet and dried by rotary evaporation and overnight vacuum. The sample was prepared for CD by dissolving in 2 mL of methanol and passed through a nylon filter to provide a clear colorless solution.

²⁹ Chel'tsova, G.V.; Karpeiskaya, E.I.; Kablunovskii, E.I. *Bull. Acad. Sci. USSR Div. Chem. Sci.*, **1990**, *39*, 727.

Table 3. ¹H NMR Spectral Data for Compounds **2.10-13**.^a

	2.10	2.11	2.12	2.13
1	δ 5.27, bs	5.94, d, <i>J</i> =5.7	5.71, s	5.22, m
2	δ 2.05, m	4.76, ddd, <i>J</i> =5.5, 4.5, <2		2.00, m
3α	δ 1.28, m	2.05, dd, <i>J</i> =11.5, 5.3	2.69, d, <i>J</i> =15.8	1.81, ddd, <i>J</i> = 12.9, 12.9,4.8
3β	δ 1.40, m	2.14, dd, <i>J</i> =, 11.3, 4.8	2.16, d, <i>J</i> = 15.8	1.45, m
5	δ 2.64, dd, <i>J</i> = 12.4, 2.3	2.22, dd, <i>J</i> = 12.4, 4.8	3.2, dd, <i>J</i> = 12.9, 4.2	2.67, dd, <i>J</i> = 13.5, 3.7
6α	δ 1.24 m	1.71, m	1.42 m	1.24 m
6β	δ 1.31 m	1.44, m	1.42 m	1.24 m
7α	δ 1.44 m	1.33, m	1.82 m	1.46 m
7β	δ 1.44 m	1.33, m	1.82 m	1.46 m
8	δ 1.56 m	1.64, m	1.77 m	1.54
11a	δ 2.22, ddd, <i>J</i> =12.4, 12.4, <2	2.05, ddd, <i>J</i> =12.6, 12.6, 3.9	2.34, ddd, <i>J</i> =12.6, 12.6, 3.0	2.13, ddd, <i>J</i> =12.3, 12.3, 3.0
11b	δ 1.33, m <i>J</i> =12.2, 12.2, <2	1.35, ddd, <i>J</i> =12.6, 12.6, 3.9	1.33 ddd, <i>J</i> =12.4, 12.4, 3.0	1.42, m
12a	δ 0.99 m	1.16, ddd, <i>J</i> =12.6, 12.6, 3.9	0.89, m	1.03, ddd, <i>J</i> = 12.3, 12.3, 6.4
12b	δ 0.99 m	1.09, ddd, <i>J</i> =12.6, 12.6, 3.9	0.89, m	1.03, ddd, <i>J</i> =12.3, 12.3, 6.4
14	δ 5.78, dd, <i>J</i> = 10.9, 17.5	5.82, dd, <i>J</i> = 10.9, 17.4	5.83, dd, <i>J</i> = 11.0, 17.4	5.80, dd, <i>J</i> = 10.6, 17.2
15A	δ 5.21, dd, <i>J</i> = 17.5, 0.7	5.14, dd, <i>J</i> = 17.5, 1.5	5.16, dd, <i>J</i> = 17.4, 1.6	5.19, dd, <i>J</i> = 17.6, 1.6
15B	δ 5.03, dd, <i>J</i> = 10.8, 0.7	4.99, dd, <i>J</i> = 10.8, 1.5	4.99, dd, <i>J</i> = 11, 1.6	4.99, dd, <i>J</i> = 10.6, 1.7
16	δ 1.28, s	1.20, s	1.25, s	1.26, s
17	δ 0.74, d, <i>J</i> = 6.8	0.83, d, <i>J</i> = 6.9	0.81, d, <i>J</i> = 7.1	0.71, d, <i>J</i> = 6.0
18	δ 1.16, s	1.18, s	1.18, s	1.09, s
20	δ 0.82, s	0.92, s	0.98, s	0.98, s
OMe				3.62, s

a. **2.10** and **2.13** in CDCl₃; **2.11** and **2.12** in CD₃OD c. *J* coupling values in Hz.

Table 4. ^{13}C NMR Spectral Data for Compounds **2.10-13.**^a

Position	2.10	2.11	2.12	2.13
1	119.9	123.5	124.3	119.8
2	23.3	73.0	201.5	23.3
3	28.4	35.9	41.9	29.7
4	44.6	45.0	45.1	45.0
5	37.4	41.4	44.1	37.8
6	24.0	22.0	23.7	23.7
7	29.1	25.9	28.2	28.8
8	39.9	39.4	41.2	39.6
9	43.4	42.2	45.1	43.3
10	141.8	149.7	172.7	141.9
11	32.0	32.0	33.0	32.2
12	36.6	36.9	36.1	36.6
13	73.6	72.4	72.5	72.7
14	143.4	145.2	144.4	144.4
15	111.7	111.0	110.4	111.4
16	29.6	27.9	27.6	29.7
17	15.7	14.4	14.5	15.5
18	182.5	183.4	182.7	178.8
19	21.8	18.0	20.6	22.1
20	23.1	21.0	21.8	22.4
OMe				51.9

a. **2.10** and **2.13** in CDCl_3 ; **2.11** and **2.12** in CD_3OD

III. PARISSAPONIN Pb FROM *CESTRUM LATIFOLIUM* LAM.

3.1 Introduction.

As part of our ongoing program to isolate anticancer compounds from terrestrial plants, the methanol extract of *Cestrum latifolium* Lam. was found to display significant biological activity versus various *Saccharomyces cerevisiae* cell lines. The known saponin parissaponin Pb (**3.14**) was isolated and found to be responsible for the bioactivity. Parissaponin Pb was characterized by degradation, spectral analysis and comparison to the known literature data.

3.1.1 Structure and Basic Properties of Saponins.

Saponins¹ are glycosides of steroids (**3.1**) or triterpenes (**3.2**); the steroid or triterpene part of the molecule is called the aglycone. They are naturally occurring compounds that were first noticed due to their physical properties: primarily, they can behave as detergents. A number of plants such as soapbark (*Quillaja saponaria*) with high saponin contents have been given common names remarking on this behavior. It should be no surprise that the Latin word *sapo* means soap.

¹ Hostettmann, K.; Marston, A. *Saponins, Chemistry and Pharmacology of Natural Products*, Cambridge University Press, Cambridge, UK, **1995**.

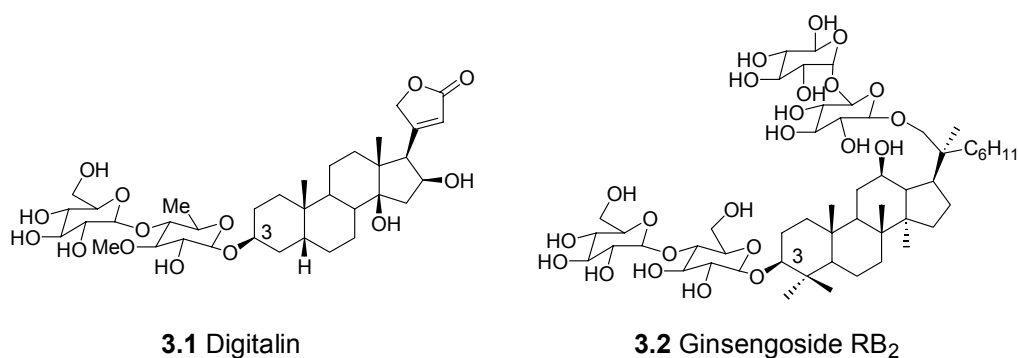


Figure 3-1. Saponins

Other general properties of saponins are their bitter taste, toxicity to fish, and the ability to cause hemolysis (they can disrupt the membranes of red blood cells thus releasing hemoglobin). They are typically found in plants (both terrestrial and marine); many vegetables have high saponin content.

Most saponins isolated to date are triterpenoid (C₃₀ aglycone-based) saponins (750 saponins with 360 different aglycones). At least six basic triterpene aglycones (3.3-3.6) exist. These structures have been well characterized and are published in the literature making structure elucidation of a typical aglycone relatively straightforward.

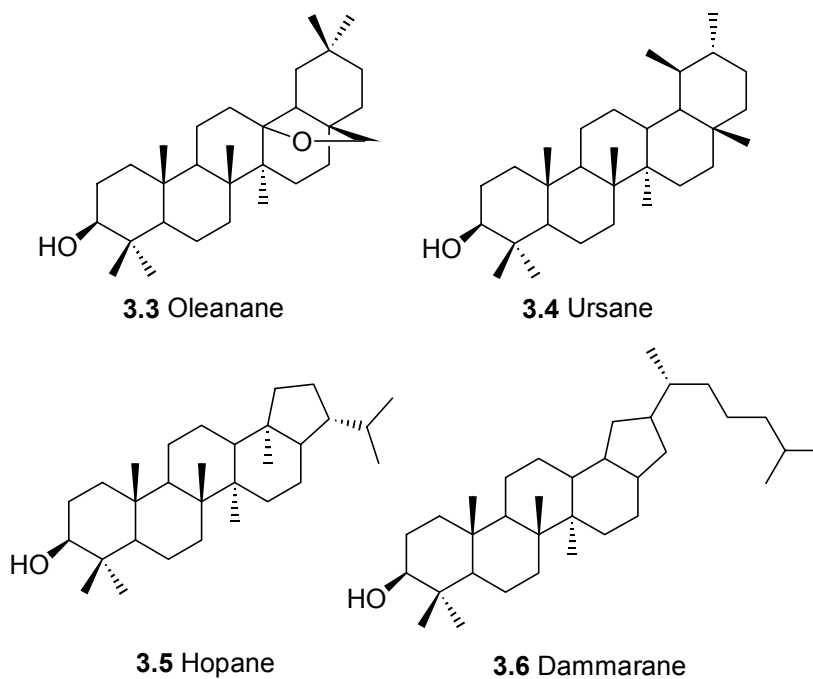


Figure 3-2. Four Common Triterpene Aglycone Skeletons

Steroidal saponins (C_{27} based aglycones) are structurally similar to triterpene saponins. In general, they possess similar physical and biological properties to the triterpene saponins. Fewer steroidal saponins have been found compared to the triterpene saponins. Steroidal saponins fall into two major and one minor classification: the spirostanol glycosides, the furostanol glycosides, and the steroidal alkaloids. The aglycones in steroidal saponins are also known as sapogenins.

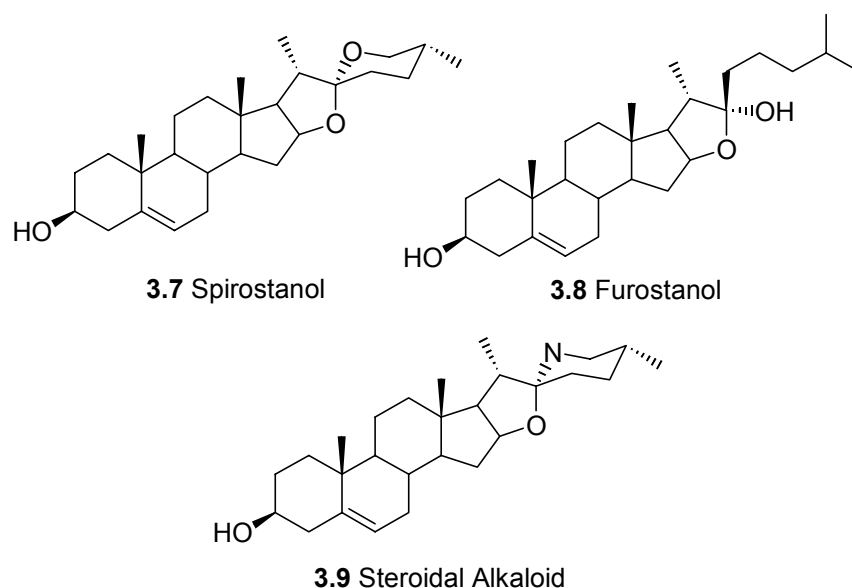


Figure 3-3. Basic Steroidal Saponin Skeletons

Triterpenes can be mono- (3.1), bi- (3.2), or tridesmosidic. The prefix indicates the number of glycosyl moieties that exist. Steroidal saponins are typically monodesmosidic. The most common sugars possessed by saponins are D-glucose, L-rhamnose, L-arabinose, and D-xylose; D-apiose, D-ribose, D-quinovose, and D-allose have also been reported but are less common. Typically, a glycosyl moiety is attached to the aglycone at the 3-O position (3.1, 3.2). However if the aglycone possesses additional oxygenated functionalities then additional glycosidal moieties may be present (3.2). The glycosidal moieties can be linear, branched, nitrogenated, oxidized, reduced, acetylated, or any combination thereof.

3.1.2 Saponins: Medicinal Applications and Other Uses.

Saponins are commonly used for poisoning fish, as drugs (the cardiotoxic digitalin from *Digitalis purpurea* L. 3.1), and as dietary supplements (the ginsenoside

RB₂ from various *Panax* (ginseng) species, **3.2**). Poisoning as a means of harvesting fish has been a tradition for many cultures; Brazilian Indians and Japanese fisherman still do so today, using saponin-rich *Serjania* and *Schima* species respectively.¹

Saponins tend to be antifungal; it has been postulated that this is their function in higher organisms.² Steroidal saponins are more potent fungicides compared to triterpenoid saponins, but have a narrower spectrum of activity against other organisms. A number of saponins have been isolated that display activity versus plant-pathogenic fungi but not human-pathogenic fungi.³ Saponins show little or no antibacterial activity and their activities versus viruses are not well characterized; however many saponins have shown cytotoxic and antitumor activity. The Ames test has detected a number of mutagenic saponins.⁴

One promising area of research is the antimolluscicidal activity of saponins, since it is estimated that 250 million people in tropical areas suffer from diseases caused by water-borne snails and other parasites. Many of these sufferers cannot afford commercially available drugs, but fortunately many of these regions possess plants rich in saponins.⁵ A 5-year control program was instituted in Ethiopia using the dried extracts of soapberry (*Phytolacca dodecandra*, locally known as 'endod'); the extract (previously used as a soap, containing up to 25% saponins) dramatically reduced infection rates of *Schistosoma mansoni*. Another medicinal use for saponins in poorer regions is as a

² Defago, G. Ber. *Schweiz. Bot. Ges.* **1977**, *87*, 79.

³ Hiller, K. in *Biologically Active Natural Products* (K. Hostettmann, ed.) **1987**, Oxford Press, Oxford, UK, 167.

⁴ Elias, R.; De Meo, M.; Vidal-Olliver, E.; Laget, M.; Balansard, G.; Dumenil, G. *Mutagenesis*, **1990**, *5*, 327.

⁵ Hostettmann, K. in *Economic and Medicinal Plant Research* (H. Wagner, H. Hikino, N.R. Farnsworth, eds.) Academic Press, London, **1989**, 73.

spermicide.⁶ The mechanism of action is presumably due to the disruption of the sperm plasma cell membrane, just as in many commercial spermicides.

Various other medicinal uses of saponins have been investigated, particularly the effect of saponins on the cardiovascular system, but they are too numerous to list here.¹ Many attempts to link the various biological activities to the hemolytic activity of saponins gave inconclusive results. The various mechanisms of action still aren't understood. Many of known triterpenoid saponins are bidesmosidic saponins, which are usually not antifungal or antimolluscicidal. They may act as prodrugs since they have superior transport properties (more water-soluble) compared to monodesmosidic saponins. In some plants, they are formed in the roots, transported to the location of infection, then enzymatically cleaved to form the monodesmosidic fungicide.^{7,8} Further research is required to fully understand the medicinal uses of saponins.

The insect antifeedant activities of saponins have been reported by a number of authors¹ although these activities can vary widely. Antifeedant activity has also been proposed to be the major reason for the biosynthesis of saponins in higher plants. It has been observed that soybeans are resistant to some insect infestations while growing yet when harvested and stored they are vulnerable to infestation. Saponins are believed to be responsible for this behavior.⁹

Dietary supplements and foodstuffs are also one of the major uses of saponin-containing plants today. Many traditional Asian folk medicines and dietary supplements are rich in saponins. Beans (family *Fabaceae*), yams (family *Dioscorea*), peas (family

⁶ Bhargava, S.K. *Fitoterapia*, **1988**, 59, 163.

⁷ Tschesche, R.; Wulff, G. *Prog. Chem. Org. Nat. Prod.* **1972**, 30, 462.

⁸ Tschesche, R. in *Pharmacognosy and Phytochemistry* (H. Wagner and L. Horhammer, ed.) **1971**, 274.

⁹ Applebaum, S.W.; Gestetner, B.; Birk, Y. *J. Agric. Food. Chem.* **1969**, 618.

Leguminosae), leeks (family *Allium*), tomatoes and potatoes (both family *Solanaceae*) are all rich in saponins. One publicized use of such supplements (in the USA) is the potential cholesterol-reducing ability of saponins. Soybeans and soybean products, such as tofu and soymilk, have been promoted to reduce cholesterol. Soybean saponins have been shown to reduce cholesterol uptake in the intestines of rats.¹⁰ Ginseng extracts can reduce total cholesterol and triglyceride concentrations but do not effect HDL-cholesterol.¹¹

Saponins are part of our everyday lives. They are present in our foodstuffs and in some cases in our medicines. Saponins appear to be very important in agriculture. They are potentially inexpensive, natural replacements for many expensive, synthetic products that are in use today. For these reasons and other reasons not yet discovered, increasing our understanding of these compounds is a worthy goal.

3.1.3 *Chemical Investigation of Cestrum latifolium Lam. and Cestrum Saponins.*

The *Cestrum* genus belongs to the *Solanaceae* (nightshade) family. This contains a number of known species such as *Cestrum sendtnerianum*, *Cestrum diurnum* (the day-blooming nightshade), and *Cestrum nocturnum* (the night-blooming nightshade). *Cestrum nocturnum* is perhaps the most commonly investigated species. These plants are commonly found in the northern parts of South America, the Caribbean, and southern United States. Traces of nicotine, nor nicotine, and solanidine S (**2.9**) have been found in this genus.¹² This genus also has been implicated in the poisoning of livestock in South

¹⁰ Sidhu, G.S.; Upson, B.; Malinow, M.R. *Nutr. Rep. Int.* **1987**, *35*, 615.

¹¹ Moon, C.K.; Kang, N.Y.; Yun, Y.P.; Lee, S.H.; Lee, H.A.; Kang, T.L. *Arch. Pharmacol Res.* **1984**, *7*, 41.

¹² Ahmad, V.U.; Baqai, F.T.; Ahmad, R. *Z. Naturforsch. B.* **1995**, *50*, 1104.

America.^{13,14,15} A number of saponins (**3.10-12**) have been isolated from these species.^{12,16,17} To date, there is little if any published data concerning *Cestrum latifolium* Lam. (Solanaceae). In Suriname, this plant is known as Bitu-uwí.

3.2 Results and Discussion

3.2.1 Isolation of Parissaponin Pb from *Cestrum latifolium* Lam.

As part of our ongoing program to isolate anticancer compounds from terrestrial plants, the methanol extract of *Cestrum latifolium* Lam. (9 g) was found to display significant biological activity in the 1138 (IC₁₂=200 µg/mL), 1140 (IC₁₂=400 µg/mL), and 1353 (IC₁₂=400 µg/mL) *Saccharomyces cerevisiae* cell lines.

A sample of this extract (4 g) was partitioned between aqueous 80% methanol and hexanes (Scheme 2). The aqueous methanol fraction was then diluted with water (to 60% methanol) and extracted with dichloromethane. Each fraction was subjected to solvent removal by rotary evaporation and bioassay; the dried aqueous fraction was determined to be the most active fraction. This fraction was then subjected to solvent partitioning between water and *n*-BuOH; the more active dried *n*-BuOH fraction was then subjected to column chromatography with MCI gel (aqueous methanol gradient). The most active fraction was then subjected to RP-18 solid phase extraction (aqueous methanol gradient) and recrystallization (ethanol) to afford 41.9 mg of compound **A** (IC₁₂= 14 (1138), 17 (1140), 18 (1353) µg/mL). The active dichloromethane fraction was also subjected to

¹³ Brevis, C.; Quezada, M.; Sierra, M.A. *et al. Arch. Med. Vet.* **1999**, *31*, 109.

¹⁴ Gava, A.; Stolf, L.; Varaschin, M.S. *et al. Pesquisa Vet Brazil*, **1996**, *16*, 4.

¹⁵ Van der Lugt, J.J.; Nel, P.W.; Kitching, J.P. *Onderstepoort J. Vet.* **1991**, *58*, 211.

¹⁶ Haraguchi, M.; Mimaki, Y.; Motidome, M.; Morita, H.; Takeya, K.; Itokawa, H.; Yokosuka, A.; Sashida, Y. *Phytochemistry*, **2000**, *55*, 715.

¹⁷ Ahmad, V.U.; Baqai, F.T.; Ahmad, R. *Phytochemistry*, **1993**, *34*, 511.

LH-20 Sephadex size exclusion chromatography and reverse phase chromatography.

Thin-layer chromatography indicated the presence of compound **A** in the active fractions.

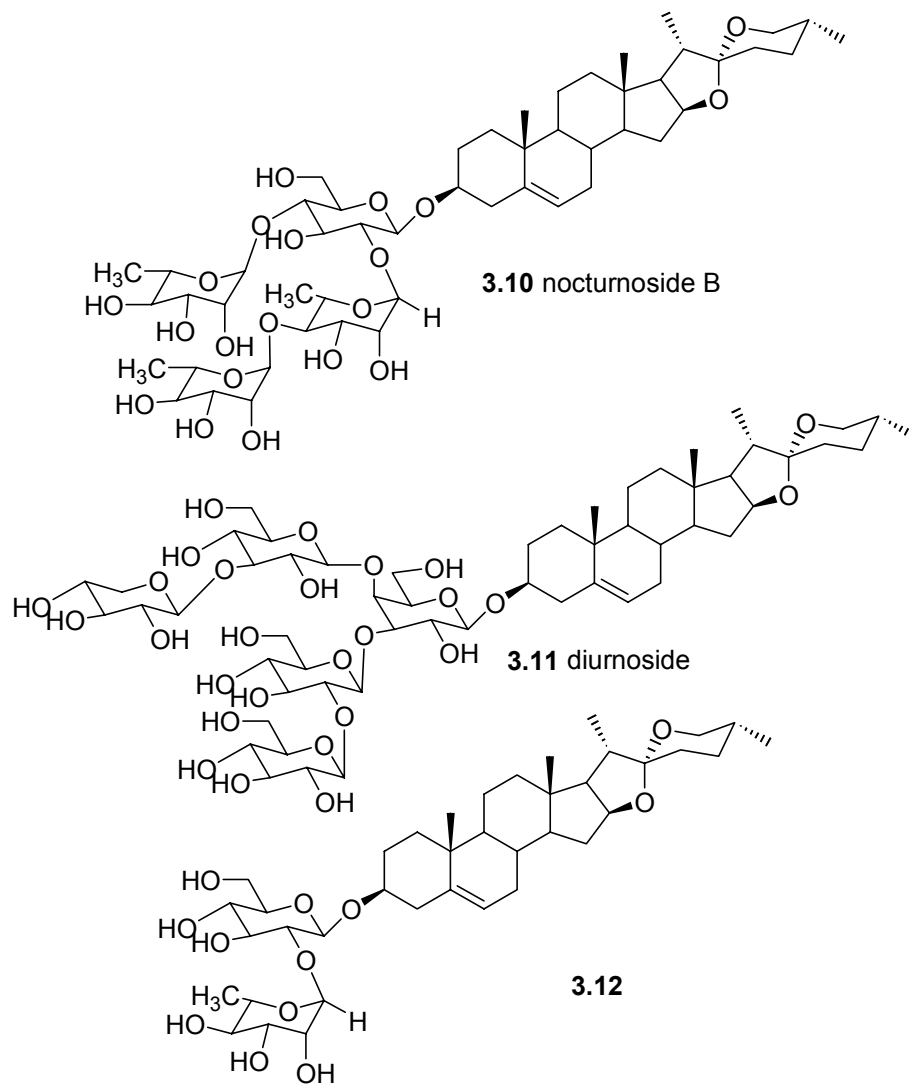
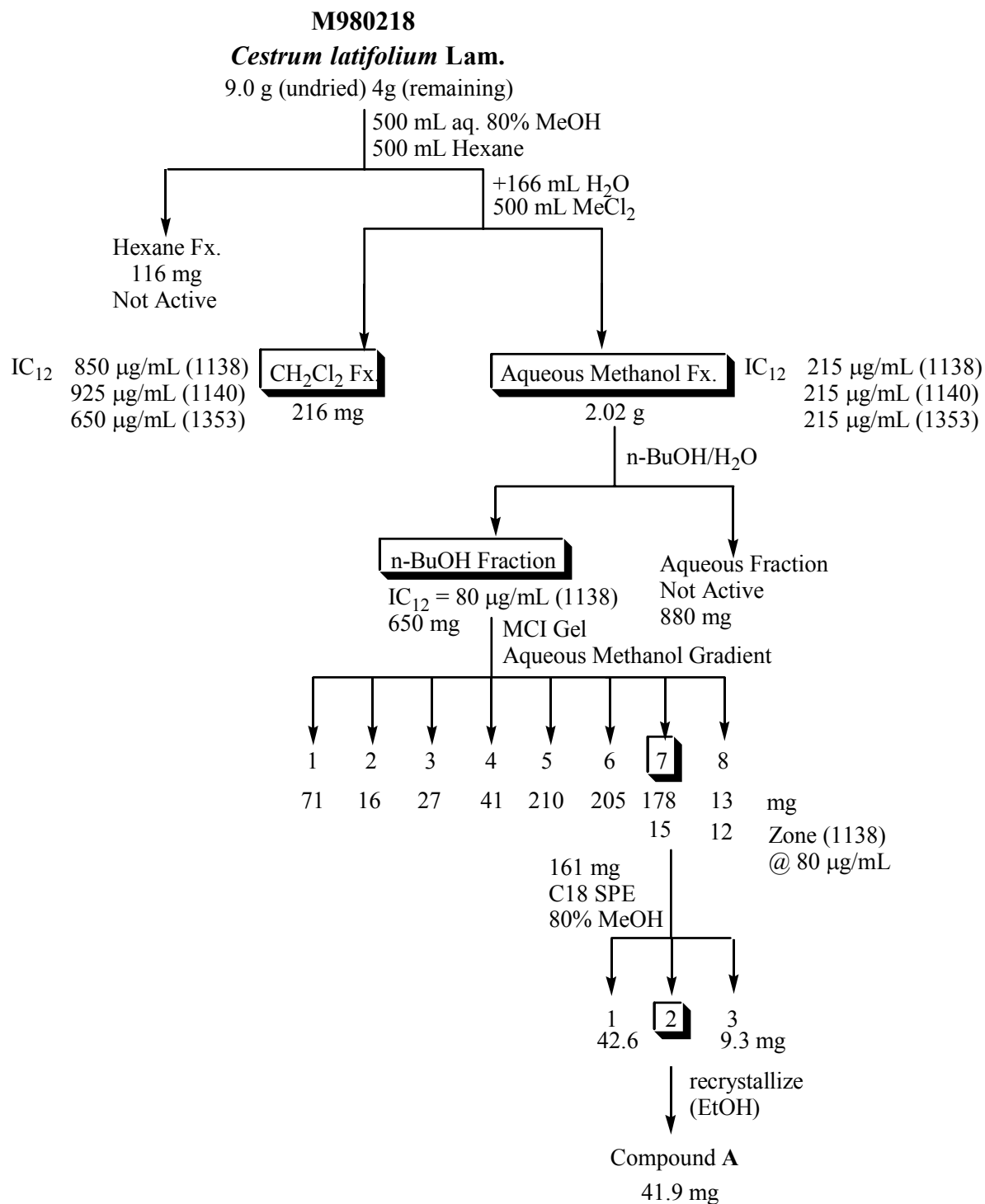


Figure 3-4. *Cestrum* Saponins



Scheme 2. Isolation Tree for M980218 (*Cestrum Latifolium* Lam.)

3.2.2 Structural Elucidation of Parissaponin Pb

A positive ion FABMS of compound **A** ($C_{51}H_{82}O_{20}$) displayed an $M+1$ of m/z 1015. The fragmentation pattern showed the loss of 4 sugars. In particular, the fragment weights correlated to the loss of three deoxy-hexoses followed by a hexose, implying the hexose is the sugar attached to the aglycone. The FABMS of **A** possessed a signal at 415 m/z , consistent with the presence of the common spirostanol diosgenin **3.13**. An IR spectrum indicated very little functionality other than a strong -OH peak at 3404 cm^{-1} . In previously reported work with Parissaponin Pb and diosgenin, IR spectroscopy was successfully used to determine the stereochemistry of the spiroketal center at C-25 in the steroidal saponin. Thus when a band at 890 cm^{-1} is more intense than that at 910 cm^{-1} a 25(*R*) stereochemistry is indicated.¹² Unfortunately, the bands at 897 and 921 in compound **A** were of equal intensity and no stereochemistry could be assigned. The stereochemistry at this position was subsequently determined through IR spectroscopy of the aglycone compound **B** (see below).

The ^1H NMR spectrum displayed signals for several methyl groups (δ 0.68, 0.85, 1.04, 1.13, 1.57, 1.60, 1.77), sugar protons (δ 3.5-4.5), a vinylic proton (δ 5.30) and four anomeric protons (δ 4.96 (d, $J=5.5$ Hz), 5.89 (bs), 6.29 (bs), 6.41(bs)). The J coupling values and broadening of these signals for the anomeric protons indicated that the sugars were connected by a β -linkage and three α -linkages.¹² ^{13}C NMR, APT, and DEPT experiments showed the presence 51 carbons (many unresolved in the sugar region). HETCOR and HMQC experiments were necessary to clearly define the 7 methyls, 10 methylenes, 30 methines, and 4 quaternary carbons. An unusual peak at δ 109.5

indicated the presence of a spiroacetal carbon. Signals for anomeric protons were correlated with those for anomeric carbons via HETCOR and HMQC.

Acid hydrolysis of compound **A** led to the aglycone **B**, which was found to be diosgenin (**3.13**) (C₂₇H₄₄O₃). Compound **3.13** was characterized by FABMS (M+H⁺, *m/z* 415), ¹H NMR, and ¹³C NMR. Confirmation of the structure **3.13** as diosgenin was made by comparison of its ¹³C NMR spectrum with that of the literature data.¹⁸ Its ¹³C NMR, APT and HMQC spectra revealed 27 (4 CH₃, 10 CH₂, 9 CH, and 4 *q*-C) carbon signals that are indicative of a steroid skeleton; the peak at δ 109.5 (C-25) revealed a spiroacetal functionality, and a peak at δ 71.4 pointed to the presence of a hydroxy group (C-3). The location of the resonance for C-27 (δ 17.2) corresponded to an (*R*)-orientation.¹² An IR spectrum also confirmed the presence of a C=C (1452 cm⁻¹), the stereochemistry of the spiroketal (intensity at 897 > 921 cm⁻¹ indicated 25(*R*)-stereochemistry),¹⁹ and a hydroxyl group (3364 cm⁻¹).

The sugars isolated from the acid hydrolysis were reduced and then acetylated to make them amenable to GC analysis. Analysis of these derivatives by GC and comparison to prepared standards revealed that the hexose was D-glucose and all of the deoxy-hexoses were L-rhamnose.

An examination of the literature reveals three saponins based upon diosgenin and containing glucose and three rhamnoses: nocturnoside B (**3.10**),¹² parissaponin Pb (**3.14**, also known as Pb),²⁰ kallstroemin-D (**3.15**),²¹ and polyphyllin E (**3.16**).²² Physical

¹⁸ Eggert, H.; Djerassi, C. *Tetrahedron Lett.* **1975**, *42*, 3635.

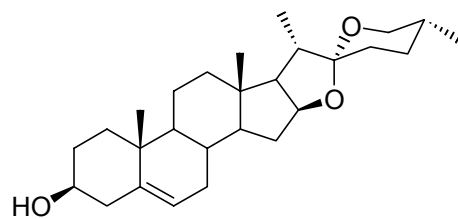
¹⁹ Asami, A.; Hirai, Y.; Shoji, J. *Chem. Pharm. Bull.* **1991**, *39*, 2053.

²⁰ a. Nohara, T.; Yabuta, M.; Suenobu, M.; Hida, R.; Miyahara, K.; Kawaski, T. *Chem. Pharm. Bull.* **1984**, *32*, 295. b. Munday, S.C.; Wilkins, A.L.; Miles, C.O.; Holland, P.T. *J. Agric. Food. Chem.* **1993**, *41*, 267.

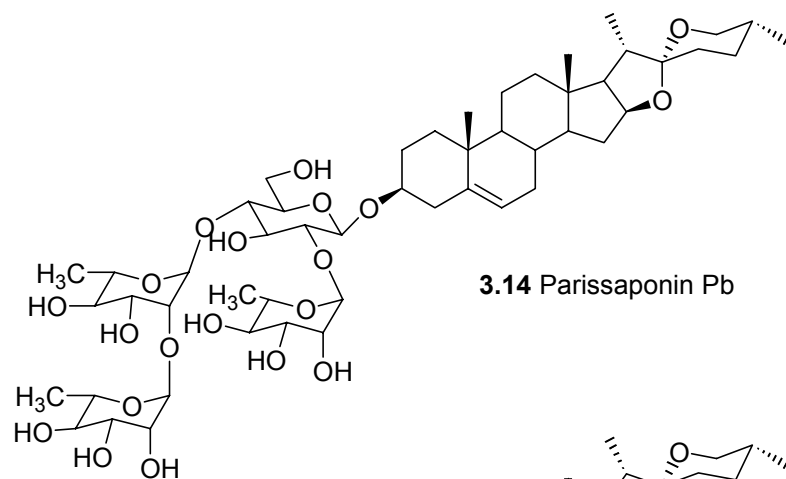
²¹ Mahato, S.B.; Sahu, N.P.; Pal, B.C.; Chakravarti, R.N. *Ind. J. Chem.* **1981**, *59*, 1328.

²² Singh, S.B.; Thakur, R.S. *Planta Med.* **1980**, *40*, 301.

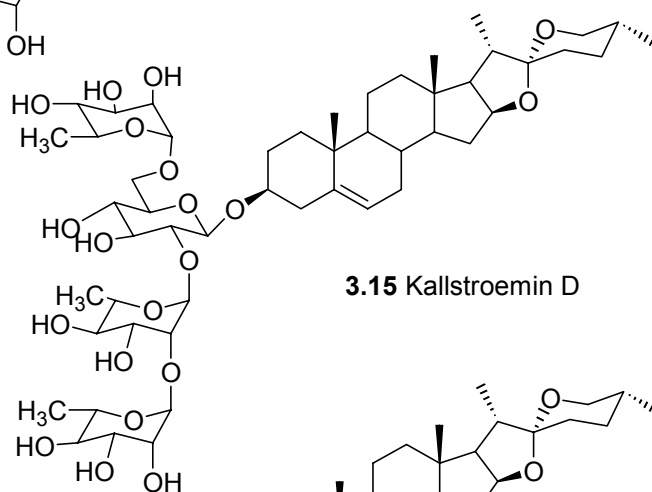
methods of analysis (optical rotation and melting points) indicated that the isolated saponin was more similar to **3.10** or **3.14**, rather than to **3.15** (although such measurements are not sufficiently accurate for confirmation). Comparison of ^{13}C NMR and ^1H NMR data of these compounds revealed that the isolated saponin had the same spectra as **3.10** and **3.14**, but differ from each other in the assignment of two positions and so a definitive choice could not be made between them. Compound **3.15** was excluded since the ^{13}C NMR spectrum indicated that the glucose was not substituted at the C-6 position (δ 61.0). The NMR data for **3.16** did not agree with that of the isolated saponin. Thus compound **A** is neither **3.15** nor **3.16**. The reported NMR assignments for parissaponin Pb were determined by COSY, HMQC, HOHAHA, and NOESY experiments (Tables 5-7);²⁰ the report NMR assignments for nocturnoside B were determined by the same techniques and HMBC.



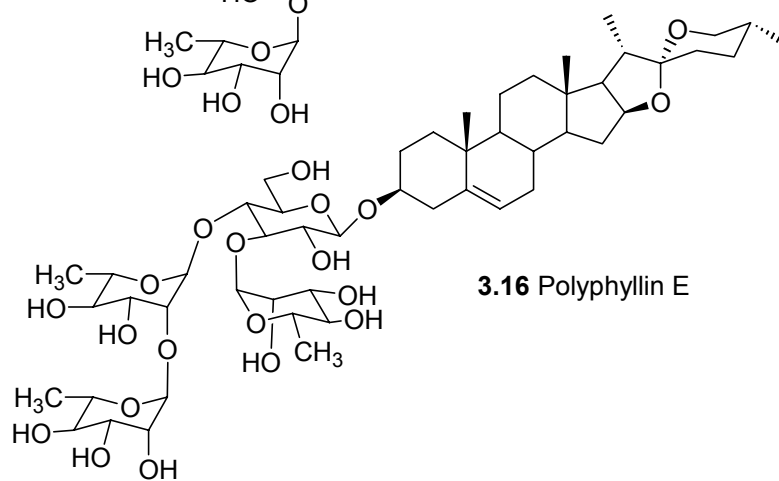
3.13 Diosgenin



3.14 Parissaponin Pb



3.15 Kallstroemin D



3.16 Polyphyllin E

Figure 3-5. Diosgenin and Related Saponins

Further characterization of compound **A** required the use of HMBC NMR spectroscopy. The significant amount of overlap in the region δ 3-5 in the ^1H NMR made assignment difficult. As stated earlier, all ^{13}C and ^1H signals reported for **3.10** and **3.14** had identical peaks with the exception of three assignments; these assignments are the rha-II-4 position, the rha-III-4 position, and the glc-4 position. These three assignments can be distinguished by HMBC to determine the identity of the compound **A**.

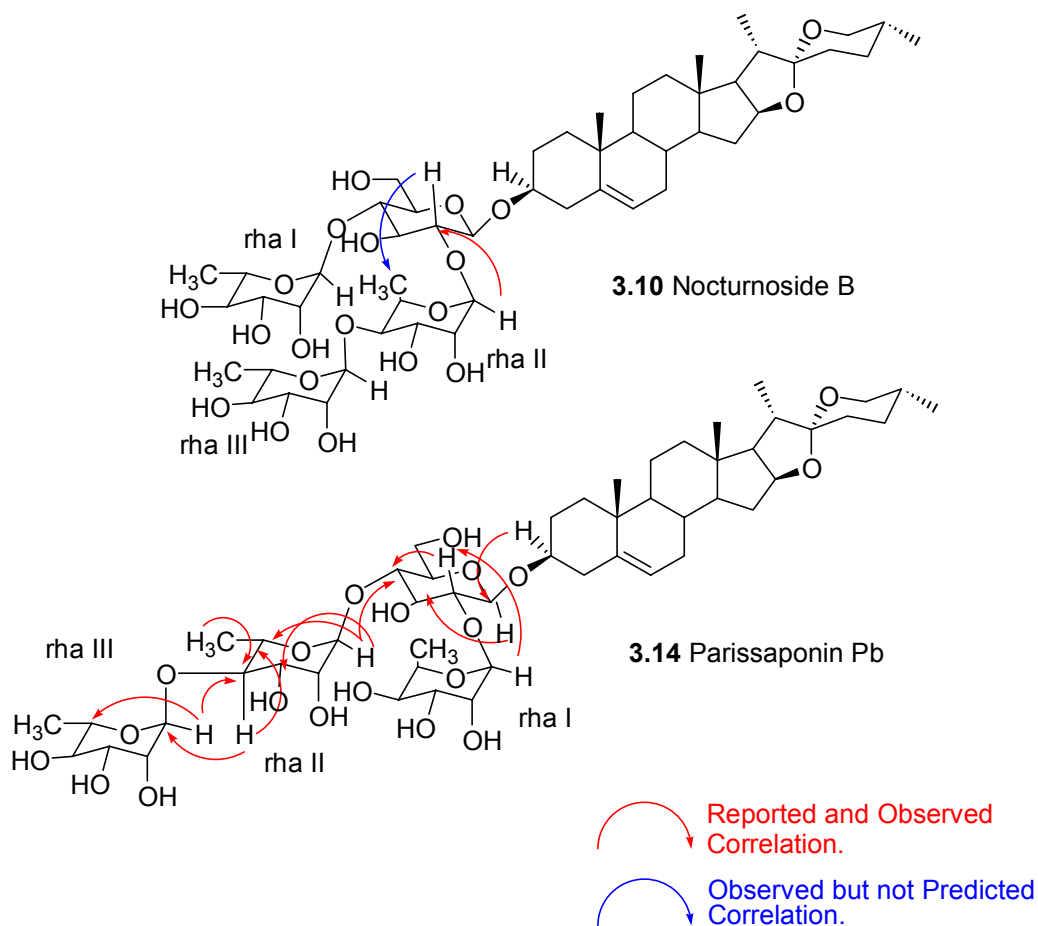


Figure 9. Predicted and Observed HMBC Correlations

As the ^1H and ^{13}C spectra were so similar, the HMBC assignments were also remarkably similar. The HMBC of compound **A** correlated all reported signals for **3.10** and **3.14** except for those three assignments: δ 4.44/80.2, 4.37/74.0, and 4.21/77.8 (δ H/C). The HMBC results did not agree with the published assignments for nocturnoside B (**3.10**), since there was an observed HMBC correlation between δ_{C} 80.2 (reported for the glc-C-2) and δ_{H} 1.59 (rhamnose CH_3 protons). This observation was in better agreement with the reported assignments for rha-II-C-4 in parissaponin Pb (**3.14**). If compound **A** was nocturnoside B (**3.10**), we would expect to see a correlation between the glucose C-2 carbon (δ 80.2) and the rha II anomeric proton (δ 6.26) but we would not observe correlations between the glucose C-2 carbon and a rhamnose CH_3 group.

Additional HMBC correlations between anomeric protons and other linkage carbons confirm the linkages. On this basis, the compound **A** has been confirmed as parissaponin Pb (**3.14**)

Parissaponin Pb has been isolated from a variety of *Paris* species,²³ *Trachycarpus* species,²⁴ *Rhapis* species,²⁵ *Allium* species,²⁶ *Dioscorea floribunda*,²⁷ and *Chamaerops humilis* L.^{24b} As this is a previously reported natural product further investigations were not necessary and the project was concluded at this point.

²³ a. Miyamura, M.; Nakano, K.; Tomimatsu, T.; Kawaski, T. *Chem. Pharm. Bull.* **1982**, *30*, 712. b. Wu, R.-T.; Chiang, H.-C., Fu, W.-C., Chien, K.-Y.; Chung, Y.-M.; Horng, L.-Y. *Anticancer Res.* **1992**, *12*, 1475.

²⁴ a. Hirai, Y.; Sanada, S.; Ida, Y.; Shoji, J. *Chem. Pharm. Bull.* **1984**, *32*, 295. b. Hirai, Y.; Sanada, S.; Ida, Y.; Shoji, J. *Chem. Pharm. Bull.* **1986**, *34*, 82.

²⁵ Hirai, Y.; Sanada, S.; Ida, Y.; Shoji, J. *Chem. Pharm. Bull.* **1984**, *32*, 4003.

²⁶ a. Mimaki, Y.; Satou, T.; Ohmura, M.; Sashida, Y. *Nat. Med.* **1996**, *4*, 308. b. Inoue, T; Mimaki, Y.; Sashida, Y.; Nishino, A.; Satomi, Y.; Nishino, H. *Phytochemistry*, **1995**, *40*, 521.

²⁷ Hoyer et. al. *Phytochemistry*, **1975**, *14*, 539.

3.2.3 *Biological Evaluation of Parissaponin Pb.*

Parissaponin Pb has been investigated for anticancer activity^{23b,28} but not for the hemolytic, antifungal or antimolluscicidal activity that saponins are noted for. A combined 5-fluorouracil/saponin treatment was more active than 5-fluorouracil or parissaponin Pb alone on solid mouse hepatoma tumors.^{23b} The anticancer activity was reportedly due to the immunomodulating effects of parissaponin Pb resulting in raised interferon levels, macrophage stimulation, and an increase in natural killer cell cytotoxicity.

Parissaponin Pb was tested against the 1138, 1140, and 1353 *Sacchararomyces cerevisiae* mutant yeast strains; it showed activities of 14, 17, and 18 µg/mL respectively. It was also tested against the A2780 human ovarian cell line and showed only a marginal activity of about 40 µg/mL. Compared to previously isolated compounds, the activity in the yeast cell lines is moderate. In general, the criterion of interest in the employed yeast or mammalian cell lines is a response of less than 1 µg/mL; thus parissaponin Pb is not really worth development as a drug candidate. The greater activity in the 1138 compared to the 1140 or 1353 is not significant since a threefold or more difference is required for significance. While parissaponin Pb shows slightly greater activity in the 1138 and 1140 vs. 1353 (indicating potential topoisomerase I inhibition) (see Table 1), the greater activity in the 1138 vs. 1140 or 1353 is probably more indicative of a cell permeability affect. Simply put, parissaponin Pb probably possesses the general antifungal activity all saponins possess. As a control, the aglycone diosgenin was also tested in the 1138/1140/1353 strains and found to be inactive.

²⁸ Wu, R.-T.; Chiang, H.-C.; Fu, W.-C.; Chien, K.-Y.; Chung, Y.-M.; Horng, L.-Y. *Int. J. Immunopharmac.* **1990**, *6*, 777.

3.3 Experimental

General Experimental Procedures. The general experimental procedures were similar to those reported earlier.²⁹ GCMS was performed on a Hewlett Packard 5890 GC with a 5970 Mass Selective Detector equipped with a HP-1 column (50m length, 0.2 mm column diameter, 0.33 μ m film thickness). Column chromatography was carried out on Supelco MCI Gel and Varian Mega Bond Elute C18 Solid Phase Extraction cartridges.

Plant Material. The bark, twigs, stems, and blooms of *Cestrum latifolium* Lam. (Solanaceae) were collected in Suriname (February, 1998). A voucher specimen was deposited at the National Herbarium of Suriname.

Plant Extraction. *Cestrum latifolium* bark, twigs, stems, and blooms were extracted with EtOAc and MeOH at Bedrijf Geneesmiddelen Voorziening Suriname (BGVS). This yielded an extract labelled BGVS M-980218.

Yeast Bioassays. The yeast bioassays was performed using yeast strains Sc-7, 1138, 1140, and 1353 as previously reported.²⁹

Cytotoxicity Bioassay. The A2780 assay was performed at Virginia Polytechnic Institute and State University as previously reported.²⁹

Extraction and Isolation. The plant material was extracted with EtOAc followed by extraction with MeOH. Solvent was removed from the MeOH extract to afford 9 g of a

dark green tar. This tar displayed activities (IC_{12}) of 200 $\mu\text{g/mL}$ (1138) and 400 $\mu\text{g/mL}$ (1140 & 1353) on the *Saccharomyces cerevisiae* (yeast) based bioassay. The dried EtOAc extract was also tested but found to be inactive. The methanol extract was dissolved in 500 mL of 80% methanol in water and defatted with hexane (500 mL). The aqueous methanol fraction was diluted with water to a composition of 60% methanol in water; this was then partitioned with 500 mL of CH_2Cl_2 . The fractions were then evaporated to dryness; biotesting revealed that the aqueous methanol fraction (2.02 g) was the most active fraction. This fraction was then partitioned between 200 mL each of *n*-butanol and water. Solvent was removed by vacuum from the *n*-butanol fraction and the active solid (650 mg, $IC_{12}=80 \mu\text{g/mL}$ in the 1138 mutant yeast strain bioassay) was chromatographed over MCI gel using a methanol:water gradient (10% methanol in water to pure methanol). The 1138 bioassay indicated the most active fraction (178 mg), which was then subjected to multiple C18 SPE column chromatography with methanol/water; finally, multiple recrystallizations from ethanol resulted in 41.9 mg of compound **A**. The aglycon diosgenin (5.3 mg) was obtained by hydrolysis of 10 mg of compound **A** with 1 mL of methanol-0.5 M aqueous HCl (1:1), heating overnight at 100 °C in a screw capped vial followed by solvent removal, partitioning into chloroform and water, and the collection and drying of the chloroform fraction. An examination of the weight ratio of aglycon to glycoside indicated that 3-4 sugars were present in the glycoside. The hydrolyzed sugars were obtained from the dried aqueous fraction. The sugars were subjected to acetylation (with 1 mL of Ac_2O and three drops of pyridine); GCMS analysis with standards confirmed the identities of the sugars.

²⁹ Chapters 2 Experimental Section.

Diosgenin-3-O- α -L-rhamnopyranosyl-(1->4)- α -L-rhamnopyranosyl-(1->4)-[α -L-rhamnopyranosyl-1->2)]- β -D-glucopyranosid (3.14) was obtained as an off white powder; m.p. 220-223 °C (ethanol). $[\alpha]_D = -85.7^\circ$ (lit. value: -104.3)²⁵. IR: 3404.6, 2935.3, 2869.9, 1597.2, 1451.0, 1366.3, 1243.0, 1046.7, 981.3, 917.7, 898.5. ¹H NMR (C₅D₅N, 500 MHz) see Table 5. ¹³C NMR (C₅D₅N, 125 MHz) see Tables 6 and 7. Positive ion FABMS: $m/z = 1038$ (M+Na)⁺(0.25), 1016 (M+1)⁺(1), 1014 (M-1)⁺(2), 869 (M-Rha)⁺(1), 723 (M-Rha-Rha)⁺(4), 577 (M-Rha-Rha)⁺(5), 415 (Diosgenin, M-Rha-Rha-Glu)⁺(45), 397 (Diosgenin-H₂O)⁺(100).

Diosgenin (3.13) was obtained as a light green solid. IR: 3364.6, 2916.0, 2849.4, 1452.9, 1372.6, 1240.9, 1054.0, 977.8, 921.7, 863.3. ¹H NMR (CDCl₃, 500 MHz) see Table 5. ¹³C NMR (CDCl₃, 125 MHz) see Table 6. Positive EIMS: $m/z = 415$ (M)⁺ (2), 414 (M-1)⁺ (3), 397 (M-H₂O)⁺ (2), 342 (5), 300 (7), 282 (23), 271 (17), 253 (9), 139 (100).

Table 5. ¹H NMR (Selected Peaks) of **3.10**, **3.13**, and **3.14**.

Proton	B	3.13 (Lit) ^{10b}	A	3.14 (Lit) ^{20b}	3.10 (Lit) ¹⁶
H-3	3.85	3.82	3.87	3.82	3.85
H-4	2.60, 2.63	2.60-2.63	2.72, 2.82	2.73-2.78	2.72, 2.79 (α, β)
H-6	5.39	5.38	5.30	5.34	5.3
H-16	4.54	4.53	4.56	4.55	4.53
H-18	0.85 (s)	0.85	0.83 (s)	0.84	0.82
H-19	1.04 (s)	1.04	1.04 (s)	1.06	1.04 (s)
H-21	1.14 (bd)	1.13	1.13 (d, <i>J</i> = 6.9)	1.14	1.12 (d, <i>J</i> = 7.0)
H-26	3.50, 3.57	3.48, 3.55	3.49, 3.59	3.51, 3.58	3.48, 3.58 (α,β)
H-27	0.69 (bd)	0.69	0.68 (d, <i>J</i> = 5.5)	0.70	0.69 (d, <i>J</i> = 5.8)
Glu-1			4.96 (d, <i>J</i> = 5.5)	4.95	4.93 (d, <i>J</i> = 6.5)
Rha-I-1			6.41 (bs)	6.39	6.37 (d, <i>J</i> = 3.7)
Rha-II-1			5.85 (bs)	5.83	5.81 (d, <i>J</i> = 2.8)
Rha-III-1			6.29 (bs)	6.28	6.26 (d, <i>J</i> = 3.6)

a. in C₅D₅N b. all *J*-coupling measurements are in Hz.

Table 6. ^{13}C NMR (Steroidal Structure) of **3.10**, **3.13**, and **3.14**.

Carbon	B	3.13 (Lit) ¹²	A	3.14 (Lit) ^{20b}	3.10 (Lit) ¹⁶
1.	37.3	37.2	37.4	37.3	37.3
2.	31.7	31.6	30.0	30.0	29.9
3.	71.8	71.5	77.9	78.0	77.9
4.	42.4	42.2	38.8	38.8	38.8
5.	141.0	140.8	140.7	140.6	140.7
6.	121.7	121.3	121.8	121.6	121.6
7.	32.2	32.1	32.2	32.1	32.1
8.	31.5	31.4	31.5	31.5	31.5
9.	50.1	50.1	50.2	50.1	50.1
10.	36.8	36.6	37.0	37.0	36.9
11.	21.0	20.9	21.0	20.9	20.9
12.	40.0	39.8	39.7	39.7	39.7
13.	40.3	40.2	40.3	40.3	40.3
14.	56.6	56.5	56.5	56.5	56.4
15.	32.0	31.8	32.1	32.0	32.0
16.	81.0	80.7	80.9	80.9	80.9
17.	62.3	62.1	62.8	62.7	62.7
18.	16.4	16.3	16.2	16.2	16.1
19.	19.5	19.4	19.3	19.2	19.2
20.	41.7	41.6	41.8	41.8	41.8
21.	14.6	14.5	14.9	14.9	14.8
22.	109.5	109.1	109.1	109.1	109.1
23.	31.6	31.4	31.7	31.7	31.6
24.	28.9	28.8	29.1	29.1	29.0
25.	30.4	30.3	30.5	30.4	30.4
26.	67.0	66.7	66.7	66.7	66.7
27.	17.2	17.1	17.2	17.2	17.1

a. **B/3.13** in CDCl_3 . b. **A/3.10/3.14** in $\text{C}_5\text{D}_5\text{N}$

Table 7. ^{13}C NMR (Glycoside Moiety) of **3.10** and **3.14**.

Carbon	A	3.14 (Lit) ^{20b}	3.10 (Lit) ¹⁶	Carbon	A	3.14 (Lit) ^{20b}	3.10 (Lit) ¹⁶
Glu-1	100.2	100.1	100.2	Rha-II-1	102.1	102.1	102.1
2	77.8	77.8	80.2	2	72.7	72.7	72.7
3	77.6	77.7	77.5	3	73.2	73.2	72.4
4	77.6	77.6	77.6	4	80.3	80.2	74.0
5	76.9	76.8	76.8	5	68.2	68.2	69.3
6	61.0	61.1	61.0	6	18.8	18.7	18.4
Rha-I-1	102.1	102.0	102.0	Rha-III-1	103.2	103.1	103.1
2	72.4	72.3	72.7	2	72.5	72.4	72.7
3	72.7	72.7	72.3	3	72.7	72.7	73.1
4	73.9	73.9	73.8	4	74.0	73.8	77.8
5	69.4	69.4	68.1	5	70.3	70.2	70.2
6	18.5	18.5	18.4	6	18.3	18.3	18.2

b. A/**3.10/3.14** in $\text{C}_5\text{D}_5\text{N}$

IV. HYDROLYSIS AND CONFIGURATION ANALYSIS OF SAPONINS (ALBIZIATRIOSIDE A) FROM *ALBIZIA SUBDIMIDIATA*

4.1 Introduction.

As part of our ongoing investigations for anticancer compounds from Surinamese flora, a new saponin, albiziatrioside A, and a known bioactive saponin were isolated from *Albizia subdimidiata* by Dr. Maged Abdel-Kader. The new saponin was partially characterized by Dr. Abdel-Kader, but additional degradative and derivatization steps were required to fully characterize it. This chapter reviews the work done by Dr. Abdel-Kader and describes the additional studies that were performed to complete the structural elucidation of albiziatrioside A.

4.1.1 Previous Investigations of *Albizia* Species.

The genus *Albizia* (Fabaceae) comprises about 150 species widely distributed in various tropical areas, especially Asia and southern Africa.¹ Of these species, approximately 15 species have been phytochemically investigated.² The most commonly investigated species is *Albizia julibrissin*, which is also known as the silk tree or mimosa (some authors have also identified it as *Albiziae cortex*, *Albizzia cortex* and *Albizziae cortex*).³ The silk tree is particularly popular as an ornamental plant, and most other *Albizia* sp. are also used as ornamental plants. Other species include *Albizia procera*

¹ Pohlhill, R. M.; Raven, P.H. *Advances in Legume Systematics*, Royal Botanic Gardens: Kew, UK, **1981**, 180.

² Scifinder Search (Chemical Abstracts/Medline): February 20, 2001

³ a. Kinjo, J.; Araki, K.; Fukui, K.; Higushi, H.; Ikeda, T.; Nohara, T.; Ida, Y.; Takemoto, N; Miyakoshi, M.; Shoji, J. *Chem. Pharm. Bull.* **1992**, *40*, 3269. b. Ikeda, T.; Fujiwara, S.; Kinjo, J.; Nohara, T.; Ida, Y.; Shoji, J. *Bull. Chem. Soc. Jpn.* **1995**, *68*, 3483.

(“Safed Siris” in Hindi),⁴ *Albizia tanganyicensis*,⁵ and *Albizia gummifera*.⁶ Besides their use as ornamental plants, a number of species have attracted the interest of the wood and pulp industries. Despite the fact that a number of species are toxic to livestock,⁵ some species are employed in animal feed.⁴ A number of species are employed in traditional African medicine (as treatments for coughs, gonorrhoea, and stomach pain) and are attracting ethnobotanical interest.⁶ Extracts and isolates from these and other species have shown interaction with DNA, cytotoxicity versus cultured mammalian cells, antibacterial activity (against both Gram positive and Gram negative bacteria) and brine shrimp lethality.⁶

Phytochemically, *Albizia* species are interesting due to their alkaloid content (predominately in the seeds) and their saponin content (in the aerial parts).

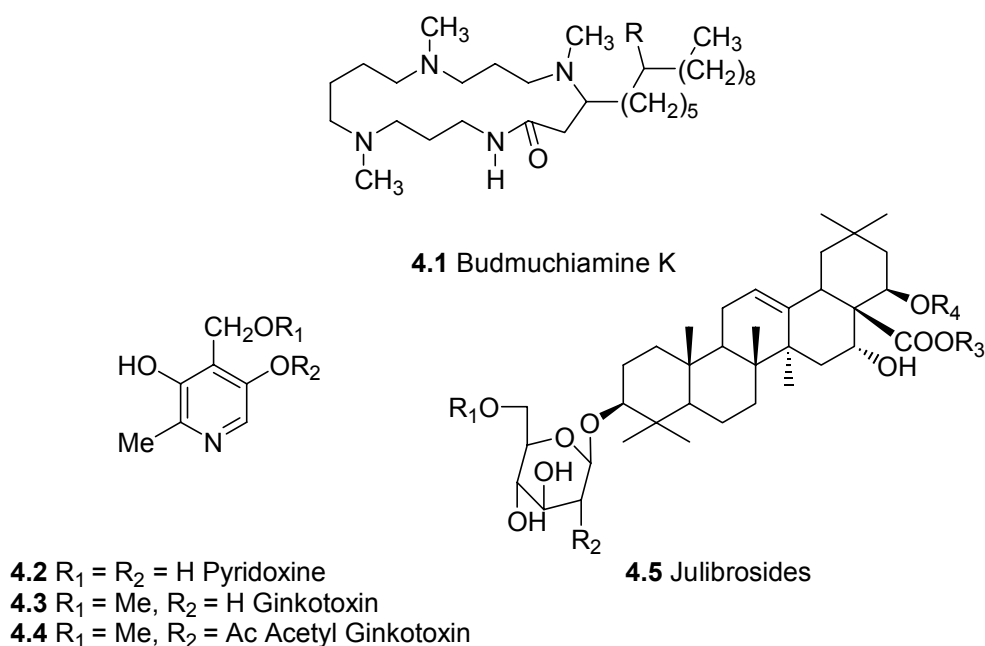


Figure 4-1. Natural Products from *Albizia* species

⁴ Yoshikawa, K.; Satou, Y.; Tokunaga, Y.; Tanaka, M.; Arihara, S.; Nigam, S.K. *J. Nat. Prod.* **1998**, *61*, 440.

⁵ Fiehe, K.; Arenz, A.; Drewke, C.; Hemscheidt, T.; Williamson, R.T.; Leistner, E. *J. Nat. Prod.* **2000**, *63*, 185.

The budmuchiamines (**4.1**)⁶ comprise an interesting class of alkaloids and appear to be responsible for some of the antibacterial activity, mammalian cytotoxicity, and shrimp lethality in *Albizia gummifera*. Unfortunately for the practitioners of traditional herbal medicine, the typical aqueous infusion would contain almost none of these lipophilic compounds. *N*-Methylation and the absence of a side chain hydroxyl group (i.e. R=H, not OH) are important for activity.

The pyridoxine (Vitamin B₆, **4.2**) derivative acetyl ginkotoxin (**4.4**) is also found in the seeds of a number of *Albizia* species.⁵ This compound and other analogs are potential inhibitors of enzymes dependent on various pyridoxyl cofactors. The most potent of these inhibitors is the neurotoxin ginkotoxin (**4.3**). Acetyl ginkotoxin may be responsible for the poisoning of livestock. This was dramatically verified when a number of poisoned sheep recovered when they were given large doses of Vitamin B₆.⁷

Most investigations of these species have involved *Albizia julibrissin* and have focused on the saponins isolated from this tree. Most saponins from *Albizia* sp. have the structural features of the julibrosides (**4.5**) with a glycoside moiety at C-3, a hydroxyl group at C-16, and terpenoid esters (R₄). It has been reported that these functionalities are crucial for the strong cytotoxicity versus the KB cell line. In addition, NH or NAc substitution at R₂ leads to stronger activity compared to the hydroxyl analog.^{3,6}

As noted earlier, only fifteen of some one hundred fifty species of *Albizia* have been investigated. Because of the interesting structures and bioactivities found in these species, it is likely that further investigations of this genus will lead to additional novel compounds with interesting bioactivities.

⁶ Rukunga, G.M.; Waterman, P.G. *J. Nat. Prod.* **1996**, *59*, 850.

⁷ Gummow, B.; Bastianello, S.S.; Labuschagne, L.; Erasmus, G.L. *Ond. J. Vet. Res.* **1992**, *59*, 111.

4.1.2 Chemical Investigations of *Albizia subdimidiata*.

Previous work on *Albizia subdimidiata* has not been reported. Work on *Albizia subdimidiata* in the Kingston group was initiated by Dr. Maged Abdel-Kader. He succeeded in isolating two cytotoxic saponins from a MeOH extract of *A. subdimidiata* stems and infructescence, (Figure 4-2) and tentatively assigned structures **4.6** and **4.7**. The resemblance of **4.6** and **4.7** to the julibrosides (**4.5**) is unmistakable. Partial hydrolysis of the saponins (Figure 4-3) led to a common aglycone, which was determined by FABMS and NMR to be oleanolic acid (**4.12**), two other triterpenoid products (**4.10**, **4.11**) which were not identified, and three sugars. The ^{13}C NMR signals of the sugar moieties in **4.6** were also comparable to those of saponins having similar sugar types and linkage sequences.⁴ Reduction and acetylation of the hydrolyzed sugars and comparison with sugar standards by GCMS permitted identification of the sugars. The sugars in **4.6** were identified as xylose, arabinose, and *N*-Ac glucosamine; the sugars in **4.7** were identified as arabinose and *N*-Ac glucosamine.

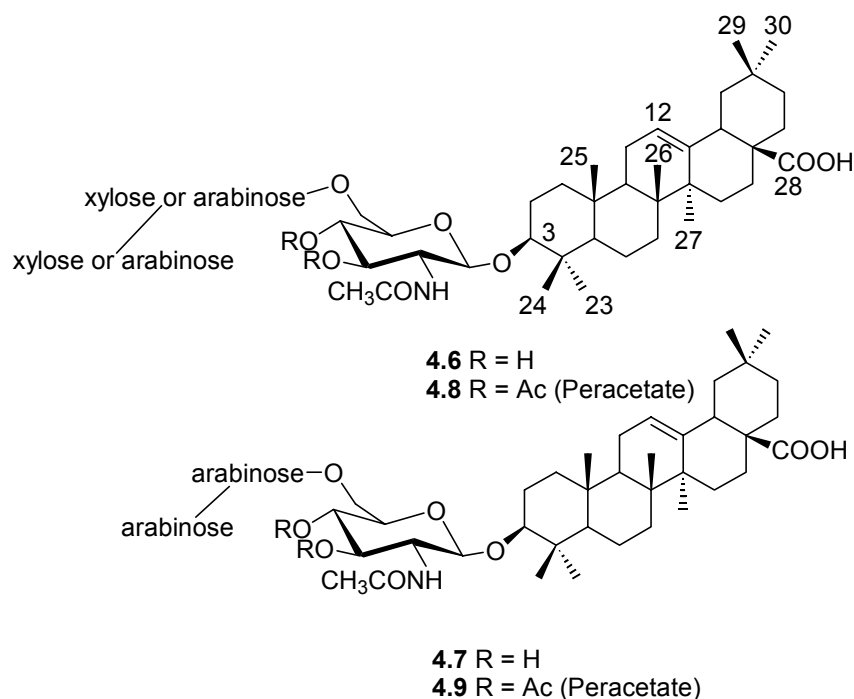


Figure 4-2. Previously Isolated and Prepared Samples from *Albizia subdimidiata*.

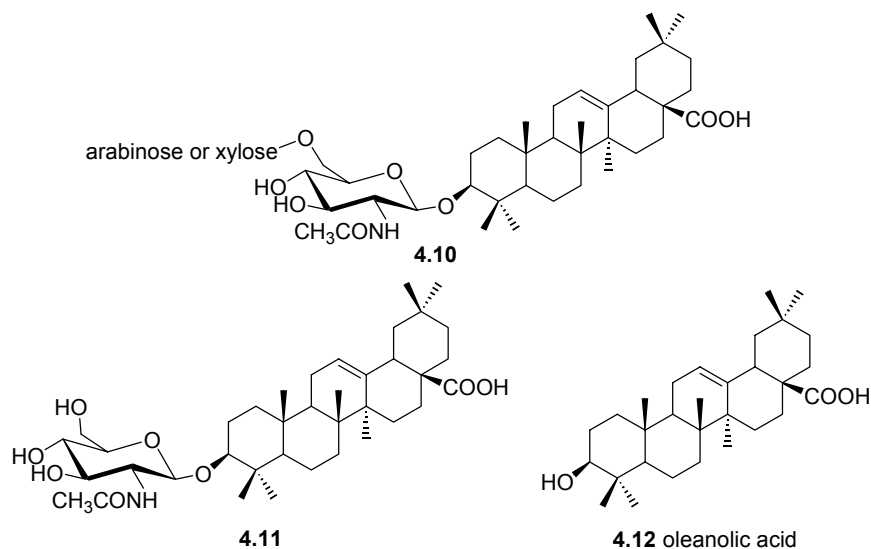


Figure 4-3. Hydrolysis Products of **4.6** and **4.7**

Permethylation of the saponins, followed by hydrolysis, reduction, peracetylation, and analysis by GCMS permitted the identification of the various saccharide linkages (Figure 4-4).⁸ The sequence of the sugar linkages was derived from analysis of the MS fragmentation of the methylated alditol acetates.⁹ Figure 4-4 shows the products separated by GC and the fragments generated by the EIMS detector. The presence of methoxy groups indicated the location of free hydroxy groups in the original saponins and the acetoxy groups indicated the location of glycosidic bonds. This allowed Dr. Abdel-Kader to deduce that the 2*N*-acetyl glucosamine (**4.13**) was unsubstituted at the C-3 and C-4 positions, the middle pentose derivative (**4.14**) was unsubstituted at the C-3 and C-4 positions, and the terminal pentose unit (**4.15**) was unsubstituted at the C-2, C-3 and C-4 positions. Not only were the essential linkage positions deduced, it was also apparent that the middle pentose derivatives (**4.14**) present in **4.6** and **4.7** in the pyranose

⁸ Jansson, P.-E.; Kenne, L.; Liedgren, H.; Lindberg, B.; Lonngren, J. *Chem. Commun.* **1976**, 8, 14.

rather than the furanose form since the C-4 positions was unsubstituted. The ring size could not be determined for the terminal pentoses (**4.15**), however, as the fragment ions necessary to determine this were not visible. The ring size of the terminal sugar was thus assigned by the positions of its anomeric carbon signal in the ^{13}C NMR spectra. The corresponding signals for the remaining anomeric carbons confirmed that all three sugars were in the pyranose form.

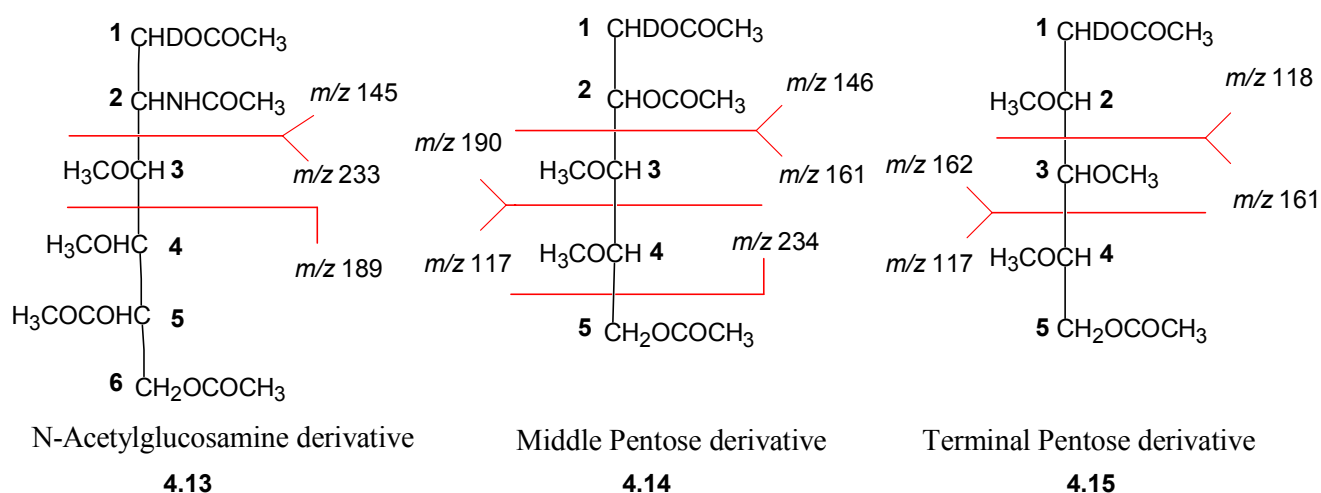


Figure 4-4. Linkage Analysis via Derivatization and GCMS

The sugar linkages were clarified by Dr. Abdel-Kader by acetylation of **4.6** and **4.7** to their peracetate derivatives followed by analysis of the ^1H NMR spectra of the products. The changes in the chemical shifts of the carbohydrate protons on acetylation made it possible to assign key signals in a COSY spectrum. This spectrum showed a correlation between H-5 signal of *N*-acetylglucosamine (δ 4.22, dd, $J = 2.1, 5.7$ Hz) and both of its unshifted H-6 proton signals (δ 3.512, dd, $J = 11.8, 9.2$ Hz; 4.18, dd, $J = 5.9, 11.8$ Hz). A second important correlation was observed between H-1 signal of the middle

⁹ a. Needs, P.W.; Selvendran, R.R. *Phytochem. Anal.* **1993**, *4*, 210. a. Jay, A. *Carbohydr. Chem.* **1996**, *15*, 897.

pentose (δ 4.57, d, $J=$ 5.9 Hz) and its unshifted H-2 signal (δ 3.82, m, overlapped with other protons) indicating that the terminal pentose is attached to the C-2 of the middle pentose linked to C-6 of *N*-acetylglucosamine (Figure 4-5).

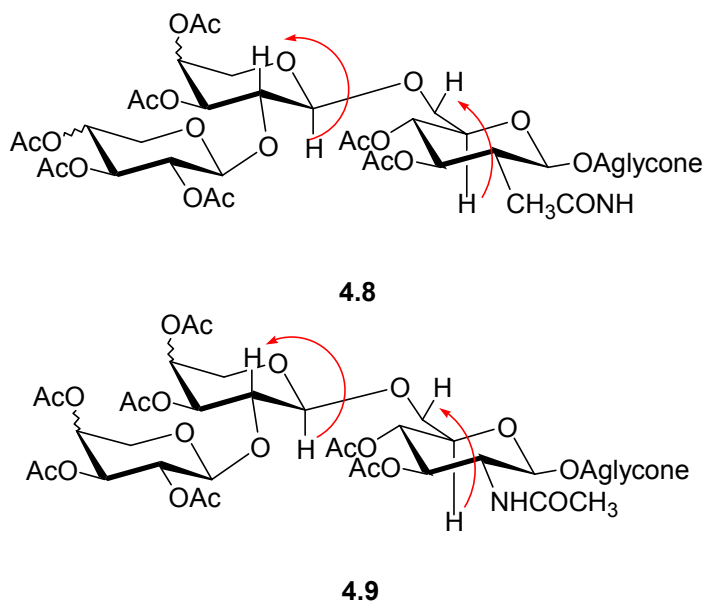


Figure 4-5. COSY Correlations Important for Linkages

The glucosamine was assigned as D-glucosamine on the basis of the conversion of **4.6** and **4.7** to the known monoside **4.11**.¹⁰

The linkages and assignment of the structures were confirmed by HMBC spectra. Compound **4.7** has been previously reported.¹¹ The structure of the saponin was confirmed as **4.7** by comparison of its spectroscopic data with those of the same compound that had been previously isolated from *Calliandra anomala*¹² and

¹⁰ Adesina, S. K.; Reisch, J. *Phytochemistry* **1985**, *24*, 3003-3006.

¹¹ a. McBrien, K. D.; Bery, R. L.; Lowes, S. E.; Nedderman, K. M.; Bursuker, I.; Huang, S.; Klohr, S. E.; Leet, J. E. *J. Antibiot.* **1995**, *48*, 1446. b. Maillard, M.; Adewunmi, C. O.; Hostettmann, K. *Helv. Chim. Acta* **1989**, *72*, 668.

¹² Tani, C.; Ogihara, Y.; Mutuga, M.; Nakamura, T.; Takeda, T. *Chem. Pharm. Bull.* **1996**, *44*, 816.

Pithecellobium racemosum.¹³ At this time, compound **4.6** has not been reported; it has been assigned the name albiziatrioside A.

Although Dr. Abdel-Kader's work established the basic structure of albiziatrioside A, there were a number of important structural and stereochemical features that needed to be established before the work could be considered complete. These included the absolute stereochemistries of the sugars and the complete structural characterization of the bioside **4.10** and the monoside **4.11**. Dr. Abdel-Kader was unable to carry out these studies because of his return to Egypt, and the work was thus undertaken as part of the present investigations. This work required the reisolation of compounds **4.6** and **4.7** and the isolation processes used is thus included here even though it closely follows that of Dr. Abdel-Kader.

4.2 Results and Discussion.

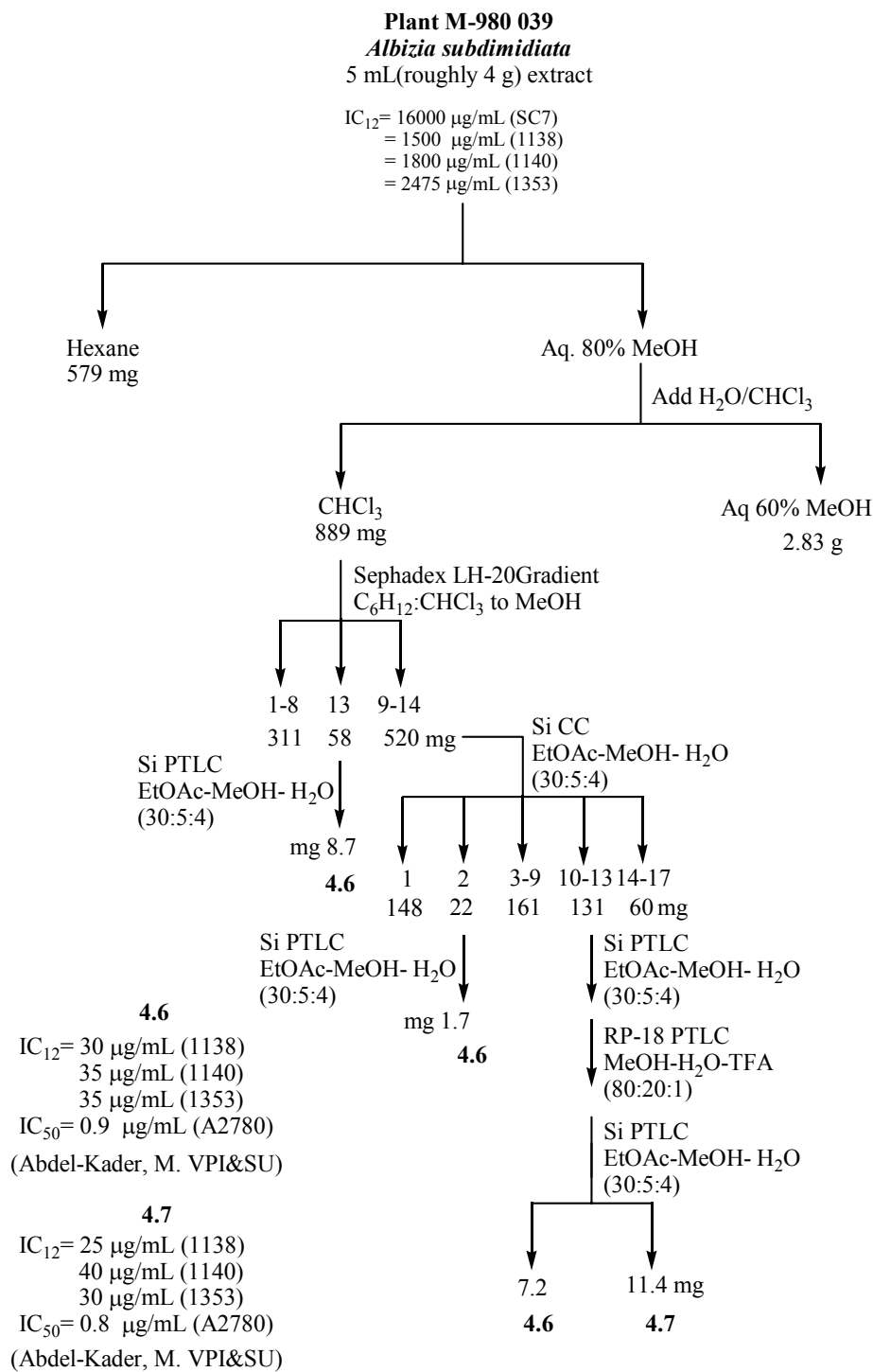
4.2.1 Isolation of Saponins from *Albizia Subdimidiata*.

As previously noted, additional quantities of **4.6** and **4.7** were required to complete the structural elucidation. The MeOH extract of *A. subdimidiata* infructescence (M980039) was subjected to liquid-liquid partitioning (Scheme 2) in a similar manner to that used by Dr. Abdel-Kader.¹⁴ The reportedly bioactive chloroform fraction was then deposited onto a Sephadex LH-20 column, which was eluted with a gradient of increasing polarity from hexane-CHCl₃ (1:1) to pure MeOH. TLC monitoring of the fractions by silica gel (EtOAc-MeOH-H₂O) permitted the identification of a number of fractions contained compounds with the desired approximate R_f (0.3). These fractions were then subjected to further purification; one sample (#13 out of 14 samples)

¹³ Khan, I.A.; Clark, A.M.; McChesney, J.D. *Pharm. Res.* **1997**, *14*, 358.

was pure enough to be separated by PTLC to yield 8.7 mg of **4.6**. The purification of the fractions after this point was also monitored by ^1H NMR spectroscopy. Observation of the anomeric proton signals indicated the purity of the fractions. The remaining material (fractions 9-14) was subjected to normal phase chromatography and reverse phase chromatography. When 1% TFA was added to the reverse phase column to improve the separation, ^1H NMR signals of the purified products were unusually shifted but no hydrolysis was observed by TLC or ^1H NMR analysis. Repurification of the samples by normal phase PTLC yielded 7.2 mg of **4.6** and 11.4 mg of **4.7** and the unusual ^1H shifts were no longer observed.

¹⁴ Personal communications from Dr. Maged Abdel-Kader (University of Alexandria, Egypt) to John Berger (VPI&SU).



Scheme 2. Isolation Tree for *Albizia* Saponins

4.2.2 Further Characterization of Saponins from *Albizia Subdimidiata*.

The major fragment in the negative ion FABMS of the isolated **4.6** (C₄₈H₇₇NO₁₆) displayed a m/z 933 (M-H⁺). The fragmentation pattern was characteristic of the loss of two pentoses followed by the loss of an *N*-acetylhexosamine. The negative ion FAB mass spectrum of **4.6** contained an ion at m/z 455, consistent with the presence of the common triterpene, oleanolic acid (**4.12**). The enhanced abundance of the negative ions compared to those of the corresponding positive ions in FABMS indicated the presence of an easily deprotonated species such as a carboxylic acid.

The identities of the isolated saponins were confirmed by comparison of its NMR data with those NMR data obtained by Dr. Abdel-Kader.¹¹ The ¹H NMR spectrum of the isolated **4.6** displayed signals for a number of methyl protons (δ 0.75, 0.86, 0.88, 0.94, 0.94, 0.96, 1.15, 1.95), a number of sugar protons (δ 3.0-4.1), a vinylic proton (δ 5.21) and three anomeric protons (δ 4.44 (d, $J=7.5$ Hz, 2H) and 4.52 (d, $J=5.5$ Hz, 1H)). The ¹³C NMR spectrum showed the presence of 48 carbon signals with heavy overlap in the sugar region. HETCOR and HMQC experiments were necessary to clearly define the 8 methyls, 13 methylenes, 18 methines, and 9 quaternary carbon signals.¹⁰ Anomeric proton signals were correlated with the anomeric carbon signals via HETCOR and HMQC.¹¹ An HMBC correlation between the signal for the anomeric proton of glucosamine at δ_H 4.44 and the signal for the C-3 carbon of oleanic acid at δ_c 90.27 indicated that the three sugars were attached to C-3. These results were all in agreement with those of Dr. Abdel-Kader.

The known compound **4.7** had spectroscopic data that were very similar to those of **4.6**. The only significant difference in the spectral data between **4.6** and **4.7** was that concerning the anomeric protons and carbons. The ¹H NMR spectrum of **4.6** possessed two signals for the three anomeric protons whereas in **4.7** there were three peaks for the

three anomeric protons. The shift (in ^{13}C NMR) of the terminal sugar anomeric carbon was also different (δ 105.84 in **4.6** compared to δ 106.47 in **4.7**).

4.2.3 *Characterization of Peracetylated Saponins*

Acetylation as previously performed by Dr. Abdel-Kader afforded the peracetates **4.8** and **4.9** respectively. These were analyzed by MALDI-TOF experiments and showed the presence of sodiated and potassiated molecular ions at m/z 1241 and 1259 respectively in the spectrum of each compound. These data are fully consistent with a molecular weight of 1218 for the parent peracetates.

4.2.4 *Partial Hydrolysis of Albizia Saponins*

Characterization of the hydrolysis products of **4.6** and **4.7** (**4.10**, **4.11** and **4.12**) was useful in that it confirms the identities of the sugars and the linkage order involved. While the connection of the acetyl glucosamine can be deduced from mass spectral information, mass spectrometry cannot determine the further linkages of **4.6**, since xylose and arabinose are isomers of each other.

Partial acid hydrolysis of the saponins **4.6** and **4.7** was previously performed by Dr. Abdel-Kader, but the products were not characterized by any method other than TLC and the method was not optimized. Further characterization was thus required and optimal experimental conditions determined. The experiments were repeated using 1% oxalic acid in aqueous methanol at 60 °C and with careful monitoring of the reaction by TLC.

Partial acid hydrolysis of both **4.6** and **4.7** yielded the same bioside (**4.10**) and monoside (**4.11**) along with the aglycone (**4.12**). Bioside **4.10** was isolated and characterized by FABMS (m/z 790 ($M-H^+$)) and by comparison of the 1H NMR data of its anomeric proton signals to those reported for the known saponin prosapogenin 10 from *Acacia concinna* (**4.16**).¹⁵ Monoside **4.11** was also isolated and characterized by 1H NMR (Table 8) and FABMS (M^- at m/z 659) as 3-*O*-2-acetamido-2-deoxy- β -D-glucopyranosyl oleanolic acid. These data indicate that **4.6** and **4.7** differ only in the terminal sugar, with a xylose in **4.6** and an arabinose in **4.7**.

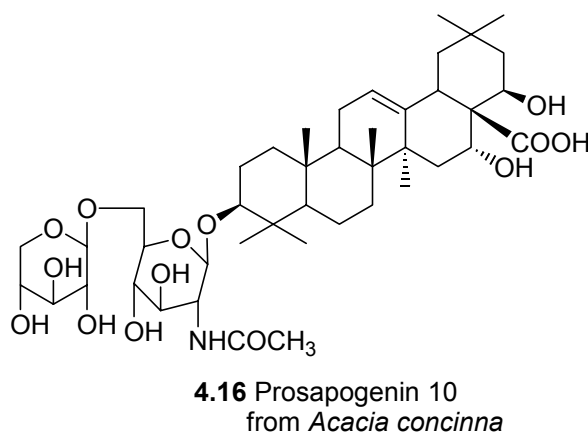


Figure 4-6. Prosapogenin 10 from *Acacia concinna*.

4.2.5 Determination of the Stereochemistries of the Pentose Sugars

The absolute stereochemistries of the hydrolyzed pentose sugars of **4.6** and **4.7** were determined by Hara's method, which involved preparing their thiazolidine peracetate derivatives (**4.21** and **4.23**) and comparison with standards by GCMS.¹⁶ Standard derivatives of arabinose were prepared by treatment of D and L-arabinose (**4.17**

¹⁵ a. Tezuka, Y.; Honda, K.; Banskota, A.H.; Thet, M.M.; Kadota, S. *J. Nat. Prod.* **2000**, *63*, 1658. b. Ikeda, T.; Fujiwara, S.; Araki, K.; Kinjo, J.; Nohara, T.; Miyoshi, T. *J. Nat. Prod.* **1997**, *60*, 102.

¹⁶ Hara, S.; Okabe, H.; Mihashi, K. *Chem. Pharm. Bull.* **1987**, *35*, 501.

and **4.18**) with methyl L-cysteine hydrochloride (**4.19**) in aqueous pyridine, which afforded the thiazolidines (**4.20** and **4.22**) in reasonable yield. The NMR spectra of each product indicated they were diastereomeric mixtures (with a diastereomeric ratio ranging from 1:1 to 8:2); these ratios were comparable to those reported in the literature.¹⁸ Column chromatography could not separate the diastereomeric mixtures. The original paper reported that the products were purified by recrystallization from ethanol, but attempts to repeat this work were not successful. The product mixtures (**4.20** and **4.22**) were therefore characterized by NMR and employed as such in the next reactions. The ¹H NMR signals were assigned on the basis of the literature.¹⁸ APT was used to identify C-2 and C-7 and HMQC was used to identify H-2 (a and e) and H-7. The remaining protons were then assigned by COSY and the corresponding carbons were assigned by HMQC. The acetates (**4.21** and **4.23**) were then prepared by treating the thiazolidines (**4.20** and **4.22**) with acetic anhydride and pyridine followed by purification by silica gel chromatography. NMR spectroscopy was used to characterize the acetates in a similar fashion as the unsubstituted thiazolidines. These spectra indicated that the products were also diastereomeric mixtures. Separation was attempted by reverse phase HPLC, but this was not successful. Analysis of each of the individual standards by GCMS gave a clean chromatogram with a single peak, even though the original arabinose thiazolidines (**4.20** and **4.22**) were individually diastereomeric mixtures. The analysis was monitored by total ion current (TIC) and mass filtering at *m/z* 146, which was reported as a major fragment ion for these standards. Co-injection of the two standards resulted in two well-resolved peaks. Since the GCMS peaks were adequately resolved, the prepared acetates were used to characterize the stereochemistries of the saponin pentoses.

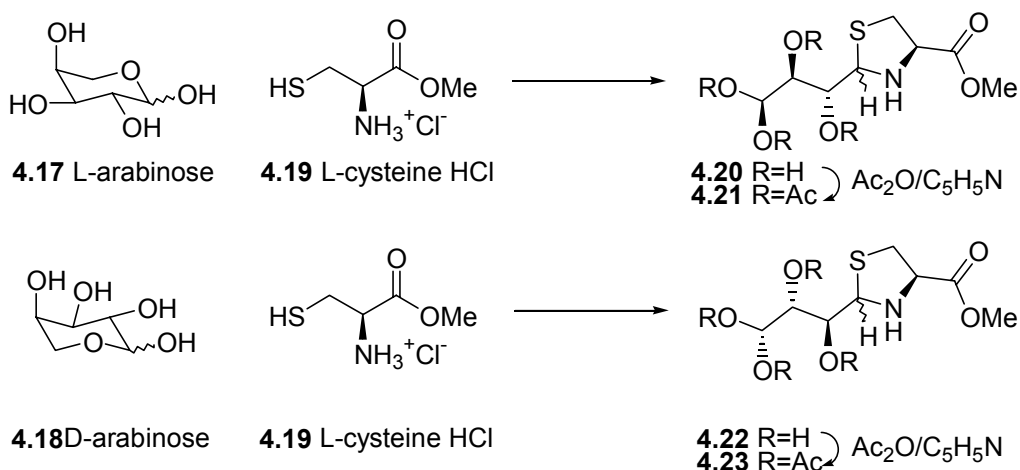


Figure 4-7. Preparation of Standards for GCMS Analysis of Sugars

Standard xylose thiazolidine acetate derivatives were prepared in a similar fashion to that of the arabinose thiazolidine standards with some minor modifications. The xylose thiazolidines were prepared as described above, but the resulting products were neither crystalline nor pure; the products were thus separated by silica gel chromatography (MeOH-CHCl₃, 3:97) to afford yellow oils. NMR analysis indicated that the products were diastereomeric mixtures with diastereomeric ratios about 1:1. Acetylation gave a mixture of diastereomeric acetates in each case that could not be separated chromatographically. Analysis of the individual standard mixtures by GCMS gave a clean chromatogram with a single peak even though the original thiazolidines were diastereomeric mixtures. Coinjection of the two xylose standards resulted in two well resolved peaks. Since the GCMS peaks were adequately resolved, the acetates were used to characterize the stereochemistries of the saponin pentoses. Although the standard acetates from D and L-arabinose and from D and L-xylose could be separated, it turned out that the standards from L-arabinose and D-xylose gave overlapping peaks on our

column. These were however clearly separated from the peaks from L-arabinose and L-xylose standards. This phenomenon has previously been reported for this method.¹⁶

The thiazolidine acetates of the sugars from **4.6** were prepared by reaction of the acid hydrolyzate of **4.6** with L-cysteine hydrochloride, followed by acetylation. Analysis of the products of this reaction by GCMS (mass filtering at m/z 146) showed the presence of only a single peak corresponding to the L-xylose and/or L-arabinose derivatives, thus clearly indicating the absence of L-xylose and D-arabinose in **4.6**. Since the previously reported GCMS data proved the presence of xylose and arabinose in the hydrolyzate, the absolute configurations of the hydrolyzed pentoses were assigned as L-arabinose and D-xylose. A similar experiment with **4.7** confirmed that both its hydrolyzed pentoses were L-arabinose.

A stereochemical determination was not performed on the hydrolyzed 2-*N*-Ac glucosamine since there are currently no reported instances of L-glucosamine occurring in Nature. In addition, the structural assignment of the monoside **3.11** was secure, because it had identical spectroscopic data to a literature compound that was assigned to the same structure.

4.2.6 *Biological Evaluation of Saponins*

Compounds **4.6** and **4.7** showed some activity in our yeast bioassay (Scheme 2); this activity was only moderate and appears to be unspecifically antifungal (i.e. no correlation to topoisomerase activity). In a cytotoxicity test using the A2780 cell line, both compounds showed significant cytotoxicity, with IC_{50} values of 0.9 and 0.8 $\mu\text{g/mL}$ for compounds **4.6** and **4.7**, respectively. As a general rule, activity of less than 1 $\mu\text{g/mL}$ for any of the bioassays is required to provoke interest, thus **4.6** and **4.7** is just interesting enough to warrant further testing. However, since they belong to a known class of

compounds which has failed to yield any anticancer drugs in the past it is unlikely that they will be developed further. The bioside (**4.10**) and the monoside (**4.11**) were also tested in the 1138 mutant yeast assay; the bioside significantly less active ($IC_{12}=1000$ $\mu\text{g/mL}$) than the parent compounds. The monoside was inactive in the same assay.

3.2 Experimental Section

The spectroscopic data of compounds **4.6-9** were originally obtained by Dr. Abdel-Kader but the data reported here are for the samples reisolated by the author. Compounds **4.8** and **4.9** were prepared by Dr. Abdel-Kader but additional spectroscopic data were obtained by the author. The remaining compounds were prepared and characterized by the author, and the determination of sugar stereochemistries was also carried out by the author.

General Experimental Procedures. General experimental procedures were essentially identical to that reported earlier.¹⁸ FAB and GC mass spectra were obtained on a VG 7070 E-HF mass spectrometer. HRFAB mass spectra were obtained on a Kratos MS50 mass spectrometer, and MALDI-TOF spectra were obtained on a Kratos Kompact SEQ instrument.

Yeast Bioassays. The bioassays were carried out as previously described.¹⁷

Cytotoxicity Bioassay. The *in-vitro* antitumor cytotoxicity assays were performed at Bristol-Myers Squibb Pharmaceutical Research Institute as previously described.¹⁷

¹⁷ Chapter 2.

Plant Material. The infructescences of *Albizia subdimidiata* (Fabaceae) were collected in the Paramaribo district on the Backboord property, Suriname, in April 1998. Voucher specimens are deposited in the National Herbarium of Suriname, Paramaribo, Suriname, and the Missouri Botanical Garden, St. Louis, Missouri.

Extraction and Isolation. Extracts of the infructescences for screening were prepared with EtOAc and MeOH by Bedrijf Geneesiddelen Voorziening, Suriname and sent for bioassay and isolation work to VPI&SU; the methanol extract was supplied to VPI&SU as BGVS M980039. The MeOH extract of the infructescences (4 g) was reported to have activities of IC₁₂ values of 1500, 1800, 2475, and 16000 µg/mL against the 1138, 1140, 1353 and Sc-7 yeast strains. The extract was dissolved in 80% aqueous MeOH and extracted with hexane (200 mL x 3). The aqueous MeOH fraction was diluted with H₂O to 60% aqueous MeOH and extracted with CHCl₃ (200 mL x 3). All of the fractions were then dried by rotary evaporation. The CHCl₃ fraction (889 mg) was purified by chromatography on Sephadex LH-20 (100 g) using the following solvents (approximately 200 mL each): hexane-CHCl₃ (1:1), hexane-CHCl₃ (1:3), CHCl₃, CHCl₃-MeOH(100:1), CHCl₃-MeOH(97:3), CHCl₃-MeOH(95:5), CHCl₃-MeOH(90:10), CHCl₃-MeOH(80:20), CHCl₃-MeOH(70:30), CHCl₃-MeOH(50:50) and MeOH. The fractions containing material with an R_f of 0.2-0.3 (Si TLC with EtOAc-MeOH-H₂O(30:5:4)) were combined and refractionated using a flash Si gel column using EtOAc-MeOH-H₂O(30:5:4) as an eluant. One fraction (#13 out of 14, R_f 0.266) was purified with Si PTLC (EtOAc-MeOH-H₂O (30:5:4)) to afford 8.7 mg of **4.6**. Two sets of fractions (22, 131 mg) were subjected individually to preparative TLC (Si gel, EtOAc-MeOH-H₂O, 30:5:4) with careful slicing to separate the bands of **4.6** and **4.7**; one purification obtained 1.7 mg of **4.6**. The second purification was subjected to reverse phase PTLC (MeOH-H₂O-TFA(80:20:1)) followed

by normal phase PTLC (Si gel, EtOAc-MeOH-H₂O, 30:5:4) affording 7.2 mg of **4.6** and 11.4 mg of **4.7**.

Albiziatrioside A (3-O-β-D-Xylopyranosyl(1→2)-α-L-arabinopyranosyl(1→6)-2-acetamido-2-deoxy-β-D-glucopyranosyl oleanolic acid (4.6) : Amorphous powder, mp 272-274 °C; $[\alpha]_D^{26} + 30^0$ (*c* 1.0, MeOH); IR (film) ν_{\max} 3373 (OH), 2942, 1658 (COOH), 1642, 1550 (NHCO) cm⁻¹; ¹H NMR see Table 8; ¹³C NMR see Table 9; FABMS *m/z* 923 (10), 922 (M-1)⁻ (18), 791 (M-Xyl)⁻ (13), 659 (M-Xyl-Ara)⁻ (32), 483 (47), 455 (C₃₀H₄₇O₃, aglycone)⁻ (100), 438 (aglycone-H₂O)⁻ (55); HRFABMS *m/z* 946.514 (M+Na)⁺ (calcd for C₄₈H₇₇NO₁₆Na, 946.514).

3-O-α-L-Arabinopyranosyl(1→2)-α-L-arabinopyranosyl(1→6)-2-acetamido-2-deoxy-β-D-glucopyranosyl oleanolic acid (4.7): Amorphous powder, dec. at 275 °C; $[\alpha]_D^{26} + 39^0$ (*c* 1.0, MeOH); IR (film) ν_{\max} 3376 (OH), 2940, 1670 (COOH), 1639, 1551 (NHCO) cm⁻¹; ¹H NMR see Table 8; ¹³C NMR see Table 9; FABMS *m/z* 923 (10), 922 (M-1)⁻ (20), 791 (M-Xyl)⁻ (70), 659 (M-Xyl-Ara)⁻ (58), 483 (55), 455 (C₃₀H₄₇O₃, aglycone)⁻ (100), 438 (aglycone-H₂O)⁻ (60); HRFABMS *m/z* 946.515 (M+Na)⁺ (calcd for C₄₈H₇₇NO₁₆Na, 946.514).

Partial Hydrolysis of 4.6 and 4.7. Compounds **4.6** and **4.7** (4 mg each) were treated separately with 10 mg of oxalic acid in 1 mL MeOH-H₂O (1:1) at 60 °C with reaction monitoring by TLC. After 48 hours the products were dried, suspended in EtOAc (*via* sonication) and purified by preparative Si gel TLC (EtOAc-MeOH-H₂O, 30:5:4) to give bioside **4.10** (1.0 mg from **4.6** and 0.9 mg from **4.7**) and monoside **4.11** (detected but not

isolated). In a separate experiment a mixture of **4.6** and **4.7** (4 mg) was hydrolyzed under similar conditions to give **4.10** (1.1 mg) and **4.11** (0.9 mg).

3-O- α -L-arabinopyranosyl(1 \rightarrow 6)-2-acetamido-2-deoxy- β -D-glucopyranosyl

oleanolic acid (3.10): ^1H NMR see Table 8; FABMS $^-$ m/z 790 (M-H, 82), 686 (16), 658 (M-ara-1, 55), 640 (23), 483 (34), 455 (C₃₀H₄₇O₃, 100).

3-O-2-Acetamido-2-deoxy- β -D-glucopyranosyl oleanolic acid (4.11): ^1H NMR see Table 8; ^1H -NMR spectrum in pyridine- d_5 matches literature data;¹⁸ FABMS m/z 660 (M $^+$ +H, 10), 659 (M $^+$, 4), 658 (M $^+$ -H, 6), 455 (aglycone, C₃₀H₄₇O₃, 16), 454 (36), 453 (100), 439 (C₃₀H₄₇O₂, 32), 437 (42).

Acetylation of 4.6 and 4.7. Compounds **4.6** and **4.7** (5 mg each) in pyridine (0.5 mL) were treated separately with Ac₂O (0.2 mL) for 24 h at room temperature. Evaporation of the resulting solutions under a stream of argon yielded chromatographically (Si gel, EtOAc-MeOH-H₂O) homogeneous acetates **4.8** and **4.9**.

3-O- β -D-Xylopyranosyl(1 \rightarrow 2)- α -L-arabinopyranosyl(1 \rightarrow 6)-2-acetamido-2-deoxy- β -D-glucopyranosyl oleanolic acid peracetate (4.8): ^1H NMR see Table 8; MALDI-TOF m/z 1257 (M+K) $^+$ (47), 1241 (M+Na) $^+$ (100).

¹⁸ Maillard, M.; Adewunmi, C.O.; Hostettmann, K. *Helv. Chim. Acta* **1989**, *72*, 668.

3-O- α -L-Arabinopyranosyl(1 \rightarrow 2)- α -L-arabinopyranosyl(1 \rightarrow 6)-2-acetamido-2-deoxy- β -D-glucopyranosyl oleanolic acid peracetate (4.9): ^1H NMR see Table 8; MALDI-TOF m/z 1241(M+Na) $^+$ (100).

Determination of the Stereochemistries of Pentoses by GCMS. Methyl 2-(D- and L-arabino-tetrahydroxybutyl)-thiazolidine-carboxylates and methyl 2-(D- and L-xylo-tetrahydroxybutyl)-thiazolidine-carboxylate standards were individually synthesized as follows:¹⁶ 0.58 g of L-cysteine methyl ester hydrochloride, 0.50 g of pentose and 0.3 mL pyridine were placed in 1 mL of H₂O and allowed to sit overnight. The arabinose derivatives crystallized when washed with large volumes of EtOH; the products of the derivatizations of the xyloses were yellow oils and were purified by Si gel column chromatography using MeOH-CHCl₃ (3:97) as an eluant. The acetates of these compounds were prepared by treating 100 mg of a thiazolidine with 0.5 mL of acetic anhydride and 0.5 mg of pyridine overnight at room temperature, followed by dilution with 50 mL each of water and CHCl₃. The mixture was shaken, the CHCl₃ layer collected, washed, dried, and evaporated, and the product purified by PTLC (Si gel, Hexane-EtOAc, 1:1). The compositions of the products were confirmed by FABMS. The corresponding derivatives of **4.6** and **4.7** were prepared by first hydrolyzing 1-2 mg each of **4.8** and **4.9** overnight at 100 °C in MeOH-1N HCl (1:1, 500 μ L), followed by extraction with H₂O-CHCl₃ and evaporation of the water-soluble fraction. This fraction was then treated with pyridine (500 μ L) and L-cysteine methyl ester hydrochloride (6 mg) and the mixture stirred overnight at room temperature. Ac₂O (300 μ L) was then added and the mixture was allowed to react overnight at room temperature. The solvent was removed in a stream of argon. Both standards and samples were analyzed by GCMS using a HP5 capillary column (60 m x 0.25mm i.d., 0.32 μ M film) with an initial

temperature of 75 °C, programmed to 250 °C at 10 °C/minute. Retention times of 26.50 (D-arabinose) 26.57 (L-arabinose and D-xylose) and 26.93 minutes (L-xylose) were observed for the standards. The chromatograms were monitored in the positive ion mode both by TIC and by selective ion monitoring at m/z 146, a major fragment ion. The thiazolidine derivatives from **4.6** resulted in a single peak at 26.44 minutes indicating (with previous GCMS data) the presence of L-arabinose and D-xylose stereochemistries. The thiazolidine derivatives from **4.7** resulted in a single peak at 26.42 minutes indicating the presence of L-arabinose and L-arabinose stereochemistries.

Methyl 2-(L-arabino-tetrahydroxybutyl)-thiazolidine-carboxylate (mixture): white solid, mp 145-146 °C; lit. 155-156 °C;¹⁶ yield 0.50 g (66%); ¹H NMR (C₅D₅N) δ 5.66 (H-2(S), d, J = 5.8 Hz, 0.2H) 5.42 (H-2(R), d, J = 5.7 Hz, 0.8 H), 4.85 (H-1'(R), bd, J = 4.6 Hz, 0.8 H), 4.65 (H-1'(S), t, J = 7.1 Hz, 0.2 H), 4.52 (H-2', dd, 11.4, 4.1), 4.42 (H-3', dd, 7.5, <2 Hz, 1H), 4.37 (H-4(S), dd, J =10.5, 5.7 Hz, 0.2 H), 4.10 (H-4(R), dd, J = 7.5, <2 Hz, 0.8 H), 3.58 (Me, s, 3 H), 3.32 (H-5a, dd, J = 9.4, 7.5 Hz, 1 H), 3.06 (H-5e, dd, J = 9.4, <2 Hz, 1 H) ; ¹³C NMR (C₅D₅N) δ 172.16 (COOMe), 74.9 (C-4), 73.51 (C-3'), 73.09(C-2'), 65.17 (C-4'), 65.17 (C-2), 51.99 (OMe), 37.42 (C-5); FABMS m/z 268 (M⁺) (50), 236 (9), 160 (13), 150 (20), 146 (C₅H₈NO₂S)⁺ (30), 136 (methyl cysteine)⁺ (22).

Methyl 2-(L-arabino-tetrahydroxybutyl)-thiazolidine-carboxylate peracetate: white solid; yield 56 mg (37%); ¹H NMR (CDCl₃) δ 5.42 (H-2(S), d, J = 6.4 Hz, 1H), 4.896 (H-2(R), dd, J = 9.2, 6.9 Hz, H), 4.56-4.54 (H-4', H-3', H-2', m, 4 H), 4.50 (H-1', dd, J =10.8, 5.3 Hz, 1 H), 4.01 (H-4, dd, J = 9.2, 6.9 Hz, 1 H), 3.60 (Me, s, 3 H), 3.32 (H-5a, dd, J = 10.1, 6.9 Hz, 1 H), 3.06 (H-5e, dd, J = 9.7, <2 Hz, 1 H), 2.19 (OAc, s, 3 H), 2.13 (OAc, s, 3 H), 2.08 (OAc, s, 3 H), 2.06 (OAc, s, 3 H), 2.03 (OAc, s, 3 H); ¹³C NMR (CDCl₃) δ

170.67 (COOMe), 169.99 (OAc), 169.96 (OAc), 169.93 (OAc), 169.72 (OAc), 169.20 (OAc), 71.67 (C-4), 68.87 (C-3'), 68.87 (C-2'), 61.47 (C-4'), 63.35 (C-1), 63.09 (C-2), 52.75 (Me), 31.92 (C-5), 22.32 (Me-OAc), 20.99 (Me-OAc), 20.75 (2 Me-OAc), 20.62 (Me-OAc); FABMS m/z 479 (M+Na)⁺ (18), 436 (M⁺) (4), 418 (4), 316 (15), 214 (43), 188 (48), 146 (C₅H₈NO₂S)⁺ (100), 136 (methyl cysteine)⁺ (33).

Methyl 2-(D-arabino-tetrahydrobutyl)-thiazolidine-carboxylate (mixture): white solid, mp 150-151 °C; lit. 156-159 °C;¹⁶ yield 0.52 g (68%); ¹H NMR (C₅D₅N) δ 5.39 (H-2(S), d, J = 6.4 Hz, 1 H), 4.96 (H-2(R), dd, J = 9.2, 6.9 Hz, 1 H), 4.56-4.49 (H-4', H-3', H-2', m, 4 H), 4.01 (H-4, dd, J = 9.2, 6.9 Hz, 1 H), 3.60 (Me, s, 3 H), 3.32 (H-5a, dd, J = 10.1, 6.9 Hz, 1 H), 3.06 (H-5e, dd, J = 9.7, <2 Hz, 1 H); ¹³C NMR (C₅D₅N) δ 172.06 (COOMe), 75.15 (C-1), 73.72 (C-6), 72.89(C-5), 65.73 (C-7), 65.73 (C-4), 65.15 (C-3), 51.98 (Me), 37.26 (C-2); FABMS m/z 268 (M⁺) (31), 236 (4), 160 (8), 150 (5), 146 (C₅H₈NO₂S)⁺ (14), 136 (methyl cysteine)⁺ (11).

Methyl 2-(D-arabino-tetrahydrobutyl)-thiazolidine-carboxylate peracetate:

Slightly yellowish solid; yield 56 mg (37%); ¹H NMR (CDCl₃) 5.42 (H-3(S), d, J = 6.4 Hz, 1 H), 4.896 (H-3(R), dd, J = 9.2, 6.9 Hz, 1 H), 4.56-4.54 (H-4', H-3', H-2', m, 4 H), 4.50 (H-1', dd, J =10.8, 5.3 Hz, 1 H), 4.01 (H-4, dd, J = 9.2, 6.9 Hz, H), 3.60 (Me, s, 3 H), 3.32 (H-5a, dd, J = 10.1, 6.9 Hz, 1 H), 3.06 (H-5e, dd, J = 9.7, <2 Hz, 1 H), 2.10 (OAc, s, 3 H), 2.03 (OAc, s, 3 H), 1.98 (OAc, s, 3 H), 1.96 (2 OAc, s, 6 H); ¹³C NMR (CDCl₃) δ 171.07 (COOMe), 170.56 (OAc), 170.21 (OAc), 170.16 (OAc), 169.96 (OAc), 169.76 (OAc), 69.08 (C-4), 69.02 (C-3'), 68.30 (C-2'), 62.53 (C-4'), 63.69 (C-1'), 63.15 (C-2), 53.22 (Me), 34.41 (C-5), 22.35 (Me-OAc), 21.05 (Me-OAc), 20.94 (Me-OAc), 20.88

(Me-OAc), 20.72 (Me-OAc); FABMS m/z 479 (M+Na)⁺ (10), 436 (M⁺) (4), 418 (2), 316 (21), 214 (83), 188 (57), 146 (C₅H₈NO₂S)⁺ (100), 136 (methyl cysteine)⁺ (43).

Methyl 2-(L-xylo-tetrahydroxybutyl)-thiazolidine-carboxylate: yellow oil; yield 0.29 g (38%); FABMS m/z 268 (M⁺) (18), 160 (17), 150 (11), 146 (C₅H₈NO₂S)⁺ (23), 136 (methyl cysteine)⁺ (26).

Methyl 2-(L-xylo-tetrahydroxybutyl)-thiazolidine-carboxylate peracetate: off white solid; yield 32 mg (42%); FABMS m/z 478 (M+Na)⁺ (3), 436 (M⁺) (2), 418 (8), 316 (14), 214 (30), 188 (17), 146 (C₅H₈NO₂S)⁺ (100), 136 (methyl cysteine)⁺ (37).

Methyl 2-(D-xylo-tetrahydroxybutyl)-thiazolidine-carboxylate: yellow oil; yield 0.43 g (57%); FABMS m/z 268 (M⁺) (20), 160 (38), 150 (23), 146 (C₅H₈NO₂S)⁺ (61), 136 (methyl cysteine)⁺ (40).

Methyl 2-(D-xylo-tetrahydroxybutyl)-thiazolidine-carboxylate peracetate: off white solid; yield 34 mg (44%); FABMS m/z 478 (M+Na)⁺ (10), 436 (M⁺) (4), 418 (4), 316 (19), 214 (60), 188 (35), 146 (C₅H₈NO₂S)⁺ (100), 136 (methyl cysteine)⁺ (36).

Table 8. Selected ¹H NMR Data for Compounds **4.6-4.11**.^a

Positions	4.6	4.7	4.8	4.9	4.10	4.11
12	5.21 (1H, s)	5.21 (1H, s)	5.21 (1H, s)	5.22 (1H, s)	5.22 (1H, s)	5.23 (1H, s)
23	0.96 (3H, s)	0.96 (3H, s)	0.96 (3H, s)	0.96 (3H, s)	0.95 (3H, s)	1.03 (3H, s)
24	0.94 (3H, s)	0.93 (3H, s)	0.94 (3H, s)	0.94 (3H, s)	0.92 (3H, s)	0.93 (3H, s)
25	0.86 (3H, s)	0.85 (3H, s)	0.83 (3H, s)	0.83 (3H, s)	0.89 (3H, s)	0.86 (3H, s)
26	0.75 (3H, s)	0.75 (3H, s)	0.76 (3H, s)	0.77 (3H, s)	0.76 (3H, s)	0.81 (3H, s)
27	1.15 (3H, s)	1.15 (3H, s)	1.16 (3H, s)	1.17 (3H, s)	1.16 (3H, s)	1.15 (3H, s)
29	0.88 (3H, s)	0.88 (3H, s)	0.89 (3H, s)	0.92 (3H, s)	0.90 (3H, s)	0.90 (3H, s)
30	0.94 (3H, s)	0.94 (3H, s)	0.94 (3H, s)	0.93 (3H, s)	0.96 (3H, s)	0.97 (3H, s)
GluNAc H-1	4.44 (d, <i>J</i> = 7.5 Hz)	4.43 (d, <i>J</i> = 8.4 Hz)	4.57 (d, <i>J</i> = 6.0 Hz)	4.65 (d, <i>J</i> = 8.4 Hz)	4.43 (d, <i>J</i> = 8.5 Hz)	4.42 (d, <i>J</i> = 7.6 Hz)
Ara H-1	4.52 (d, <i>J</i> = 5.5 Hz)	4.55 (d, <i>J</i> = 5.8 Hz)	4.80 (d, <i>J</i> = 7.2 Hz)	4.80 (d, <i>J</i> = 6.8 Hz)	4.34 (d, <i>J</i> = 6.5 Hz)	-
Term. xyl H-1	4.44 (d, <i>J</i> = 7.5 Hz)	-	4.63 (d, <i>J</i> = 8.0 Hz)	-	-	-
Term. ara H-1	-	4.49 (d, <i>J</i> = 6.7 Hz)	-	4.49 (d, <i>J</i> = 5.6 Hz)	-	-
CH ₃ CONH	1.95 (3H, s)	1.95 (3H, s)	1.95 (3H, s)	1.95 (3H, s)	1.94 (3H, s)	1.97 (3H, s)

^a Obtained in CD₃OD. Chemical shifts in ppm from internal TMS, coupling constants in Hz.

Table 9. ^{13}C NMR Data for Compounds **4.6** and **4.7**^a in CD_3OD .

Position	4.6	4.7	Position	4.6	4.7
1	39.99	39.93	27	26.56	26.53
2	27.05	27.00	28	184.68	184.70
3	90.27	90.64	29	33.80	33.82
4	39.65	39.69	30	24.22	24.22
5	56.92	56.85	GluNAc		
6	19.35	19.38	1	104.85	104.93
7	29.05	29.05	2	57.72	57.63
8	40.53	40.53	3	76.59	76.34
9	49.13	49.11	4	72.24	72.96
10	37.93	37.92	5	75.68	75.67
11	24.57	24.59	6	69.59	69.47
12	122.99	122.96	Ara		
13	145.96	146.02	1	103.32	103.37
14	42.91	42.94	2	81.26	80.43
15	35.24	35.25	3	73.10	74.16
16	24.53	24.54	4	68.49	68.75
17	47.71	47.72	5	65.40	65.72
18	43.11	43.12	Terminal sugar	Xyl.	Ara.
19	47.76	47.78	1	106.47	105.84
20	31.71	31.72	2	75.69	71.95
21	34.06	34.08	3	77.50	73.41
22	34.10	34.91	4	71.05	69.65
23	28.57	28.56	5	67.20	67.11
24	15.97	16.00	$\underline{\text{C}}\text{H}_3\text{CONH}$	23.16	23.19
25	18.02	18.06	$\text{CH}_3\underline{\text{C}}\text{ONH}$	173.47	173.47
26	17.07	17.11			

^a Assignment made by combination of DEPT, HMQC data, and comparison with literature data.

V. PITTOVIRIDOSIDE, A NOVEL TRITERPENOID SAPONIN

FROM *PITTOSPORUM VIRIDIFLORUM*

5.1.1 Introduction.

While investigating rainforest flora for anticancer activity, a methanol extraction of *Pittosporum viridiflorum* collected in Madagascar showed activity versus our yeast based cell assays. Pittoviridoside (**5.7**), a novel saponin, was isolated and partially characterized by Dr. Youngwan Seo and found to be responsible for the activity of the extract. Dr. Seo returned to Korea before he could complete the structural elucidation of the pittoviridoside, thus this work was undertaken by the author.

5.1.1 Previous Investigations of *Pittosporum* species.

The *Pittosporum* genus belongs to the Pittosporaceae family. These plants are commonly found throughout Africa, Australia, and the Pacific islands.¹ The leaves, fruit, and flowers have been employed as therapeutics. In particular, they are used as snakebite antidotes, as baths for women after childbirth, and as treatments for skin diseases malaria.¹ A number of investigators have investigated extracts of the leaves of *Pittosporum* species for their antimicrobial effect,^{2,3} which is apparently due to a number of volatile mono and sesquiterpenes.^{4,5,6} Molluscicidal activity was also reported.⁷

¹ Flor, S. C. *Antimicrobial Saponins of Pittosporum viridiflorum* (Thesis) University of Mississippi, **1974**, Accession No. AAG7510681, Source: *Diss. Abs. Int.* **35**, 11B (**1974**), 5511.

² Mogg, V.; Gundidza, M. University of Zimbabwe, Honors Project Publications, **1982**. <http://www.uz.ac.zw/medicine/pharmacy/pubs/1982.html>.

³ Ramanandraibe, V.; Rakotovao, M.; Andriamaharavo, R.N.; Bessiere, J.-M.; Ravaonindrina, N.; Ramanoelina, A.R.P. *J. Essent. Oil. Res.* **2000**, *12*, 650.

⁴ Mananjarasoa, E.; Rakotovao, M.; Ramanoelina, A.R.P.; Andriantsiferana, M.H. *J. Essent. Oil Res.* **1998**, *10*, 459.

⁵ Nemethy, E.K.; Calvin, M. *Phytochemistry* **1982**, *21*, 2981.

⁶ Gurib-Fakim, A.; Demarne, F.-E. *Planta Med.* **1994**, *60*, 584.

⁷ El-Nahas, H.A. *J. Pharm. Sci.* **1998**, *7*, 68.

Along with alkanes such as *n*-heptane and nonane, a number of volatile terpenes (pinene, myrcene and limonene) have been found in the fruits and leaves of *Pittosporum* species.^{1,4,5,6} Steroids such as stigmasterol and sitosterol have also been found.¹ The most commonly investigated natural products from *Pittosporum* species are the saponins. The saponins are typically glycosides of ursolic acid (**5.1**), R₁-barrigenol (**5.2**), or R₁-barringtogenol (**5.3**).^{1,8} While the R₁-barrigenols resemble the julibrosides (**4.5**), their substituents are quite different. The hydroxy groups in julibrosides tend to be glycosylated whereas the hydroxy groups in barrigenol tend to be acylated with angelic acid (**5.4**). The glycosyl moieties for R₁-barrigenol saponins usually include glucuronic acids; it is uncommon to find glucuronic acid in other saponins.

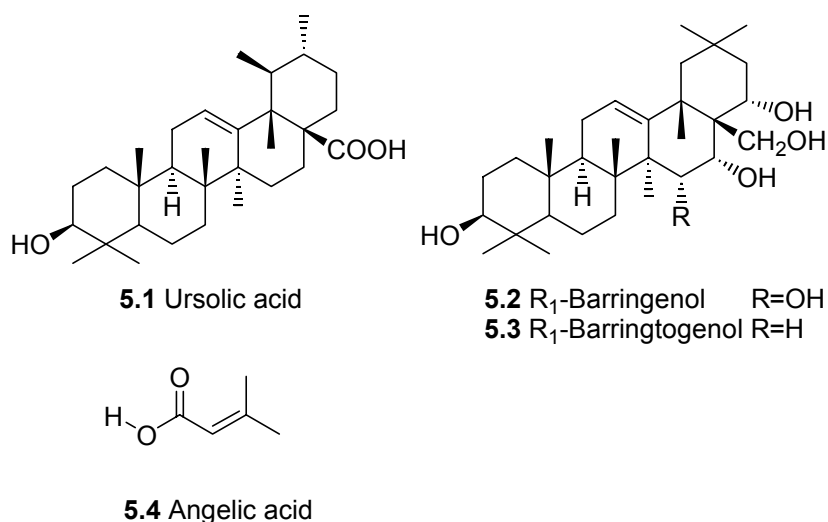


Figure 5-1. *Pittosporum* Terpenes.

⁸ Higuchi, R.; Kubota, S.; Komori, T.; Pandey, V. B.; Singh, J. P.; Shah, A. H. *Phytochemistry*, **1984**, *23*, 2597.

5.1.2 Chemical Investigations of *Pittosporum viridiflorum*.

Pittosporum viridiflorum is a small to large species of evergreen tree that occurs widely in forests throughout much of Madagascar and tropic Africa.

A single investigation into *Pittosporum viridiflorum* has been reported.¹ This investigation dealt with the characterization of the saponin aglycones from the wood and bark of *Pittosporum viridiflorum*. In addition, the antimicrobial activities of the crude extracts were evaluated. In this work the individual ethanol extracts of the bark and wood were found to be active against *Candida albicans* and *Saccharomyces cerevisiae*, weakly active against *Pseudomonas aeruginosa* and inactive against *Staphylococcus aureus*, *Escherichia coli*, *Mycobacterium smegmatis*, and *Aspergillus niger*. The freeze-dried extracts were subjected to Soxhlet extraction. Testing against *Saccharomyces cerevisiae* indicated that the polar *n*-butanol and water fractions contained the activity. *In-vivo* antitumor studies of the extracts were ineffective since the toxicity dose appeared to be only slightly higher than the effective dose (6 mg/kg in mice). Crude extracts were purified by polyamide and silica gel chromatography and monitored with the *C. albicans* bioassay. The most active fractions were subjected to hydrolysis and purification to afford a number of sapogenins (5.2, 5.5, and 5.6). The glycoside moieties were not characterized, nor were the identities of the sugars determined.

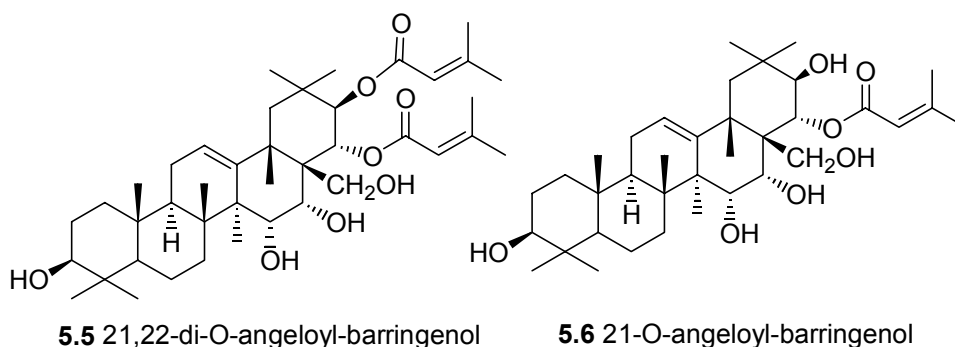


Figure 5-2. Previously isolated *Pittosporum viridiflorum* Sapogenins

Pittosporum viridiflorum was also investigated by Dr. Youngwan Seo.⁹ A crude methanol extract of the aerial parts was subjected to liquid-liquid partitioning, reverse phase chromatography, and normal phase preparative TLC to afford the new saponin pittoviridoside (**5.7**).

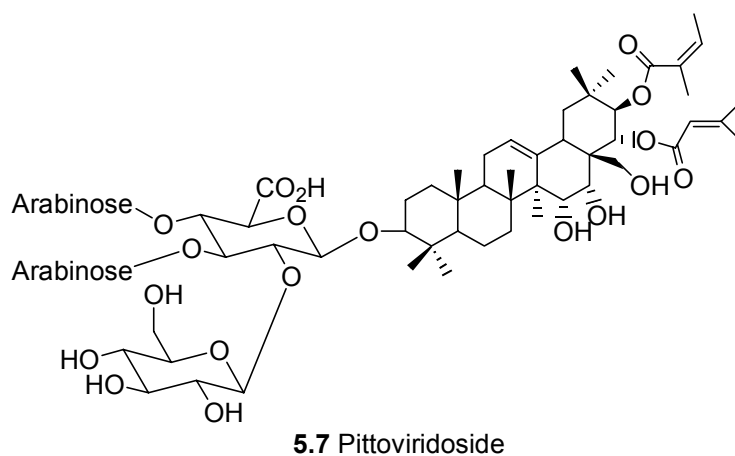


Figure 5-3. Pittoviridoside from *Pittosporum viridiflorum*

⁹ VPI&SU (Blacksburg, VA) and KORDI (Korea Ocean Research & Development Institute, Seoul, South Korea).

Pittoviridoside was characterized by NMR and MS; various degradations and derivatizations were employed as necessary. Hydrolysis of the saponin provided the sugars and the free aglycone. The aglycone was determined by NMR spectroscopy and MS to be 21,22-di-O-angeloyl-barringenol 21-angeloyl-22-senecieryl-12-oleanene-3, 15, 16, 21, 22, 28-hexol, which was named pittoviridagenin. The sugars were determined by methanolysis, acetylation and GCMS analysis to be glucuronic acid, glucose, and arabinose; these assignments were also confirmed by TLC. The glycosyl linkages were determined by methylation, reduction, hydrolysis, further reduction, acetylation, and GCMS analysis;¹⁰ the products of this treatment and the fragment ions generated by the EIMS are displayed in Figure 5-4. The locations of methyl ethers indicated sites that were unsubstituted in pittoviridoside; sites that possessed ester functionalities were substituted in pittoviridoside. These results show that in pittoviridoside the glucuronic acid was fully substituted, with sugars at C-2, C-3 and C-4 positions. The other sugars were unsubstituted and attached to the glucuronic acid. This experiment was unable to determine whether the pentoses existed as furanoses or pentoses since the necessary fragment ions were not visible; various NMR experiments of the saponin were however adequate to determine the secondary structure of the pentoses.

¹⁰ Jansson, P.-E.; Kenne, L.; Liedgren, H.; Lindberg, B.; Lonngren, J. *Chem. Commun.* **1976**, 8, 14.

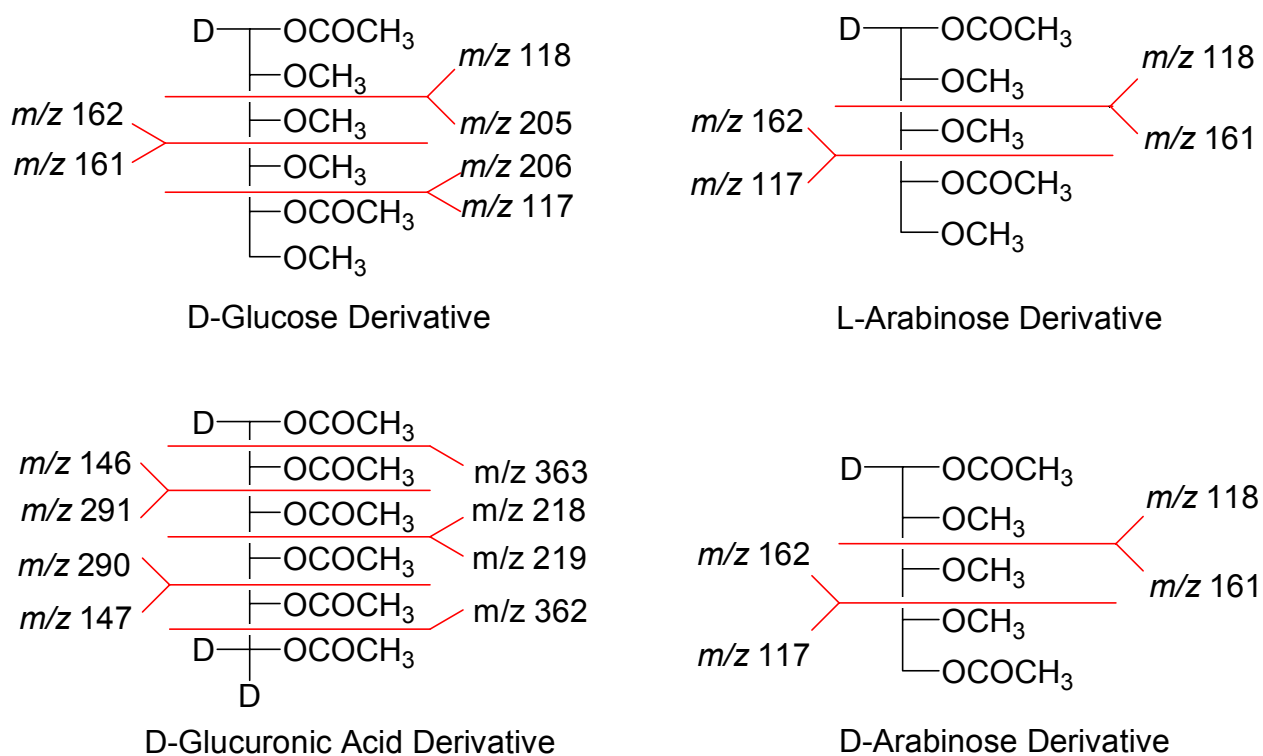


Figure 5-4. Mass Spectroscopic Fragmentations of Reduced Alditol Acetates from **5.7**

Although the structure of pittoviridoside was largely determined by these results, a few details remained to be elucidated before the work could be considered complete. Specifically the ring size (furanose or pyranose) and the absolute configuration of the sugars were not determined.

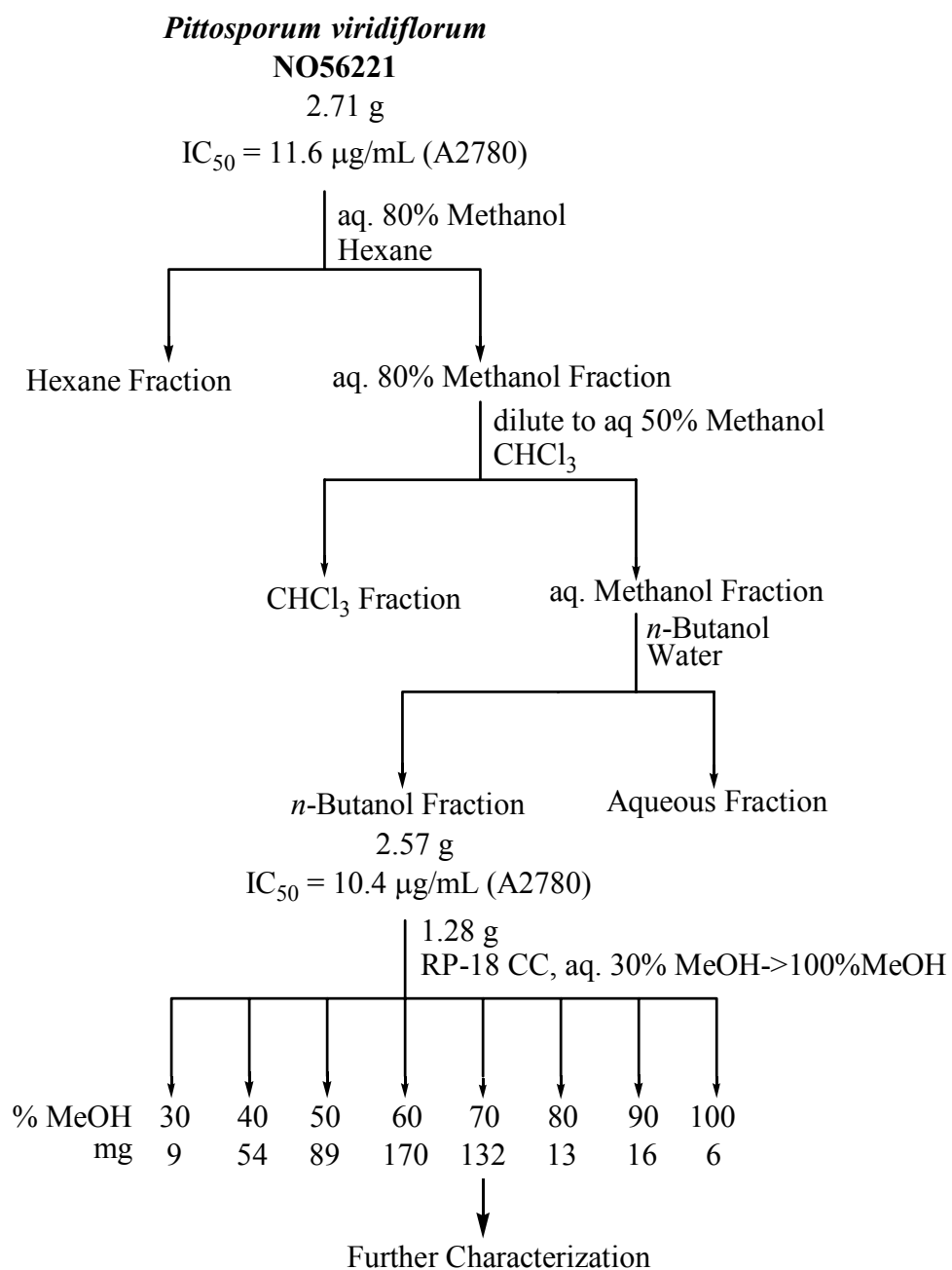
5.2 Results and Discussion.

5.2.1 Isolation of Crude Pittoviridoside from *Pittosporum viridiflorum*.

It was desirable to determine the stereochemistries of the pentoses by the same method used to characterize the *Albizia subdimidiata* pentoses, namely by preparation of thiazolidine acetate derivatives followed by GCMS analysis, Figure 4-7. As only a small quantity of pure pittoviridoside (**5.7**) was available, re-isolation of the saponin was required to obtain material for the purpose of determining method validity.

The methanol extract of the aerial parts of *Pittosporum viridiflorum* (2.71g) was partitioned with aqueous methanol and hexane (Scheme 4). The aqueous methanol fraction was diluted with water and extracted with CHCl₃. The aqueous methanol fraction was dried and partitioned between water and *n*-butanol.

The dried *n*-butanol fraction (1.28 g) was purified by reverse phase chromatography. Thin layer chromatography revealed that the aqueous 70% methanol fraction was enriched with pittoviridoside, as determined by comparison with a pure sample. Although this fraction was not completely pure, it was suitable for preliminary studies to optimize the derivatization procedure required for the characterization of the sugars.



Scheme 4. Isolation of Crude Pittoviridoside

5.2.2 Determination of the Stereochemistries of the Pentose Sugars

The stereochemistries of the hydrolyzed pentose sugars of pittoviridoside (**5.7**) were determined in a similar manner to those of the sugars from the *Albizia* saponins. As

noted above, since pure pittoviridoside was available only in a small quantity, crude pittoviridoside was employed first to ensure method validity. Thiazolidine derivatives were prepared from the hydrolyzed sugars by treatment with L-cysteine methyl ester hydrochloride (Figure 4-7), followed by conversion into their peracetates and comparison with standards by GCMS.¹¹ The chromatograms were monitored by total ion current (TIC) and at m/z 146, a major fragment ion, and revealed two peaks of roughly equivalent area corresponding to D- and L-arabinose derivatives (monitoring m/z 146). These results were confirmed by matching the fragmentation patterns of the derivatives against those of the standards. After this favorable result, thiazolidine acetate derivatives were prepared from pure pittoviridoside. When subjected to GCMS analysis, these derivatives also gave two peaks corresponding to the D- and L-arabinose derivatives. These results were confirmed by coinjecting the prepared standards with the derivatives; the stereochemistries of the pentoses were thus assigned as those corresponding to D- and L-arabinose.

Several saponins containing R₁-barrigenol and glucuronic acid moieties have been isolated from phytochemical sources.¹² Pittoviridoside however has two unusual structural features when it is compared with them. First, it has both D-arabinopyranose and L-arabinofuranose at the same time in the sugar moiety. A literature survey revealed the existence of a few compounds containing arabinopyranose and arabinofuranose with the same stereochemistry,¹³ and also very few compounds possessing arabinose units

¹¹ Hara, S.; Okabe, H.; Mihashi, K. *Chem. Pharm. Bull.* **1987**, *35*, 501.

¹² a. Arda, N.; Goren, N.; Kuru, A.; Pengsuparp, T.; Pezzuto, J.M.; Qiu, S.-X.; Cordell, G.A. *J. Nat. Prod.* **1997**, *60*, 1170. b. Schopke, T.; Janka, M.; Nimitz, M.; Wray, V.; Hiller, K. *Planta Med.* **1998**, *64*, 83.

¹³ a. Encarnacion, R.; Kenne, L.; Samuelsson, G.; Sandberg, F. *Phytochemistry*, **1981**, *20*, 1939. b. Higuchi, R.; Fujioka, T.; Iwamoto, M.; Komori, T.; Kawasaki, T.; Lassak, E. *Phytochemistry*, **1983**, *22*, 2565. Higuchi, R.; Kubota, S.; Komori, T.; Pandey, V.B.; Singh, J.P.; Shah, A.H.; *Phytochemistry*, **1984**, *23*, 2597. Nakayama, K.; Fujino, H.; Kasai, R.; Tanaka, O.; Zhou, J. *Chem. Pharm. Bull.* **1986**, *34*, 2209. Bhandari, S.P.S.; Agrawal, P.K.; Garo, H.S. *Phytochemistry*, **1990**, *29*, 3889.

with opposing stereochemistries¹⁴ Pittoviridoside appears however to be the first non-polymer compound to combine both enantiomers of arabinose and both ring sizes in the same structure. Another uncommon feature is the consecutive 1,2,3,4-tetrasubstituted glycosidic linkage in the glucuronic acid moiety. This kind of functionality has been reported previously on one only occasion.^{14b}

5.2.3 NMR Confirmation of Structure

NOE correlations were used to confirm the overall structure, since it was necessary to determine which arabinose had which stereochemistry i.e. is the structure D-arabinopyranose/L-arabinofuranose (**5.8**) or L-arabinopyranose/D-arabinofuranose (**5.9**)? 1D-GOESY spectra were acquired by Dr. Youngwan Seo but the interpretation of these spectra required the stereochemical determination described in the previous section and thus was carried out as part of the present work following the return of Dr. Seo to Korea. Interpretation was greatly assisted by the use of molecular models. The correlations are shown for the two possibilities in Figure 5-5. The structures have been drawn so those NOE interactions to the anomeric protons can be visualized. Structure **5.8** clearly shows that the predicted NOE interactions based on this structure were observed; in particular it explains the NOE interaction from the furanose C-4 proton to the pyranose C-4 proton observed between the pyranose and the furanose rings. In contrast, structure **5.9** does not explain several observed correlations. Thus as noted above an interaction is observed between the furanose C-4 proton and the pyranose C-4 proton; this signal, clearly seen by GOESY, cannot be explained by structure **5.9**. On the other hand, a signal for the

¹⁴ Martinez-Vartinez, M.; Garcia-Argaez, A.N.; Bueno, J.L.; Espinosa, G.; Calderon, J.S. *Phytochemistry*, **1998**, *48*, 1221.

interaction between the furanose C-2 proton and the pyranose C-2 proton would be expected but was not observed. After comparing the two possible structures with their predicted and observed NOE signals, the structure and stereochemistry of the sugar moiety was assigned as that of structure **5.8**.

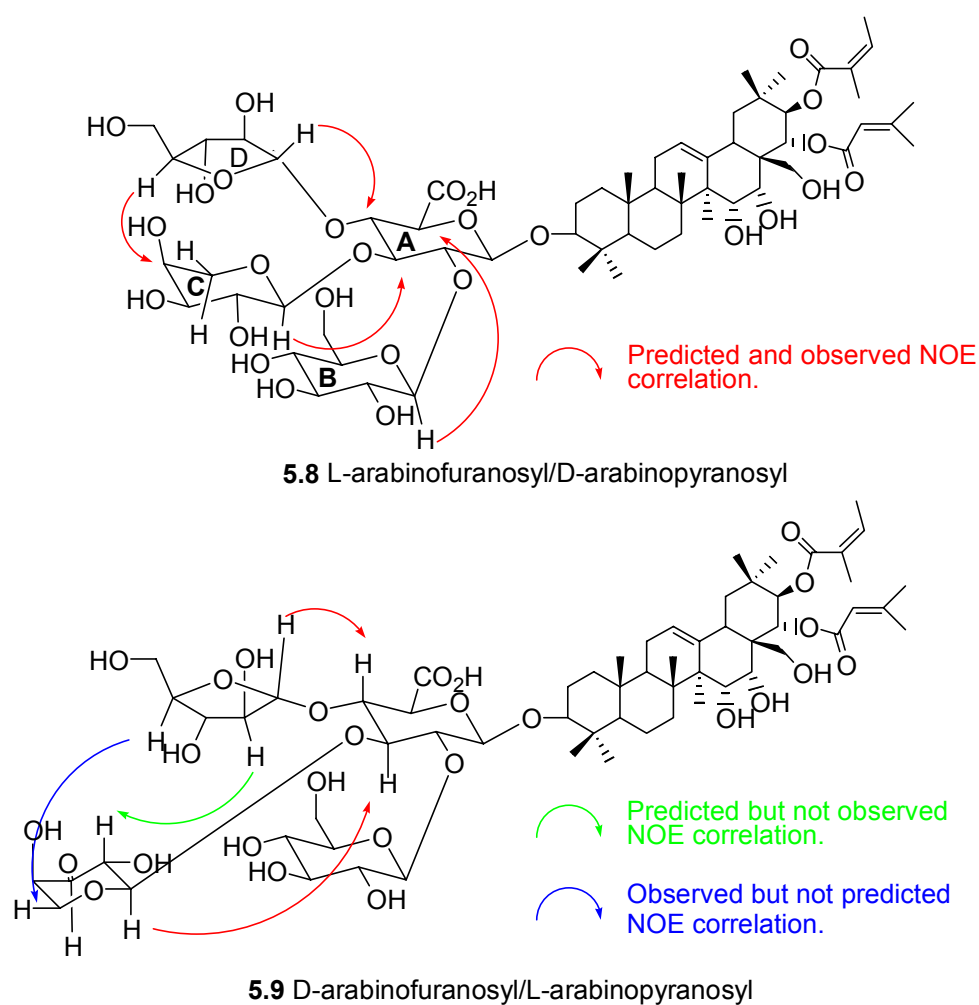


Figure 5-5. Predicted and Observed NOE Correlations.

5.2.4 *Biological Evaluation of Pittoviridoside.*

Pittoviridoside **4.7** showed weak activity (IC_{12} 85, 80, 140, and 100 $\mu\text{g/mL}$) against 1138, 1140, 1353, and Sc-7 yeast bioassays. While this activity might indicate weak topoisomerase I activity, the selectivity was not really adequate to support this conclusion. Thus, pittoviridoside probably possesses the general antifungal activity that all saponins possess. Pittoviridoside exhibited only moderate cytotoxicity (IC_{50} 10.1 $\mu\text{g/mL}$) against the A2780 human ovarian cancer cell line; this activity is insufficient to warrant further investigation.

5.3 **Experimental**

General Experimental Procedures. The general experimental procedures were identical to those previously reported in Chapters 2 and 4 with the following differences: mass spectral data were obtained at the Nebraska Center for Mass Spectrometry and on a VG 7070EHF mass spectrometer in the Department of Biochemistry, Virginia Polytechnic Institute and State University; UV spectra were measured on a Shimadzu UV1201 spectrophotometric instrument; and IR spectra were recorded on a Perkin-Elmer FT-IR 1600 instrument.

Plant Material. The aerial parts of *Pittosporum viridiflorum* were collected in the Ankarana Reserve in Madagascar, by D.K. Harder and M.C. Merello from the Missouri Botanical Gardens assisted by S. Razafimandimbison and G. Razafindrabaeza from the Centre National des Recherches Pharmaceutiques.

Extract Preparation. The plant samples were dried, ground, and extracted with EtOAc

and then with MeOH. The MeOH extract was assigned the code number N056221.

Yeast Bioassay. The 1138/1140/1353/Sc-7 yeast bioassays were carried out as previously described.¹⁵

Cytotoxicity Bioassay. The A2780 assay was performed at Virginia Polytechnic Institute and State University as previously reported.¹⁵

Isolation of Pittoviridoside. Isolation studied by Dr. Youngwan Seo gave 13 mg of **Pittoviridoside (5.7)**: white solid; mp 276 °C (dec.); $[\alpha]_D^{25}$ -19.0°(c 0.30, MeOH); UV (MeOH) λ_{\max} (log ϵ) 214 (3.71); IR (KBr) ν_{\max} 3400 (br), 2920, 1720, 1610, 1380, 1240, 1160, 1080, 1040, 1000 cm^{-1} ; ^1H and ^{13}C NMR data, see Tables; HRFABMS m/z 1317.5857(M-H+2Na)⁺(calcd for C₆₁H₉₃O₂₇Na, 1317.5876).

Isolation of Crude Pittoviridoside. The bioactive MeOH extract (2.71 g) described was active against the mutant 1138, 1140, 1353, and Sc7 yeast strains. The MeOH extract (IC₁₂ 650, 700, 800, 1150 $\mu\text{g}/\text{mL}$ in the 1138, 1140, 1353, and Sc7 yeast strains) was dissolved in 80% aqueous MeOH (250 mL) and extracted with *n*-hexane (300 mL x 2). The bioactive aqueous MeOH layer was diluted with H₂O to 60% aqueous MeOH, and then partitioned with CH₂Cl₂ (300 mL x 2). The activity was retained in the 60% aqueous MeOH, which was fractionated between *n*-BuOH and H₂O to afford 1.62 g of *n*-BuOH-soluble bioactive extract. Half of the *n*-BuOH fraction was subjected to C₁₈ reversed-phase vacuum flash chromatography using gradient mixtures of MeOH and H₂O (elution

order: 50%, 60%, 70%, 80%, 90% aqueous MeOH, 100% MeOH) to give 132 mg of crude saponin.

Determination of Pentose Stereochemistries. A crude fraction containing pittoviridoside (10 mg) was placed in 0.5 mL of MeOH and 0.5 mL of 1 N HCl. This was heated at 100 °C for 12 hours and allowed to stand at room temperature for 12 h. Water and chloroform were added, shaken, and the water-soluble fraction dried by rotary evaporation (6.9 mg). This fraction was placed in 1 mL of pyridine and 11.8 mg of cysteine methyl ester hydrochloride added; this was heated for 2 h at 100 °C. Acetic anhydride (0.3 mL) was then added and allowed to react for a further 2 h. The sample was cooled and solvent removed by blowing off with argon to yield a mixture of thiazolidine-4-carboxylate derivatives, which were analyzed by GC-MS using a 30 m x 0.32 mm id HP5 capillary column connected to the VG7070EHF mass spectrometer. D and L arabinose thiazolidine-carboxylate standards were also prepared (as described previously). Injector temperature was 200 °C. A temperature gradient was used for the oven; the initial temperature was maintained at 75 °C for 1 min and then raised to 250 °C at the rate of 10 °C/min. Individual signals for L-arabinose (26.28 min) and D-arabinose (26.41 min) thiazolidine acetate standards were observed; it was apparent from the mass spectral data of these peaks that the predominant ion possessed a mass-to-charge ratio of m/z 146. The analysis of the derivatized crude saponin sugars (with monitoring at m/z 146) indicated the presence of L-arabinose (26.24 minutes) and D-arabinose (24.41 minutes); a mass spectral examination of the peaks revealed that they possessed identical fragmentation patterns with the standards. Following this analysis, pure pittoviridoside

¹⁵ Chapter 2.

was derivatized in a similar fashion to that of the crude material. Pittoviridoside (1 mg) was placed in 0.25 mL of MeOH and 0.5 mL of 1-N HCl. This was heated at 100 °C overnight. Water and chloroform were added, shaken, and the water-soluble fraction dried by rotary evaporation. This fraction was placed in 0.3 mL of pyridine and 3 mg of cysteine methyl ester hydrochloride was added; this was heated for 2 h at 100 °C. Acetic anhydride (0.3 mL) was then added and allowed to react for a further 2h. After cooling and solvent removal, the products were analyzed in a similar fashion to that of the crude material; the results also indicated the presence of D and L-arabinose.

Table 10. ^1H and ^{13}C NMR Spectral Data for Pittoviridagenin (21-angeloyl-22-senecieryl-12-oleanene-3, 15, 16, 21, 22, 28-hexol) (Seo).

Position	^{13}C	^1H	position	^{13}C	^1H
1	39.4t	1.61 (1H, m), 1.06 (1H, m)	21	78.9d	6.25 (1H, d, 10.2)
2	28.2t	1.87 (2H, m)	22	72.5d	6.65 (1H, d, 10.2)
3	78.0d	3.48 (1H, m)	23	28.7q	1.23 (3H, s)
4	39.3s		24	16.6q	1.05 (3H, s)
5	55.6d	0.95 (1H, m)	25	16.0q	0.96 (3H, s)
6	19.2t	1.68 (1H, m), 1.45 (1H, m)	26	17.6q	1.08 (3H, s)
7	36.8t	2.23 (1H, m), 2.12 (1H, m)	27	21.0q	1.84 (3H, s)
8	41.5s		28	62.8t	3.73 (1H, dd, 9.8, 4.6), 3.43 (1H, dd, 9.8, 4.6)
9	47.3d	1.78 (1H, dd, 11.2, 5.7)	29	29.5q	1.11 (3H, s)
10	37.4s		30	20.1q	1.33 (3H, s)
11	24.1t	1.92 (2H, m)	1'	166.7s	
12	125.5d	5.57 (1H, t, 3.1)	2'	116.5d	5.22 (1H, m)
13	143.7s		3'	156.2s	
14	47.9s		4'	19.9q	2.10 (3H, d, 1.0)
15	67.6d	4.20 (1H, dd, 9.4, 4.2)	5'	26.8q	1.51 (3H, d, 1.0)
16	73.0d	4.35 (1H, dd, 4.2, 4.2)	1''	169.0s	
17	48.6s		2''	129.2s	
18	40.9d	3.13 (1H, m)	3''	136.5d	5.90 (1H, brq, 7.1)
19	46.9t	3.08 (1H, m), 1.46 (1H, dd, 11.5, 2.7)	4''	15.8q	2.05 (3H, dq, 7.2, 1.5)
20	36.3s		5''	20.9q	1.99 (3H, m)

^1H and ^{13}C NMR spectra were measured in pyridine- d_5 at 100 and 400 MHz, respectively. Assignments were aided by DEPT, ^1H COSY, TOCSY, HMQC, and HMBC experiments, and literature comparison.

Table 11. ^1H and ^{13}C NMR Spectral Data for Pittoviridoside (**5.7**) (Seo).

Position	^{13}C	^1H	Position	^{13}C	^1H
1	40.2t	1.61 (1H, m), 0.96 (1H, m)	21	79.8d	5.85 (1H, d, 10.2)
2	27.1t	1.90 (1H, m), 1.70 (1H, m)	22	73.1d	5.51 (1H, d, 10.2)
3	91.9d	3.17 (1H, dd, 11.8, 4.1)	23	28.4q	1.07 (3H, s)
4	40.4s		24	17.0q	0.87 (3H, s)
5	56.7d	0.78 (1H, d, 12.0)	25	16.3q	0.98 (3H, s)
6	19.5t	1.55 (1H, m), 1.40 (1H, m)	26	17.9q	1.00 (3H, s)
7	37.2t	1.75 (2H, m)	27	21.0q	1.40 (3H, s)
8	42.3s		28	62.8t*	2.98 (1H, d, 11.3), 3.26 (1H, d, 11.3)
9	48.2d	1.57 (1H, m)	29	29.6q	0.87 (3H, s)
10	37.9s		30	20.1q	1.07 (3H, s)
11	24.8t	1.91 (2H, m)	1'	168.3s	
12	127.0d	5.47 (1H, t, 3.3)	2'	116.7d	5.67 (1H, m)
13	143.6s		3'	159.1s	
14	48.4s		4'	27.5q	1.87 (3H, d, 1.0)
15	68.5d	3.70 (1H, m)	5'	20.4q	2.11 (3H, d, 1.0)
16	74.1d	3.73 (1H, m)	1''	169.5s	
17	49.1s		2''	129.5s	
18	41.4d	2.62 (1H, m)	3''	138.4d	6.03 (1H, qq, 7.1, 1.5)
19	47.5t	2.61 (1H, m), 1.21 (1H, m)	4''	15.9q	1.88 (3H, dq, 7.2, 1.5)
20	36.7s		5''	20.8q	1.81 (3H, m)

^1H and ^{13}C NMR spectra were measured in CD_3OD at 100 and 400 MHz, respectively. Assignments were made by DEPT, ^1H COSY, TOCSY, HMQC, and HMBC experiments.

Table 12. ^1H and ^{13}C NMR Spectral Data of the Sugar Moiety for Pittoviridoside (**5.7**) (Seo).

Position	^{13}C	^1H	Position	^{13}C	^1H
$\beta\text{-D-GluA}$			$\alpha\text{-D-Araf}$		
1'''	105.7s	4.46 (1H, d, 7.8)	1''''	104.1s	4.91 (1H, d, 7.4)
2'''	79.9d	3.89 (1H, m)	2''''	73.1d	3.56 (1H, dd, 8.3, 7.4) ^a
3'''	80.2d	3.87 (1H, m)	3''''	74.5d	3.52 (1H, dd, 9.7, 3.7) ^a
4'''	75.1d	3.85 (1H, m)	4''''	70.4d	3.77 (1H, brs) ^a
5'''	78.6d	3.68 (1H, m)	5''''	67.5t	3.82 (1H, m), 3.54 (1H, brd, 15.6) ^a
6'''	176.7s				
$\beta\text{-D-Glu}$			$\alpha\text{-L-Araf}$		
1''''	102.9s	5.00 (1H, d, 7.8)	1'''''	108.2s	5.18 (1H, brs)
2''''	76.2d	3.20 (1H, dd, 9.1, 7.8)	2'''''	81.8d	3.97 (1H, d, 1.2)
3''''	78.0d	3.39 (1H, dd, 9.1, 9.0)	3'''''	79.5d	3.75 (1H, brd 5.0) ^a
4''''	72.6d	3.12 (1H, dd, 9.5, 9.0)	4'''''	87.4d	4.43 (1H, dt, 5.0, 4.5)
5''''	78.2d	3.31 (1H, m)	5'''''	63.5t ^b	3.66 (2H, m)
6''''	63.6t ^b	3.83 (1H, dd, 12.0, 2.0) ^a , 3.58 (1H, dd, 12.0, 7.2) ^a			

^1H and ^{13}C NMR spectra were measured in CD_3OD at 100 and 400 MHz, respectively. Assignments were made by DEPT, ^1H COSY, TOCSY, HMQC, and HMBC experiments. ^aCoupling constant is based on 1 D TOCSY Experiment. ^bExchangeable.

VI. SYNTHESIS OF 2-METHOXY-6-N-ALKYL BENZOQUINONES AND BIS-BENZOQUINONES: POTENTIAL DNA INTERCALATORS AND TOPOISOMERASE INHIBITORS

6.1 Introduction

In continuation of our search for anticancer compounds, bioactivity-directed fractionation of an EtOAc extract from the leaves of a *Miconia lepidota* (Melastomaceae) by Dr. A. A. Leslie Gunatilaka afforded two benzoquinones, primin (**6.1**) and its *n*-heptyl analog (**6.2**).¹

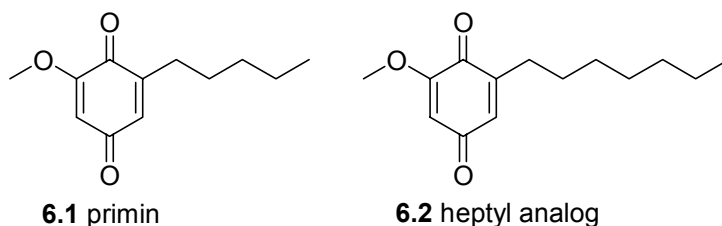


Figure 6-1. Benzoquinones from *Miconia lepidota*.

Both **6.1** and **6.2** exhibited activity towards mutant yeast strains based on *Saccharomyces cerevisiae* indicative of their cytotoxicity and potential anticancer activity. Interestingly, it was observed that the *n*-heptyl analog (**6.2**) was significantly more active than primin (**6.1**), and this observation raised the possibility that analogs with longer side chains would be even more active. This chapter describes synthetic efforts to test this hypothesis, and also to test the hypothesis that analogs with two benzoquinone units linked by an alkyl chain would be significantly active.

¹ Gunatilaka, A.A.L.; Berger, J.M.; Evans, R.; Miller, J.S.; Wisse, J.H.; Neddermann, K.M.; Bursuker, I.; Kingston, D.G.I. *J. Nat. Prod.* **2001**, *64*, 2.

6.1.1 A Benzoquinones as Potential DNA Intercalators and Topoisomerase Inhibitors.

Quinones and hydroquinones are biochemically important compounds, functioning as oxidizing and reducing agents, respectively. They have been found in plants, animals and various microbial sources. The K series of vitamins (**6.3**) are probably the best known quinones; they are important for oxidative metabolism.² Other biochemically important compounds are the hydroquinone Vitamin E (**6.4**), an important antioxidant, and the ubiquinones (**6.5**), which are involved in electron transport in mitochondria.

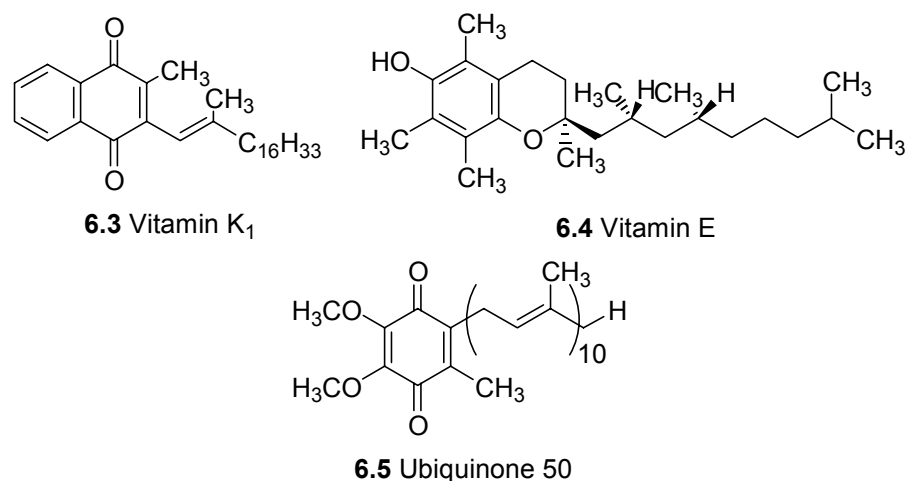


Figure 6-2. Biochemically Important Benzoquinones and Hydroquinones.

Many medicinally important natural products contain quinone or hydroquinone functionalities. Mitomycin C from *Streptomyces caespitosus* (**6.6**) and doxorubicin (adriamycin, **6.7**) from *Streptomyces peuketius* are important anticancer compounds. While the mechanisms of activity for these two compounds are different (doxorubicin inhibits RNA synthesis and topoisomerase II whereas mytomycin C is a DNA alkylating agent)^{3,4} both possess an important

² *Biochemistry of Quinones* (R.A. Morton, ed.) **1965**, Academic Press, New York.

³ Dewick, P. *Medicinal Natural Products*, **1997**, John Wiley and Sons, New York, 85.

physical property: they both intercalate into DNA. Intercalation (literally: “inserting dates into a calendar”) occurs when a compound can reversibly insert itself into a host structure while maintaining the structural features of the host.⁵ Intercalation is usually studied as a component of material science but it is also an important subject involving DNA(host)-drug(guest) relationships. A number of important synthetic drugs such as the antimalarial chloroquinone (6.8) have been found to be strong intercalators.

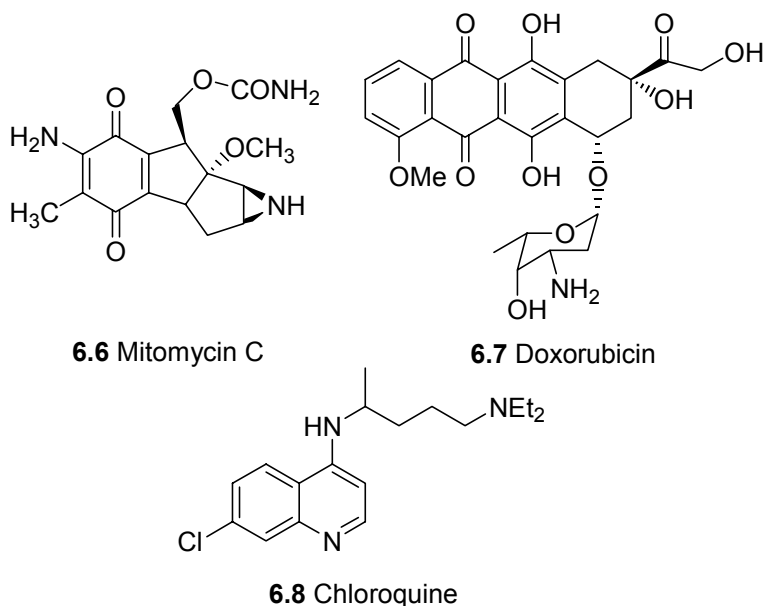


Figure 6-3. Intercalating Drugs.

Intercalating drugs have some common features: they tend to be planar, aromatic, polycyclic compounds that can be cationic at physiological pH. The binding of intercalators to DNA can be summarized as two types: Type I and Type II binding. Type I binding is due to hydrogen bonds between the intercalator and the DNA base pairs; it is strong bonding essentially

⁴ Kim, J.Y.; Su, T.-L.; Chou, T.-C.; Koehler, B.; Scarborough, A.; Ouerfelli, O.; Watanabe, K.A. *J. Med. Chem.* **1996**, *39*, 2812.

unaffected by concentration. The weaker Type II binding is due to π -stacking and π -cation interactions; these interactions are ionic strength dependent and are considered not important under physiological conditions.

Intercalation is considered very important for the activity of the drugs above; it may explain the selectivity for a number of compounds. It is easy to imagine that an intercalator forms a complex with DNA (which by itself does not lead to metabolic disruption); when an important enzyme (such as topoisomerase II) comes into contact with the complex, the guest disrupts the enzyme eventually leading to cell death (Figure 6-4).⁶

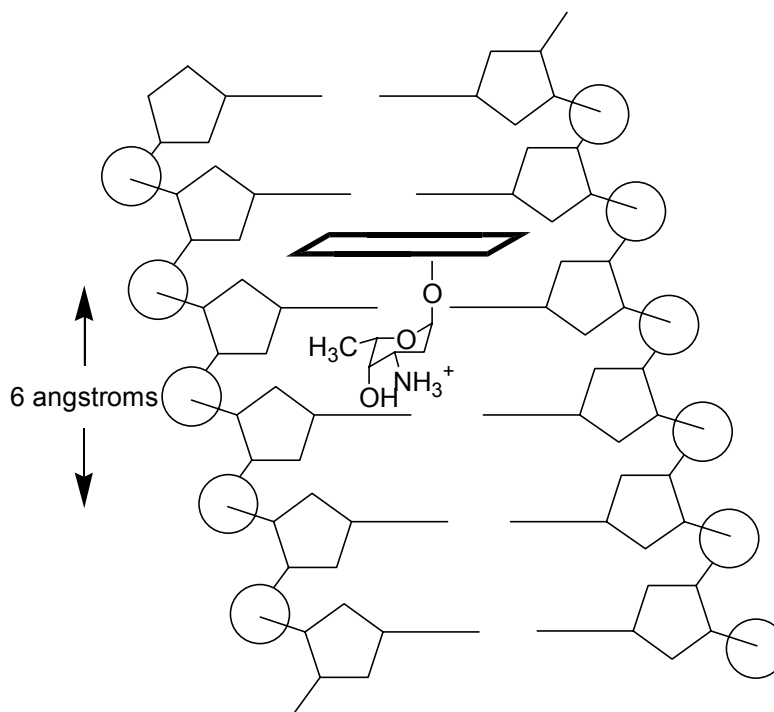


Figure 6-4. Representation of the Intercalation of Anthracycline Antibiotics in DNA.⁶

⁵ Wilson, W.I.; Jones, R.L. Intercalation in Biological Systems (Chapter 14) in *Intercalation Chemistry* (M.S. Whittingham and A.J. Jacobsen, eds.) **1982**, Academic Press, New York.

⁶ Chaires, J.B.; Leng, F.; Przewlaka, T.; Fokt, T.; Ling, Y.-H.; Perez-Soler, R.; Priebe, W. *J. Med. Chem.* **1997**, *40*, 261.

Investigations into a number of intercalator-DNA complexes have revealed that minor and major groove binding can occur; groove selectivity is usually a function of the bulkiness of the intercalator.⁴ The theoretical maximum number of intercalating molecules per DNA base pair has been determined to be 0.5 (neighbor exclusion principal). Partial intercalation can occur; this is when only a portion of a compound intercalates into DNA.

Perhaps the most interesting intercalators are the bis-intercalators. These compounds are typically composed of two intercalator moieties linked together by a spacer unit. These compounds were very useful in early investigations to probe DNA structure and intercalator interactions. Bis-intercalators were also investigated for therapeutic usage (Figure 6-5).

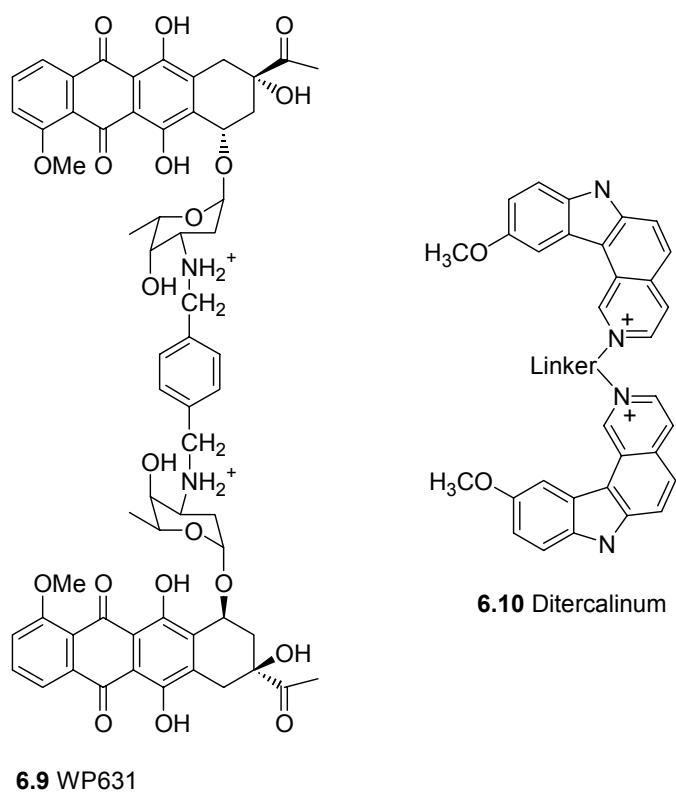


Figure 6-5. Bis-Intercalators^{6,7}

⁷ DePascual-Teresa, B.; Gallego, J.; Ortiz, A.R.; Gago, F. *J. Med. Chem.* **1996**, *39*, 4810.

There are a number of potential advantages of bis-intercalators over monointercalators.^{5,8} The binding constant of a bis-intercalator should be the square of the binding constant of the mono-intercalator; if the mono-intercalator was already a good binder, enhanced activity should be seen. Another advantage is the possibility of increased selectivity since the bulkier bis-intercalators can only fit into a limited range of sites. These advantages are important; many useful drug candidates that intercalate have been found to be too toxic for therapeutic use. These advantages may permit the development of useful drugs with lower dosages or side effects.

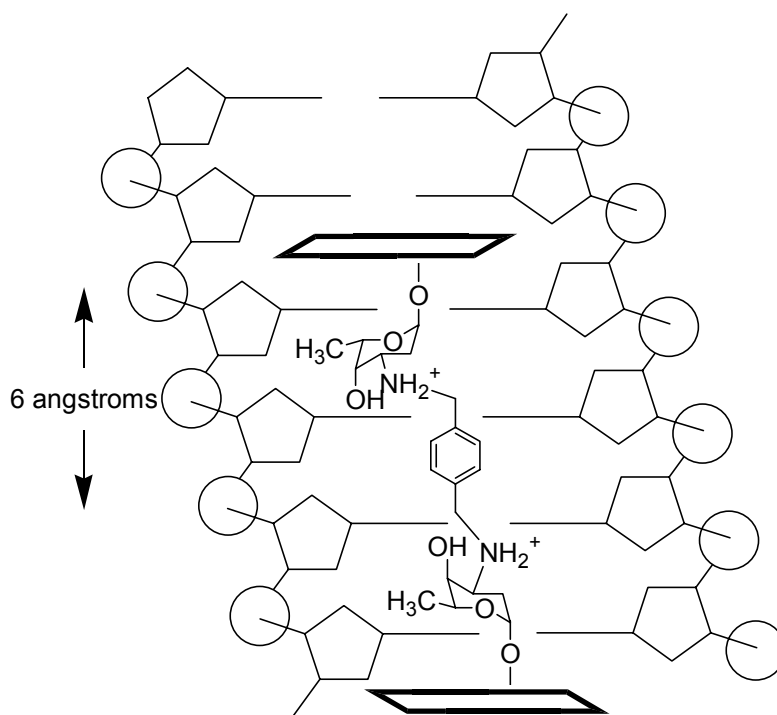


Figure 6-6. Intercalation of WP 631 into DNA.

There are important considerations when choosing linker units: size, polarity, etc. A range of compounds must be synthesized to develop a worthy drug candidate. If the spacer was long enough to permit intercalation between every other base pair, both rings will intercalate in

⁸ Wakelin, L.P.G. *Polyfunctional DNA Intercalating Agents. Med. Res. Rev.* **1986**, 375.

agreement with the neighbor exclusion principal. However, if the spacer is only long enough to permit intercalation between adjacent base pairs, only one ring normally intercalates; there has been some evidence that some bis-intercalators can intercalate at adjacent sites in violation of the neighbor exclusion principal (possibly by partial intercalation).⁵ Substituents on the aromatic rings can also effect bis- versus mono-intercalation.

Natural products that possess structures similar to known intercalators may be good templates for bis-intercalators; these bis-intercalator analogs may show enhanced bioactivities compared to the parent compounds. There has been at least one successful example of this.⁶

6.1.2 Previous Investigations of Primin and Primin Derivatives.

Primin (**6.1**) was originally isolated from the leaves of *Primula obconica*⁹ and later the roots of *Miconia* sp. (Melastomaceae).¹⁰ Although **6.2** has been synthesized in a structure-activity relationship study of primin-type benzoquinones as cell-mediated allergens causing contact dermatitis¹¹ and has been reported as a minor component of *Primula obconica*,¹² it had not previously been isolated as a homogenous compound. Previous phytochemical studies of *Miconia* species have resulted in the isolation of primin (**6.2**)¹³ its quinol analog miconidin,^{13,14} and several triterpenes.^{14,15} Insect feedant,¹³ antimicrobial,^{14,15} and antineoplastic^{14,15} activities of primin and miconidin have also been evaluated.

⁹ Nugteren, D.H. *Biochim. Biophys. Acta*, **1975**, 380, 299.

¹⁰ Miyamoto, T.; Ogino, N.; Yamamoto, S.; Hayashi, O. *J. Biol. Chem.* **1976**, 251, 2629.

¹¹ König, W.A.; Faasch, H.; Heitsch, H.; Colberg, C.; Hausen, B.M. *Z. Naturforsch. B. Chem. Sci.* **1993**, 48, 387.

¹² Schlegel, R.; Ritzau, M.; Ihn, W.; Stengel, C.; Gräfe, U. *Nat. Prod. Lett.* **1995**, 6, 171.

¹³ Bernays, E.; Lupi, A.; Bettolo, R.M.; Mastrofrancesco, C.; Tagiatesta, P. *Experientia*, **1984**, 40, 1010.

¹⁴ Marini-Bettolo, G.B.; Delle Monache, F.; Goncalves da Lima, O.; de Barros Coelho, S. *Gazz. Chim. Ital.* **1971**, 101, 41.

¹⁵ a. Chan, W.R.; Sheppard, V.; Medford, K.A.; Tinto, W.P.; Reynolds, W.P.; McLean, S. *J. Nat. Prod.* **1992**, 55, 963. b. Macari, P.A.T.; Emerenciano, V. de. P.; Ferreira, Z.M.G.S. *Quim. Nova*, **1990**, 13, 260.

The bioactivity profiles for **6.1** and **6.2**¹⁶ in our bioassays are depicted in Table 13. Both compounds exhibited moderate activity in all cell lines.

Table 13. Bioactivity Data for the Isolated Benzoquinones.

Compound	Yeast Based Cell Lines				Cancer Cell Lines	
	Sc-7	1138	1140	1353	A2780	M109
6.1	48 ± 1	240 ± 40	170 ± 40	285 ± 40	3.53 ± 0.31	10
6.2	16 ± 10	120 ± 10	130 ± 10	220 ± 10	3.42 ± 0.32	10

However, it is interesting to note that compound **6.2**, having two additional carbon atoms in the side-chain, was significantly more active than its lower homologue, primin (**6.1**) in the yeast strains. These results were in agreement for results from an investigation reported by Dr. König in Germany, who studied benzoquinones as skin allergens.¹¹ This encouraged us to initiate an investigation concerning the structure-activity relationships of benzoquinones involving the alkyl side chain. A number of primin analogs were synthesized with varying sizes of the alkyl side chain; these compounds were then tested in a variety of cell lines.

6.2 Results and Discussion.

6.2.1 *Synthesis of Benzoquinones.*

A variety of 2-methoxy-6-*n*-alkyl-1,4-benzoquinones were synthesized or resynthesized by a previously reported method.¹¹ In this method, commercially available *o*-vanillin (**6.11**) was allowed to react with an excess of a selected Grignard reagent. Although this process requires at least two equivalents of Grignard reagent, because of the hydroxy group present in *o*-vanillin, it is more efficient than alternate routes involving protecting group chemistry. The benzylic

¹⁶ The *n*-heptyl analog (**6.2**) was referred to as “miconin” in the author’s notebook and other documents.

alcohols were obtained in good yield where R was a smaller alkyl group (methyl to butyl), but only in low yields where R was a larger group.

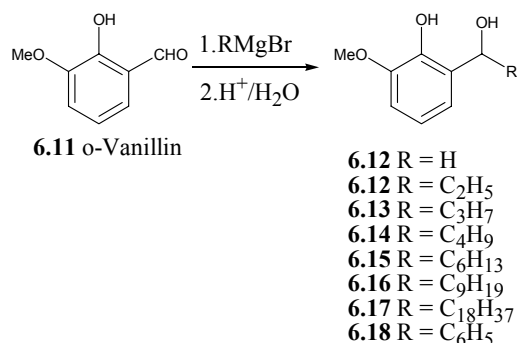


Figure 6-7. Synthesis of Benzylic Alcohols

Conversion of the phenols **6.12-6.17** into the final quinones was accomplished in two steps. In the first step, the benzylic hydroxyl group was removed by hydrogenolysis over palladium on charcoal to give the desoxy derivatives **6.20-6.26**. The methyl analog **6.19** was prepared from the hydrogenolysis of *o*-vanillin. Finally, oxidation of the desoxyphenols with Fremy's salt gave the quinones **6.1-6.2**, **6.28-6.33**. The hydroxyprimin analog (**6.34**) was also prepared from the oxidation of **6.14** with Fremy's salt.

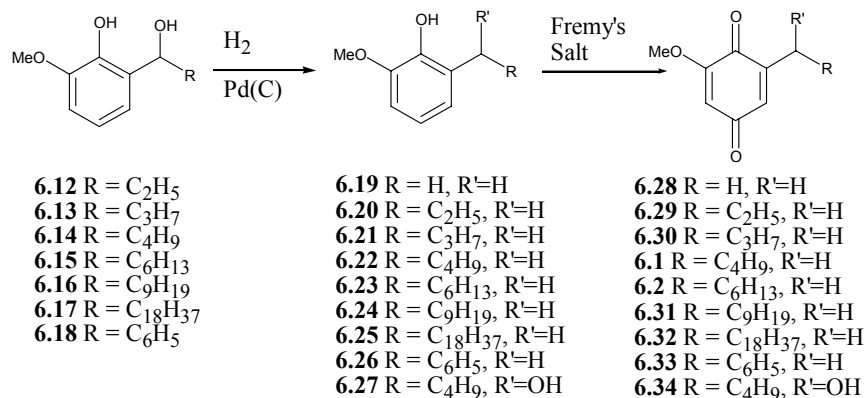


Figure 6-8. Hydrogenolysis and Oxidation of Phenolic Alcohols to Benzoquinones.

These benzoquinones were all tested, in triplicate, in the mutant yeast strains. The most potent of these compounds in the yeast cell lines were then tested in the A2780 cell line (**6.1-2, 6.30**) and in the M109 cell line (**6.1-2, 6.31**). The results are summarized in Table 14. It was found that moderate length side chains (C₄H₉ to C₁₀H₂₁) generally showed greater activity than those of shorter or longer length; these results also agreed with those of Konig.¹¹ These results were promising enough to initiate an investigation into the anticancer activities of bis-benzoquinones with moderate length spacer groups.

Table 14. Bioactivity Data for Compounds **6.1-2, 6.28-6.34**.

Compound	Yeast Based Cell Lines				Cancer Cell Lines	
	Sc-7	1138	1140	1353	A2780	M109
6.28	530 ± 100	580 ± 100	630 ± 180	830 ± 110	NT	NT
6.29	220 ± 50	200 ± 30	140 ± 20	233 ± 20	9.8 ± 0.36	NT
6.30	80 ± 25	220 ± 30	150 ± 20	210 ± 30	3.35 ± 0.31	NT
6.1	48 ± 1	240 ± 40	170 ± 40	285 ± 40	3.53 ± 0.31	10
6.2	16 ± 10	120 ± 10	130 ± 10	220 ± 10	3.42 ± 0.32	10
6.31	3 ± 1	380 ± 180	380 ± 180	380 ± 180	NT	10
6.32	>2000	>2000	>2000	>2000	NT	NT
6.33	440 ± 120	536 ± 40	430 ± 50	577 ± 40	12.30 ± 1.51	NT
6.34	180 ± 120	460 ± 80	420 ± 150	590 ± 80	10.16 ± 0.15	NT

6.2.2 Synthesis of Bis-Benzoquinones

The synthesis of the bis-benzoquinones was very similar to that of the mono-benzoquinones with the following changes. The bis-Grignard reagents were prepared from various α,ω -dibromoalkanes. Benzyl protected *o*-vanillin was also employed. Protection was found to be a requirement in the addition step. Addition occurred in the earlier synthesis since a large excess of Grignard reagent was employed. Addition was unable to occur when the

Grignard reagent was employed as a limiting reagent; simple deprotonation of the phenol was the result.

Hydrogenolysis occurred without incident. It is noteworthy that the benzyl groups were preferentially hydrogenated before the benzylic hydroxy groups; rehydrogenation was found to adequately resolve this problem.

Due to the poor yields afforded by Fremy's salt in the previous oxidations of the phenols to benzoquinones, salcomine (N-,N'-bis(salicylidene)-ethylenediaminocobalt(II)) was employed as a catalyst in the oxidation of the bis-phenols to bis-benzoquinones with O₂ in DMF; these oxidations occurred in very good yields. The single example of a poor yield involved an oxygen atmosphere instead of oxygen bubbling through solution; poor oxygen uptake by the catalyst under these circumstances is suspected.

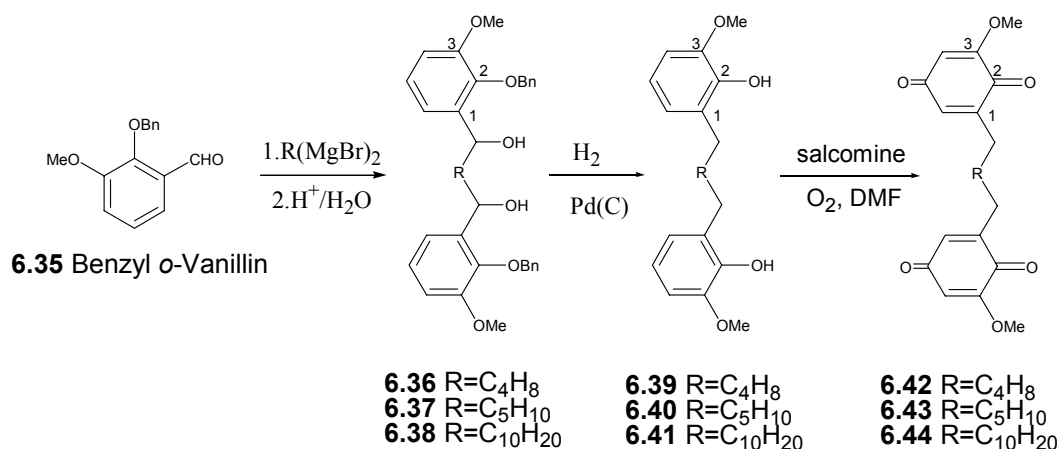


Figure 6-9. Preparation of Bis-Benzoquinones (6.42-6.44)

All three of the bis-benzoquinones prepared were tested in the same cell lines as the prepared mono-quinones (Table 15).

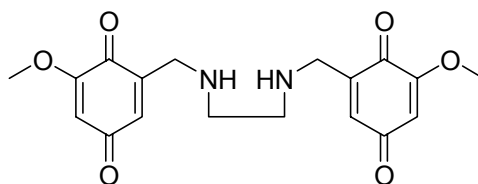
Table 15. Bioactivity Data for Compounds **6.42-44**.

Compound	Yeast Based Cell Lines				Cancer Cell Lines	
	Sc-7	1138	1140	1353	A2780	M109
6.42	>2000	>2000	>2000	>2000	16.54 ± 1.51	NT
6.43	>2000	>2000	>2000	>2000	14.47 ± 0.20	NT
6.44	>2000	>2000	>2000	>2000	15.76 ± 1.86	NT

The results were disappointing. The bis-benzoquinones did not appear to be as active as the mono-benzoquinones. A comparison of the bis-benzoquinones to reported bis-intercalators reveals some differences. Most bis-intercalators are water-soluble and either cationic or protonizable under physiological conditions (Figure 6-5). Compounds **6.42-44** do not fit this description. This initiated a short investigation into more water-soluble bis-intercalators.

6.2.3 *Synthesis of Bis-Schiff Bases.*

Nitrogen can permit organic compounds to become more water soluble; nitrogen is also an important element in hydrogen bonding. As discussed earlier, Type I binding in intercalation is due to hydrogen bonding. A short investigation was initiated to test the hypothesis that nitrogen-containing bis-benzoquinones may possess interesting biological activity. An example of such a target can be seen in Figure 6-10.



6.45

Figure 6-10. Nitrogen Containing Bis-Benzoquinone Target.

The synthetic strategy for such a target is quite simple. By analogy with our previous syntheses, *o*-vanillin was treated with selected diamines to form bis-Schiff bases. The Schiff bases can then be subjected to hydrogenolysis followed by oxidation to the benzoquinone.

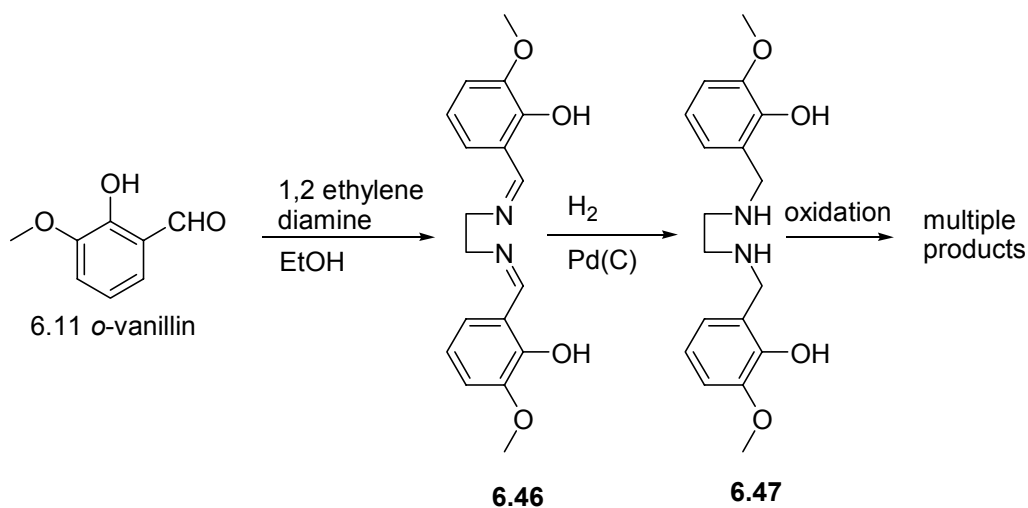


Figure 6-11. Attempted Preparation of **6.45**.

The Schiff base **6.46** was prepared by a known procedure in high yield.¹⁷ The reduced product **6.47** was prepared in low yield by hydrogenation of **6.46** over palladium on charcoal. Conversion of **6.47** to **6.45** with either Fremy's salt or salcomine-catalyzed failed. Attempts to convert **6.46** into quinones also failed. Attempts to synthesize compounds similar to **6.45** would require an alternative strategy.

A number of previously prepared intermediates and compounds including **6.46** and **6.47** were subjected to biotesting on the 1138 and Sc-7 yeast assays. Almost all of the compounds lacked activity (including **6.47**), but **6.46** displayed significant activity in a single dose test; it displayed an inhibitory zone >30 mm at 1000 µg/mL against Sc-7. It displayed almost no

¹⁷ Choudhary, N.F.; Connelly, N.G.; Hitchcock, P.B.; Leigh, G.J. *J. Chem. Soc. Dalton Trans.*, **1999**, 24, 4437.

activity versus the 1138 yeast. Compound **6.46** was then submitted for A2780 cytotoxicity testing.

Encouraged by this result, an additional nitrogen containing bis-Schiff base was prepared from commercially available 1,6 hexamethylene diamine in a similar fashion as **6.46**.

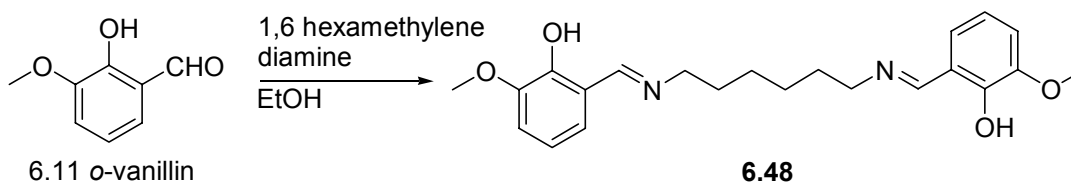


Figure 6-12. Preparation of a Bis-Schiff Base.

Compound **6.48** was also subjected to biotesting.

6.2.4 Biological Evaluation of the Benzoquinones, Bis-Benzoquinones and Bis-Schiff Bases.

Table 16 summarizes the results for the biotesting of the prepared benzoquinones and Schiff Bases. Of the mutant yeast strains, the Sc-7 line shows the most sensitivity to benzoquinones. In the Sc-7 cell line, it is apparent that lengthening the alkyl side chain results in increased activity. The activity reaches a maximum with a decyl side chain (**6.31**), yet the activity is lost when a significantly longer nonadecyl side chain (**6.32**) is introduced; this trend has been noted in previous investigations for benzoquinones as cell allergens.¹¹

Table 16. Bioactivity Data for **6.1-2, 6.28-34, 6.42-44, 6.46-6.48.**

Compound	Yeast Based Cell Lines (IC ₁₂ , µg/mL)				Cancer Cell Lines (IC ₅₀ , µg/mL)	
	Sc-7	1138	1140	1353	A2780	M109
6.28	530 ± 100	580 ± 100	630 ± 180	830 ± 110	NT	NT
6.29	220 ± 50	200 ± 30	140 ± 20	233 ± 20	9.8 ± 0.36	NT
6.30	80 ± 25	220 ± 30	150 ± 20	210 ± 30	3.35 ± 0.31	NT
6.1	48 ± 1	240 ± 40	170 ± 40	285 ± 40	3.53 ± 0.31	10
6.2	16 ± 10	120 ± 10	130 ± 10	220 ± 10	3.42 ± 0.32	10
6.31	3 ± 1	380 ± 180	380 ± 180	380 ± 180	NT	10
6.32	>2000	>2000	>2000	>2000	NT	NT
6.33	440 ± 120	536 ± 40	430 ± 50	577 ± 40	12.30 ± 1.51	NT
6.34	180 ± 120	460 ± 80	420 ± 150	590 ± 80	10.16 ± 0.15	NT
6.42	>2000	>2000	>2000	>2000	16.54 ± 1.51	NT
6.43	>2000	>2000	>2000	>2000	14.47 ± 0.20	NT
6.44	>2000	>2000	>2000	>2000	15.76 ± 1.86	NT
6.46	30mm @ 1000 µg/mL	1300	1500	1300	18.46 ± 1.40	NT
6.47	NT	NA	NA	NA	NA	NT
6.48	NT	950	1950	1000	27.96 ± 6.40	NT

NT=Not tested

These results seem to show some dependency on lipophilicity over a selected range. A number of physical properties including lipophilicity (log P) have been calculated for the benzoquinones; they are summarized in Table 17.

Table 17. Calculated Physical Properties of Compounds **6.1-2, 6.28-44, 6.46-6.48.**

Compound	Molar Volume ^b	Dipole Moment ^c	Log (P) ^d	Molecular Weight ^e
6.28	129.2	0.632	0.86	152.15
6.29	145.7	0.540	1.40	166.18
6.30	178.5	0.498	2.46	194.23
6.1	194.9	0.496	2.99	208.26
6.2	227.5	0.483	4.05	236.31
6.31	276.4	0.471	5.65	278.39
6.32	422.1	0.474	10.43	404.63
6.33	189.4	0.868	2.63	228.25
6.34	193.0	0.902	1.99	224.25
6.42	292.5	0.003	3.10	358.39
6.43	308.6	0.455	3.63	372.42
6.44	389.3	0.030	6.29	442.55
6.46	280.5	2.159	3.06	328.37
6.47	344.3	3.872	2.34	388.50
6.48	334.8	2.942	4.34	384.47

a. All geometrically dependent calculations assume 'anti' conformations. b. cm³. Calculated with ACD CNMR 2.0. c. debye. Calculated with Chem 3D (AM1), MM2+ minimization. d. Calculated with ACD/Log P 1.0. e. g/mol (avg.)

A plot of activity versus lipophilicity (log P) for compounds the 2-methoxy-6-n-alkyl-1,4-benzoquinones is shown in Figures **6.13-14**. It shows a fairly good exponential relationship ($R^2=0.90$) existed between activity and lipophilicity in n-alkyl benzoquinones of small to moderate size (**6.1-2, 6.28-31**). Larger benzoquinones (**6.32**) do not fit this relationship. This plot predicts that the activity is a maximum when log P=5 (**6.31**).

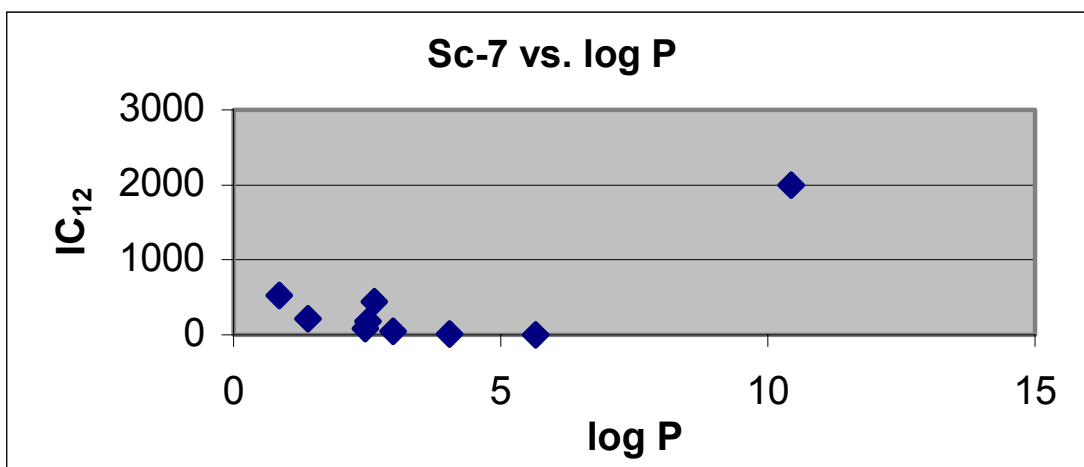


Figure 6-13. Relationship Between Lipophilicity and Activity in the Sc-7 Cell Line.

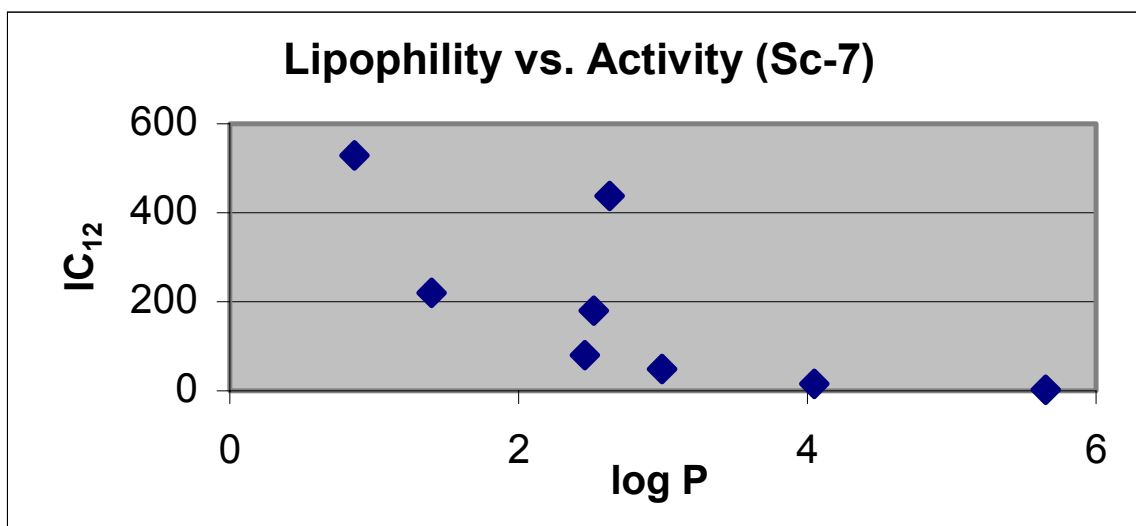


Figure 6-14. Relationship Between Lipophilicity and Activity in the Sc-7 Cell Line (Expanded Scale).

In Figure 6-14, the two points above the curve are the benzyl (**6.33**) and hydroxy-primin (**6.34**) analogs. Interestingly, the ACD Log P 1.0 software that predicted the lipophilicity of the hydroxy primin predicted two structures and two different Log P's for the hydroxy primin. The software predicted that a tautomerism would occur and that the hydroquinone is favored over the quinone form. The log P of the hydroquinone form does fit the curve better than that of the quinone form. However, NMR results (in various solvents) indicate that the quinone form is favored in solutions.

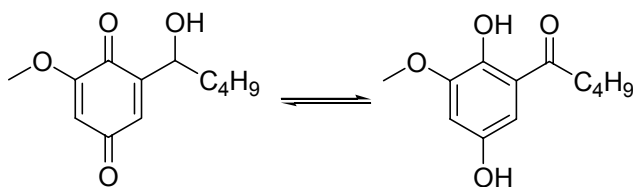


Figure 6-15. Calculated but not Seen Tautomerism of Hydroxy Primin

The other yeast strains (1138/1140/1353) were useful indicators of potential topoisomerase I and topoisomerase II inhibitors.¹⁰ Selective activity of the 1138 and 1140 strains versus the 1353 strain indicate a potential topoisomerase I inhibitor, whereas activity solely on the 1138 strain indicates a potential topoisomerase II inhibitor. Activity in all three strains indicates general DNA damaging compounds and/or antifungal activity. The moderate size alkyl chains (**6.1**, **6.2**, **6.29**, **6.30**) gave similar results, indicative of antifungal activity and possible general DNA damaging activity. All other side chain modifications led to significantly weaker activity. While there appeared to be some selectivity against the 1138 and 1140 versus the 1353, the selectivity was not large enough to indicate potential topoisomerase I activity. The most active of these compounds in the Sc-7 strain (**6.1**, **6.2**, **6.31**) were also tested in the M109 tumor

cell line, where they displayed activities of 10 $\mu\text{g/mL}$ (IC_{50}). The benzoquinones **6.1**, **6.2** and **6.30** were also tested in the A2780 human ovarian cancer cell lines where they showed good activity (about 3 $\mu\text{g/mL}$) but insufficient activity for further development. No correlations can be drawn from comparison of the bioactivity versus physical properties (R^2 for these cases was usually 0.6-0.7). The only pattern that can be concluded was that moderate length side chains (C_4H_9 to $\text{C}_{10}\text{H}_{21}$) generally showed greater activity than those of shorter or longer length; these results also agreed with those of Konig.¹¹

A review of the literature indicated that quite a number of benzoquinones have been previously synthesized. One interesting subset of reported compounds are bis-benzoquinones. These bis-benzoquinones contained long aliphatic spacer groups ($\text{C}_{14}\text{-C}_{16}$);¹⁸ however our results suggested that moderate length spacer groups may provide stronger bioactivity. The three bis-benzoquinones (**6.18-20**) showed poor solubility in the alcoholic and aqueous DMSO solutions prepared for biotesting. They displayed no activity versus the various mutant yeast strains. This was surprising since the lipophilicities ($\log P$) of the bis-benzoquinones were similar to those of the most active mono-benzoquinones. The bis-benzoquinones did display some activity against the A2780 human ovarian cancer cell line (approximately 15 $\mu\text{g/mL}$). While the activities of the bis-benzoquinones were significantly less than those of the mono-benzoquinones, it is possible that the benzoquinones show more selective cytotoxicity against cancer cells than against other (yeast) cells. However, this conclusion requires further investigation to be proven valid; this may be an artifact of the testing conditions.

The bis-Schiff bases also showed significantly less activity against the cell lines than the mono-benzoquinones. Nevertheless, it is still surprising to see any biological activity for Schiff bases. The ethylene analog **6.46** showed A2780 cytotoxicity comparable to that of the bis-

benzoquinones; the larger analog (**6.48**) showed less activity in the cell lines. The bis-Schiff bases were considerably more soluble in the alcoholic and aqueous DMSO solutions used for dilution. Compounds **6.46** and **6.48** were also considerably more active than the bis-benzoquinones against the yeast cell lines. The mechanism of action for these compounds has not yet been established; while they are roughly the same size and shape as the bis-benzoquinones, they are chemically different. The bis-benzoquinones are oxidizing agents whereas compound **6.46** has been shown to chelate nickel.¹⁶ Further investigation would be required to elucidate these results.

6.3 Experimental Section

General Experimental Procedures. Experiment procedures were carried out as previously reported in Chapter 2. Elemental Analysis was performed by Atlantic Microlab, Inc. (P.O. Box 2288, Norcross, GA 30091 Tel. No. 770-242-0082).

Yeast Bioassay. The yeast bioassay was performed using the yeast strains Sc-7, 1138, 1140 and 1353 as previously reported.

Cytotoxicity Bioassay. The A2780 assay was performed at Virginia Polytechnic Institute and State University as previously reported. The M109 assay was performed at Bristol Myers Squibb as reported in the literature.¹⁹

¹⁸ Croft, J.A.; Ritchie, E.; Taylor, W.C. *Aust. J. Chem.* **1976**, *29*, 1979.

¹⁹ a. Marks, T.A.; Woodman, R.J.; Geran, R.I.; Billups, L.H.; Madison, R.M. *Cancer Treat.* 1977, *61*, 1459. b. McBrien, K.D.; Bery, R.L., Lowes, S.E.; Neddermann, K.M.; Bursuker, I.; Huang, S.; Klohr, S.E.; Leet, S.E. *J. Antibiot.* **1995**, *48*, 1446.

General Procedures for the Synthesis of Alkyl and Benzyl Benzoquinones. Various 2-methoxy-6-alkyl-1,4-benzoquinones were synthesized in a manner similar to that reported by Konig. Alkyl and benzyl Grignard reagents were prepared by the slow addition of 0.009 mol of alkyl or benzyl bromide in 8 mL of THF to 0.629 g (0.026 mol) of magnesium turnings in a vented 20 mL vial with vigorous shaking until the addition was complete. The mixture was allowed to stir for 1 hour. 0.5 g (0.003 mol) of *o*-vanillin in 8 mL of THF was slowly added with vigorous shaking at 0 °C until either the addition was complete or until the yellow color (indicative of unreacted *o*-vanillin) persists. The vial was allowed to stand at room temperature overnight. The reaction was worked up with 100 mL of 10% hydrochloric acid in water, extracted with 200 mL of diethyl ether, and the ether layer dried over sodium sulfate; the solvent was removed under reduced pressure to afford the crude addition product as an oil. This crude product was purified with 25% EtOAc in hexane over silica gel; if necessary further purification was performed using a reverse phase 5 g Varian C18 SPE with gradient of 70-100% methanol in water.

The reduced phenol was prepared from the hydrogenation of the addition product with an equivalent weight of 5% palladium on carbon in 50 mL of methanol over a period of 2-5 days at atmospheric pressure and room temperature. The reaction was monitored by TLC until the reaction was complete or five days have passed. The reaction was filtered over Celite, with the Celite washed with additional methanol. The methanol was removed under reduced pressure; the product usually did not require further purification; if further purification was necessary it was subjected to Si gel PTLC with 25% EtOAc in hexane

The benzoquinone was synthesized by oxidizing 50-100 mg of the reduced phenol in with 0.5 g of Fremy's salt in either 100 mL of aqueous 5% sodium carbonate or with 20 mL of pH 9 phosphate buffer in 80 mL water with vigorous stirring overnight. The solution was extracted

twice with 100 mL of chloroform; the chloroform layer was dried over sodium sulfate, filtered, and solvent removed under reduced pressure. The crude product was then purified by Si gel PTLC with 25% EtOAc in hexane and/or recrystallization with hexane/CHCl₃ or hexane/EtOAc.

Compound **6.28** was synthesized in a similar fashion; however, the addition of a Grignard was not performed. *o*-Vanillin was reduced by 5% palladium on carbon with hydrogen followed by oxidation with Fremy's salt.¹¹

2-Methoxy-6-methyl-1,4-benzoquinone (6.28) was obtained as a tan-yellow solid, mp 144-145 °C (from hexane/CHCl₃); lit. 150 °C;¹¹ ¹H NMR Refer to Table 18; ¹³C NMR Refer to Table 19. Anal: Calcd for C₈H₈O₃•1/3H₂O: C, 60.76; H 5.52. Found C, 60.49; H, 5.36. Overall yield: 20%.

2-Methoxy-6-ethyl-1,4-benzoquinone (6.29) was obtained as a bright yellow solid, mp 109-111 °C (from hexane/CHCl₃); lit. 106 °C;¹¹ ¹H NMR Refer to Table 18; ¹³C NMR Refer to Table 19. Anal: Calcd for C₉H₁₀O₃: C, 65.05; H 6.07. Found C, 64.82; H, 6.21. Overall yield: 24%.

2-Methoxy-6-butyl-1,4-benzoquinone (6.30) was obtained as a bright yellow solid, mp 52-54 °C (from hexane/CHCl₃); lit. 55 °C;¹¹ ¹H NMR Refer to Table 18; ¹³C NMR Refer to Table 19. Anal: Calcd for C₁₁H₁₄O₃: C, 68.02; H 7.26. Found C, 67.74; H, 7.19 Overall yield: 19%.

2-Methoxy-6-pentyl-1,4-benzoquinone (Primin) (6.1) was obtained as a yellow solid, mp 62-64 °C (from hexane/CHCl₃); lit. 62-63 °C;¹¹ ¹H NMR Refer to Table 18; ¹³C NMR Refer to Table 19. Anal: Calcd for C₁₂H₁₆O₃: C, 69.21; H 7.74. Found C, 68.99; H, 7.74. Overall yield: 8%.

2-Methoxy-6-heptyl-1,4-benzoquinone (6.2) was obtained as yellow solid, mp 64-66 °C (from hexane/CHCl₃); lit. 63 °C; ¹¹ ¹H NMR Refer to Table 18; ¹³C NMR Refer to Table 19. Anal: Calcd for C₁₄H₂₀O₃: C, 71.16; H 8.53. Found C, 70.92; H, 8.56. Overall yield: 6%.

2-Methoxy-6-decyl-1,4-benzoquinone (6.31) was obtained as a tan-yellow solid, mp 62-63 °C (from hexane/EtOAc); lit. 60-61 °C; ¹¹ ¹H NMR Refer to Table 18; ¹³C NMR Refer to Table 19; EIMS *m/z* 278 (M⁺, 48), 193 (13), 179 (27), 166 (17), 154 (98), 139 (14), 124 (19), 109 (10), 69 (43); HREIMS *m/z* 278.1884 (calcd. For C₁₇H₂₆O₃ 278.1881). Anal: Calcd for C₁₇H₂₆O₃•1/3H₂O: C, 71.80; H 9.45. Found C, 71.98; H, 9.33. Overall yield: 17%.

2-Methoxy-6-nonadecyl-1,4-benzoquinone (6.32) was obtained as a tan-yellow waxy solid, mp 86-87 °C (from hexane/EtOAc); lit. 93 °C; ¹¹ ¹H NMR see Table 18; ¹³C NMR see Table 19; EIMS *m/z* 404 (M⁺, 75), 193 (6), 179 (12), 166 (11), 154 (100), 139 (13), 124 (15), 109 (12), 69 (37); HREIMS *m/z* 404.3297 (calcd. For C₂₆H₄₄O₃ 404.3290). Overall yield: 10%.

2-Methoxy-6-benzyl-1,4-benzoquinone (6.33) was obtained as a bright yellow solid, mp 128-130 °C (from hexane/CHCl₃); ¹H NMR See Table 18; ¹³C NMR See Table 19; overall yield: 19%; EIMS *m/z* (rel. int.) 228 (M⁺, 80), 213 (70), 196 (50), 185 (20), 168 (22), 157 (28), 143 (44), 129 (36), 128 (28), 115 (90), and 69 (100). Anal: Calcd for C₁₄H₁₂O₃: C, 73.67; H 5.30. Found C, 73.37; H, 5.32. Overall Yield: 7%.

Procedure for the Synthesis of 2-methoxy-6-(1'-hydroxy)-n-pentyl-1,4-benzoquinone. 2-Methoxy-6-(1'-hydroxy)-n-pentyl-1,4-benzoquinone was the result of inadequate hydrogenation

of 2-methoxy-6-(1'-hydroxy)-*n*-pentyl-phenol followed by oxidation with Fremy's salt. It was recovered in an overall yield of 21%.

2-Methoxy-6-(1'-hydroxy)-*n*-pentyl-1,4-benzoquinone (6.34) was obtained as a yellow-tan solid, mp 94-95 °C (from hexane/CHCl₃); ¹H NMR See Table 18; ¹³C NMR See Table 19. EIMS *m/z* (rel. int.) 224 (M⁺, 5), 196 (8), 195 (7), 182 (30), 168 (98), 167 (100), 159 (15), 158 (22), 140 (42), 139 (78), 125 (36), 122 (22) and 69 (62). Anal: Calcd for C₁₂H₁₆O₄: C, 64.27 H 7.19. Found C, 64.02; H, 7.18.

Preparation of Benzyl Protected *o*-Vanillin. (6.35). Benzyl bromide 2 g (1 eq.) was added to a stirred solution of 2.0 g *o*-vanillin (1.1 eq) and 7.6 g K₂CO₃ (5 eq.) in 26 mL of DMF. The mixture was allowed to react overnight. Water and CHCl₃ were added to the mixture; the solution was shaken and the organic layer collected by separatory funnel. The organic layer was washed three times with aqueous 10% NaOH followed with water. The organic layer was dried over Na₂SO₄, filtered and solvent was removed by rotary evaporation. Yield: 2.69 g (96%)

Benzyl *o*-vanillin (2-benzyloxy, 3-methoxy-benzaldehyde) (6.35) was obtained as an oil; ¹H NMR (CDCl₃) δ 10.25 (1H, s, CHO), 7.37 (6H, m, Bn-H, H-6), 7.15 (1H, dd, 8, 1.8 Hz, H-4), 7.09 (1H, dd, 7.75, 7.75, H-5), 5.17 (2H, s, CH₂), 3.89 (3H, s, OMe); ¹³C NMR (CDCl₃) δ 190.27 (CHO), 153.17 (C-2), 151.14 (C-3), 136.56 (C-1'), 130.36 (C-1), 128.97 (C-3'), 128.78 (C-2'), 128.60 (C-4'), 124.38 (C-5), 119.04 (C-6), 118.17 (C-4), 76.37 (CH₂), 56.15 (OMe); EIMS *m/z* (rel. int.) 242 (M⁺, 12), 214 (M-CHO, 14), 213 (M-OMe, 34), 181 (M-C₅H₅, 8), 150 (M-C₇H₇, 45), 136 (M-C₇H₇O, 7), 122 (M-C₇H₇-OMe, 21), 108 (C₇H₇OH, 53), 91 (C₇H₇, 100) (15) and 65 (C₅H₅).

General Procedures for the Synthesis of Alkylated-Bis-Benzyloxy-1'-Hydroxy-Guaiacols.

Various bis-benzoquinones were synthesized in a manner similar to that reported earlier. Alkyl bis-Grignard reagents were prepared by the slow addition of 0.002 mol of 1,n-dibromoalkane in 5 mL of freshly dried THF to 0.629 g (0.006 mol) of magnesium turnings under argon in a 20 mL vial with vigorous stirring. This was allowed to stir an additional 6h after addition 1.0 g (0.006 mol) of benzyl o-vanillin in 5 mL of THF was slowly added with vigorous stirring at 0 °C under argon until the addition was complete. The vial was allowed to stir at room temperature overnight under argon. The reaction was worked up with 100 mL of 10% hydrochloric acid in water, extracted with 200 mL of diethyl ether, and the ether layer dried over sodium sulfate; the solvent was removed under reduced pressure to afford the crude addition product as an oil. This crude product was purified with 25% EtOAc in hexane over silica gel; if necessary further purification was performed using PTLC.

1,6-Di-(2-benzyloxy, 3-methoxyphenyl)-hexan-1,6-diol (6.36) was obtained as an oil; ¹H NMR see Table 20; ¹³C NMR see Table 21; FABMS⁺ *m/z* (rel. int.) 566 (M+Na⁺, 70), 524 (M-H₂O, 12), 506 (M-2H₂O, 12), 474 (M-2H₂O-OMe, 12), 434 (M-Bn-H₂O, 18), 416 (M-Bn-2H₂O, 100), 325 (M-2Bn-2H₂O, 76); FABMS⁻ *m/z* (rel. int.) 542 (M, 40), 459 (43), 458 (41), 451 (M-Bn, 100), 433 (M-Bn-H₂O, 38), and 410 (25); yield: 34%.

1,7-Di-(2-benzyloxy, 3-methoxyphenyl)-heptan-1,7-diol (6.37) was obtained as an oil; ¹H NMR see Table 20; ¹³C NMR see Table 21; EIMS *m/z* (rel. int.) 556 (M⁺, <1), 538 (M-H₂O, <1), 520 (M-2H₂O, <1), 430 (3, M-Bn-2H₂O), 340(7,M-2Bn-2H₂O), 204 (C₁₃H₁₆O₂, 13), 137 (38, C₉H₉O₂), 91 (C₇H₇, 100) and 65 (C₅H₅, 20); yield: 43%.

1,12-Di-(2-benzyloxy, 3-methoxyphenyl)-dodecan-1,12-diol (6.38) was obtained as an oil; ^1H NMR see Table 20; ^{13}C NMR see Table 21; FABMS⁺ m/z (rel. int.) 649 (M+Na⁺, 22), 608 (M-H₂O, 6), 591 (M-2H₂O, 61), 500 (M-Bn-2H₂O, 82), 410 (100), 409 (M-2Bn-2H₂O, 88), 377 (62); FABMS⁺ m/z (rel. int.) 626 (M, 11), 625 (M-1, 28), 536 (M-Bn, 88), 459 (M-Bn-Ph, 29), 367 (C₂₁H₃₆O₅, 100); yield: 25%.

General Procedures for the Synthesis of Alkylated Bis-Guaiacols. The reduced phenols were prepared from the hydrogenation of the addition product with an equivalent weight of 5% palladium on carbon in 50mL of methanol over a period of 2-5 days at atmospheric pressure and room temperature with vigorous stirring. The reaction was monitored by TLC until the reaction was complete or five days have passed. The reaction was filtered over Celite; the Celite washed with additional methanol. The methanol was removed under reduced pressure; the product usually did not require further purification; if further purification was necessary it was subjected to Si PTLC with EtOAc-hexane(1:4)

1,6-Di-(2-benzyloxy, 3-methoxyphenyl) hexane (6.39) was obtained as a slightly pink solid, 98-100 °C mp; ^1H NMR see Table 20; ^{13}C NMR see Table 21; FABMS⁺ m/z (rel. int.) 368 (M+K⁺, 32), 353 (M+Na⁺, 5), 331 (M+1, 50), 330 (M, 100), 312 (M-H₂O, 23), 307 (42), and 289 (38); FABMS⁻ m/z (rel. int.) 367 (M+K-1, 32), 352 (M+Na-1, 3), and 329 (M-1, 22); yield: 58%.

1,7-Di-(2-benzyloxy, 3-methoxyphenyl) heptane (6.40) was obtained as a white solid; ^1H NMR see Table 20; ^{13}C NMR see Table 21; FABMS⁻ m/z (rel. int.) 343 (M-1, 11), 329 (M-Me, 2), 313 (M-OMe, 2), 293 (3), 275 (5), 273 (3), 221 (M-C₇H₇O₂, 5), and 217 (11); yield: 47%.

1,12-Di-3-(2-benzyloxy, 3-methoxyphenyl) dodecane (6.41) was obtained as a white solid, mp 68-70 °C; ¹H NMR see Table 20; ¹³C NMR see Table 21; FABMS⁻ *m/z* (rel. int.) 414 (M, 11), 413 (M-1, 40), 306 (7); yield: 98%.

General Procedures for the Synthesis of Alkylated Bis-Benzoquinones. The bis-benzoquinones were synthesized by oxidizing 50-300 mg of the reduced guaiacol with 12-80 mg of salcomine under bubbled oxygen in 10 mL DMF. Water was added and the solution was extracted twice with 100mL of chloroform; the chloroform layer was dried over sodium sulfate, filtered, and solvent removed under reduced pressure. The crude product was then purified by Si gel PTLC with 25% EtOAc in hexane and/or recrystallization with hexane/CHCl₃ or hexane/EtOAc. If necessary, the product was subjected to RP-18 PTLC with MeOH:H₂O (70:30).

1,6-Di-(3-methoxy-1,4-benzoquinonyl) hexane (6.42) was obtained as an earthy yellow solid, mp 177-178 °C; ¹H NMR see Table 18; ¹³C NMR see Table 19; FABMS *m/z* (rel. int.) 358 (M⁺, 10), 206 (C₁₂H₁₄O₃, 17), 205 (C₁₂H₁₃O₃, 43), 177 (42), 153 (51), 152 (28), and 69 (100); yield: 32%.

1,7-Di-(3-methoxy-1,4-benzoquinonyl) heptane (6.43) was obtained as a tan solid, mp 121-123 °C; ¹H NMR see Table 18; ¹³C NMR see Table 19; FABMS *m/z* (rel. int.) 374 (51), 372 (M⁺, 21), 263 (28), 244.1 (60), 221 (28), 219 (7), 201 (95), and 193 (63); yield: 70%.

1,12-Di-(3-methoxy-1,4-benzoquinonyl) dodecane (6.44) was obtained as a yellow solid, mp 144-145 °C; ¹H NMR see Table 18; ¹³C NMR see Table 19; FABMS *m/z* (rel. int.) 443 (M⁺, 73), 391 (39), and 371 (23); yield: 5 %.

Preparation of Bis-Schiff Bases. The compound **6.46** were prepared from the addition of 0.02 mol of ethylene diamine to a stirred solution of 0.04 mol of *o*-vanillin in 200 mL of ethanol. Compound **6.48** was prepared identically at one-tenth the scale of **6.46**. The mixtures were allowed to react for four hours. Compound **6.46** precipitated out of solution. It was filtered, washed with ether, and dried. Compound **6.48** did not precipitate out of solution. Instead, solvent was removed to afford a residue; compound **6.44** was recrystallized from this residue with EtOAc and hexane.

Ethylene diamine, *o*-vanillin bis-Schiff base (6.46) was obtained as a yellow solid, mp 155-156 °C; IR Spectrum (neat): 2998, 2935, 2900, 2849, 2838, 1630, 1464, 1252, 1080, 966, 834; ¹H NMR see Table 22; ¹³C NMR see Table 23; FABMS⁺ *m/z* (rel. int.) 329 (M+1)(100) and 328 (M⁺) (43); FABMS⁻ *m/z* (rel. int.) 327 (M-1) (43), 306 (100), 305 (98); yield: 85 %.

Hexamethylene diamine, *o*-vanillin bis-Schiff base (6.48) was obtained as yellow crystals, mp 74-75 °C; IR Spectrum (neat): 3000, 2929, 2855, 2838, 1630, 1464, 1252, 1160, 1080, 966, 840; ¹H NMR see Table 22; ¹³C NMR see Table 23; FABMS⁺ (*m/z*) 386 (M+1), (100), 372 (72), 328 (76), 283.9 (89); HRFABMS⁺ (*m/z*) 385.2123 (calc. For C₂₂H₂₉O₄N₂ 385.2127); yield: 75 %.

Preparation of Reduced Schiff Base (6.47). Compound **6.46** (1.25 g) in 50 mL of EtOAc was hydrogenated with 0.4 g of palladium charcoal and hydrogen for three days at room temperature

and atmospheric pressure. The mixture was passed over celite and washed with 100 mL of acetone. The solvent was removed by rotary evaporation.

Diamine 6.47: tan solid, mp 151-152 °C; ¹H NMR see Table 22; ¹³C NMR see Table 23; FABMS⁺ *m/z* (rel. int.) 355 (M+Na)⁺(40), 333 (M+1) (12), 245 (40), and 328 (M⁺) (43); FABMS⁻ *m/z* (rel. int.) 331 (M-1) (12), 306 (100), 305 (78), 304 (20); yield: 6.4 %.

Table 18. ¹H NMR Spectral Data for Compounds **6.1-2**, **6.28-34**, and **6.42-44**.

Proton	6.28	6.29	6.30	6.1	6.2	6.31
H-3 (1H)	5.87, d, <i>J</i> = 2.3	5.87, d, <i>J</i> = 2.3	5.86, d, <i>J</i> = 2.5	5.86, d, <i>J</i> = 2.8	5.86, d, <i>J</i> = 2.3	5.86, d, <i>J</i> = 2.5
H-5 (1H)	6.52, dt <i>J</i> = 2.3, 1.6	6.47, dt <i>J</i> = 2.7, 1.7	6.47, bd, <i>J</i> = 1.9	6.46, dt, <i>J</i> = 2.5, 1.4	6.46, bd, <i>J</i> =2.6	6.47, bd, <i>J</i> = 2.6
H-1' (2H)		2.46, dq, <i>J</i> = 7.6, 1.8	2.44, dt <i>J</i> = 6.5, 1.6	2.41, dt, <i>J</i> = 8.0, 1.3	2.41, dt <i>J</i> = 7.5, 1.4	2.41, d <i>J</i> = 7.0
H-2' (2H)			1.47, m	1.49, m	1.49, m	1.47, m
(CH ₂) _n			1.37, m	1.31, m	1.31, m	1.24, m
CH ₃ (3H)	2.05, bs	1.13, t, <i>J</i> = 7.3	0.92, t, <i>J</i> = 7.3	0.87, t, <i>J</i> = 6.9	0.87, t, <i>J</i> =7.0	0.86, t <i>J</i> = 6.9
OMe (3H)	3.81, s	3.80, s	3.80, s	3.80, s	3.79, s	3.80, s
Proton	6.32	6.33	6.34	6.42	6.43	6.44
H-3 (1H)	5.86, d, <i>J</i> = 2.5	5.86, d, <i>J</i> = 2.3	5.89, d <i>J</i> = 2.5	5.86, d, <i>J</i> = 2.5	5.86, d, <i>J</i> = 2.5	5.85, d, <i>J</i> = 2.5
H-5 (1H)	6.47, dt <i>J</i> = 2.5, 1.3	6.29, dt, <i>J</i> = 2.3, 1.6	6.69, dt <i>J</i> = 2.5, 1.2	6.45, dt <i>J</i> = 2.3, 1.2	6.47, dt <i>J</i> = 2.5, 1.3	6.46, dt <i>J</i> = 2.2, 1.6
H-1' (2H)	2.41, dt <i>J</i> = 7.9, 1.4	3.74, d, <i>J</i> = 1.4	4.69, m	2.41, dt <i>J</i> = 8.0, 1.3	2.41, dt <i>J</i> = 7.9, 1.4	2.41, dt <i>J</i> = 7.6., 1.6
H-2' (2H)	1.49, m		1.7, m	1.49, m	1.49, m	1.48, m
(CH ₂) _n	1.24, m		1.38, m	1.36, m	1.24, m	1.30-1.23
CH ₃ (3H)	0.87, t, <i>J</i> =6.9		0.89, t, <i>J</i> = 7.3	0.87, t, <i>J</i> =6.9	0.87, t, <i>J</i> =6.9	0.87, t, <i>J</i> =6.9
Ar-H-3' (1H)		7.19, bd <i>J</i> = 6.7				
Ar-H-4' (1H)		7.31, bt <i>J</i> = 7.1				
Ar-H-5' (1H)		7.24, tt, <i>J</i> = 7.3, 1.4				
OMe (3H)	3.80, s	3.81, s	3.81, s	3.81, s	3.80, s	3.79, s

Table 19. ¹³C NMR Spectral Data for Compounds **6.1-2**, **6.28-34**, and **6.42-44**.

Carbon	6.28	6.29	6.30	6.1	6.2	6.31	6.32	6.33	6.34	6.32	6.43	6.44
C-1	182.1	182.2	182.4	182.2	182.3	182.4	182.2	182.0	182.4	182.1	182.2	182.2
C-2	158.8	158.9	159.0	158.9	159.3	158.7	158.8	158.9	158.4	158.9	158.9	158.9
C-3	107.1	107.0	107.4	107.1	107.2	107.0	107.0	107.3	107.0	107.2	107.2	107.2
C-4	187.7	187.8	187.7	187.8	188.1	187.8	187.8	187.6	187.1	187.8	187.7	187.7
C-5	132.8	132.0	133.5	132.2	133.1	132.9	132.9	133.9	131.9	133.0	133.0	132.9
C-6	147.6	147.7	144.1	148.7	148.1	147.4	147.7	146.7	148.1	147.4	147.4	147.6
CH ₃ O	53.6	56.4	56.4	55.9	56.4	55.8	56.4	56.5	56.4	56.3	56.4	56.3
C-1'	28.7	28.8		21.9	29.8	28.8	28.8	35.0	68.4	29.1	29.0	29.6
C-2'	27.7	27.5			28.5	27.8	27.7	136.4	35.9	28.7	28.7	29.5
C-3'	29.0	31.5			22.4	29.3	29.3	129.5	27.7	27.8	27.7	29.4
C-4'	29.2	22.4				29.6	29.4	128.9	22.2	29.0		29.3
C-5'	31.7					29.6		127.1				28.8
C-6'	22.6					29.4						27.8
C-7'						29.4						
C-8'						32.0	29.6					
C-9'						22.7						
(CH ₂) ^a							29.8 ^a					
C-16'							29.4					
C-17'							32.1					
C-18'							22.8					
CH ₃	14.1	13.9	15.4	11.5	13.9	14.1	14.1		13.6			

a. Includes C-5', C-6', C-7', C-9' to C15' b. in CDCl₃

Table 20. ¹H NMR of Bis-Benzoquinone Intermediates.

Proton	6.36	6.37	6.38	6.39	6.40	6.41
H-3 (1H)	7.06, bt, <i>J</i> = 8.0	7.06, m	7.06, m	6.76, m	6.73, m	6.75, m
H-4 (1H)	6.95, dd, <i>J</i> = 7.8, 0.9	6.95, m	6.96, m	6.76, m	6.73, m	6.75, m
H-5 (1H)	6.87, bd, <i>J</i> = 8.0	6.87, m	6.88, m	6.76, m	6.73, m	6.75, m
Ph (5H)	7.35, m	7.35, m	7.37, m			
Ph-CH ₂ (2H)	5.05, m	5.05, m	5.05, m			
H-1' (2H)	4.84, bt <i>J</i> = 6.4	4.86, m	4.84, bt <i>J</i> = 5.6	2.63, d <i>J</i> = 7.6	2.61, d <i>J</i> = 7.6	2.63, <i>J</i> = 5.5
H-2' (2H)	1.66-1.37, m	1.62, m	1.63, m	1.61, m	1.59, m	1.59, m
(CH ₂) _n	1.19, m	1.48-1.19, m	1.63-1.25, m	1.42, m	1.35-1.24, s	1.33-1.25, m
-OH (1H)				5.70	5.65	5.67
OMe (3H)	3.87, s	3.89, s	3.89	3.89	3.87	3.87

Table 21. ¹³C NMR of Bis-Benzoquinone Intermediates.

Carbon	6.36	6.37	6.38	6.39	6.40	6.41
C-1	144.8	144.8	144.8	143.5	143.5	146.3
C-2	138.8	137.7	138.9	128.8	128.8	128.9
C-3	118.7	118.6	137.7	122.4	122.4	122.4
C-4	124.4	124.4	124.4	119.2	119.2	119.2
C-5	111.4	111.4	111.4	108.2	108.2	108.2
C-6	152.5	152.5	152.5	146.4	146.5	143.5
Bn-CH ₂	75.0	75.0	75.0			
OMe	55.9	55.9	55.9	56.1	56.0	56.0
Bn-C-1	137.6	136.8	137.7			
Bn-C-2	128.4	128.4	128.4			
Bn-C-3	128.6	128.5	128.5			
Bn-C-4	128.2	128.2	128.2			
C-1'	69.4	69.4	69.6	29.8	29.8	29.9
C-2'	38.0	38.0, 32.7	38.0	29.8	29.7	29.8
C-3'	25.7	29.4, 26.0	29.7	29.5	29.6	29.8
C-4'		25.8, 25.6	29.4		29.5	29.7
C-5'			26.1			29.7
C-6'			24.3			29.7

Table 22. ^1H NMR data for **6.46-48**.

Proton	6.46	6.47	6.48
1'	8.54 s	4.07 s	8.29 s
2'	4.00 s	2.81s	3.57 t, $J = 6.4$ Hz
3'			1.69 m
4'			1.42 m
OMe	3.79 s	3.75 s	3.879 s
Ar-3	6.77 d, $J = 7.8$ Hz	6.88, m	6.75, d, $J = 8.0$ Hz
Ar-4	6.97 ddd, $J = 12.6,$ 8.1, 1.4 Hz	6.90, m	6.88, ddd, $J = 13.7,$ 7.4, 1.3 Hz
Ar-5	6.78 d, $J = 8.0$ Hz	6.94, m	6.77, d, $J = 7.9$ Hz

a. Compounds **6.46** and **6.48** measured in d_6 -acetone. b. Compound **6.47** measured in d_5 -pyridine.

Table 23. ^{13}C NMR data for **6.46-48**.

Carbon	6.46	6.47	6.48
1'	163.09	50.82	164.80
2'	55.55	48.23	56.28
3'			30.84
4'			26.95
OMe	59.46	55.79	58.78
Ar-1	151.79	148.34	152.92
Ar-2	148.55	147.48	148.85
Ar-3	117.96	118.55	122.99
Ar-4	114.07	111.65	113.96
Ar-5	123.40	125.86	122.99
Ar-6	118.98	121.66	117.77

a. Compounds **6.46** and **6.48** measured in d_6 -acetone. b. Compound **6.47** measured in d_5 -pyridine.

VII. CONCLUSIONS

As part of ongoing investigations for anticancer drugs from rainforest flora, five plant extracts were determined to contain interesting bioactivity. These extracts were subjected to various separation techniques, affording a number of bioactive compounds that were then characterized by spectral and degradative methods.

Two new diterpenes were isolated from *Hymenaea courbaril*, which in an earlier investigation had provided a new diterpene. The absolute configurations of these diterpenes were assigned on the basis of anisotropic NMR studies, X-ray crystallography, circular dichroism analysis and previously reported literature. Derivatization with chiral reagents afforded amides whose conformations were determined by NOE interactions. Knowledge of these conformations permitted predication of the absolute configuration of the major diterpene from the measured anisotropic induced shifts in the ^1H NMR spectra.

A methanol extract of *Cestrum latifolium* Lam. yielded the known compound parissaponin Pb. Hydrolysis afforded its aglycone, the known spirostanol diosgenin. GCMS analysis characterized the derivatized, hydrolyzed sugars.

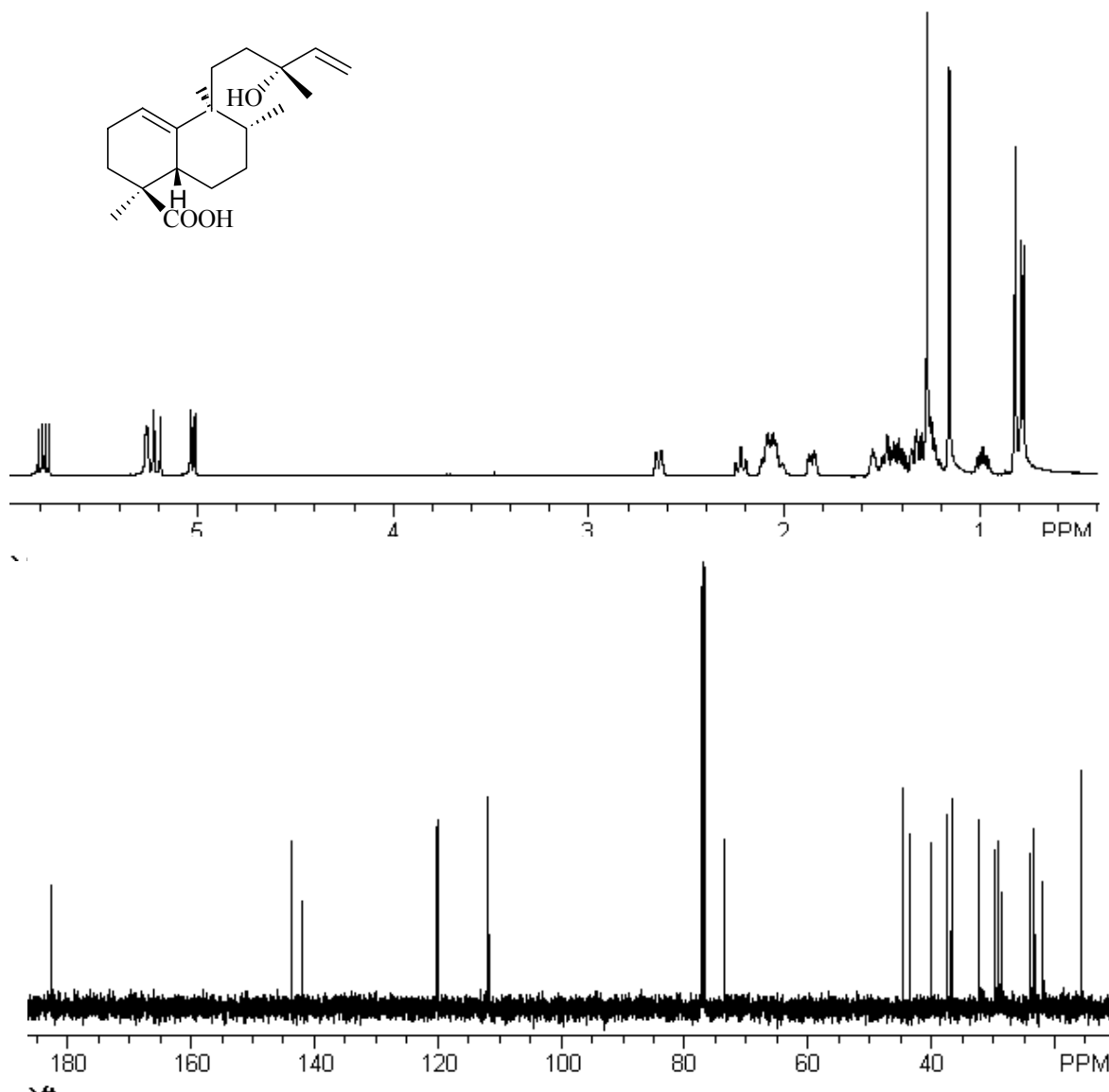
Previous investigations of *Albizia subdimidiata* provided two saponins including the new compound albizatrioside A. The sugar moieties of these two compounds required further characterization. They were characterized by spectral analysis of the partially hydrolyzed products and by GCMS analysis of the hydrolyzed sugars. Conversion of the hydrolyzed sugars into chiral thiazolidine acetates permitted identification of the absolute configuration of the pentoses by GCMS

Pittoviridoside, a saponin from *Pittosporum viridiflorum*, was isolated in a previous investigation. Further investigation was required to characterize the stereochemical environment of the sugar moiety. The stereochemistries of the pentose sugars were determined by conversion into thiazolidine acetates of known stereochemistries and analysis with standards by GCMS.

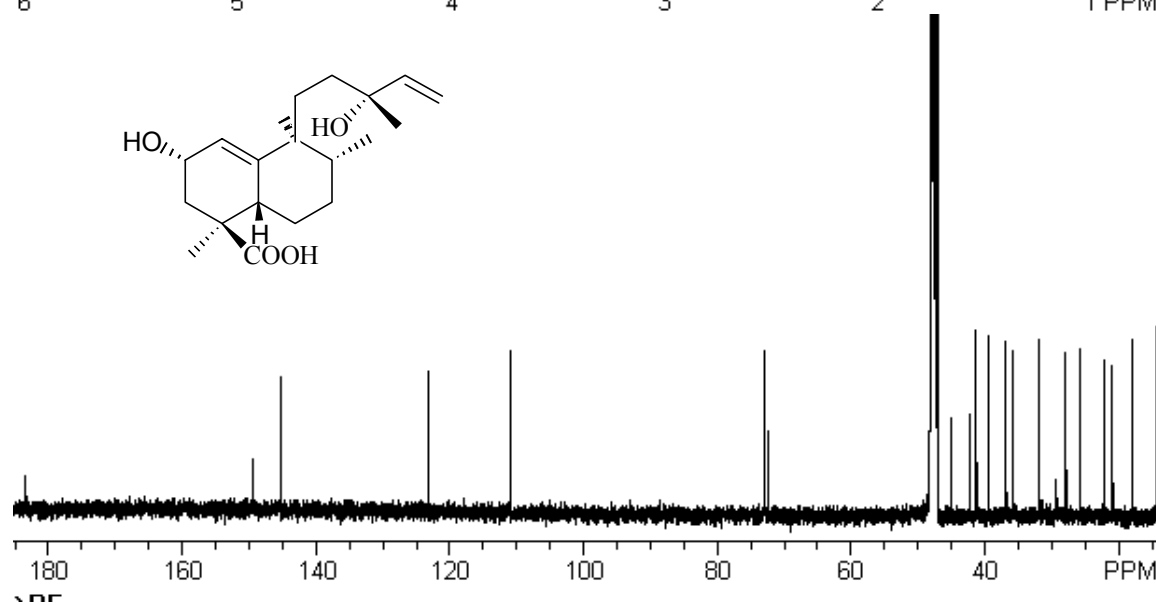
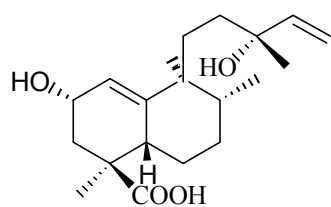
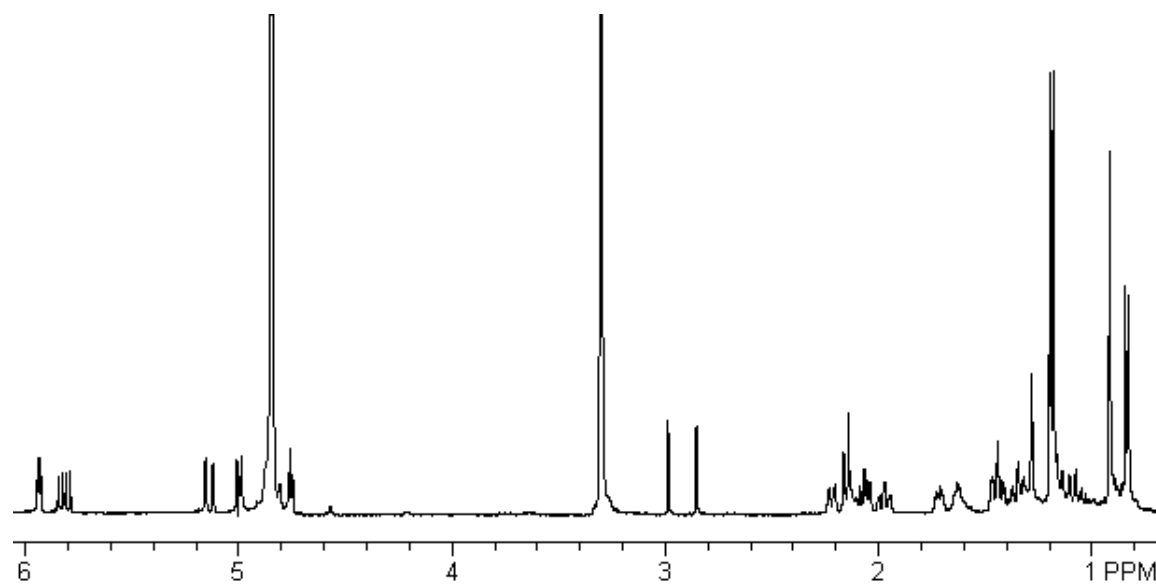
A previous investigation of *Miconia lepidota* isolated two benzoquinones, primin and its *n*-heptyl analog. Fifteen analogs were synthesized for structure-activity relationship determination. It was found that benzoquinones with moderate-length alkyl side chains displayed the strongest activity in our yeast and cancer cell lines.

APPENDIX

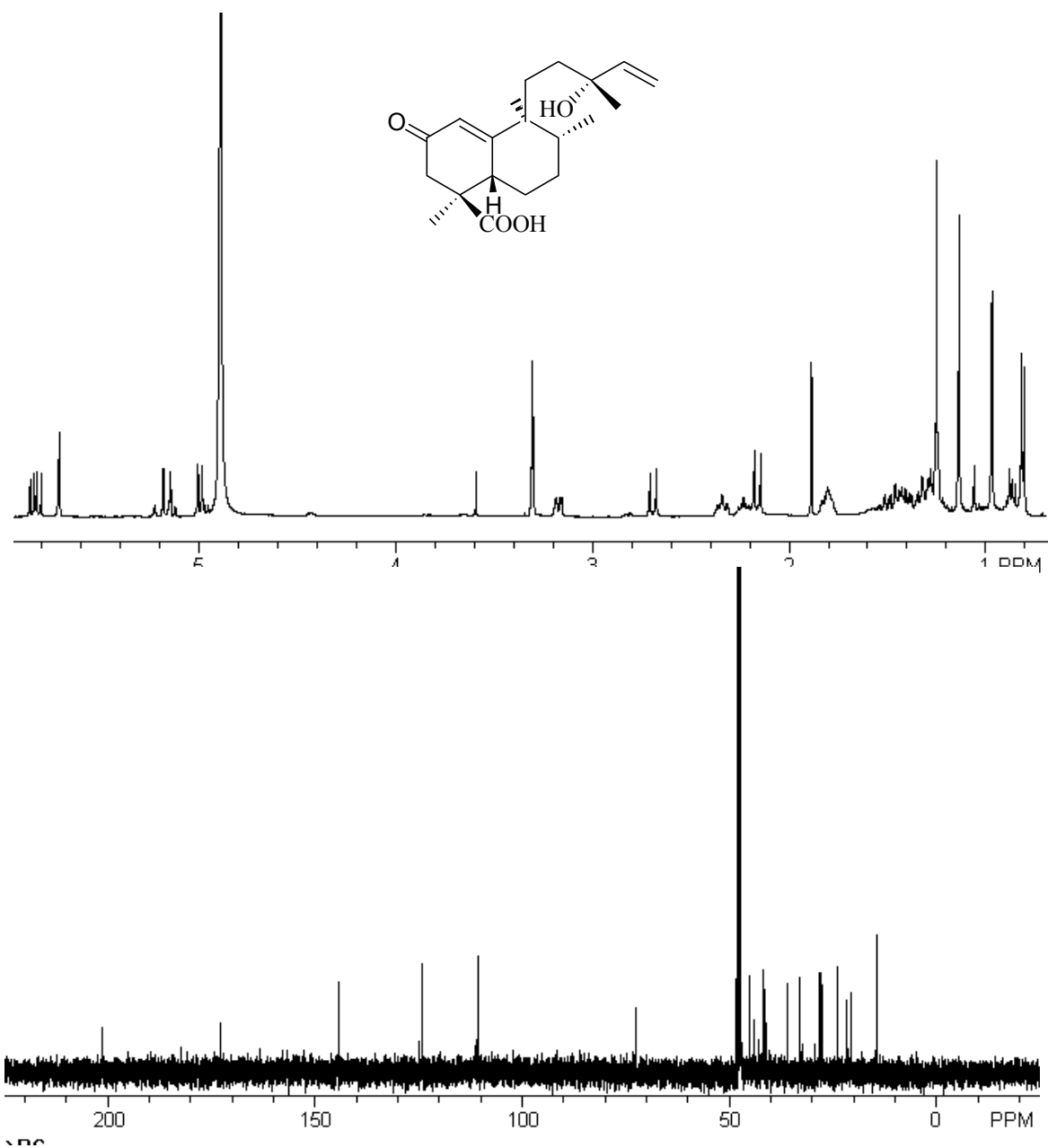
JMB-151-183-4 (**2.10**) (13*R*)-13-Hydroxy-1(10),14-*ent*-halimadien-18-oic acid



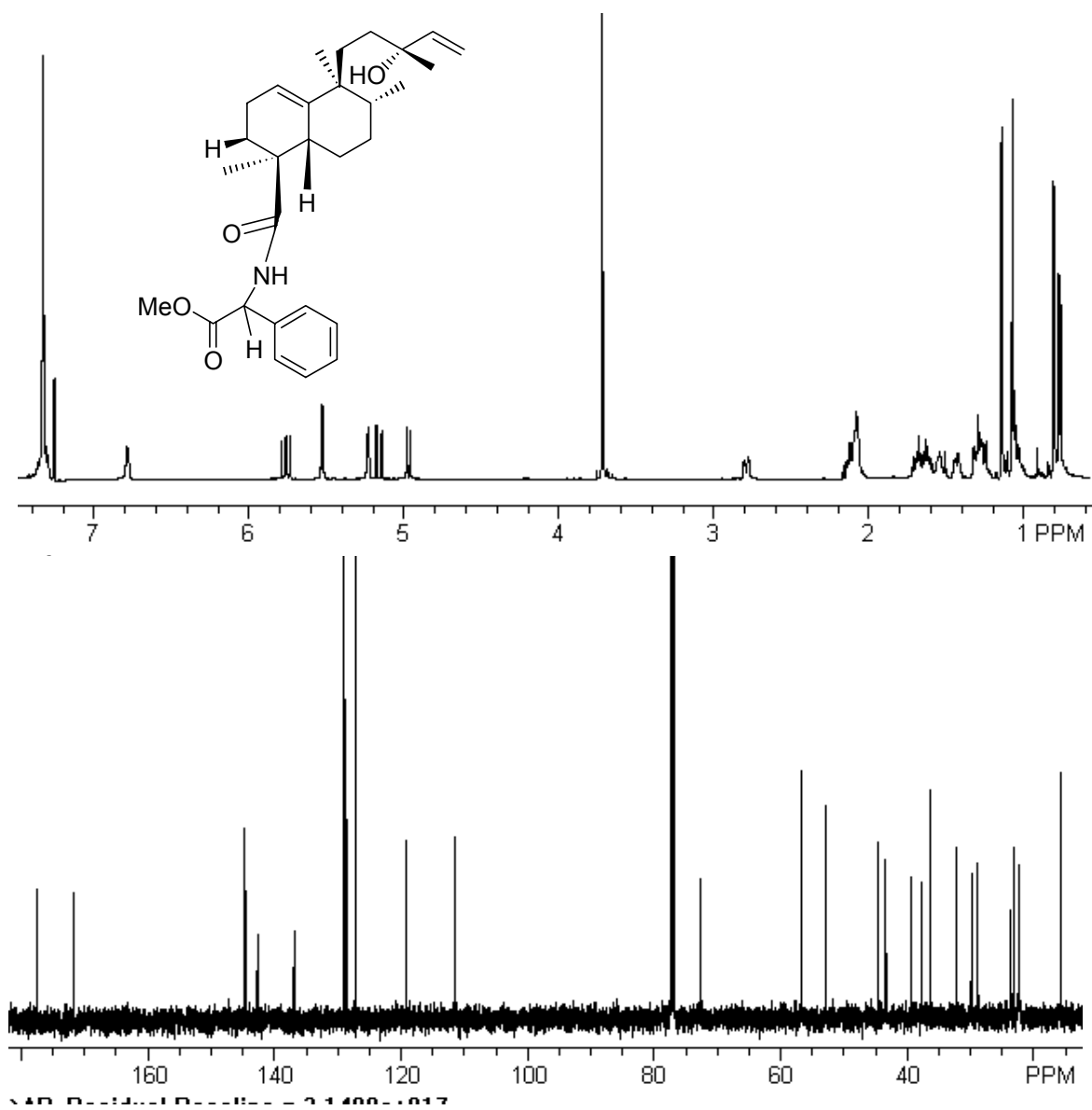
JMB-147-297-6 (**2.11**) (2*S*,13*R*)-2,13-Dihydroxy-1(10),14-*ent*-halimadien-18-oic acid



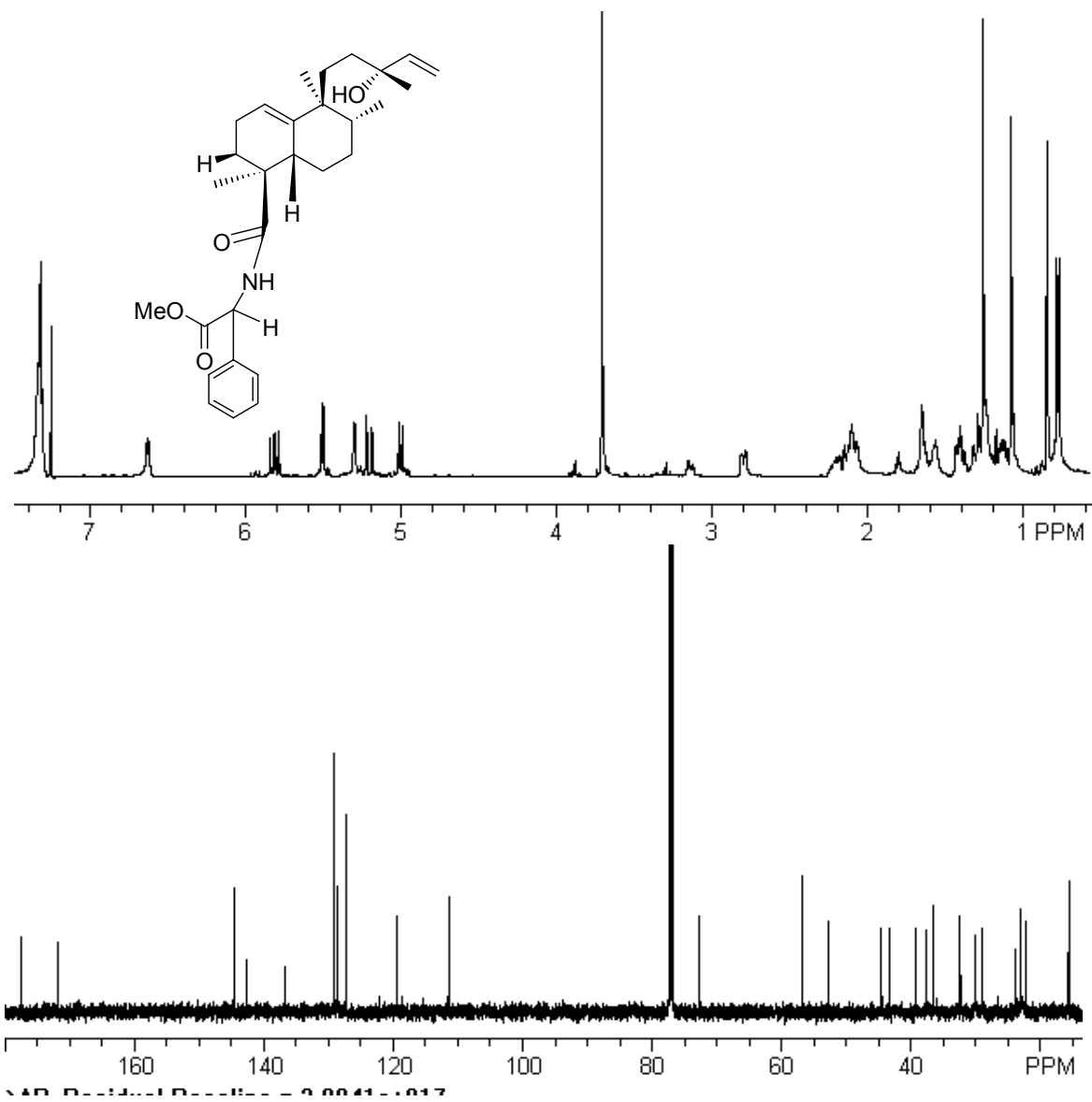
JMB-151-252-2 (2.7) 2-Oxo-(13*R*)-13-hydroxy-1(10),14-*ent*-halimadien-18-oic acid
JMB-147-255-6
JMB-151-266-2



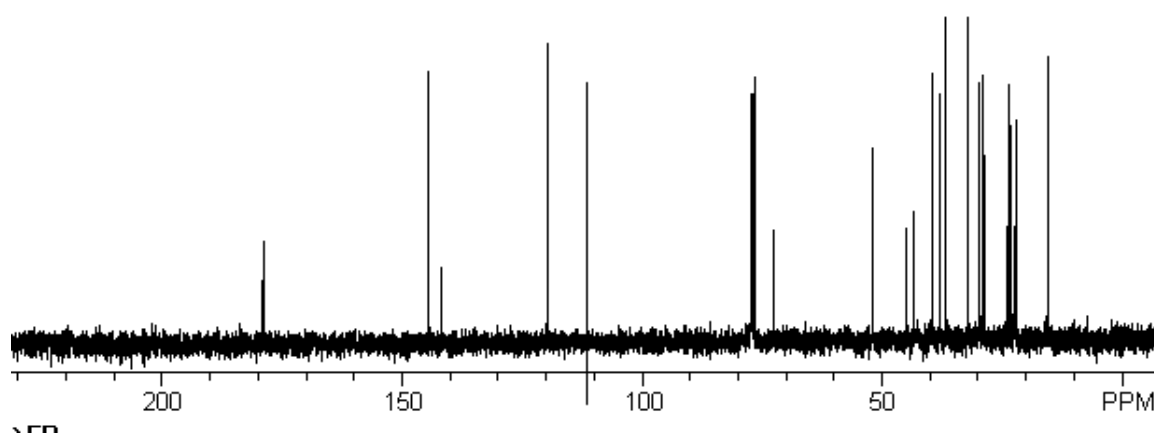
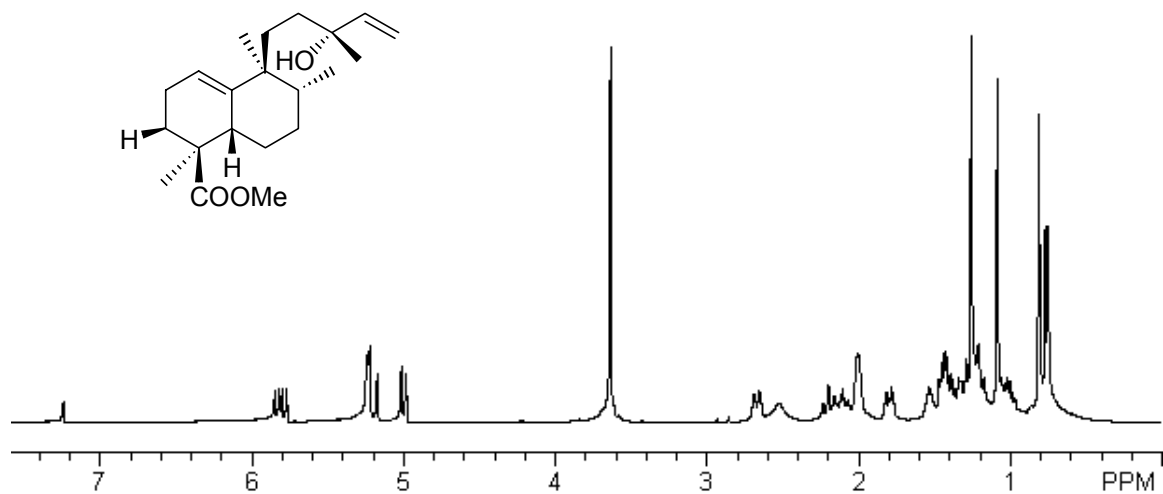
JMB-151-214-2 (13*R*)-13-hydroxy-1(10),14-*ent*-halimadien-18-oic acid (*S*)-PGME amide



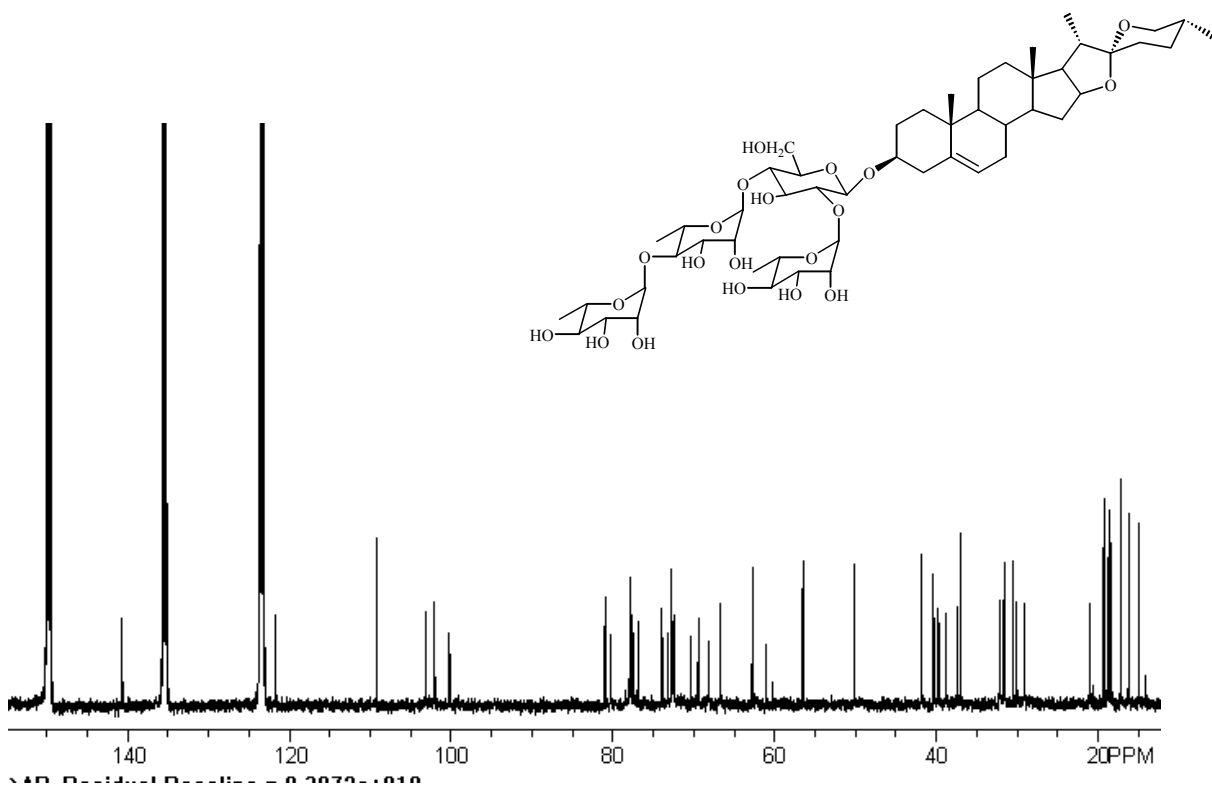
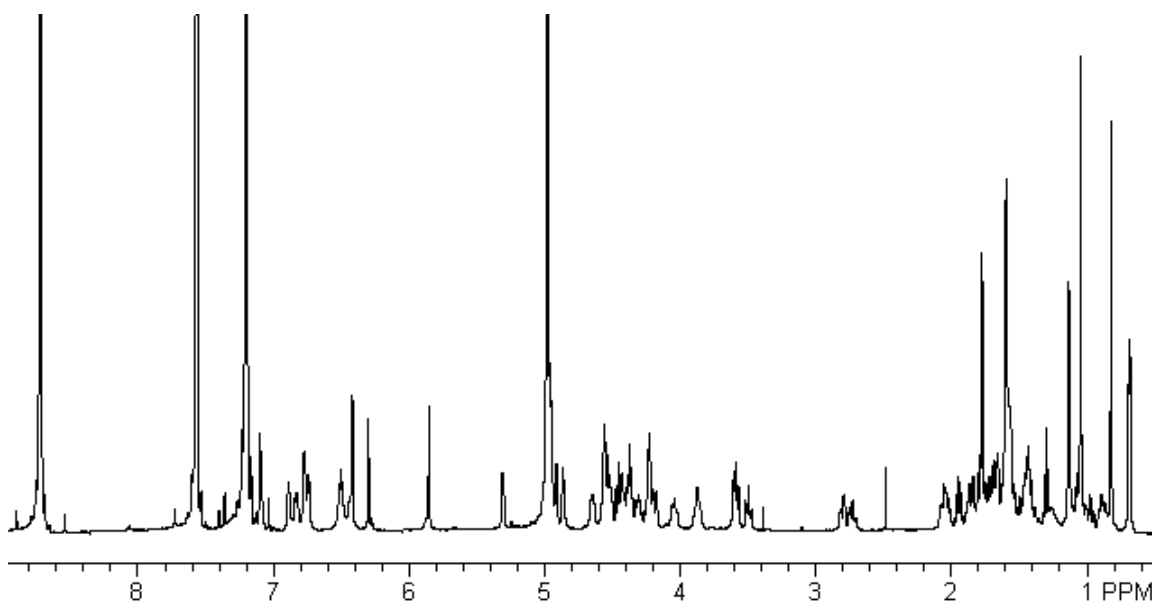
JMB-151-215-5 (13*R*)-13-hydroxy-1(10),14-*ent*-halimadien-18-oic acid (*R*)-PGME amide



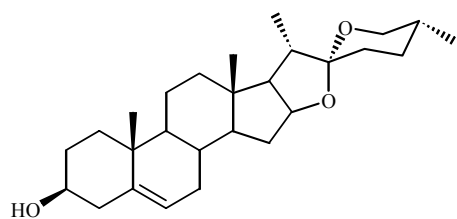
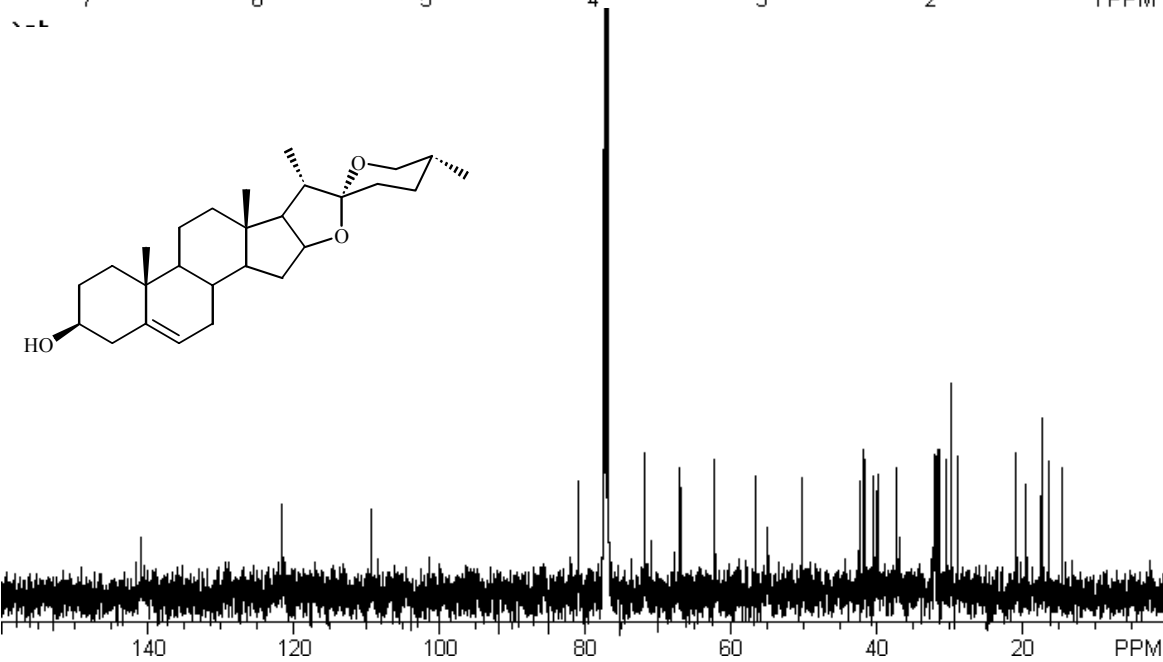
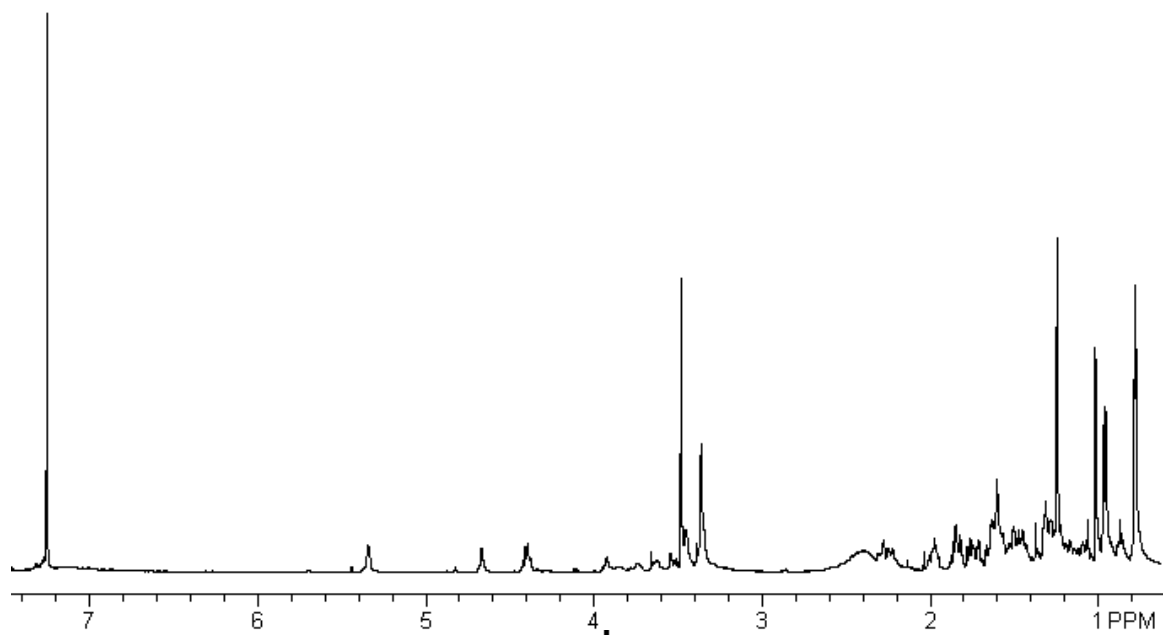
JMB-151-273 (**2.13**) (13*R*)-13-hydroxy-1(10),14-*ent*-halimadien-18-oic acid methyl ester



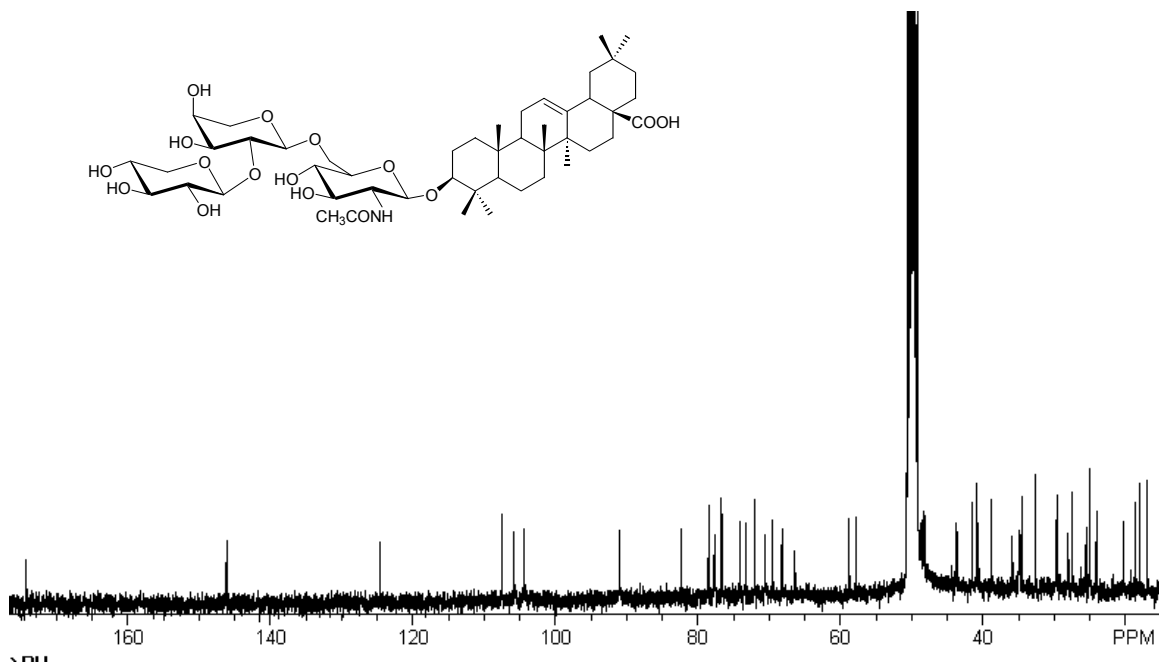
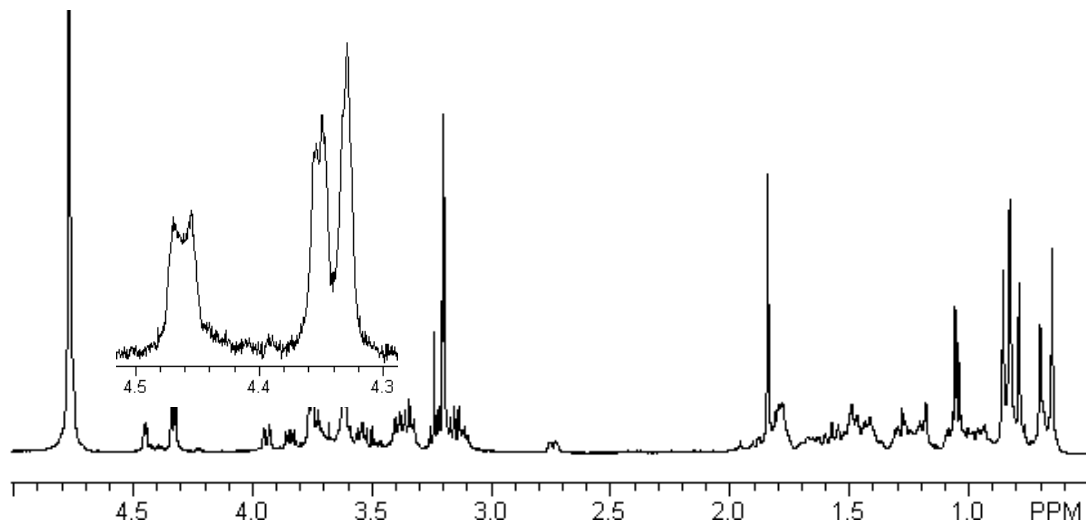
JMB-147-245-3 (3.14) Parissaponin Pb



JMB-147-246 (3.7) Diosgenin, Parissaponin Aglycone



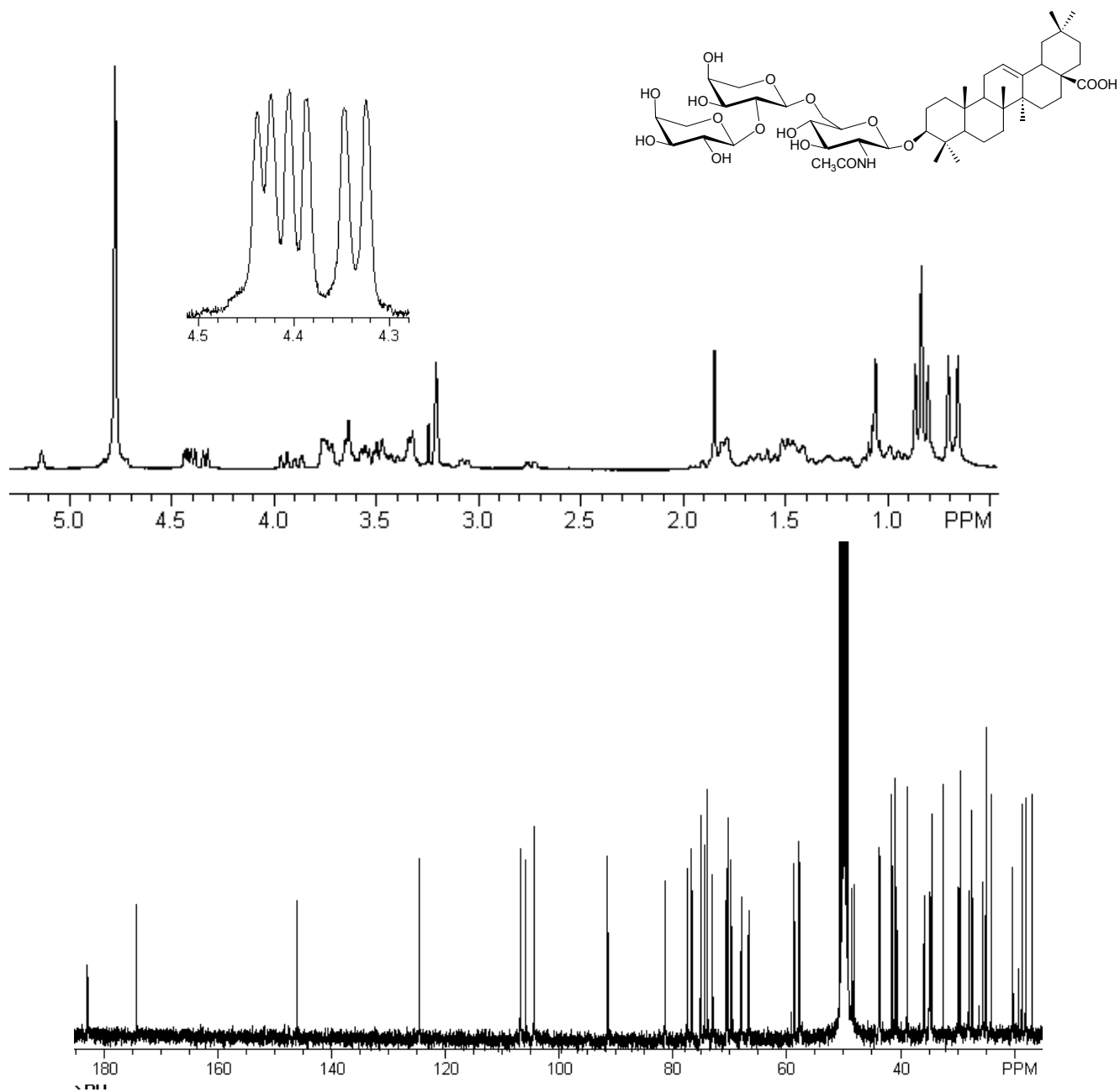
JMB-151-255-2 (4.6) Albiziatriside A
JMB-151-257-2
JMB-151-266-1



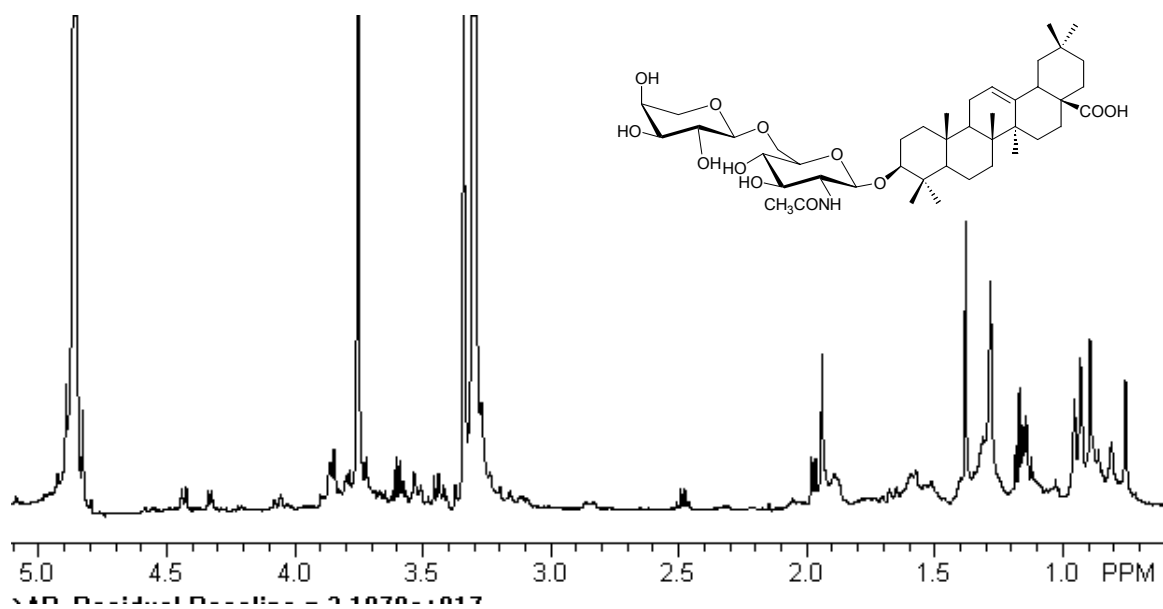
JMB-151-261-3 (4.7)

JMB-151-262-3

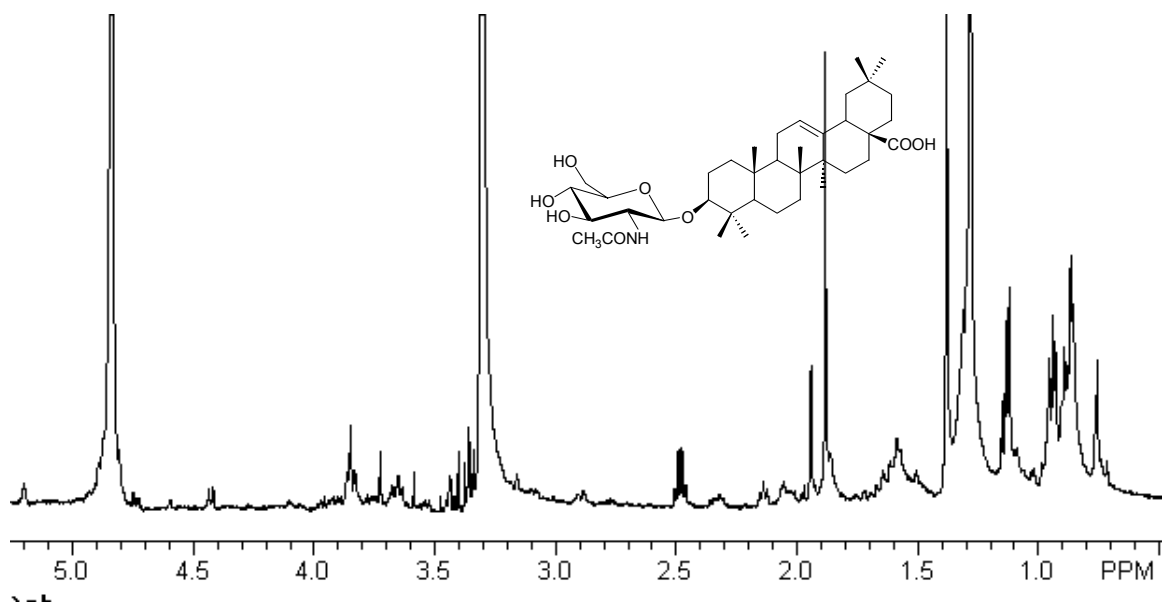
JMB-151-266-2



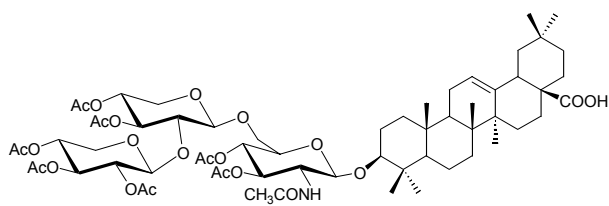
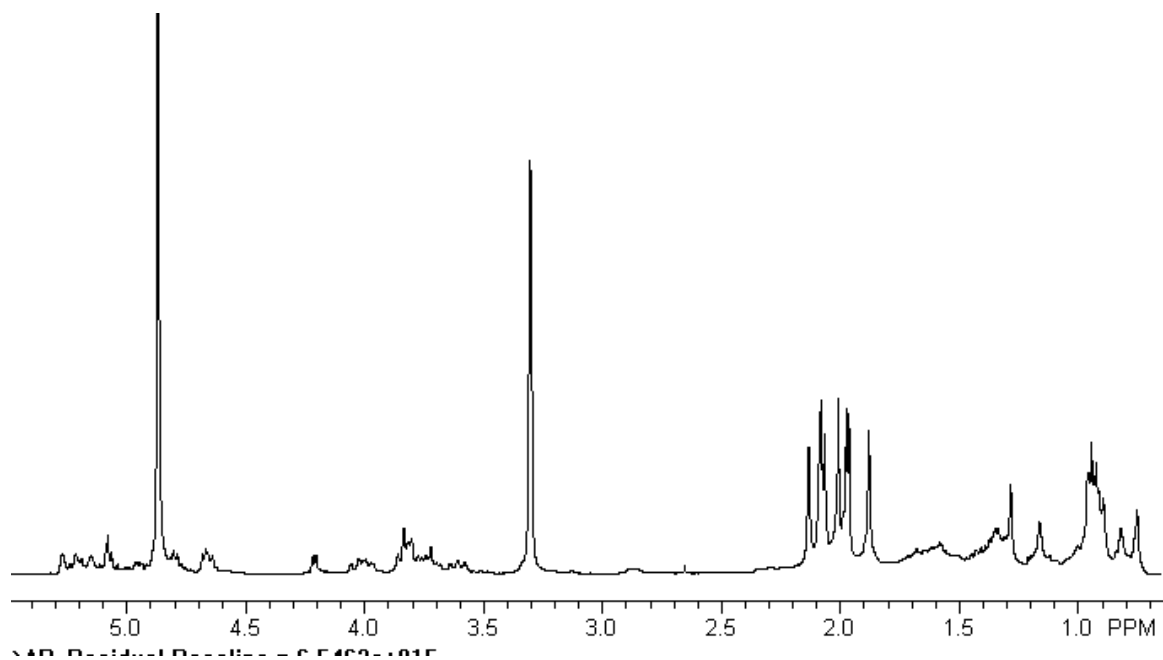
JMB-151-259-4 (4.10) Alibiza Bioside



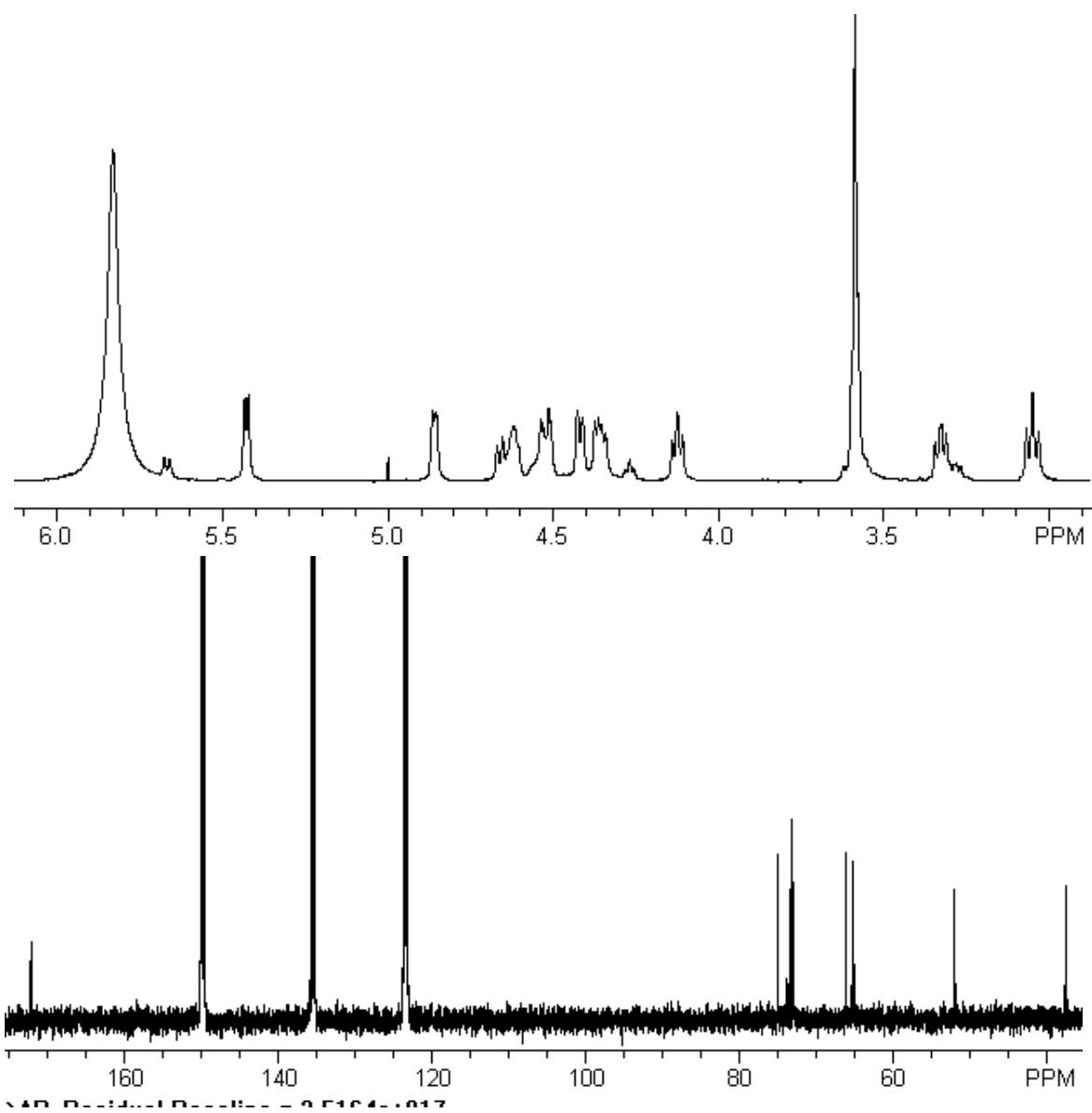
JMB-151-258-2 (4.11) Alibiza Monoside



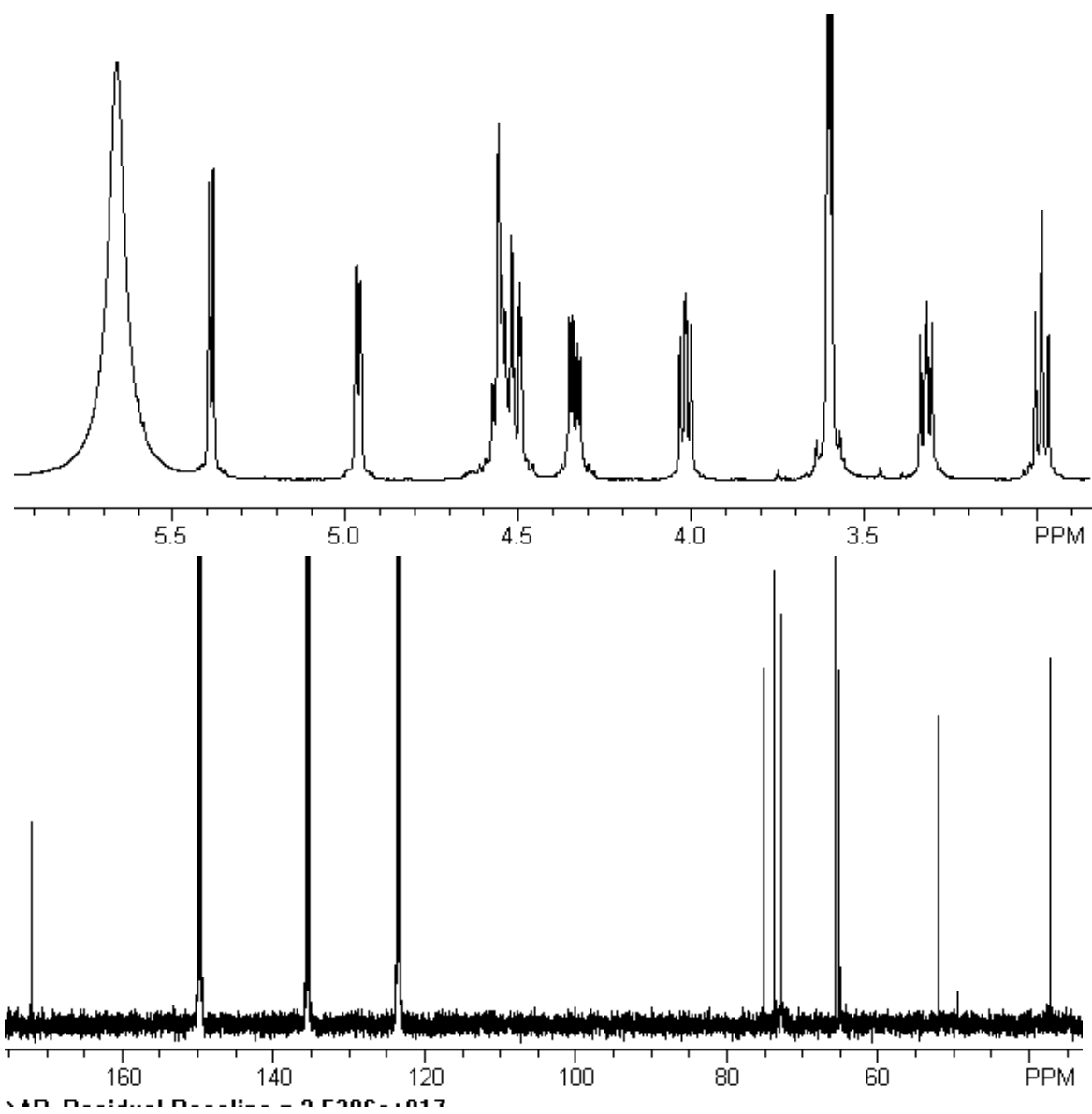
MSA-970-39-L-Acetate-1HNMR-CH3OH (4.9) Peracetate



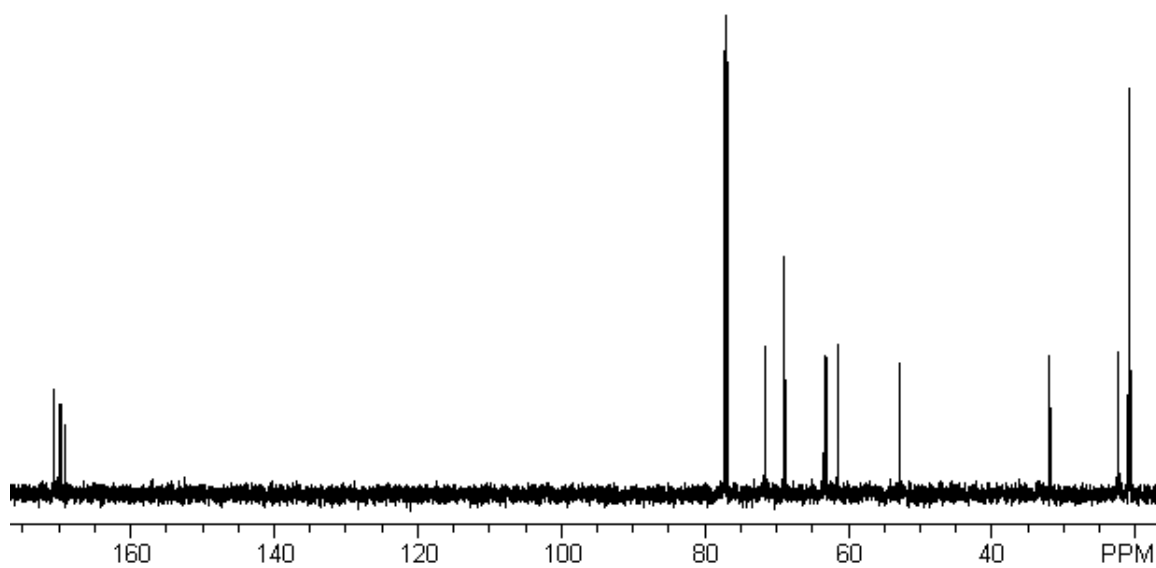
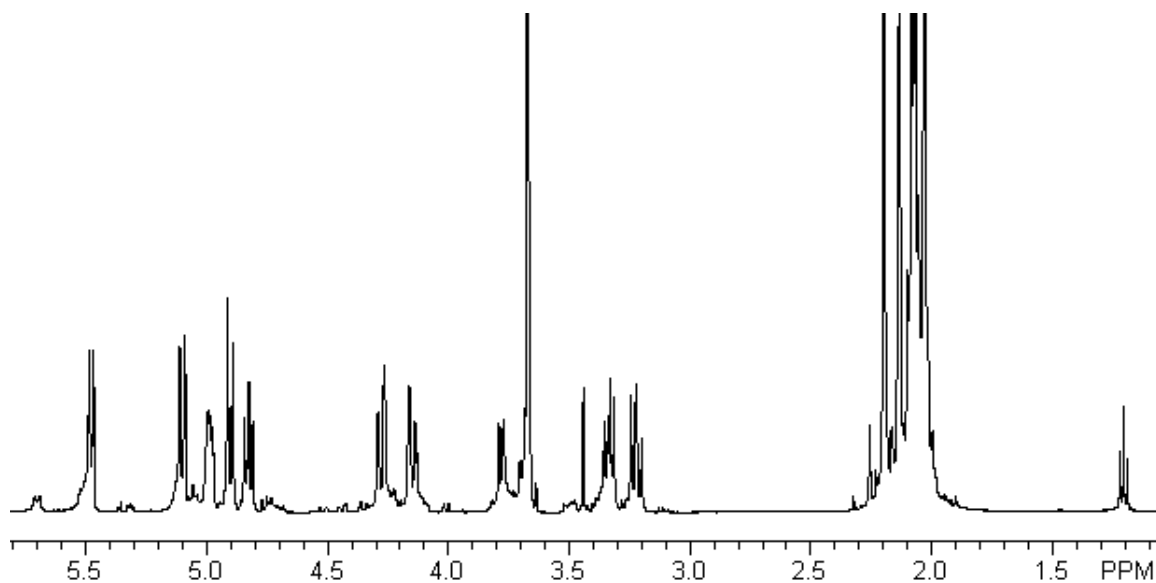
JMB-151-224-4 (4.19) L-Arabinose Thiazolidine



JMB-151-224-5 (4.21) D-Arabinose Thiazolidine

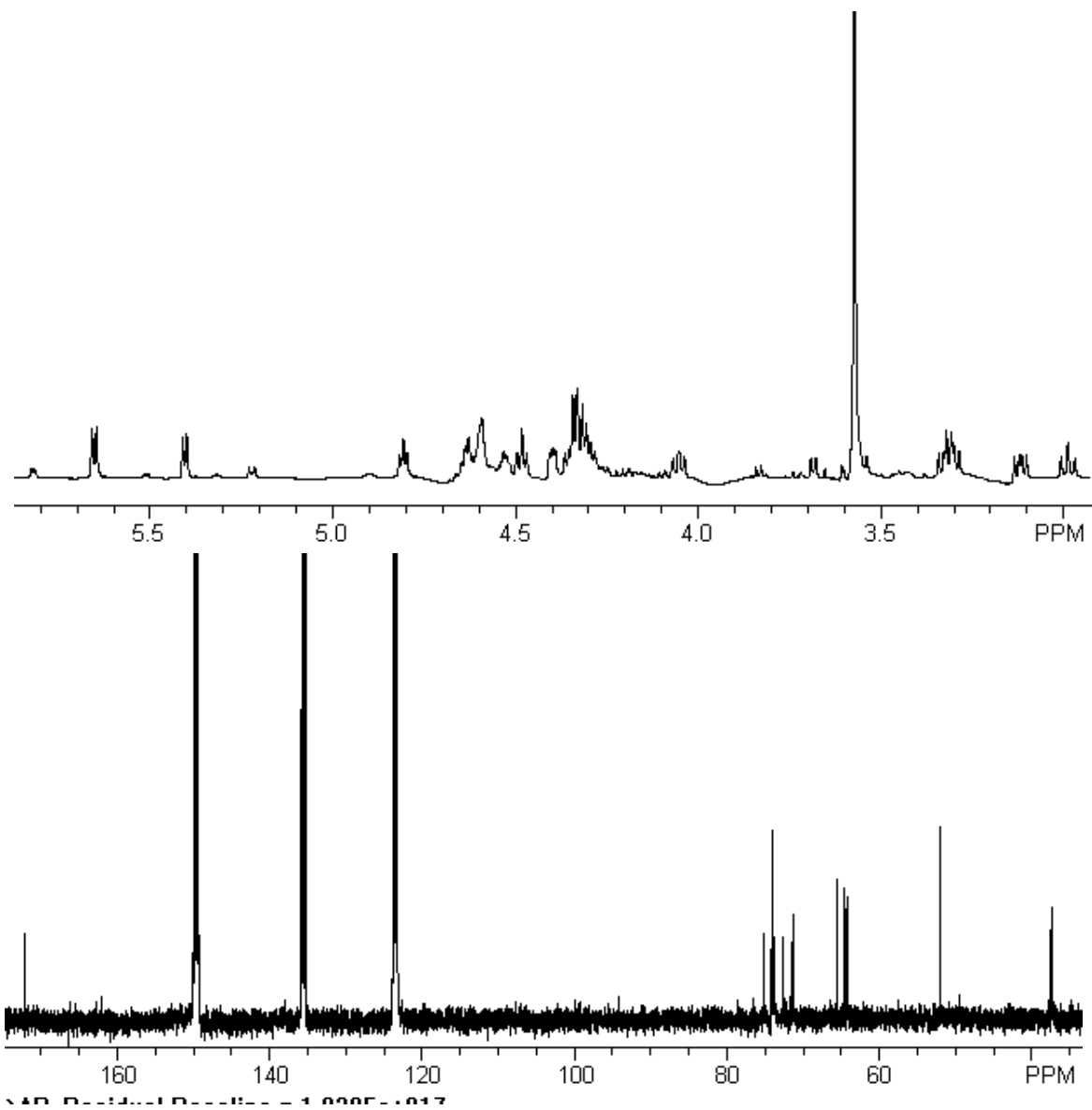


JMB-151-227-4 (4.20) L-Arabinose Thiazolidine Peracetate

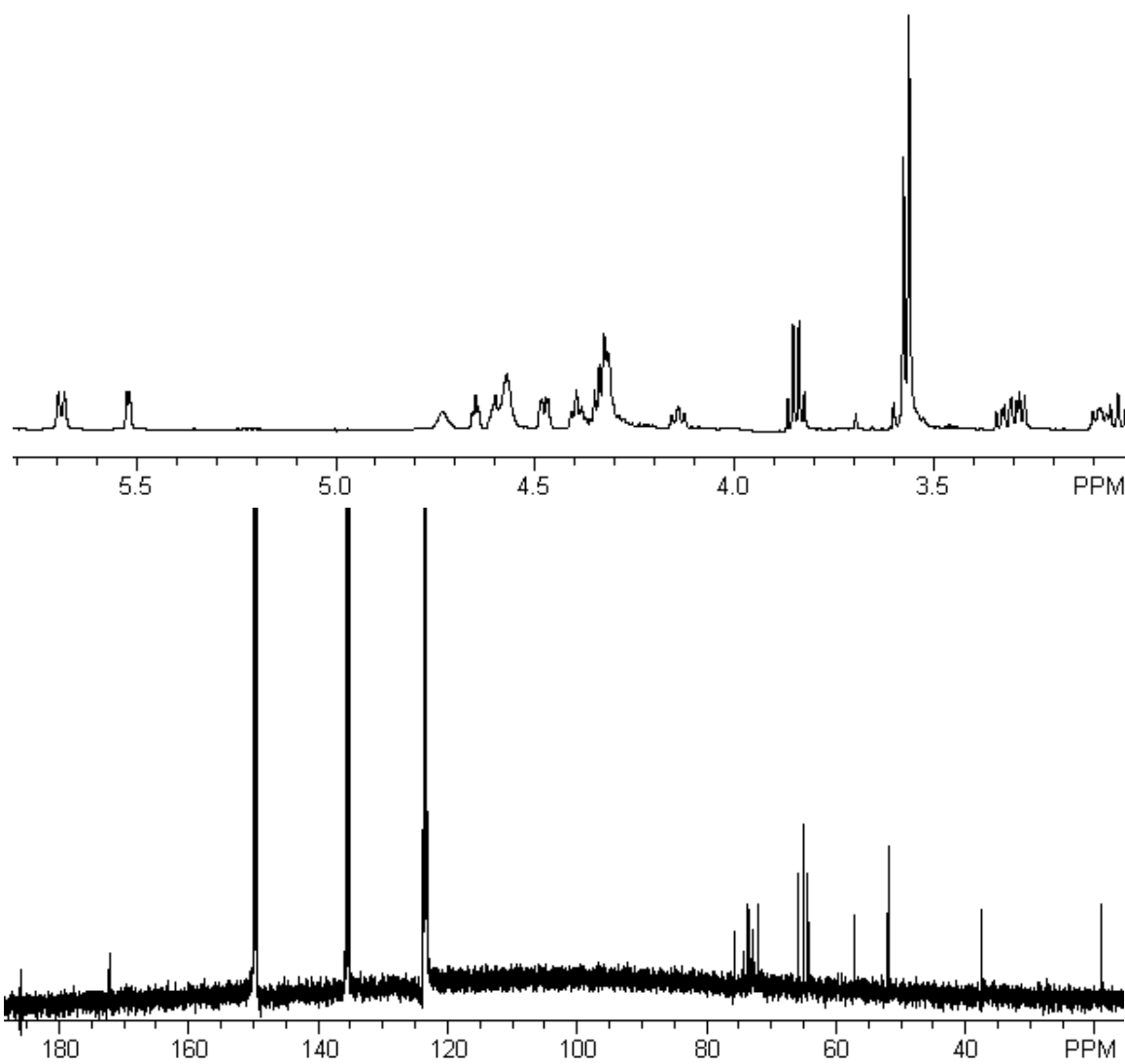


13C NMR Data: 3.0101-016

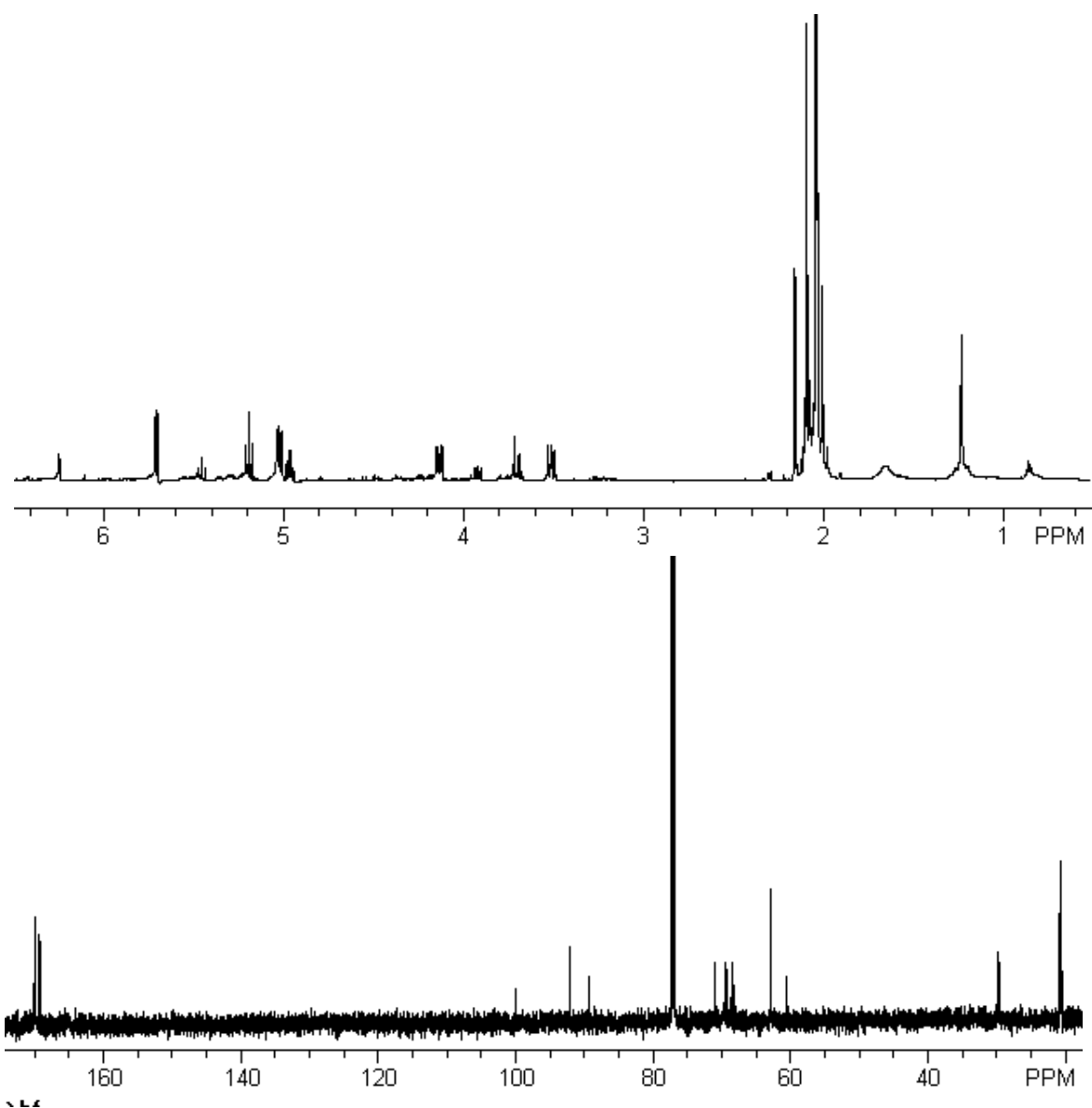
JMB-151-226-13 L-Xylose Thiazolidine



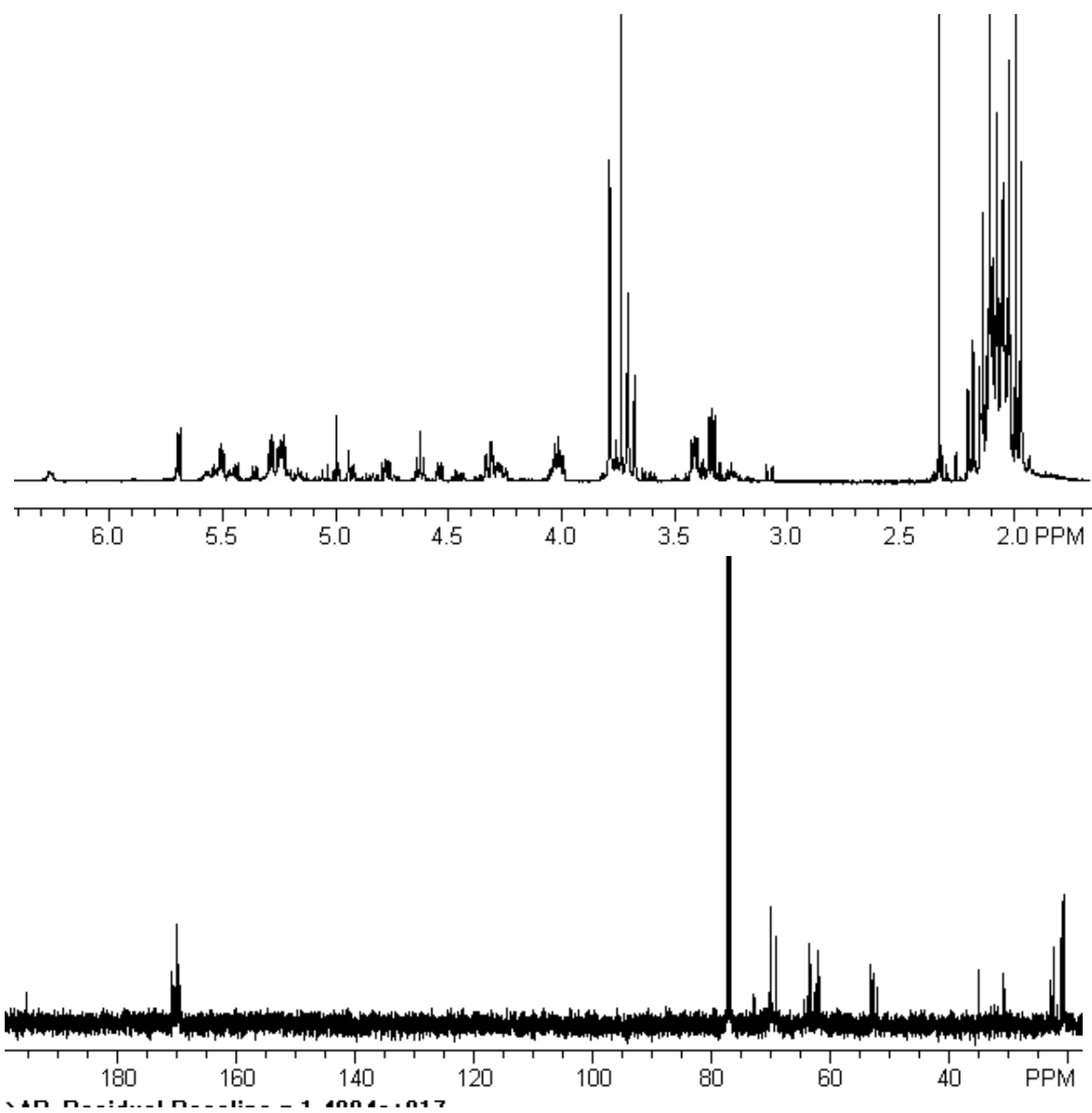
JMB-151-231-3 D-Xylose Thiazolidine



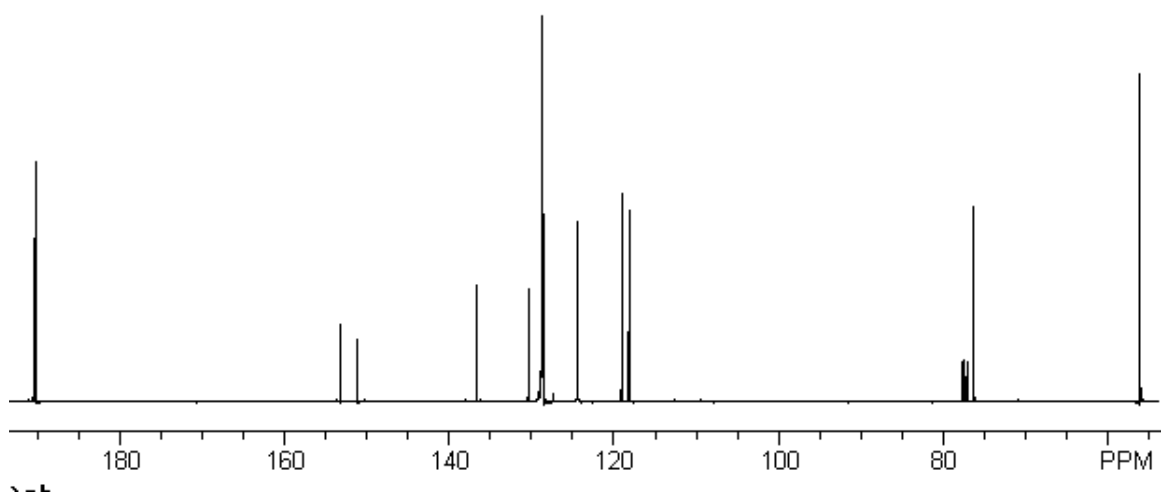
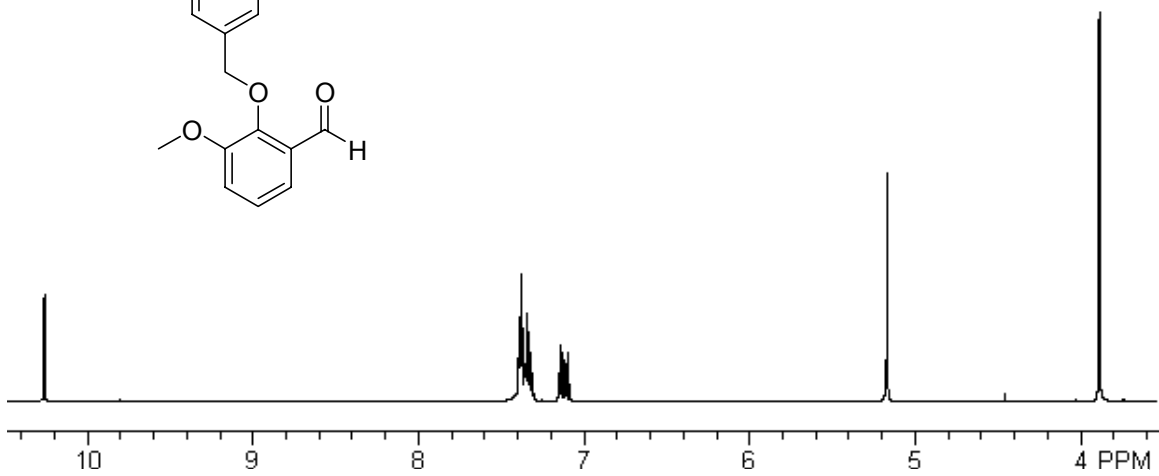
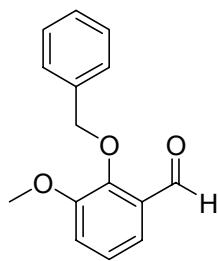
JMB-151-235-2 D-Xylose Thiazolidine Peracetate



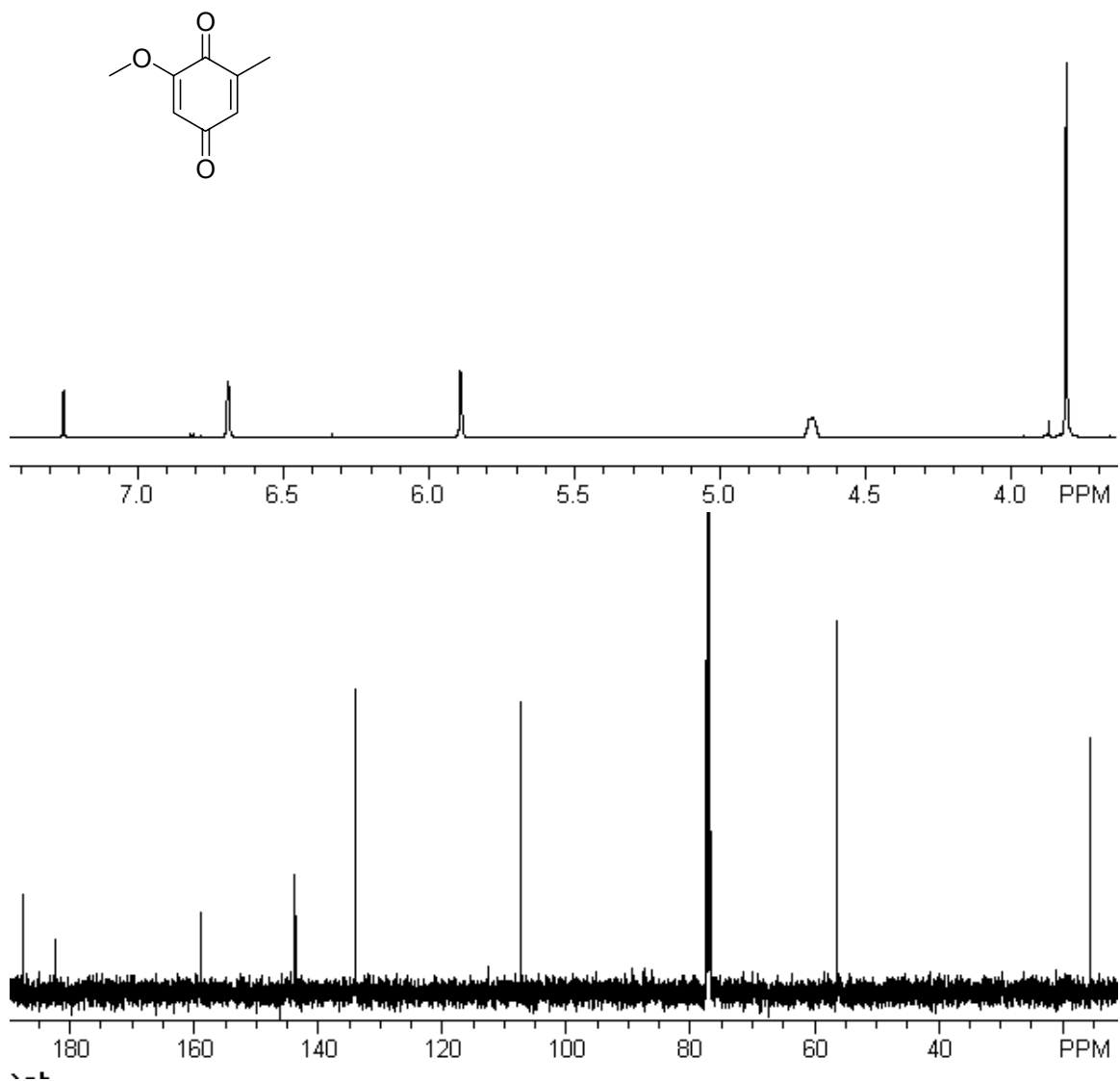
JMB-151-241-2 L-Xylose Thiazolidine Peracetate



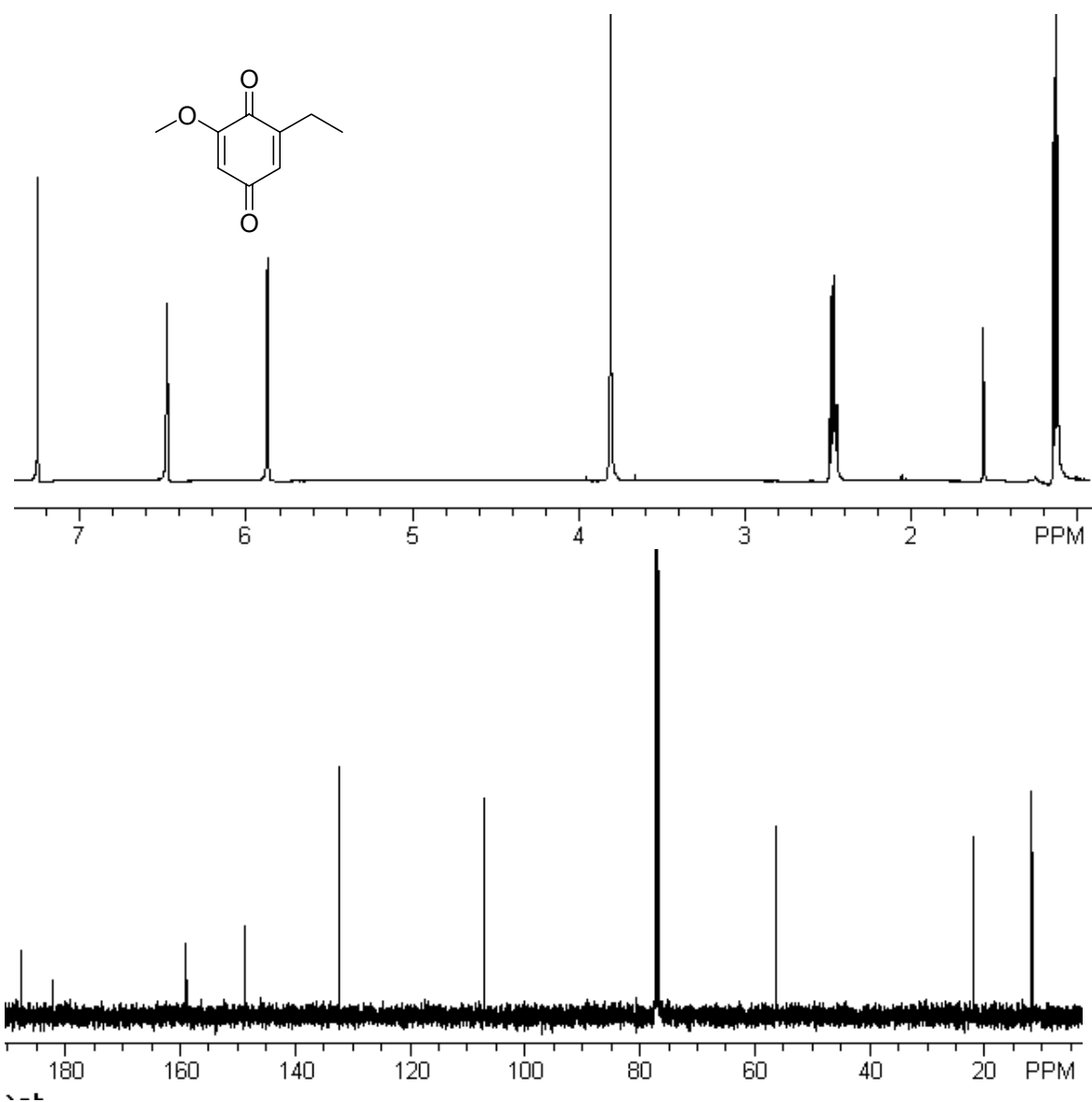
Benzyl *o*-Vanillin



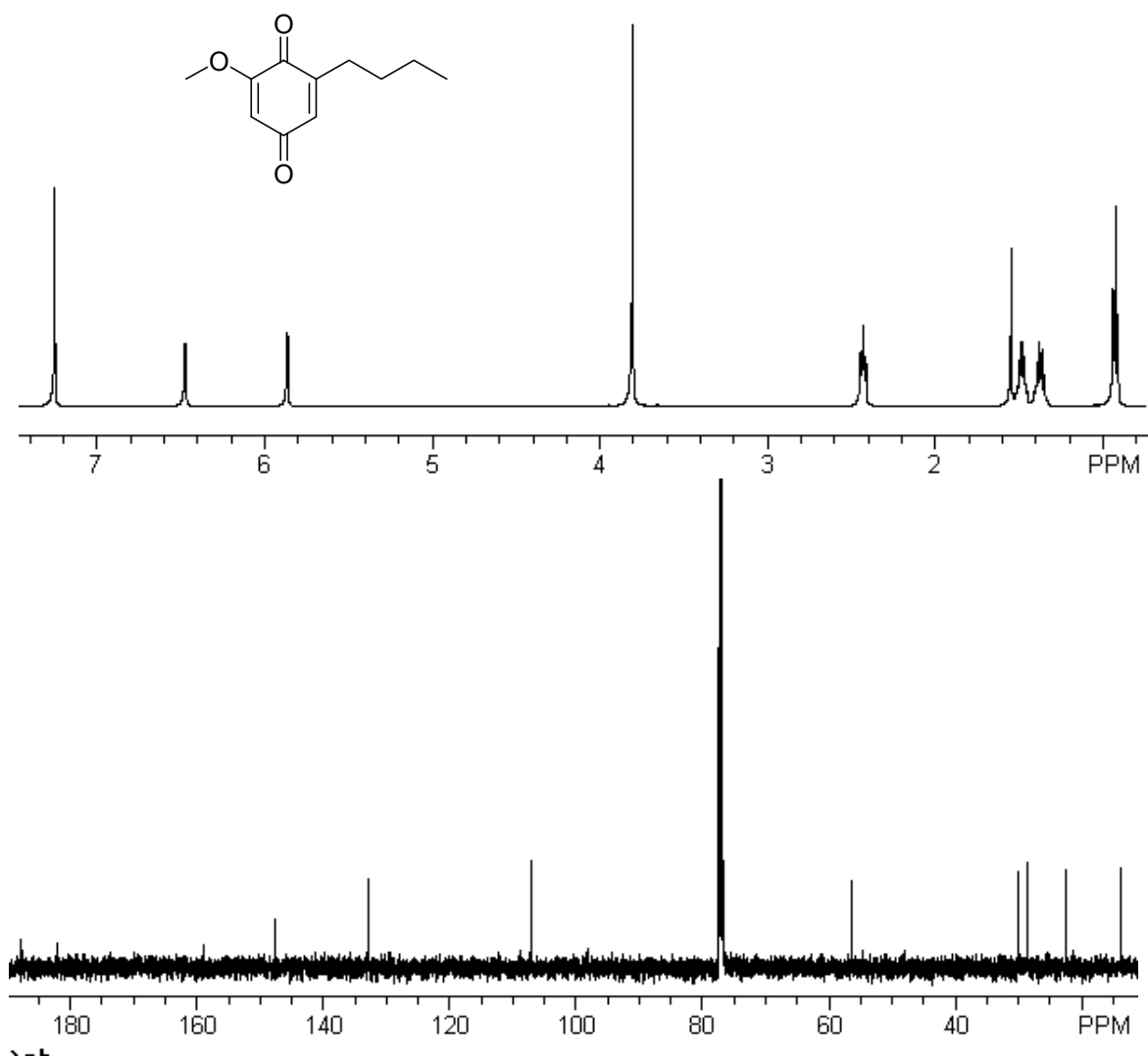
JMB-147-275 (6.9) 2-Methoxy-6-methyl-1,4-benzoquinone



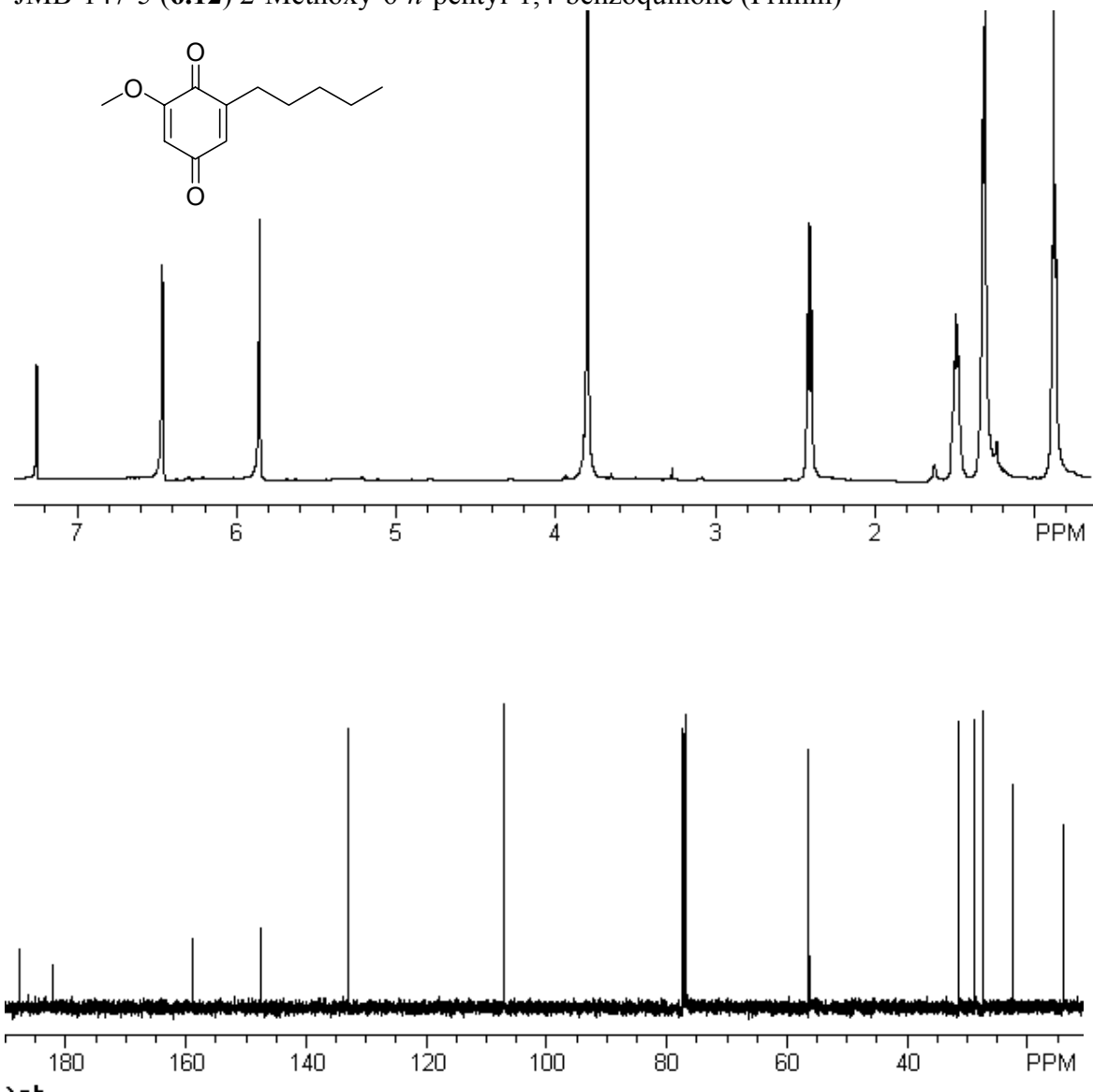
JMB-147-24 (6.10) 2-Methoxy-6-*n*-ethyl-1,4-benzoquinone



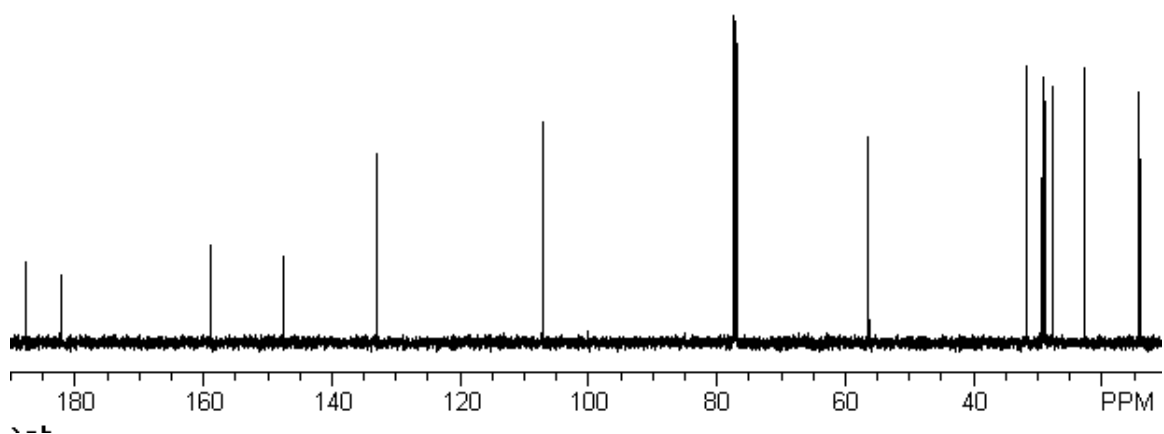
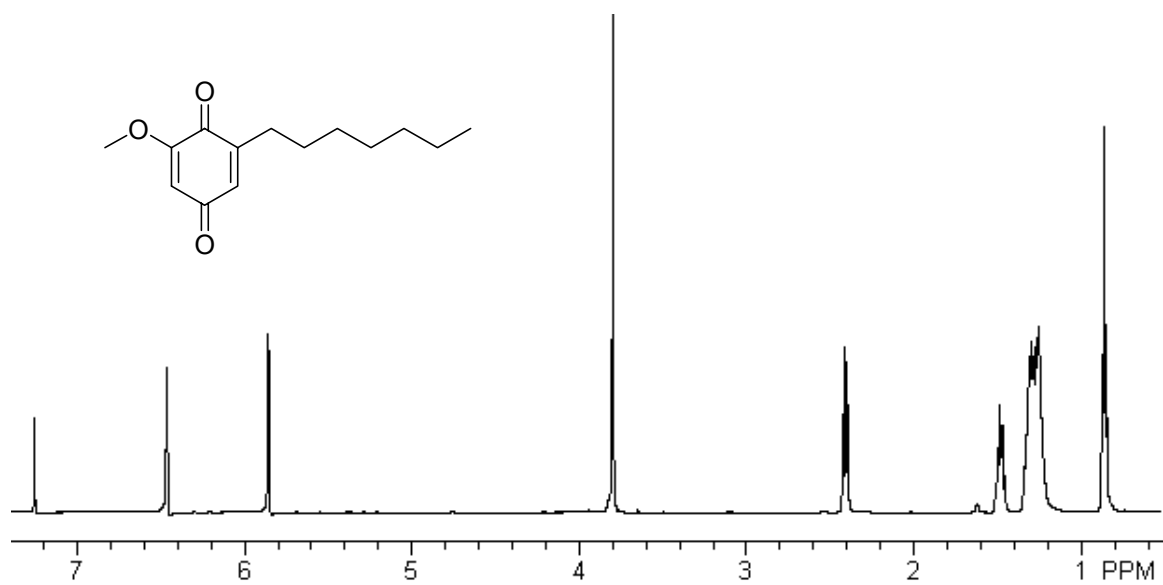
JMB-147-22 (6.11) 2-Methoxy-6-*n*-butyl-1,4-benzoquinone



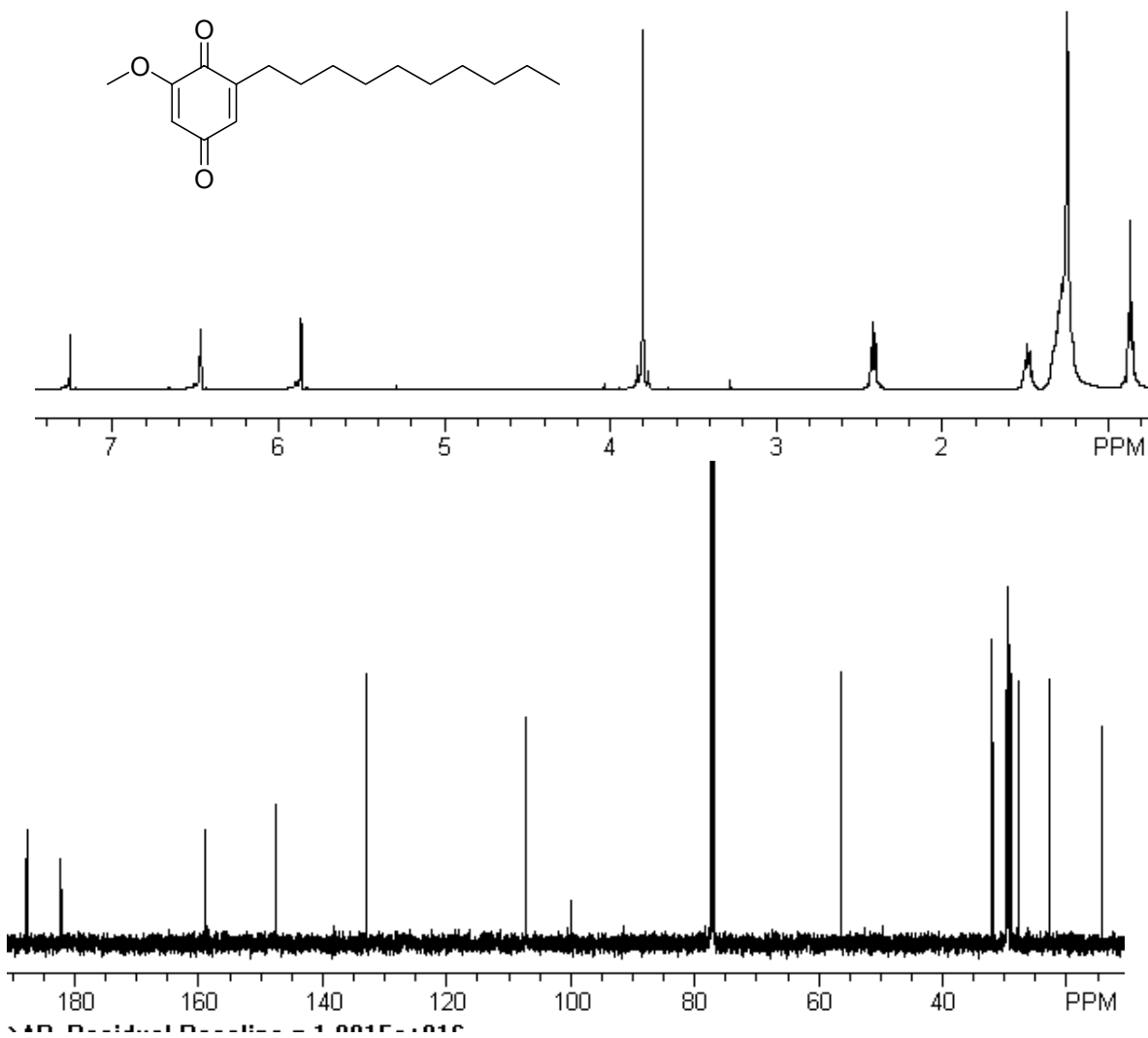
JMB-147-5 (6.12) 2-Methoxy-6-*n*-pentyl-1,4-benzoquinone (Primin)



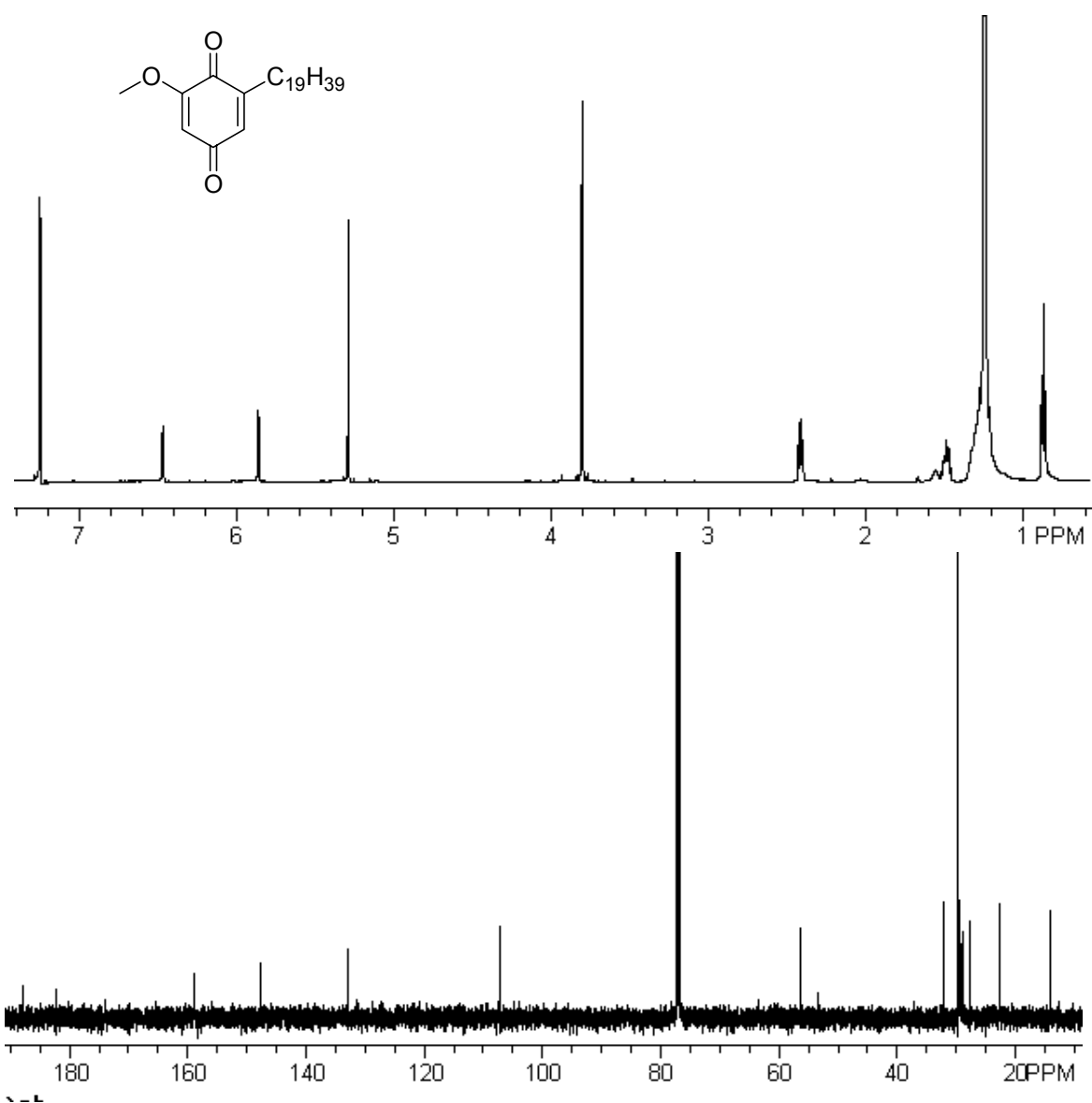
JMB-147-7 (6.13) 2-Methoxy-6-*n*-heptyl-1,4-benzoquinone (Miconin)



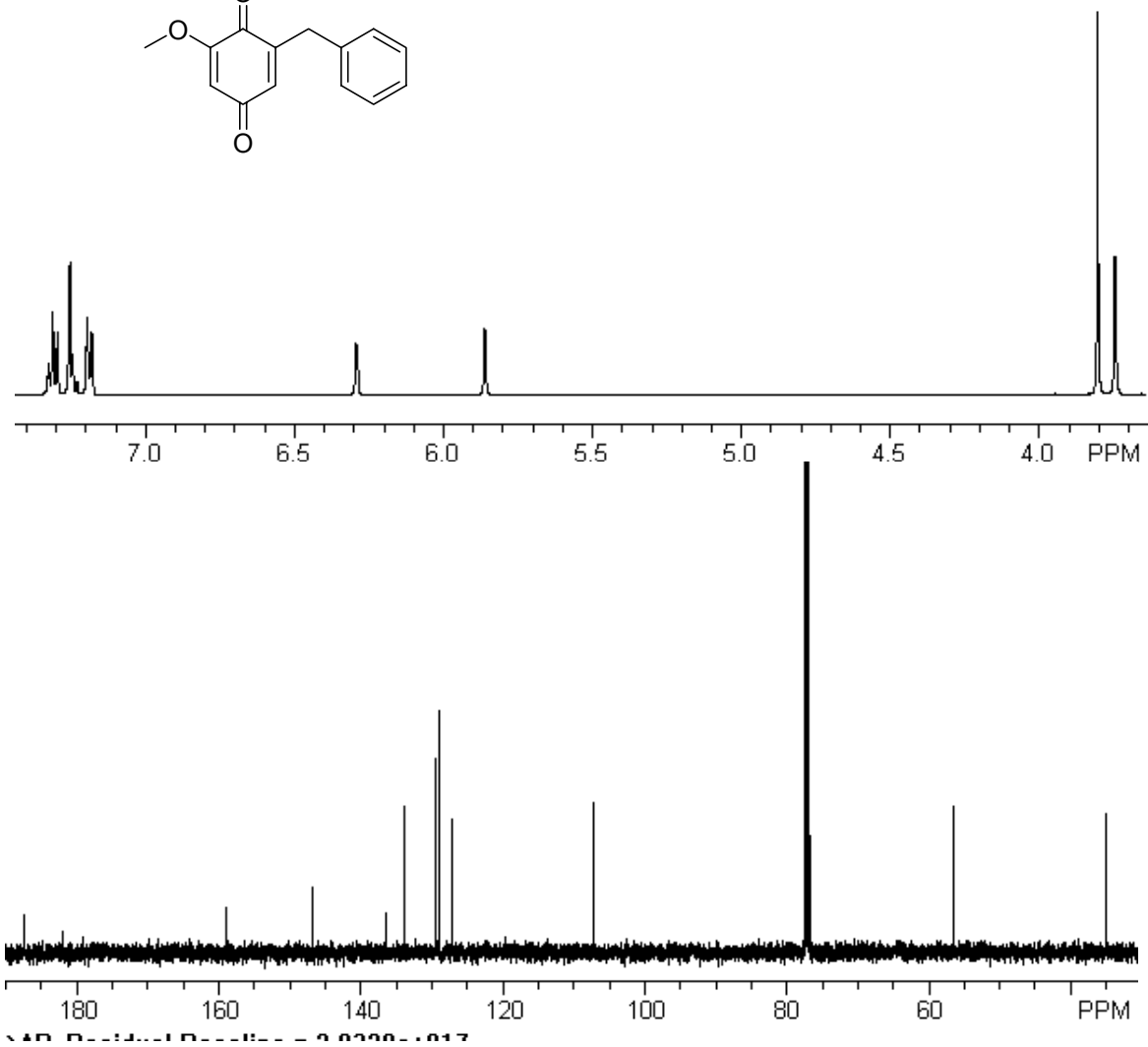
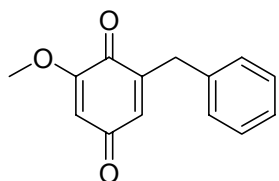
JMB-147-272 (6.14) 2-Methoxy-6-*n*-decyl-1,4-benzoquinone



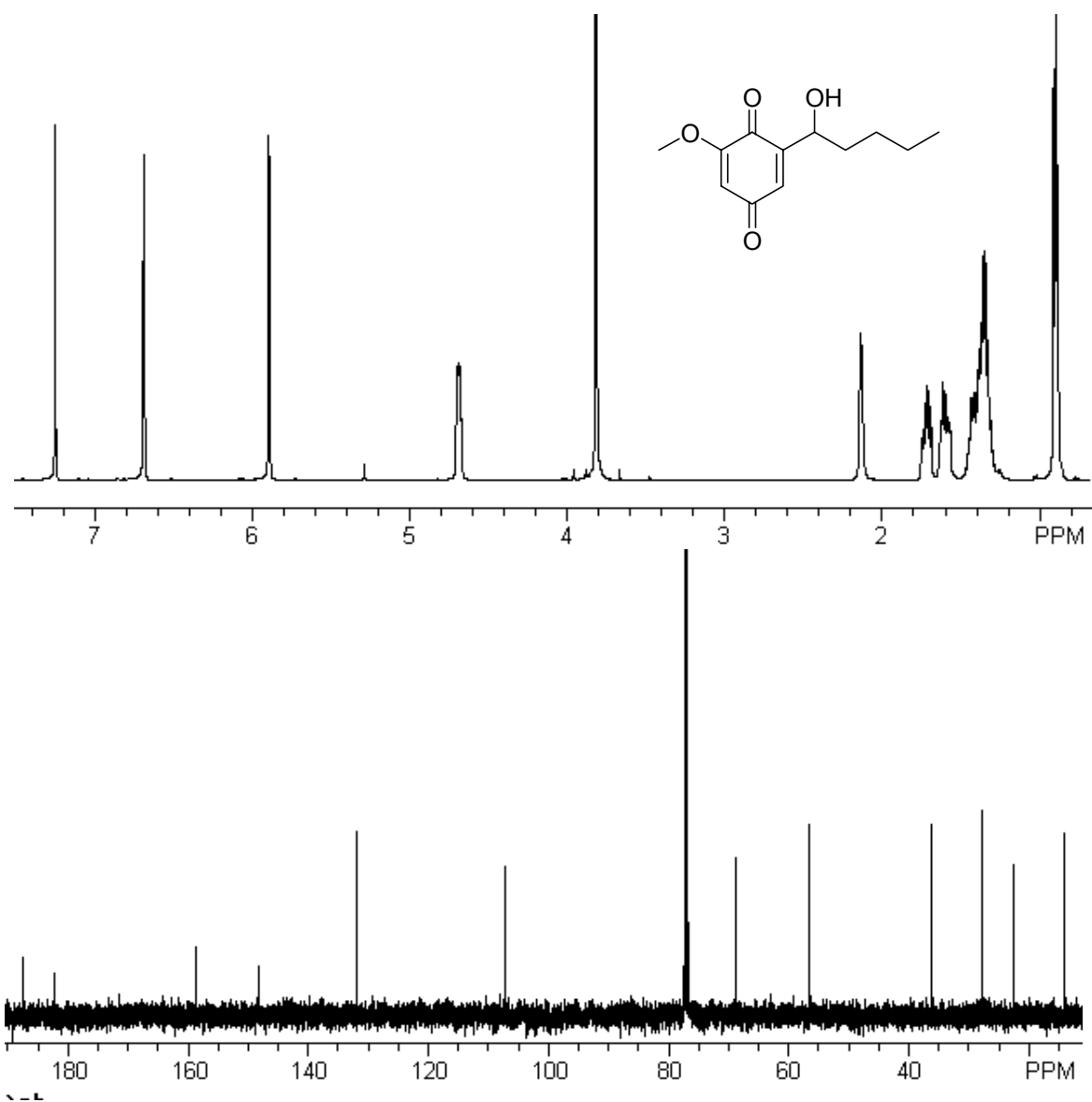
JMB-147-273 (6.15) 2-Methoxy-6-*n*-nonadecyl-1,4-benzoquinone



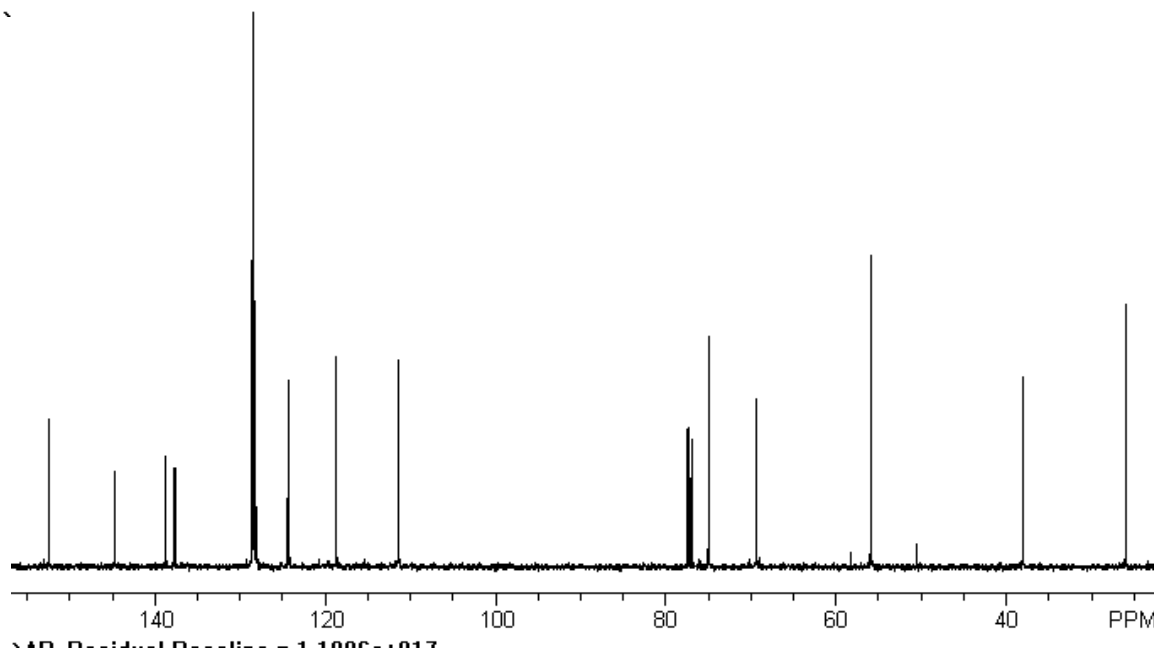
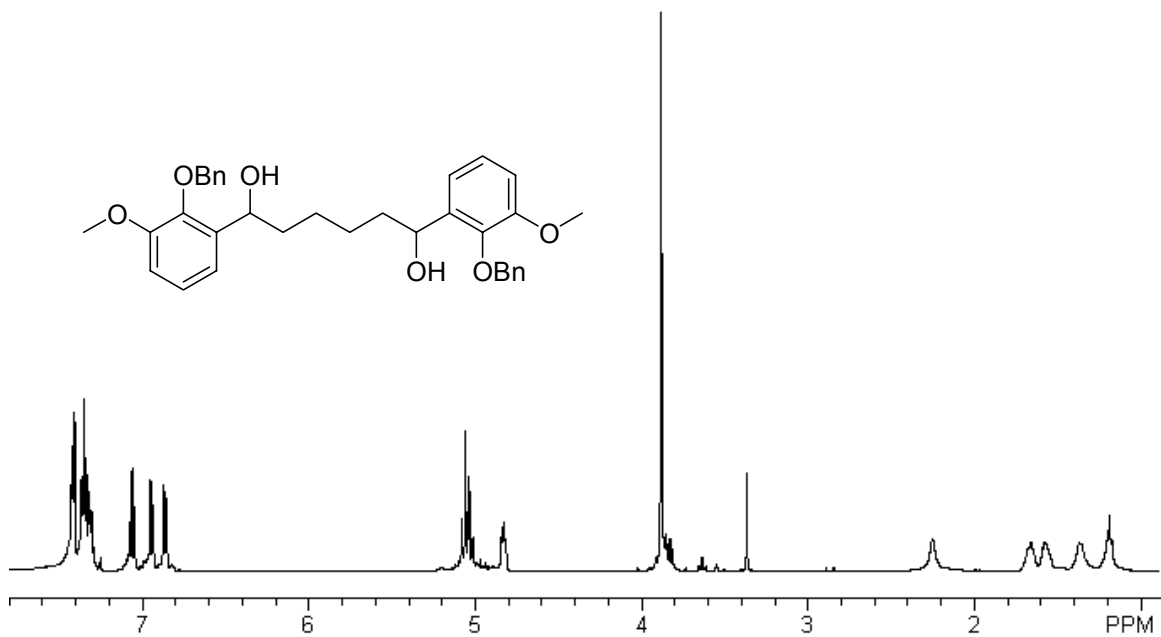
JMB-147-13' (6.16) 2-Methoxy-6-benzyl-1,4-benzoquinone



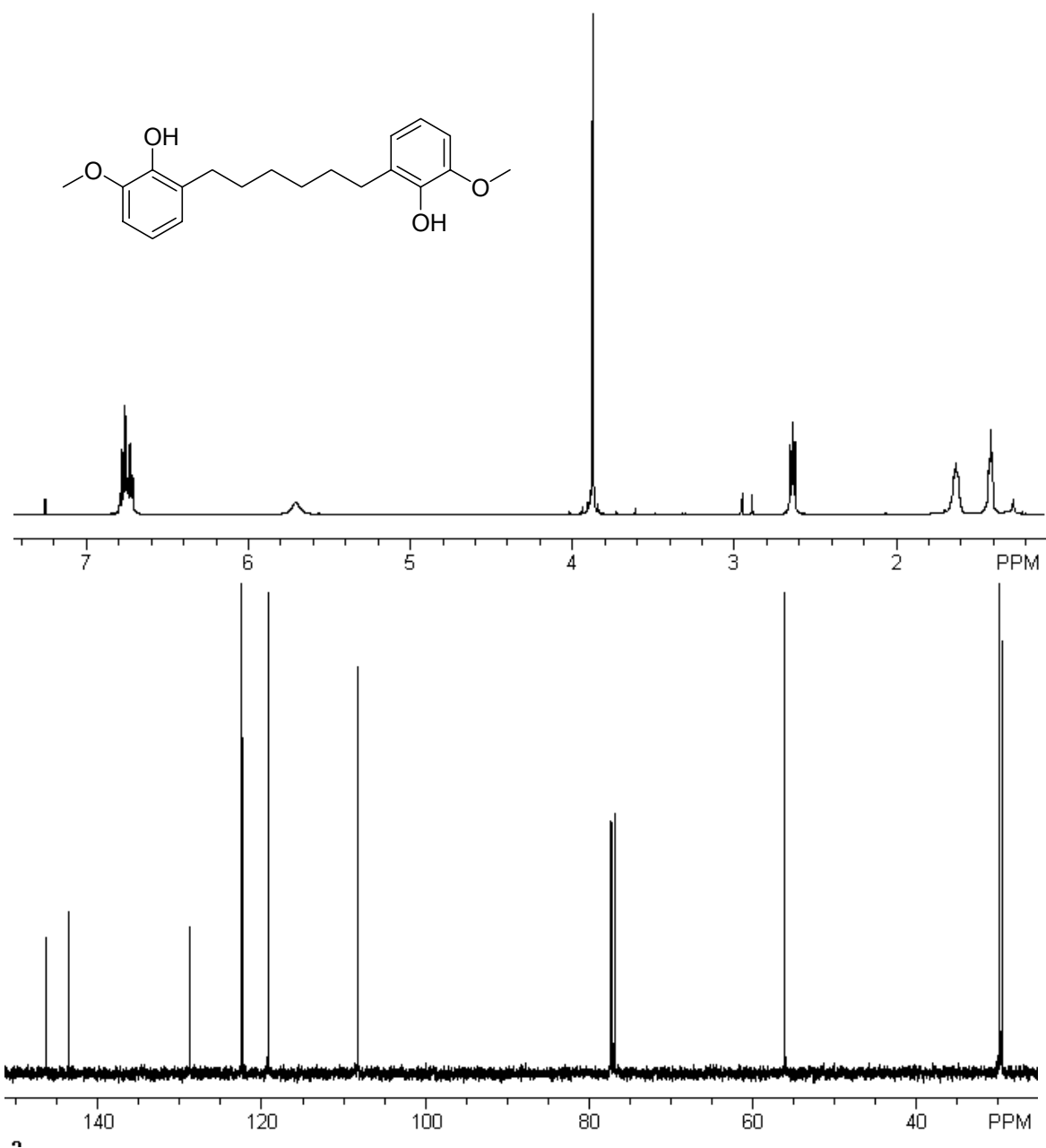
JMB-147-205 (6.17) 2-Methoxy-6-*n*-pentyl-1'-hydroxy-1,4-benzoquinone



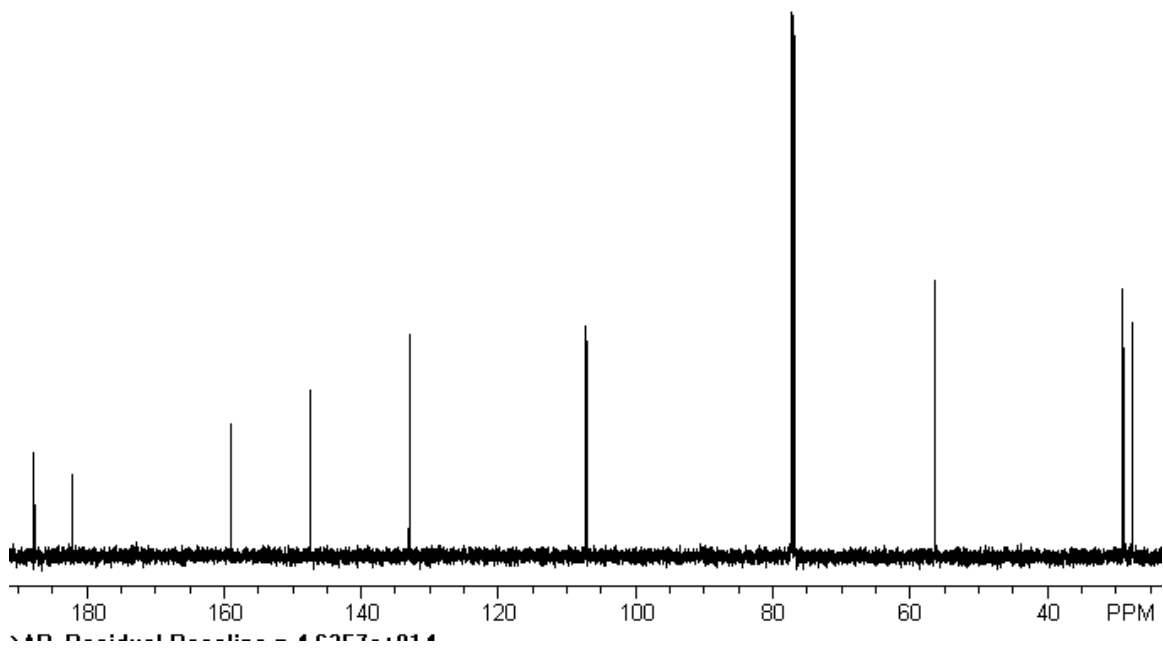
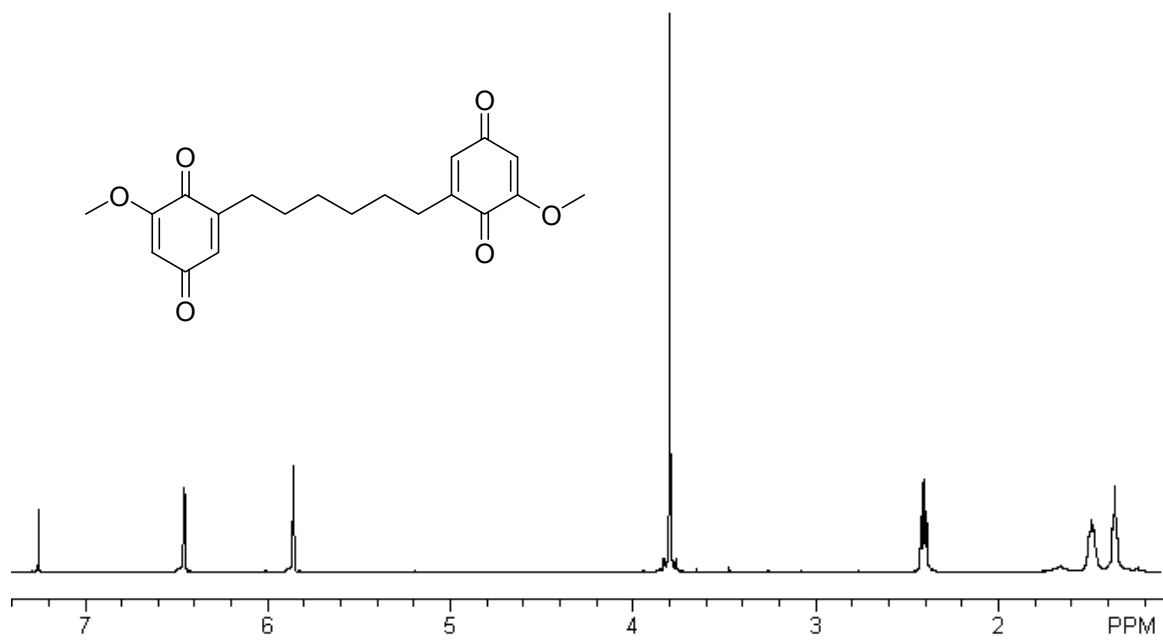
JMB-151-217-13 1,6-Di-(2-benzyloxy, 3-methoxyphenyl)-hexan-1,6-diol.



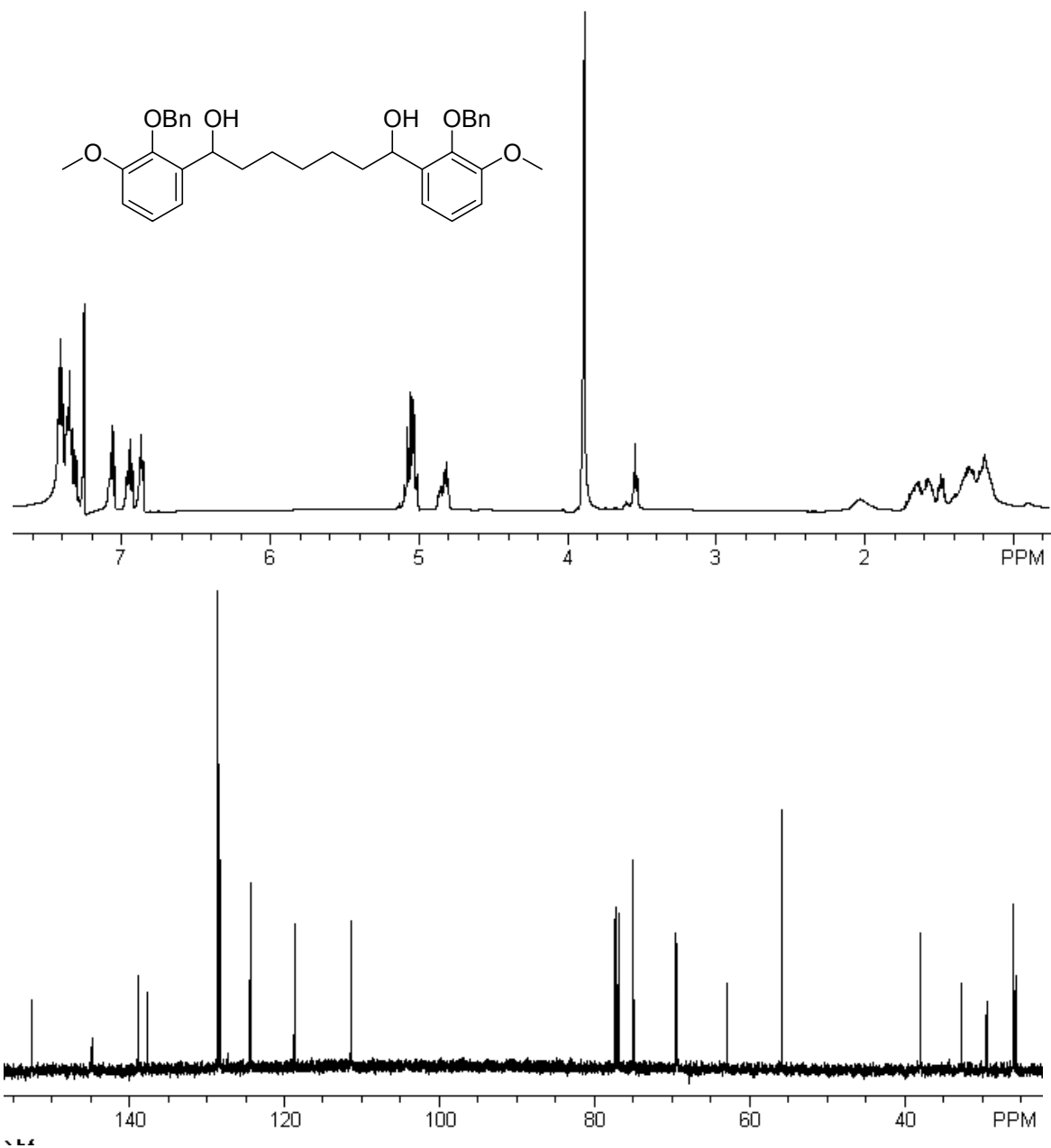
JMB-151-218-2 1,6-Di-6-(3-methoxy-phenol) hexane



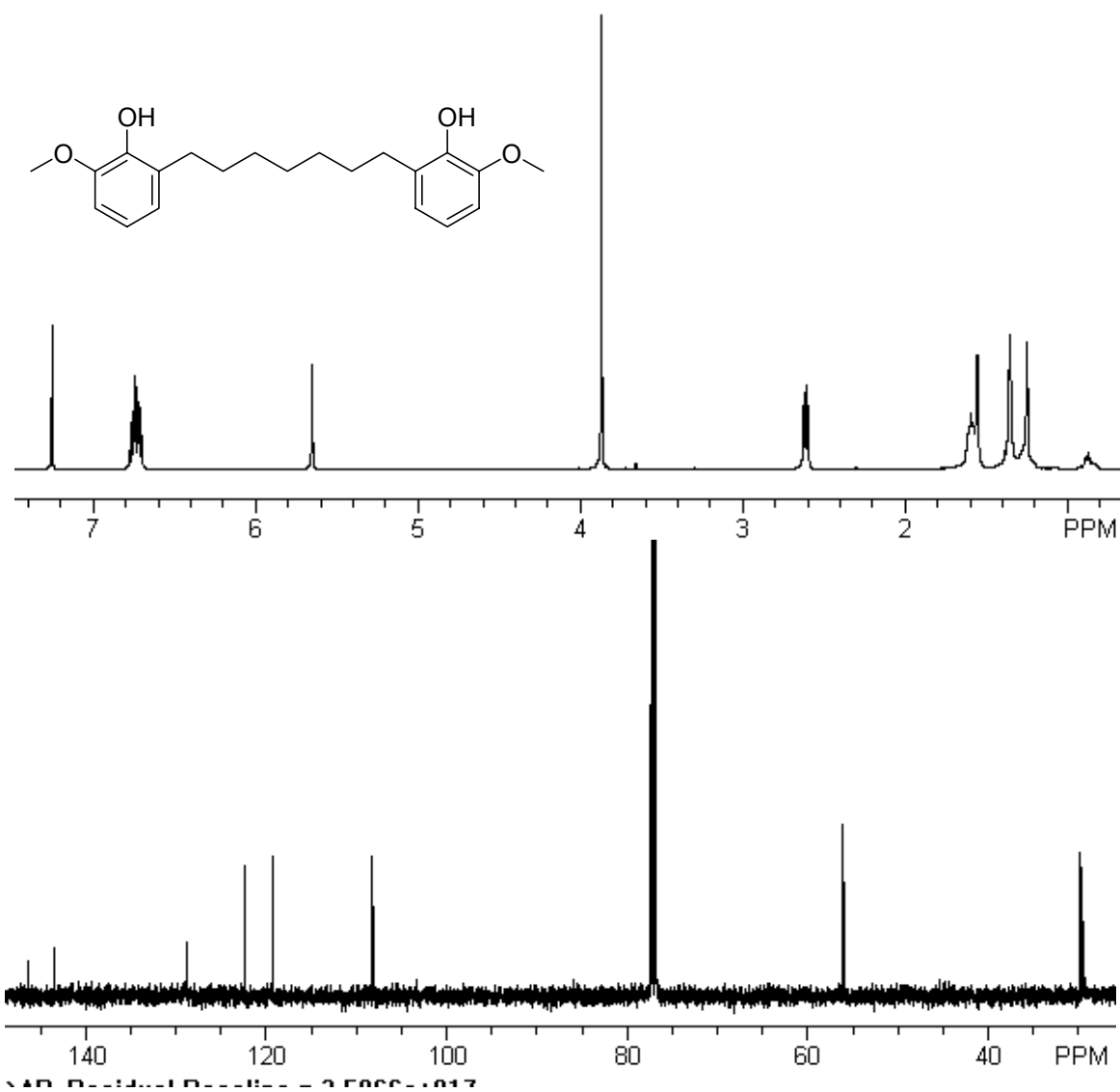
JMB-151-218-5 (6.18) 1,6-Di-(2-methoxy-1,4-benzoquinonyl) hexane



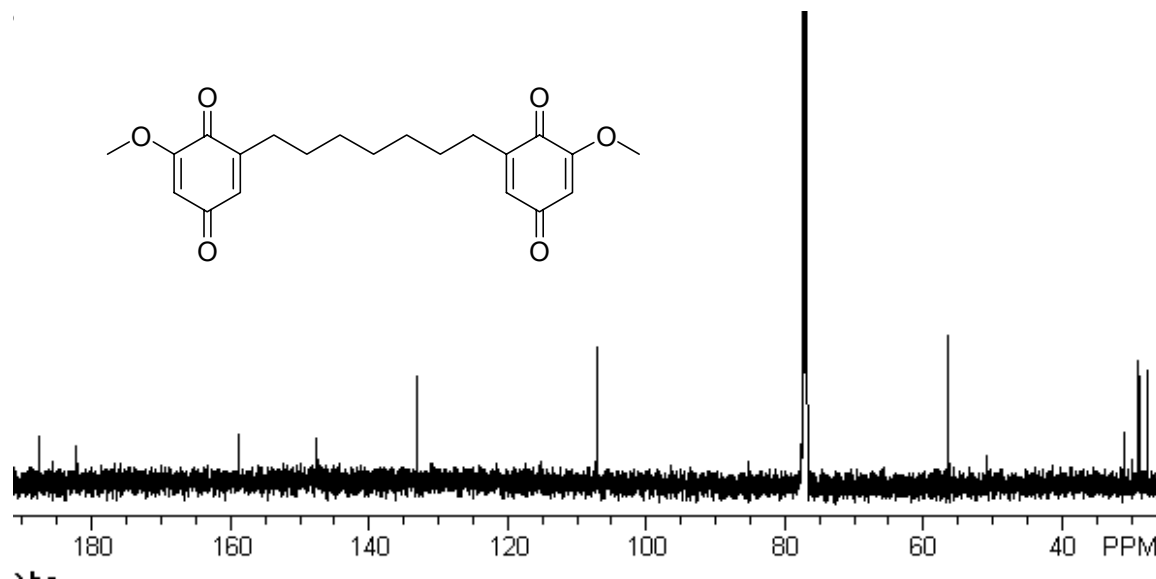
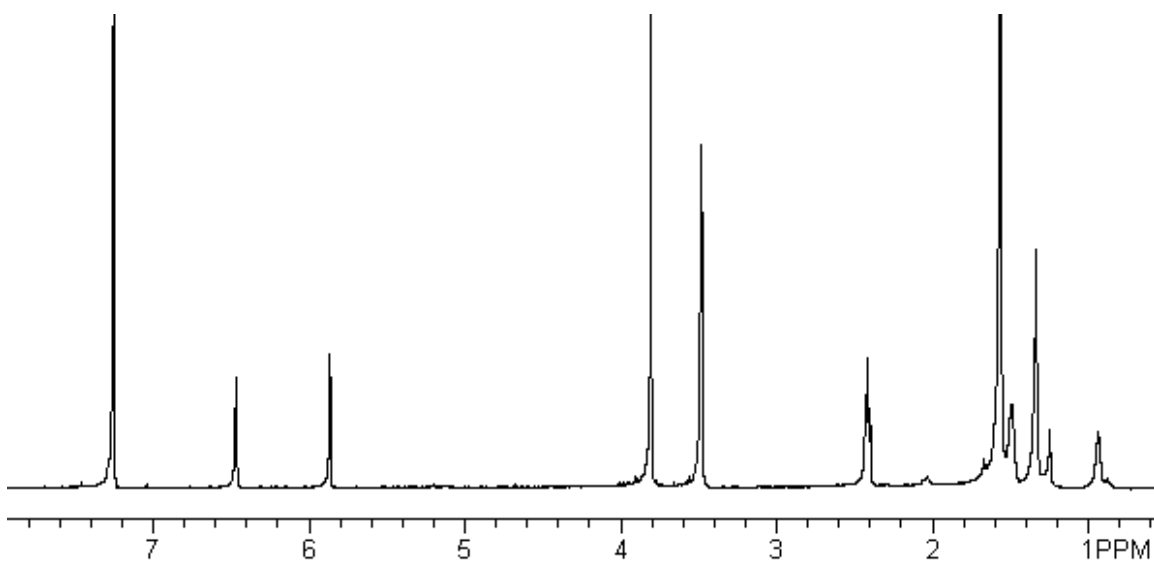
JMB-151-186-7 1,7-Di-(2-benzyloxy, 3-methoxyphenyl)-heptan-1,7-diol



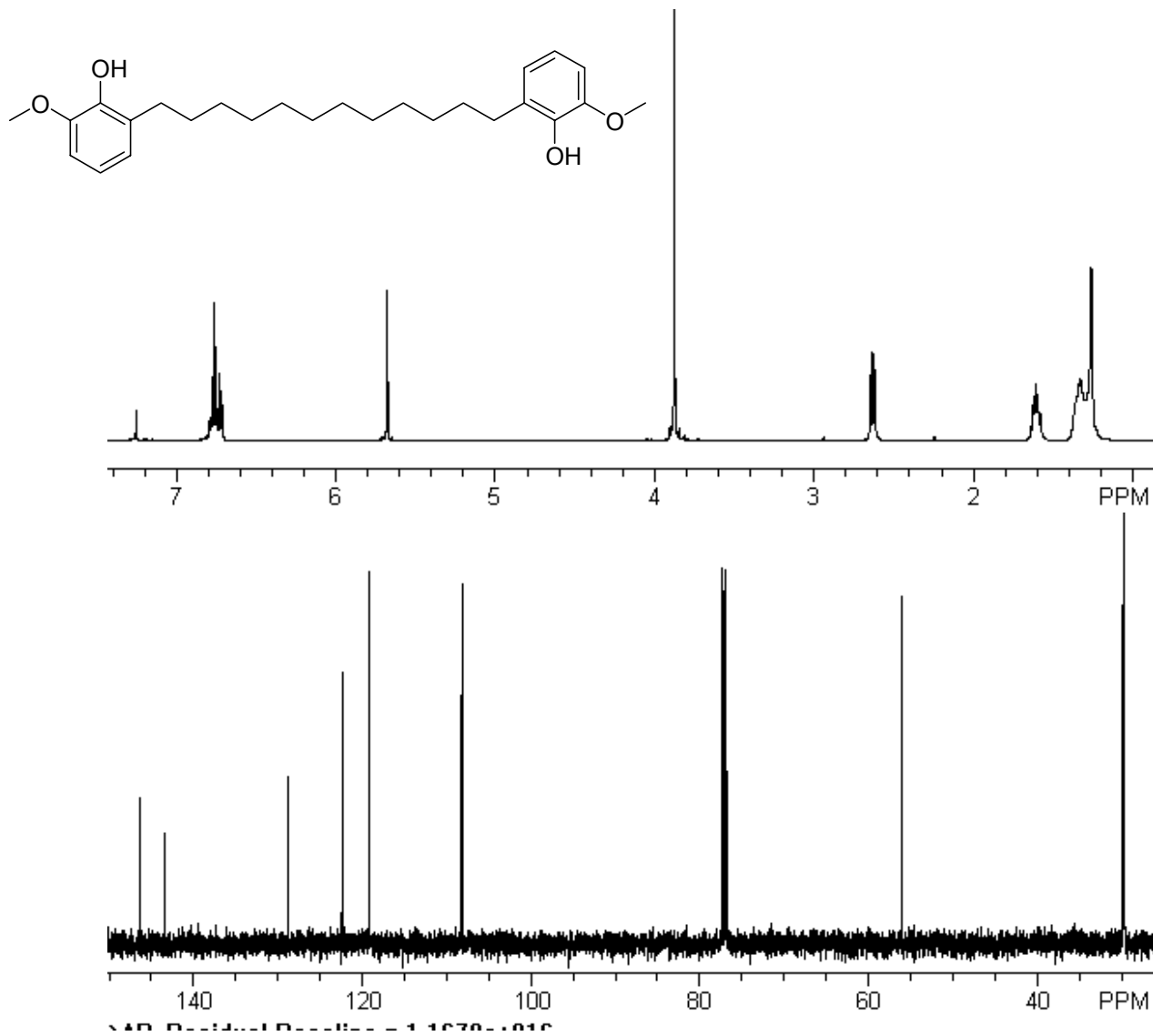
JMB-151-191-1 1,7-Di-6-(2-methoxyphenol) heptane



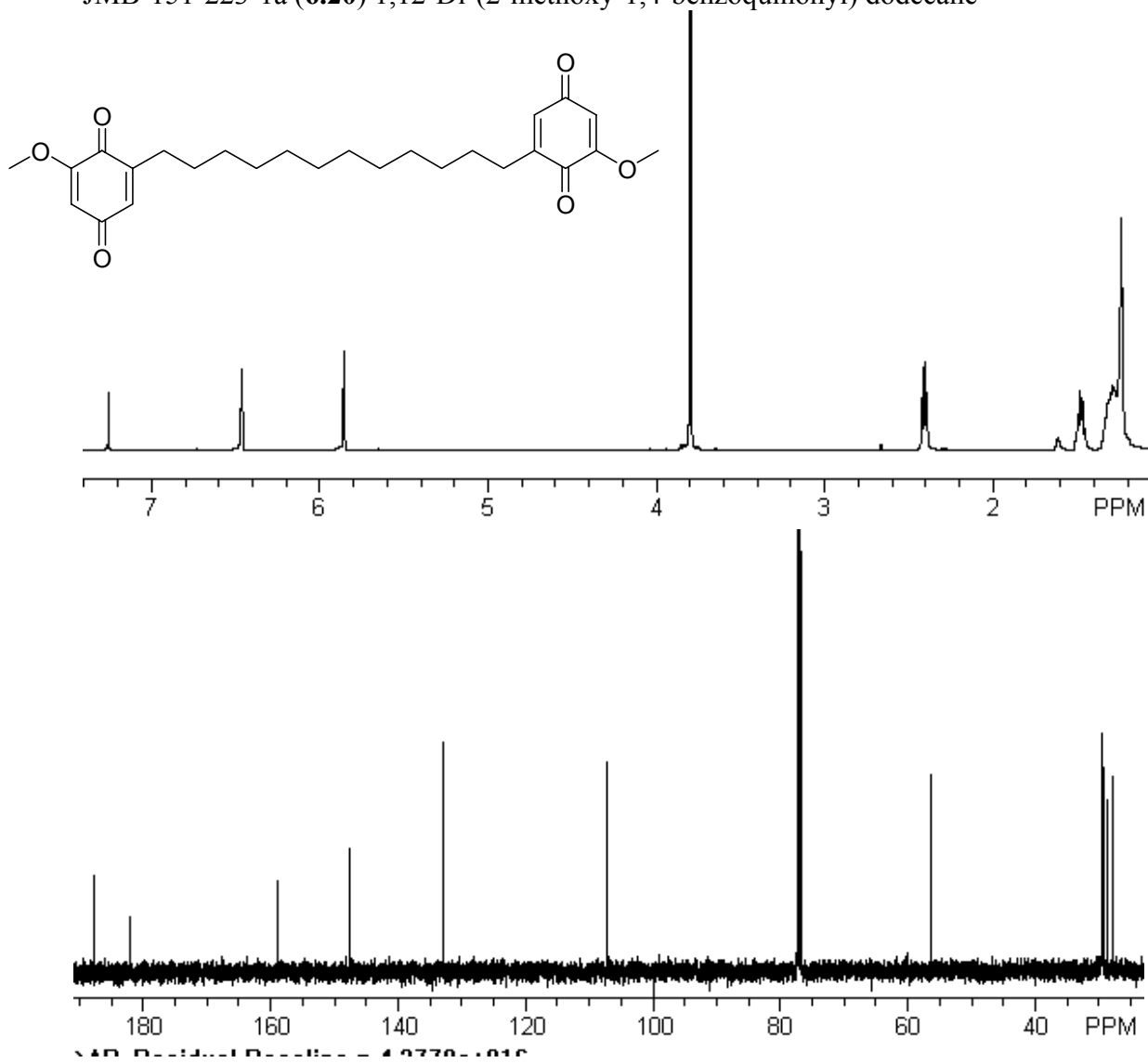
JMB-151-194-3 (6.19) 1,7-Di-(2-methoxy-1,4-benzoquinonyl) heptane



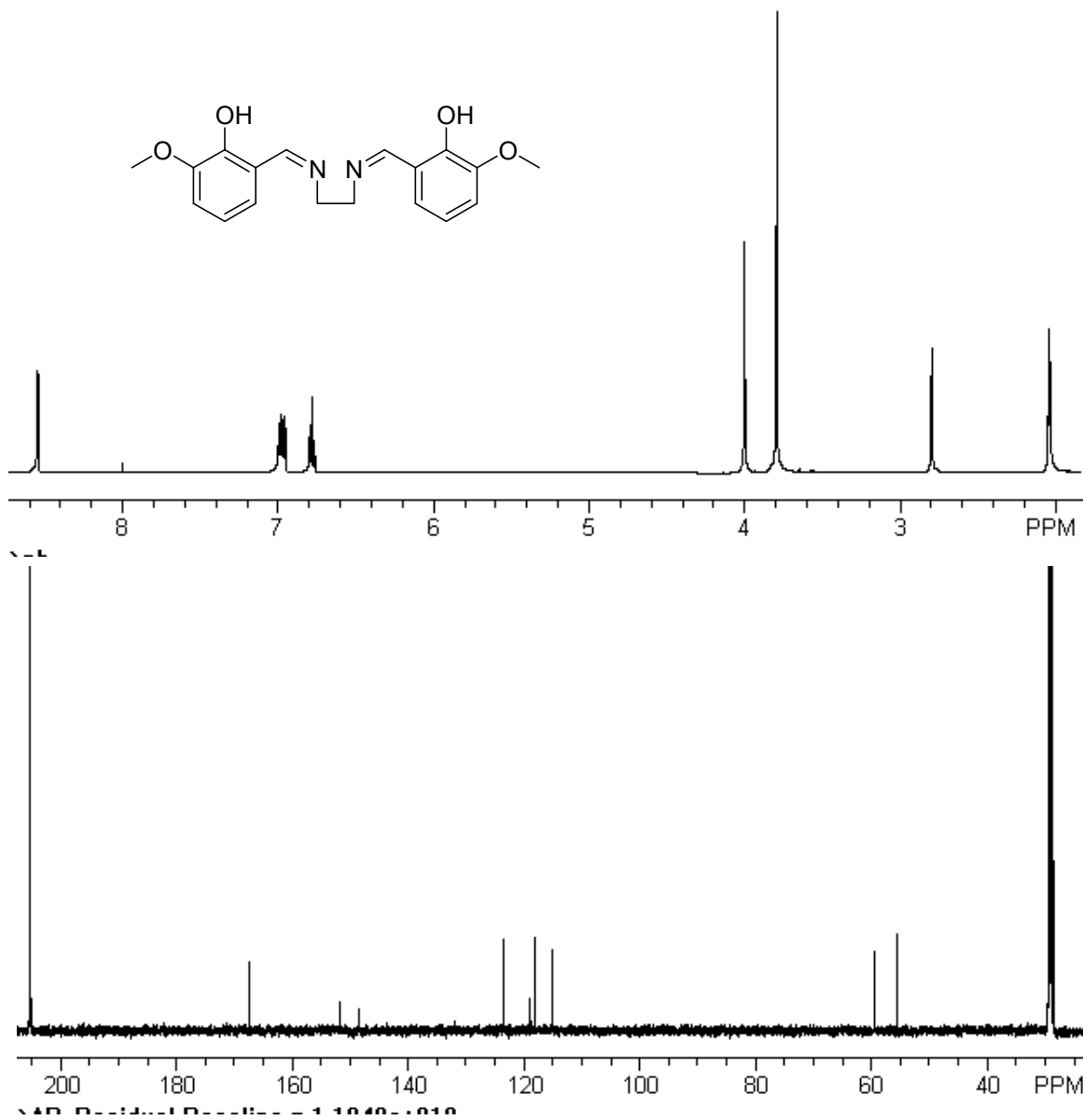
JMB-151-220-1 1,12-Di-6-(2-methoxyphenol) dodecane



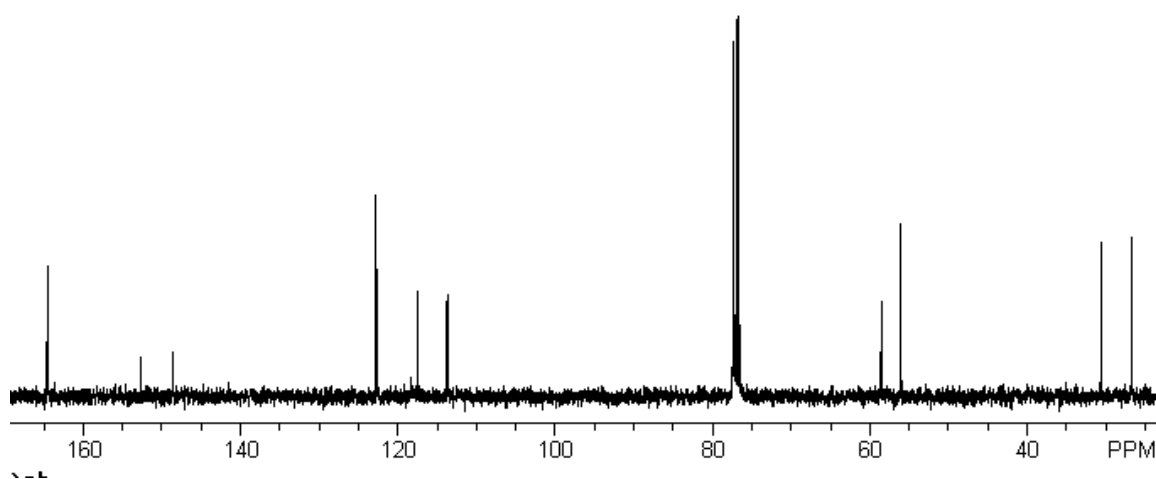
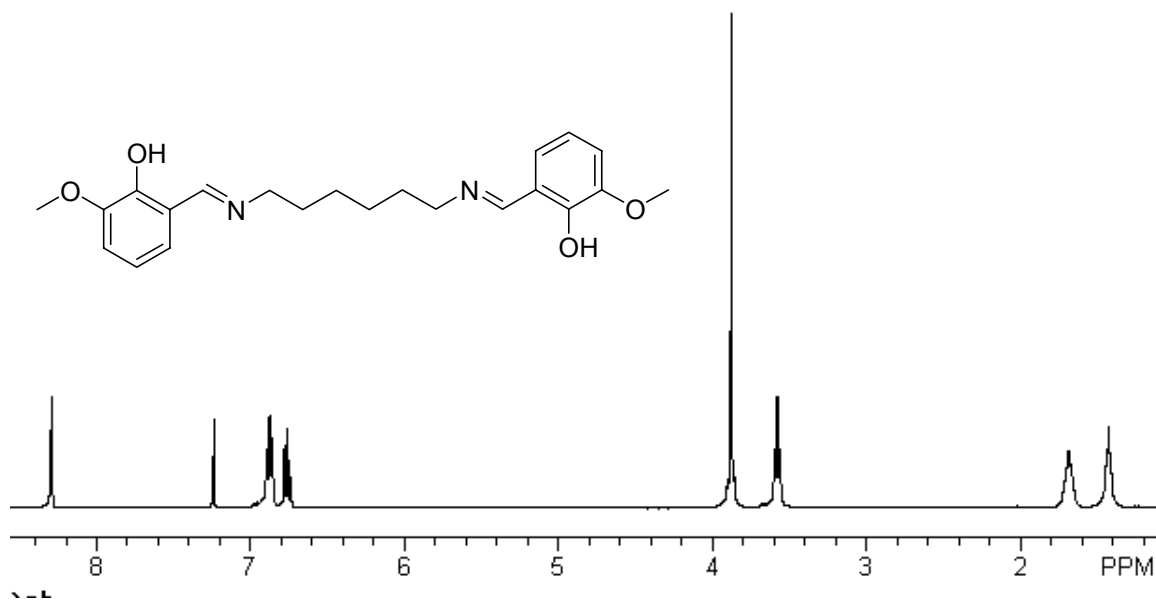
JMB-151-223-1a (6.20) 1,12-Di-(2-methoxy-1,4-benzoquinonyl) dodecane



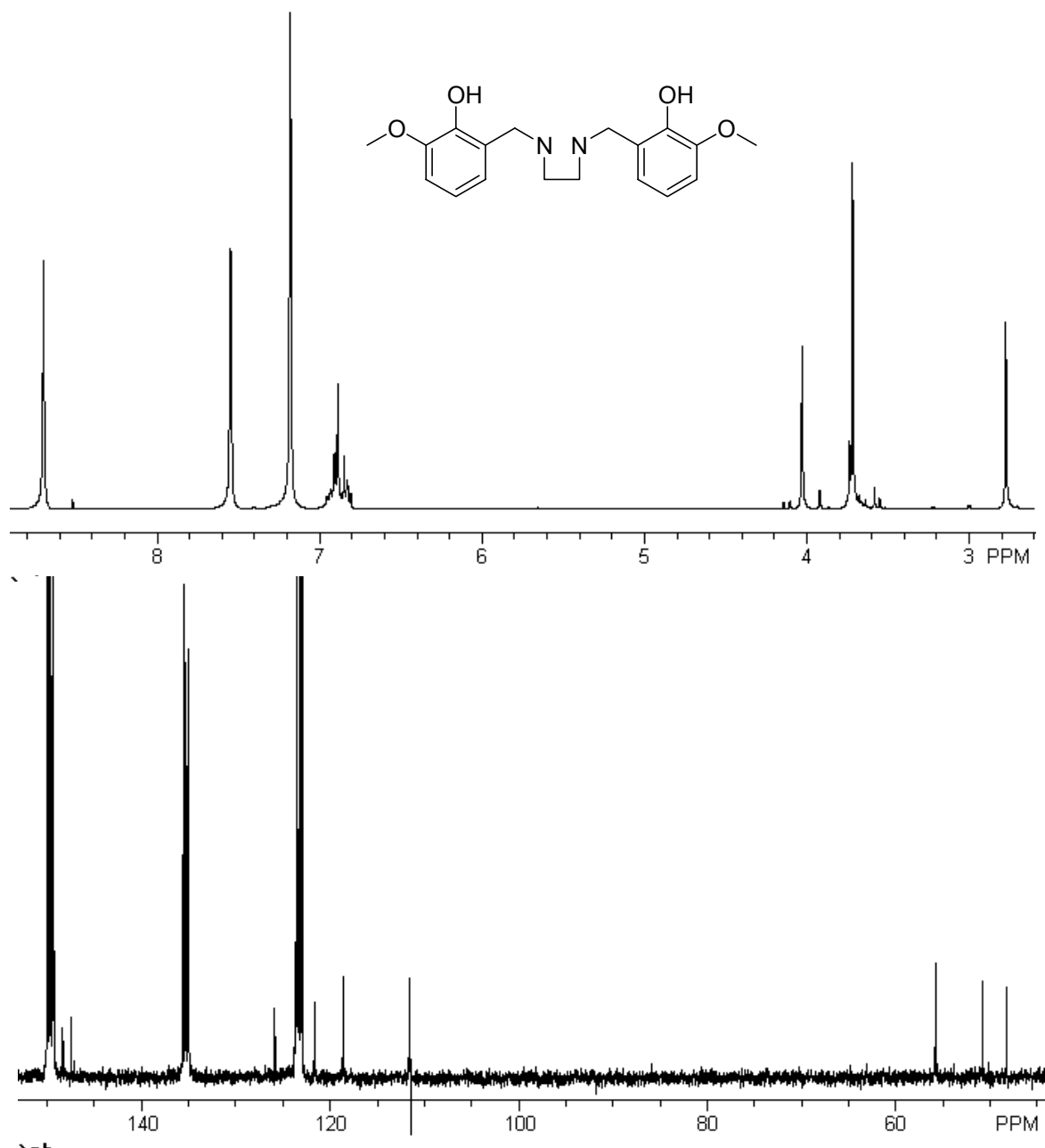
JMB-151-277 (6.44) Ethylene diamine, *o*-vanillin bis-Schiff base



JMB-151-285 (6.48) Hexamethylene diamine, *o*-vanillin bis-Schiff base.



JMB-151-279 Diamine **6.47**.



VITA

John M. Berger was born on May 27, 1967 in New York City, NY. He attended St. Francis Xavier High School and graduated in 1985. During the summer of 1984, he studied undergraduate chemistry at Harvard University, Cambridge, MA. He entered Stevens Institute of Technology in 1985 under the Gerald T. Hass Scholarship awarded from the International Brotherhood of Electrical Workers (IBEW). As a student at Stevens Institute of Technology, he became involved in the UPTAM Project (Undergraduate Participation in Technology and Medicine). Mentored by Dr. A.K. Bose and Dr. M.S. Manhas, his undergraduate research focused on the enantioselective synthesis of β -lactams. From 1987-1988, he studied abroad at the University of Dundee, Dundee, Scotland, U.K. He was awarded his Bachelor of Science in Chemistry degree in 1989.

He attended the graduate program at Stevens Institute of Technology from 1989-1994, and was awarded a Masters of Science in Chemistry degree in 1992. Dr. E. Robb was his mentor; his graduate research focused on the use of molecular modeling and NMR to characterize the conformations of penicillins in aqueous solutions.

From 1995-1996, he worked at Xechem Inc. initially as an analytical chemist, eventually becoming head of Quality Assurance.

He entered the graduate program at Virginia Polytechnic Institute and State University in 1996 and joined the natural products group of Dr. D.G.I. Kingston. In 2001, he was awarded a Ph.D. in chemistry.

John Berger is a member of the American Chemical Society, the American Society of Pharmacognosy, and *Phi Lamda Upsilon*, a chemistry honor society.